CHRISTIAN MATTHIAS HÜLS

MILLENNIAL-SCALE SST VARIABILITY AS INFERRED FROM PLANKTONIC FORAMINIFERAL CENSUS COUNTS IN THE WESTERN SUBTROPICAL ATLANTIC

GEOMAR
Forschungszentrum
für marine Geowissenschaften
der Christian-Albrechts-Universität
zu Kiel

KIEL 2000

GEOMAR REPORT 95

GEOMAR
Research Center
for Marine Geosciences
Christian Albrechts University
in Kiel

Dissertation
zur Erlangung des Doktorgrades
der mathematisch-naturwissenschaftlichen Fakultät
der Christian-Albrechts-Universität zu Kiel
zum Druck genehmigt am 21.7.1999

Redaktion der Serie: Gerhard Haass

GEOMAR REPORT
ISSN 0936 - 5788

GEOMAR
Forschungszentrum
für marine Geowissenschaften
Wischhofstr. 1-3
D - 24148 Kiel
Tel. (0431) 600-2555, 600-2505

Manging Editor: Gerhard Haass

GEOMAR REPORT
ISSN 0936 - 5788

GEOMAR
Research Center
for Marine Geosciences
Wischhofstr. 1-3
D - 24148 Kiel
Tel. (49) 431 / 600-2555, 600-2505

Content

Summary

For two sediment cores from the western tropical North Atlantic and the Caribbean Sea, sea-surface temperatures (SST) were reconstructed, based on planktonic foraminiferal census counts. For SST estimates, the **M**odern **A**nalog **T**echnique (MAT; Prell, 1985) and the **T**ransfer **F**unction **T**echnique (TFT; Imbrie and Kipp, 1971) was used.

Core M35003-4 (12.09 °N, 61.23 °W, 1299 m water depth) is located in the Tobago Basin near the Grenada Passage (SE Antilles), a main gateway for warm surface waters from the North Equatorial Current (NEC) and the Guayana Current (GC), which both enter the Caribbean Sea. The age model for core M35003-4 is based on a benthic $\delta^{18}O$ record and 19 ^{14}C-age datums. Core M35003-4 covers the last 55,000 years, with mean sedimentation rates between 10 - 48 cm/ kyr. Planktonic foraminiferal census counts were carried out at 5 cm sample intervals, equal to a mean time resolution of 300-500 years.

Foraminiferal assemblages of core M35003-4 reveal a high temporal variability of the sea-surface hydrography over the last 55,000 years. During glacial stages, abundances of high-latitude planktonic foraminiferal assemblages increased relative to the tropical assemblages. Increased abundances of *Neogloboquadrina dutertrei*, *N. pachyderma* (left coiling) and *Globigerina bulloides*, indicate an increase in productivity, possible due to an expansion of today's upwelling areas off Venezuela due to increased glacial trade wind intensity. Inferred seasonal sea-surface temperatures, estimated with TFT and MAT, show a glacial-interglacial amplitude of 2.5° - 3 °C. Seasonal SST for the upper 0-150 m indicates a shoaling of mixed-layer and the thermocline depths during these times. For marine isotope stage 3 (MIS), surface and sub-surface temperature estimates are lower by 1 °C than during glacial stage 2, which points to stronger trade wind intensities during this period. During MIS 3, inferred surface productivities, estimated from organic carbon flux to the sea floor, are equal or slightly higher than during the Holocene, while during stage 2 inferred productivity is low. Faunally-derived SST estimates agree well within the uncertainty of the methods with $U^{k'}_{37}$-SST of the same core. A conspicuous feature of the SST record is the opposite direction of the thermal evolution compared to northern hemisphere climatic records, such as the GISP 2 ice-core $\delta^{18}O$ record during Termination I. SST estimates from core M35003-4 during Heinrich event 1 and the Younger Dryas period show a warming at the core location, whereas North Atlantic sediment cores and Greenland's GISP 2 ice core $\delta^{18}O$ display a cooling. Conversely, during the northern hemisphere warm Bølling-Allerød period, SST at the core location decrease.

Core M35027-1 (17.64 °N, 67.17 °W, 1814 m water depth) is located in the northern Venezuela Basin, on the western side of the Anegada Passage. According to the benthic $\delta^{18}O$ record and by com-

parison with the SPECMAP stack, core M35027-1 extends back into marine isotope stage 10 (340,000 years B.P.). Planktonic foraminiferal census counts are carried out at 2.5 cm sample interval for the last glacial-interglacial cycle (marine isotope stage 6 to Holocene), giving a mean time resolution of 800 years. Planktonic foraminiferal assemblage variations are similar to those seen in core M35003-4, but display lower amplitudes. Estimated SST amplitudes for Terminations I and II are 2 °-2.5 °C and 1.5 °C, respectively. During the last interglacial, SST in the northern Venezuela Basin are 1 °C colder than Holocene SST.

SST estimates from cores M35003-4 and M35027-1 are compared to other published paleoceanographic records from the equatorial and North Atlantic, and to the climatic record from the GISP 2 record. The equatorial hydrography during the last glacial is mainly influenced by variations in the zonality of the trade winds, which in turn is driven by precessional forcing of the monsoon system with periodicities from 7.4 - 8.6 kyrs (McIntyre and Molfino, 1996). As proposed by McIntyre and Molfino (1996), increased upwelling should lead to a warming within the Caribbean and the Gulf of Mexico. High resolution SST estimates from core M35003-4 display the local response to varying intensity of the trade winds. Enhanced upwelling in the southern Caribbean seems to have compensated the expected effect on Caribbean SST due to advection of surface waters from the equatorial and southern Atlantic.

Zusammenfassung

Für zwei Sedimentkerne aus dem westlichen, subtropischen Atlantik und der Karibik wurden Paläo-Meeresoberflächentemperaturen (Sea Surface Temperatures, SST), basierend auf der Faunenzusammensetzung planktischer Foraminiferen, rekonstruiert. Für die SST-Berechnungen wurden die **M**odern **A**nalog **T**echnique (MAT; Prell, 1985) und die **T**ransfer **F**unktion **M**ethode (Transfer Function Technique, TFT; Imbrie und Kipp, 1971) angewendet.

Kern M35003-4 (12.09°N, 61.23°W, 1299 m Wassertiefe) stammt aus dem Tobago Becken, nahe der Grenada Passage, wo warme Oberflächenwassermassen des Nordäquatorial Stroms (NEC) und des Guyana Stroms (GC) in die Karibik einfließen. Das Altersmodel für den Kern M35003-4 basiert auf der Messung benthischer Sauerstoffisotopen sowie 19 AMS ^{14}C Datierungen an planktischen Foraminiferen. Danach umfasst der Sedimentkern die letzten 55 000 Jahre mit mittleren Sedimentationsraten zwischen 10 - und maximal 48 cm / 1000 Jahren. Die Fau-nenzusammensetzung der planktischen Foraminiferen wurde in Intervallen von 5 cm, entsprechend einer zeitlichen Auflösung von 300 bis 500 Jahren, bestimmt.

Die Foraminiferenfauna dokumentiert eine hohe zeitliche Variabilität in den Eigenschaften der Meeresoberflächenwassermassen. Während des Glazials ist die Häufigkeit von planktischen Arten,

die charakteristisch für gemäßigte bis kalte Klimazonen sind, im Vergleich zu den tropischen Arten erhöht. Die SST zeigen einen Glazial - Interglazial Temperaturunterschied von 2.5 °C bis 3 °C. Die durch die Planktonforaminiferenfauna abgeleiteten saisonalen SST stimmen im Rahmen der für die Methoden charakteristischen Genauigkeit mit $U^{k'}_{37}$ – SST Abschätzungen am selben Sedimentkern überein.

Erhöhte Häufigkeiten von *Neogloboquadrina dutertrei*, *N. pachyderma* (links drehend) und *Globigerina bulloides* während des Glazials deuten auf eine Zunahme der Produktivität, möglicherweise infolge einer nordwärtigen Ausweitung des Küstenauftriebes vor Venezuela durch eine Intensivierung des Passats. Die berechneten saisonalen Temperaturen der oberen 0 -150 m Wassertiefe während dieser Zeiten indizieren eine Mächtigkeitsabnahme der durchmischten Oberflächenwasserschicht und Verflachung der Thermokline.

Während des Isotopen Stadiums 3 (MIS 3) sind die berechneten Oberflächen- und Sub-Oberflächenwassertemperaturen rund 1 °C kälter als im Stadium 2 (MIS 2). Dies wird als ein Hinweis auf verstärkte Passatwindintensitäten interpretiert. Die aus dem organischen Kohlenstoffgehalt der Sedimente abgeleiteten Produktivitäten sind im MIS 3 ähnlich bzw. leicht höher als im Holozän, wohingegen sie im MIS 2 deutlich niedriger sind.

Eine besonders auffällige Struktur der Paläo-Temperaturen von M35003-4 ist der im Vergleich zur nördlichen Hemisphäre entgegengesetzte Verlauf der Temperaturentwicklung während des Deglazials. Berechnete SST während des Schmelzwasserereignisses ('Heinrich event') H1 und der Jüngeren Dryas zeigen eine Erwärmung im Tobago Becken an, während in der nördlichen Hemisphäre eine deutliche Abkühlung erfolgt. Im Gegensatz dazu wird während des Bølling-Allerød eine Abkühlung in der SST abgeleitet, während in der nördlichen Hemisphäre eine erste Erwärmung stattfindet.

Kern M35027-1 (17.64 °N, 67.17 °W, 1814 m Wassertiefe) liegt im nördlichen Venezuela Becken auf der westlichen Seite der Anegada Passage. Die Alterseinstufung erfolgte mit Hilfe von benthischen $\delta^{18}O$-Messungen im Vergleich zur SPECMAP –Kurve. Danach reicht der Kern M35027-1 zurück ins Isotopenstadium 10 (340 000 Jahre vor heute). Für den letzten Glazial - Interglazialzyklus (MIS 6 - Holozän) wurden Planktonforaminiferenzählungen in 2.5 cm Intervallen durchgeführt, was einer mittleren zeitlichen Auflösung von 800 Jahren entspricht.

Die Fluktuationen der Planktonforaminiferenfauna zeigt einen ähnlichen Verlauf wie im Kern M35003-4, jedoch mit geringeren Amplituden. Der SST-Hub für die Terminationen I und II beträgt 2 °C bzw. 1.5 °C. Meeresoberflächentemperaturen während des letzten Interglazials (Stadium 5.5) waren im nördlichen Venezuela Becken rund 1 °C kälter als heute.

Die SST entlang der Kerne M35003-4 und M35027-1 wurden mit Klimakurven aus dem äquatorialen und dem nördlichen Atlantik sowie Grönland verglichen. Während des letzten Glazials wurde die Oberflächenhydrographie im äquatorialen Atlantik im wesentlichen durch Variationen in der Zonalität der Passatwinde geprägt. Diese wird wiederum durch den Einfluss der Präzession auf das Mon-

soon System mit Perioden von 7.4 bis 8.6 ka (= 1000 Jahre) gesteuert. Von McIntyre und Molfino (1996) wurde vermutet, dass es durch verstärkten Wassermassentransport zu einem Aufstau warmer Wassermassen und damit zu einer Erwärmung in der Karibik und dem Golf von Mexico führen sollte. Die hochauflösenden SST-Berechnungen entlang M35003-4 spiegeln den lokalen Einfluss variierender Passatwindintensitäten wider. Der erhöhte Auftrieb in der südlichen Karibik während des Glazials hat hier den vermuteten Temperatureffekt durch Advektion von Oberflächenwassermassen aus dem äquatorialen Atlantik kompensiert.

1 Introduction

Ice-core records from Greenland have revealed a high temporal variability during the last glacial of North Atlantic climate, with temperature shifts of up to 6-7 °C within a few decades (Grootes and Stuiver, 1997). The rapid climate cycles start with an abrupt rapid warming, followed by a gradual cooling at periods of 1.5 kyrs (Dansgaard-Oeschger-Events, Johnsen et al., 1992). During the terminal cold stadials of theses cycles, increased abundances of ice-rafted debris (IRD) are observed in marine records from the northern North Atlantic (Bond et al. 1993; Bond and Lotti, 1995; Rasmussen et al., 1996), as far south as the region off Portugal (Lebreiro et al., 1996; Zahn et al., 1997). From this it has been inferred that large-scale drifts of icebergs occurred over the northern North Atlantic, with the accompanying meltwater fluxes suppressing or even stopping the production of deep water, by lowering surface water density (Sarnthein et al.,1994; Maslin et al., 1995).

McAyeal (1993) proposed a conceptual model which involves internal ice-sheet stability-instability processes: ice-sheet buildup accumulated ice masses up to a threshold, where basal melting due to increased pressure occurred, and iceberg flotillas were released into the North Atlantic.

Another mechanism involves changes in the trade wind-monsoon system at low latitudes. Particularly, linear and non-linear responses of low-latitude climate to the orbital precessional signal have been inferred as a possible cause for sub-Milankovitch climate variability (Curry and Oppo, 1997). During times of enhanced zonality of the trade wind circulation, warm waters were advected into today's warm water pool of the Caribbean and Gulf of Mexico, while at the equator increased upwelling occurred (McIntyre et al.,1989; McIntyre and Molfino, 1996; Little et al., 1997). During monsoon maxima, when the tropical easterlies diminish, these warm waters are released into the North Atlantic subtropical gyre and are delivered into the subpolar North Atlantic, causing the rapid melting of ice and hence the Heinrich events (McIntyre and Molfino, 1996). A slightly modified conceptual model is suggested by Little et al. (1997). Using the relative abundances of the polar species *N. pachyderma* (left) as an upwelling indicator, they found a high variability of coastal upwelling off SW Africa during the last glacial, with maxima in upwelling intensity preceding the North Atlantic Heinrich events by approximately 3 kyrs. At times of increased trade wind strength, tropical and subtropical waters are forced across the equator, enhancing the pool of warm waters to be transferred to the high latitudes of the North Atlantic. The increased supply of warm waters to the northern high latitudes accelerates ice sheet growth and may lead to ice sheet instability and subsequent collapse (Little et al., 1997).

In this thesis, sea-surface temperatures (SST) are reconstructed for 2 sediment cores from the western tropical north Atlantic and the Caribbean Sea. The Caribbean is the source area for the Gulf Stream and North Atlantic Drift system, which provides the high northern latitudes with heat and moisture. As such, the Caribbean is a key position to link low-latitude paleoceanographic variability

to high-latitude climate change as described previously.

Core M35003-4 is located in the Grenada Passage, one of the main gateways for warm waters entering the Caribbean. Core M35027-1 is located in the northern Venezuela Basin, at the western end of the Anegada Passage. Both sediment cores are expected to monitor the varying strength of cross-equatorial heat flux.

Paleo-sea-surface and sub-surface temperatures are estimated by determination of the relative abundances of planktonic foraminiferal assemblages. To assess the validity of SST estimates, SST are reconstructed with the Modern Analog Technique (MAT; Prell, 1985) and the transfer function technique (TFT; Imbrie and Kipp, 1971). For core M35003-4, planktonic foraminiferal based SST are compared to independent alkenone ($U^{k'}_{37}$) SST estimates.

The resulting paleoceanographic reconstructions are compared to similar data from the equatorial Atlantic, the Caribbean, and the North Atlantic. With these data, changes in the cross-equatorial and northward heat transport and connections to rapid, sub-Milankovitch climate variability as seen from Greenland ice-cores is discussed.

1.1 Core locations and oceanographic setting

Gravity cores M35003-4 and M35027-1 were retrieved during R/V METEOR cruise M35 from April to May 1996 (Hemleben et al., 1998; Figure 1, Table 1).

Core M35003-4 is located at the western flank of the Tobago Basin at the SE Lesser Antilles, on the Atlantic side near the Grenada Passage. The core lies at 1300 m water-depth, well above the modern lysocline of the Atlantic (Berger, 1968).

Core M35027-1 lies in the NE Venezuela Basin, at the Atlantic side of the Anegada Passage.

Both cores represent different environmental settings: Core M35003-4 in the south is influenced by higher terrigenous inputs from Amazon and Orinoco River suspension load (Müller-Karger et al., 1995), leading to higher sedimentation rates due to dilution of pelagic sedimentation. Core M35027-1 in the north, on the other hand, shows mainly pelagic sedimentation.

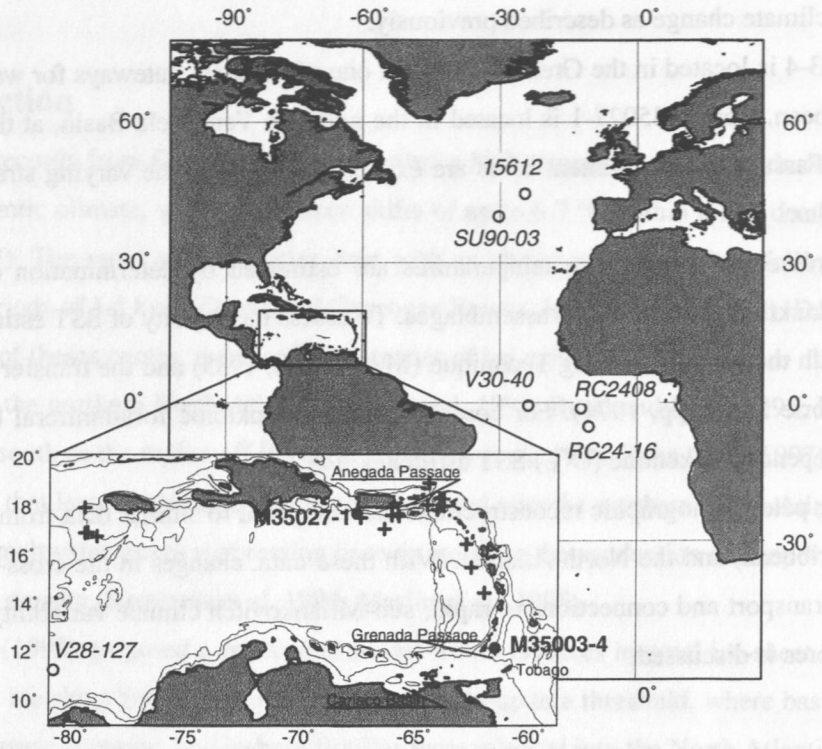

Figure 1. Position of cores and surface samples used in this thesis. Bathymetry of detailed map shows isolines of 1000 m and 2000 m water depth.

Table 1. Location of core top samples and sediment cores

Station	Latitude	Longitude	Water depth (m)	Device	Recovery (m)
M35002-1	12.0317	-61.1767	1506	GKG [1]	0.5
M35003-4	**12.0830**	**-61.2330**	**1299**	**SL [2]**	**9.63**
M35003-6	12.0850	-61.2450	1299	GKG	0.47
M35004-1	14.4100	-61.6617	2885	GKG	0.38
M35005-1	15.4533	-62.2317	2289	RKG	0.36
M35006-6	16.4217	-62.4533	888	RKG	0.33
M35008-1	18.0317	-64.1633	2820	RKG	0.37
M35010-2	18.9333	-64.0900	2696	RKG	0.25
M35012-6	18.3050	-63.6267	1121	RKG	
M35013-3	18.3150	-63.4500	899	RKG	0.26
M35014-1	17.8417	-63.7367	1604	RKG	0.32
M35015-1	17.9933	-63.4517	1230	RKG	0.31
M35018-1	17.5750	-65.3700	1728	RKG	0.3
M35019-1	17.6717	-65.4350	1815	RKG	0.32
M35020-2	17.9300	-65.6700	2005	RKG	0.4
M35023-3	17.6033	-65.6817	1192	RKG	0.21
M35024-6	17.0433	-66.0017	4710	RKG	0.35
M35026-2	17.5083	-67.0433	3815	RKG	0.41
M35027-1	**17.6483**	**-67.1667**	**1814**	**SL**	**11.06**
M35030-1	16.7550	-78.6100	1298	RKG	0.2
M35033-1	16.9133	-79.0183	1124	RKG	0.18
M35035-1	16.8933	-79.1317	1252	RKG	0.2
M35039-1	17.9267	-79.1450	1142	RKG	0.23

[1] RKG and GKG: box corer
[2] SL: gravity core

Today, warm waters of the North Equatorial Current (NEC) and the Guyana Current (GC), which comprise the northwestern extension of the Atlantic's cross-equatorial surface flow, enter the Caribbean through the Grenada Passage and the Lesser Antilles Passages (Stramma and Schott, 1996; Schott and Molinari, 1996). These warm waters are further advected by the Caribbean Current into the Gulf of Mexico, and later reach the North Atlantic to contribute to the Gulf Stream and North Atlantic Drift current (Kinder et al., 1985) (Figure 2).

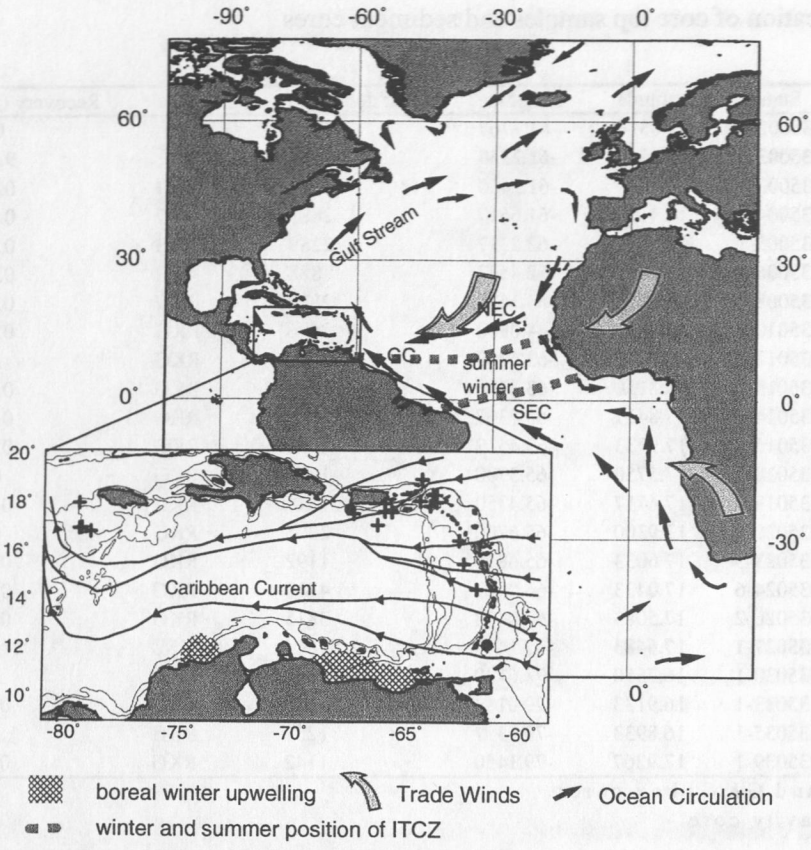

Figure 2. Ocean and atmospheric circulations schematics, based on Schott and Molinari (1996), Stramma (1991), Peterson and Stramma (1991), and Kinder et al. (1985).

During boreal winter and spring, trade winds are strongest, and the volume of Atlantic water entering the Caribbean is largest. During this season, coastal upwelling along the continental margin of Venezuela occurs due to increased Ekman transport (Kinder et al., 1985, Muller-Karger and Castro, 1994). Higher concentrations of phytoplankton during the cold boreal winter seasons northwest of Tobago island, in the islands wake, are possibly caused by higher phytoplankton abundance due to upwelling or deep mixing, since the Orinoco plume is located south of Tobago.

During boreal summer and fall, when the Intertropical Convergence Zone (ITCZ) is at its northern position, trade wind intensity and coastal upwelling in the southern Caribbean weaken, and river discharge from the Orinoco reaches up to Tobago island, as shown by Coastal Zone Color Scanner (CZCS) images which display high phytoplankton pigment concentration in the area (Muller-Karger and Castro, 1994).

Pelagic sedimentation in the southern Caribbean is influenced by high input amounts of terrigenous material, coming from the Amazon river and to some extent from the Orinoco (Milliman and Meade, 1983; Bowles and Fleischer, 1985).

Because of sill-depths ranging from 1000 m to 2000 m, Caribbean deep-water is mainly comprised of intermediate Atlantic deep water masses: North Atlantic Intermediate Water (NAIW) and Upper North Atlantic Deep Water (UNADW) enter the Caribbean through the northern Windward and Anegada Passages with sill depths of 1650 m and 2000 m, respectively. (Sturges, 1975; Metcalf, 1976). Antarctic Intermediate Water enters the Caribbean along the eastern and southeastern passages of the lesser Antilles with sill depths between 750 m and 950 m (Wüst, 1964 ; Stalcup, 1971).

2 Materials and methods

2.1 Sample preparation and analytical procedures

In general, the cores were sampled in 5 cm intervals. To enhance the time resolution, sample density in core M35027-1 was further increased to 2.5 cm intervals between the core top and 395 cm core depth (see also chapter 3.1). Sedimentation rates at the site of core M35003-4 are high, so that stratigraphic resolution at 5 cm sample intervals sufficed for the detection of fine-scale paleoceanographic variability.

For estimation of physical properties and measurement of chemical parameters (total organic carbon, inorganic carbon, carbonate phases with X-ray diffractometry), sample volumes of 5 ml were taken. 10 ml samples were taken for micropaleontological investigation and stable isotope analysis on benthic foraminifera.

All samples were weighed and dried at 50°C. Water content and dry bulk density were estimated from the difference of wet and dry weight. Samples for micropaleontological investigations were wet sieved over a >63 µm sieve, and then further subdivided into 150-250 µm and >250 µm subfractions.

2.1.1 Isotope measurements

The stratigraphy of the cores is based on benthic stable oxygen isotope and ^{14}C AMS stratigraphy. Stable isotope measurements were made on the epibenthic species *Cibicidoides wuellerstorfi*, *C. kullenbergi*, and *C. pseudoungerianus*. Below 450 cm depth in core M35003-4, the measurements were done on *Uvigerina peregrina*, since epibenthic species abundances were low in the deep core sections. To generate a composite $\delta^{18}O$ record for this core, the epibenthic $\delta^{18}O$ signal was adjusted to the *Uvigerina* scale by adding 0.64‰ (Duplessy et al., 1984).

3-5 specimens were picked for each measurement from the size fraction >250 µm. Prior to isotope analysis, the samples were ultrasonically rinsed in methanol for 10 seconds, and then transferred to a CARBO KIEL automated carbonate preparation device that is linked online to a FINNIGAN MAT 251 mass spectrometer. Reproducibility of $\delta\ ^{18}O$-measurements was 0.066 ‰ as determined by 80 replicate analysis of an internal carbonate standard (Solnhofen Limestone). All isotope data are referred to the PDB scale.

For core M35003-4, ^{14}C-AMS measurements were carried out on 12 monospecific samples of the planktonic foraminifera *Globigerinoides ruber* (white) at the Leibniz-Laboratory of Kiel University. Additionally, 8 ^{14}C-AMS datings from mixed planktonic foraminiferal samples which contained *G. ruber* and *Globigerinoides sacculifer* (Rühlemann et al., subm.) were used. In general, between 500 and 1000 specimens were picked. The ^{14}C-AMS datings were carried out at the Leibniz-Laboratory AMS facility at Kiel University using a 3 MV Tandetron system, and applying analytical procedures

described in Nadeau et al. (1997) and Schleicher et al. (1998). After cleaning with 0.5 ml 30% H_2O_2, the H_2O_2 wet samples were evacuated, and sample CO_2 for ^{14}C determination was released using concentrated H_3PO_4 at 80°C.

2.1.2 Faunal analysis: Planktonic foraminiferal census counts and factor analysis

Following the convention of the CLIMAP Group, planktonic foraminiferal census counts were done on the >150 µm size fraction and, whenever possible, a minimum of 300 specimens was counted. This number is a compromise between counting efforts and statistical precision (Chang, 1967). Lower numbers will lead to higher statistical errors, particularly for less abundant species. For example, the 2σ error for a relative abundance of 20 % on a 300 specimen count is less than 5% (van der Plas and Tobi, 1965). To achieve a higher statistical precision the test numbers to be counted must be unproportionally increased.

To facilitate the counting and determination procedure, the >150 µm size fraction was subdivided into subfractions of 150 µm - 250 µm and >250 µm. Because of high abundances of pteropod tests and fragments, the >250 µm size fraction for all samples from core M35027-1 was further subdivided into 250 µm - 400 µm and >400 µm subfractions. These subsamples were then subdivided with a microsplitter into subsets containing 150 - 200 specimens. The species percentages were calculated by combining the counts of all subfractions.

43 plankton foraminiferal species and morphotypes have been differentiated. Planktonic foraminiferal taxonomy follows the species concepts of Bé (1977), Kennett and Srinivasan (1983), Saito et al. (1981), and Hemleben et al. (1989). Following Kipp (1976), intergrades between *Neogloboquadrina pachyderma* (dextral) and *N. dutertrei* were identified and labeled as P/D intergrades. *Globoratalia menardii* and *G. tumida* were grouped together (Dowsett and Poore, 1990; Pflaumann et al., 1996), since a discrimination between both species in fossil samples is difficult.

Statistical investigation of the relative abundance information of planktonic foraminiferal communities in cores M35003-4 and M35027-1 was conducted by principal component analysis (PCA, Davis, 1986). This method was first introduced by Imbrie and Kipp (1971) and summarizes the relative abundance information of a modern reference data set (=modern core-top data) with a Q-mode PCA into statistical plankton foraminiferal assemblages, so called 'factors' (Imbrie and Kipp, 1971). In a second step, the core-top factor model is applied to down core data by simple matrix operation (Jöreskog et al., 1976).

In this thesis, a modern reference data set of 750 core-tops was compiled from published core-top foraminiferal census counts from Pflaumann et al. (1996), SPECMAP (Imbrie et al., 1990), and 19 new Caribbean core top data (this thesis) from the Atlantic between 65°N and 40°S (Figure 3). PCA

was performed using Fortran routines CABFAC and THREAD (Imbrie and Kipp, 1971; Klovan and Imbrie, 1971).

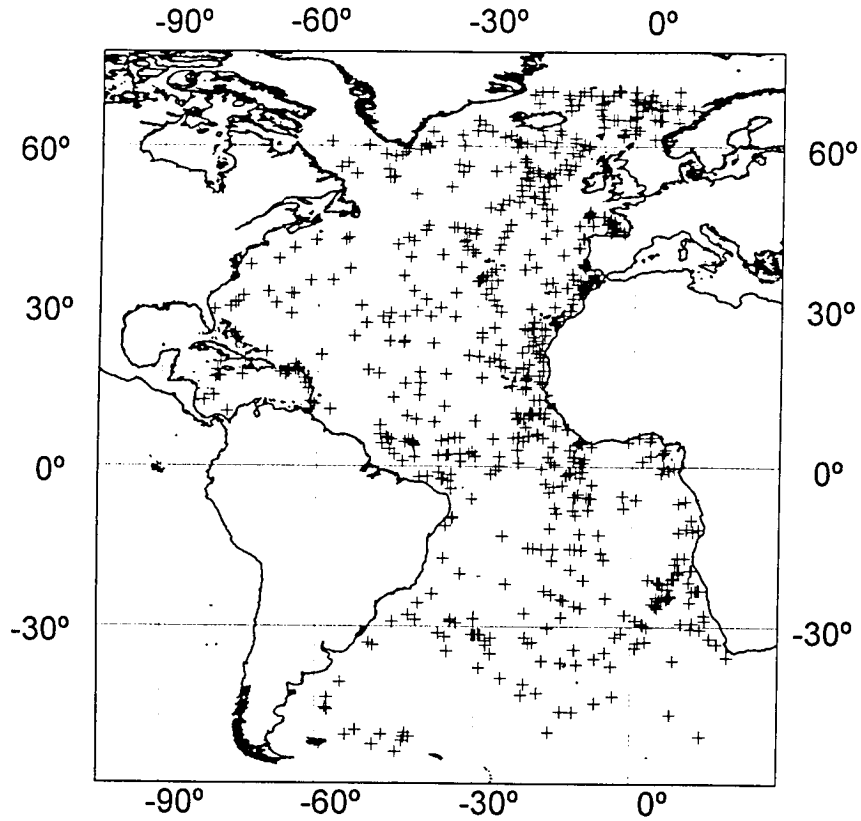

Figure 3. Location of the modern reference core top samples.

2.2 Reconstruction of sea-surface temperatures

Using the relative abundance information of planktonic foraminifera Imbrie and Kipp (1971) developed a method for quantitative reconstruction of past sea-surface environments such as sea-surface temperature and salinity. The method is based on the assumption that the pelagic ecosystem of today remained essentially unchanged during the Pleistocene. In particular, it is assumed that the ecological response of a species or a species assemblage to physical and chemical parameters of the ocean has remained the same through time (Imbrie and Kipp, 1971). The concept of the method is to compare species abundances in fossil samples with a compilation of a modern set of surface samples and to deduce environmental parameters (e.g., sea-surface temperature (SST) or ocean productivity) from a comparison with its modern analogs.

In this study, SST is estimated using two different techniques:

a) development of a transfer function with regression analysis which relates variations in foraminiferal assemblage (factors, see above) to overlying SST (**T**ransfer **F**unction **T**echnique, TFT; Imbrie and Kipp, 1971). A stepwise 2nd degree nonlinear regression analysis with factors and SST was performed with the STATVIEW software. The resulting transfer function has the form

$$SST_{ct} = f_1^2 * k_1 + f_2^2 * k_2 + ... f_9^2 * k_9 + f_1 * k_{10} + ... f_9 * k_{18} + f_1 F_2 * k_{19} + ... f_9 F_8 * k_{54} + k_0 \quad (1)$$

which is in matrix notation

$$SST_{ct} = F_{ct}^2 K + K_0 \quad (2)$$

where SST_{ct} is the core top SST, f_n (F in matrix notation) are the planktonic foraminiferal assemblages (factors 1 - n), k_n (K in matrix notation) are the regression coefficients, and k_0 (K_0 in matrix notation) is a constant.
The resulting SST Transfer Function from the regression analysis was applied to down-core assemblages from cores M35003-4 and M35027-1.

b) a direct comparison of foraminiferal census data of a sample with unknown SST with foraminiferal census data of samples with known SST by means of their similarity, assuming that similar assemblages have lived in similar environments (**M**odern **A**nalog **T**echnique, MAT; Prell [1985]).

As has been demonstrated previously (Prell, 1985; Pflaumann et al., 1996; Gonzalez-Donoso and Linares, 1998), SST estimates derived from modern assemblages using MAT reflect *in situ* SST from the modern calibration (control) data set more accurately than TFT. Additionally, MAT is shown to be less susceptible to effects of so called no-analog conditions. No-analog-conditions can be discerned, for example, if species abundances in samples exceed their maximum abundances of a modern reference data set (Hutson, 1977, Prell, 1985).

For the MAT SST estimation, the Squared Chord Distance as the best index of dissimilarity was used (DSML; Overpeck et al., 1985). This method compares the faunal information of a sample with unknown SST with faunal information from the modern assemblage control data set. SST is then estimated by a weighted average of the 'measured' temperature (interpolated SST at core top location from Levitus and Boyer, 1994) with the best analogs (=highest similarity or lowest dissimilarity). For SST estimation 10 best analogs were used.

$$D_{ij} = \sum_{1}^{n} (P_{ik}^{1/2} - P_{jk}^{1/2}) \quad (3)$$

$$S_{ij} = \sum_{1}^{n} (P_{ik} * P_{jk})^{1/2} \quad (4)$$

$$t = \frac{\sum_{n}^{k} (T_n - S_n)}{\sum_{n}^{k} S_n} \quad (5)$$

where D_{ij} is the Squared Chord Distance as dissimilarity index, S_{ij} is the similarity index, P_{ik} and P_{jk} are the kth species of the i^{th} and j^{th} samples of the analog and subject data matrix, respectively, t is estimated SST, and T_n is the SST of the n^{th} analog sample. A highly similar analog sample for a subject sample will have a dissimilarity near zero and a similarity near one.

Table 2. Comparison of MAT (Squared Chord Distance) and SIMMAX (Scalar Product) SST estimates for caloric warm and cold SST at 0-50 m water depth.

	MAT Squared Chord Distance		SIMMAX Scalar Product	
	T_c	T_w	T_c	T_w
Number of core tops	750		752	
Mean dissimilarity / mean similarity index	0.10/ 0.95		/ 0.96	
Correlation coefficient R	0.99	0.99	0.98	0.98
R^2	0.98	0.98	0.95	0.95
Mean Standard deviation of selected best analogs	0.74	0.74	0.85	0.83
Standard deviation (SD) of residuals	1.10	1.05	1.56	1.45

Another MAT technique, the SIMMAX technique (Pflaumann et al., 1996), uses the Scalar Product as a measure of similarity. The technique also uses a geographical distance weighting for SST estimation, which improves the precision of the SST estimation with respect to a calibration run (Pflaumann et al., 1996). However, in case of a broad geographical range of selected best analogs, the distance weighting may dominate the similarity weighting during the SST estimation, thus giving artificial higher or lower SST estimates. Without distance weighting, the scalar product gives a lower correlation coefficient during calibration and is therefore rejected (Table 2).

For the modern reference data set (see above), mean seasonal SST of the upper 0-50 m (the aver-

age of winter and summer SST at the 0 m, 30 m and 50 m depth level) were assigned, which were extracted from the World Ocean Atlas 1994 (Levitus and Boyer, 1994). To cover both hemispheres, caloric seasons instead of calendar seasons were used, so that the cold season is always colder than the warm season.

As planktonic foraminifera inhabit the upper few hundred meters of the water column (e.g., Hemleben et al., 1989), the TFT and MAT technique can also be used to estimate the temperature of deeper water layers (Pflaumann et al., 1996, 1999). For deep water layers, the annual temperature of the 75 m, 100 m, and 150 m layer are extracted from the World Ocean Atlas 1994. Since the modern seasonal signal for these water-depth levels is small, I use the annual water temperature. From the temperature gradient between the surface and the deep-water layers, changes in the thermocline depth can be inferred.

$SST_{0\text{-}50m}$-estimations from TFT and MAT show high correlation with 'measured' LEVITUS 94 sea surface temperature (Figure 4 A and 5A, 5C, 5E). A higher accuracy for MAT based SST estimations is indicated by lower standard deviation of the residuals (estimated - measured SST). Both methods, MAT and TFT, tend to underestimate SST at the warm end, and to overestimate SST at the cold (Figure 4 B and 5B, 5D, 5F), due to the limits of the modern reference data set. To estimate correct SST at the warm and cold end, warmer / colder 'measured' SST than existing would be necessary.

To investigate the sensitivity of planktonic foraminiferal assemblage based SST estimates, both techniques are used for the seasonal 0-50 m level. For deep-surface water temperature estimates, only the MAT is used.

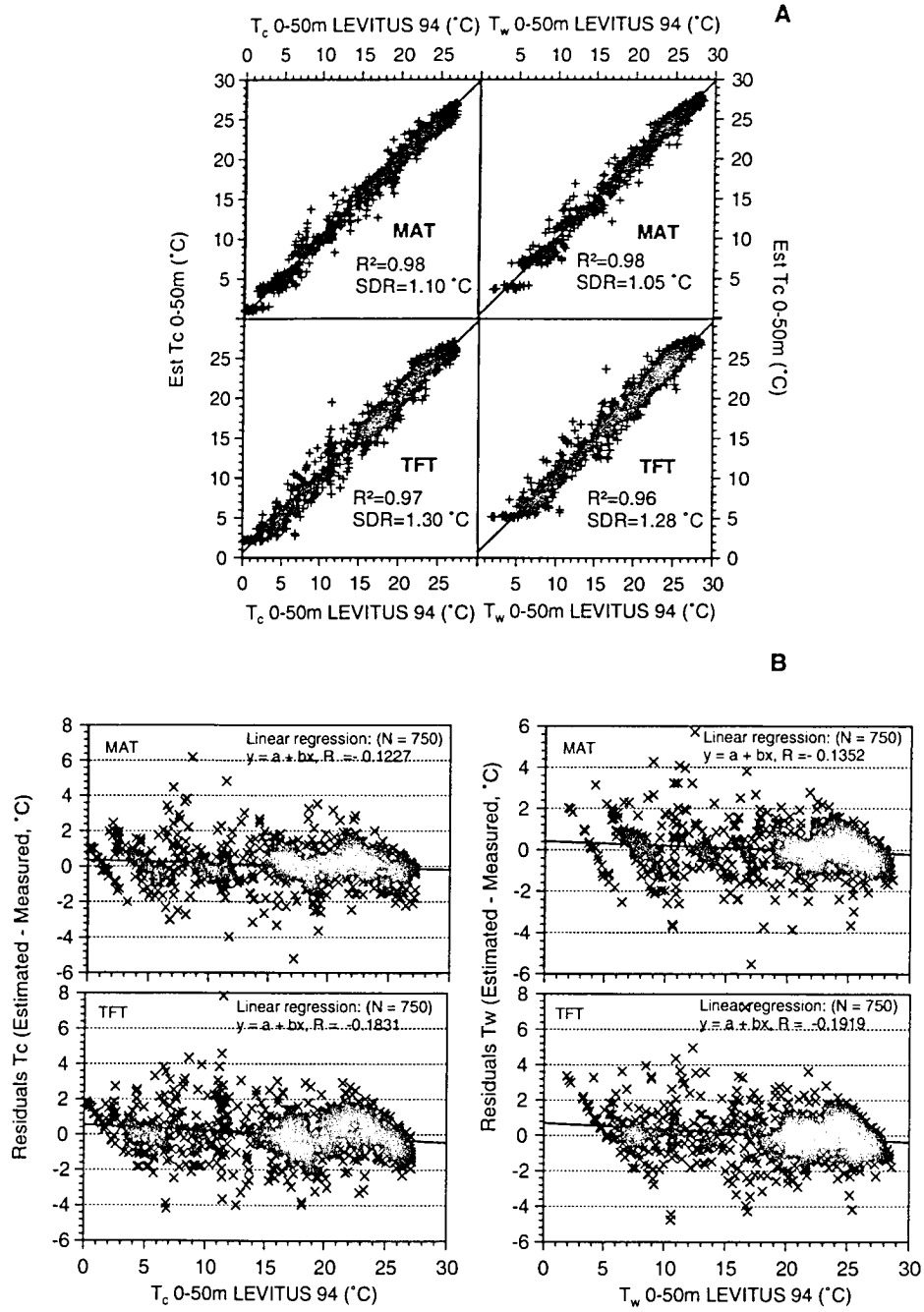

Figure 4 A). Comparison between estimated SST vs. measured SST (0-50 m water depth) of the modern calibration data set; B) Residual statistics of MAT and TFT.

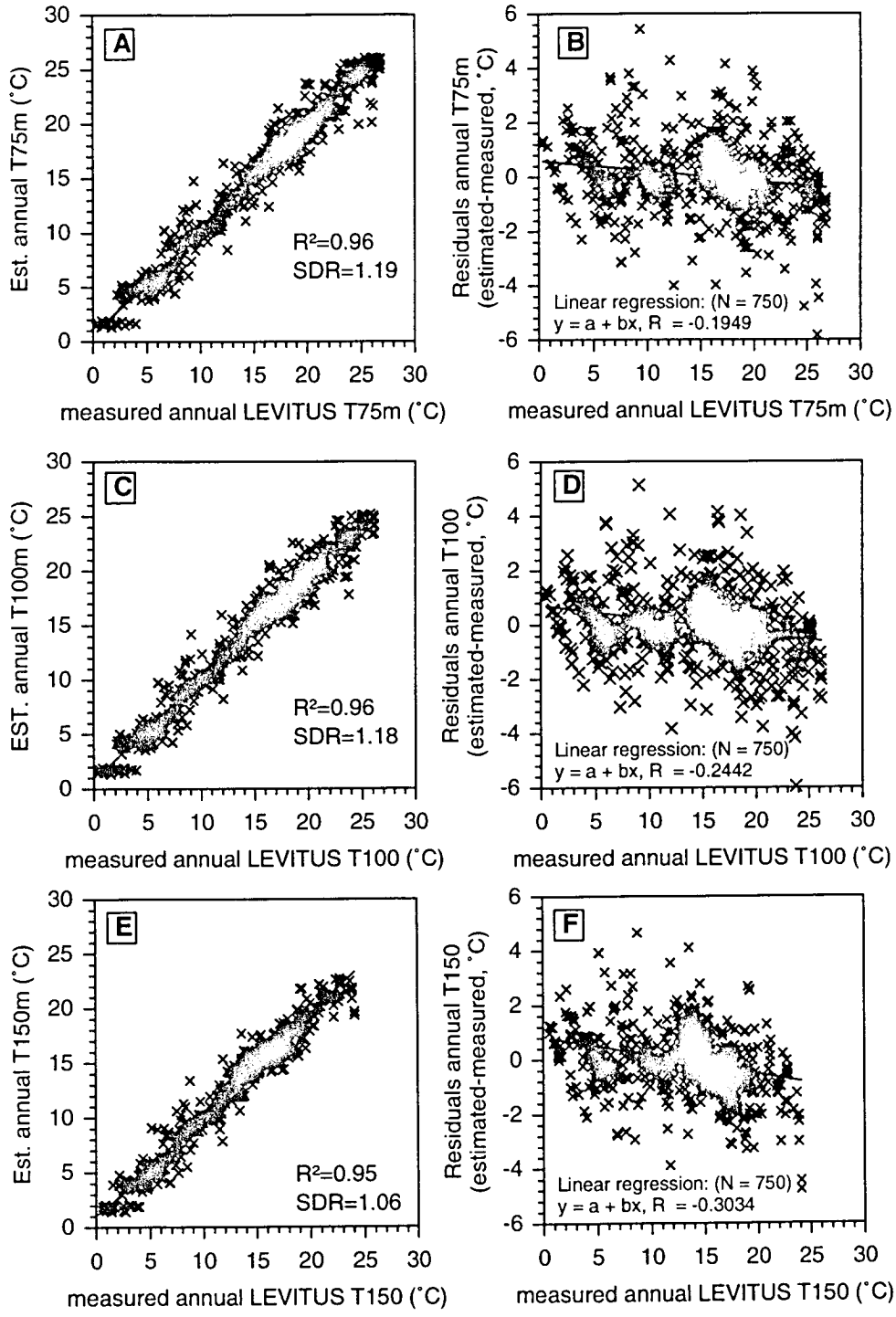

Figure 5. Statistic for deep-water MAT-SST estimations. A+B) Correlation between estimated annual SST 75 m vs. measured annual SST 75 m; residual statistic, resp.; C+D) Correlation between estimated annual SST 100 m vs. measured annual SST 100 m; residual statistic, resp.; E+F) Correlation between estimated annual SST 150 m vs. measured annual SST 150 m; residual statistic, respectively.

2.3 Estimation of bulk carbonate and metastable carbonate phases

Carbonate dissolution has the potential to alter down-core species abundances distribution through selective dissolution of thin-walled tests that are mainly secreted by warm-water species. As such, dissolution may skew the SST estimates towards colder temperatures (Le and Shackleton, 1992; Le and Thunell, 1996). To gain control on dissolution-driven SST artifacts, the down-core carbonate preservation of M35003-4 was determined by measurements of total and organic carbon, as well as the composition of the carbonate phases.

For core M35003-4, organic and inorganic carbonate analyses have been performed on 3 cm spaced samples (C. Rühlemann, University of Bremen, unpubl. data.).

Organic and total carbon were determined on 5 cm^3 dried sediment samples using a LECO C-200 analyzer. Carbonate was estimated by subtracting organic carbon from total carbon content ($CaCO_3$= [$Unit_{TOTCARBON}$ - $Unit_{orgCARBON}$] *8.33).

The precision for total carbon of the analyses was < 3 weight %. Aragonite, low and high magnesium calcite (LMC and HMC, respectively) were determined by X-ray diffraction. Samples were carefully ground with an achate mortar and pestle. The sample powder was mounted on an aluminium holder that was transferred to a multi-holder cassette. X-ray analyses were done with a PHILLIPS X-Ray DIFFRACTOMETER (PW1170 sample exchange, PW 1830 generator, and PW 1710 control unit). Data output was processed with MacDiff v3.2 (Petschick, 1996), quantitative estimation of the carbonate phases was done by quantification of peak area (Tucker, 1996), and comparison to reference samples (synthetic calcite for 100 % LMC and a Red Sea coral for 100 % aragonite; N. Andresen, unpubl.; Reijmer et al., 1988; Milliman, 1974). Concentration of carbonate phases is given in % $CaCO_3$.

3 Results

3.1 Stratigraphy and age models

3.1.1 Core M35003-4

The age model for core M35003-4 is based on the benthic $\delta^{18}O$ record (Figure 6) in conjunction with 19 ^{14}C-AMS dates (Table 3), and on comparison with the GISP2 ice core.

The benthic $\delta^{18}O$ record (Figure 6) shows the last glacial-interglacial transition between 200 and 300 cm core depth, and the isotope stage 3/2 boundary as displayed in a $\delta^{18}O$ increase at 450 cm core depth.

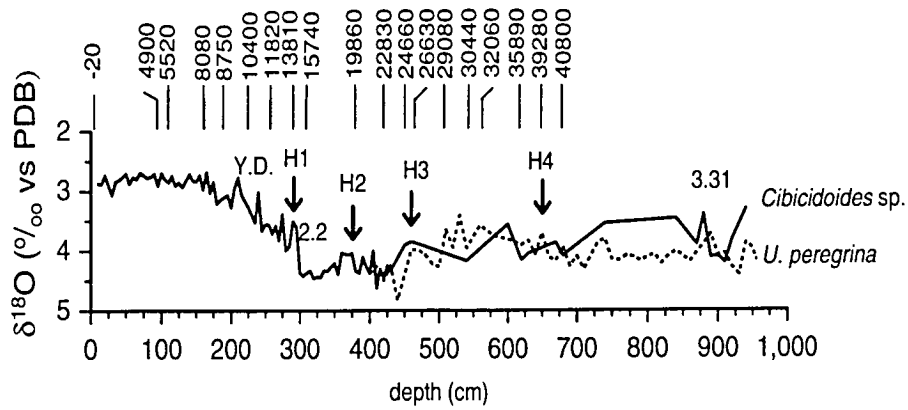

Figure 6. Benthic $\delta^{18}O$ record of M35003-4. Vertical lines and numbers give the position and reservoir corrected ^{14}C-ages in years B.P. Additional age control points are the anomalies in the benthic Cd/Ca ratio (A. Stüber, 1999), which correspond to Heinrich events 1 - 4. *C.wuellerstorfi* $\delta^{18}O$ have been adjusted by +0.64‰.

The $\delta^{18}O$-change during Termination I is 1.5 ‰, and exceeds the concomitant mean-ocean $\delta^{18}O_w$ -change by 0.25 ‰. This amplitude is distinctly smaller than that observed at mid-depth core sites in the North Atlantic, and implies that ambient bottom water temperatures changed only little ($\Delta T \sim 1°C$) during Termination I, if water mass effects on seawater $\delta^{18}O$ are assumed to be minor. At the end of the LGM, at 290 cm core depth, an abrupt decrease in $\delta^{18}O$ by 0.9 ‰ is observed which, according to the ^{14}C- dates (13.8 ^{14}C -kyrs, equiv. 15.7 cal. kyrs), is coeval with North Atlantic 'Heinrich' event 1 (H1). The Younger Dryas (Y.D.) climatic rebound is documented in the isotope record with an only small increase in benthic $\delta^{18}O$ between 210-240 cm, but is confirmed by ^{14}C- datings of 10.4 ^{14}C-kyrs at 225 cm (equiv. 12.2 cal. kyrs) which fit well into similar datings at northern North Atlantic sedi-

ment cores (e.g. Sarnthein et al., 1995). The $\delta^{18}O$ minima at 900 and 945 cm core depth correspond to the marine isotope substages 3.31 and, most likely, 3.33 with ages of 50 and 55 kyrs, resp. (Martinson et al., 1987).

Conventional ^{14}C-ages were corrected for the reservoir effect of 400 years (Hughen et al., 1998). For a first age scale the ^{14}C-ages <20 kyrs were converted to calendar years, considering the changing and variable $\Delta\ ^{14}C$-content of the atmosphere in the past, by using the CALIB conversion routine of Stuiver and Reimer (1993) and Stuiver et al. (1998). For ^{14}C-ages older than 20 kyrs, corrections according to Laj et al. (1996) were applied (Table 3). Additional age control points are directly compared to the GISP 2 $\delta^{18}O$ record as follows:

Table 3. ^{14}C-AMS dates and calendar years for core M35003-4.

Sample ID	Sample	depth (cm)	Species	Conventional Age BP (years)	Error ±	^{14}C-age (-400 years)	Calendar age (years)
KIA 4693[x]	M35003-4	3.0	Mixed planktic foraminifera	380	30	-20	0
KIA 5085[x]	M35003-4	98.0	*G ruber* (pink)	5300	50	4900	5650
KIA 4223	M35003-4	110.0	*G ruber* (white)	5920	40	5520	6300
KIA 5084[x]	M35003-4	163.0	Mixed planktic foraminifera	8480	60	8080	8950
KIA 4224	M35003-4	190.0	*G ruber* (white)	9150	50	8750	9920
KIA 4225	M35003-4	225.0	*G ruber* (white)	10800	90	10400	12220
KIA 4226	M35003-4	257.5	*G ruber* (white)	12220	70	11820	13940
KIA 4227	M35003-4	290.0	*G ruber* (white)	14210	90	13810	15670
KIA 4228	M35003-4	310.0	*G ruber* (white)	16140	100	15740	17410
KIA 6973	M35003-4	380.0	*G ruber* (white)	20260	110	19860	23900
KIA 4229	M35003-4	420.0	*G ruber* (white)	23230	210	22830	26620
KIA 4230	M35003-4	450.0	*G ruber* (white)	25060	260	24660	28660
KIA 4115[x]	M35003-4	463.0	Mixed planktic foraminifera	27030	220	26630	29550
KIA 4116[x]	M35003-4	508.0	Mixed planktic foraminifera	29480	260	29080	32780
KIA 4231	M35003-4	542.5	*G ruber* (white)	30840	520	30440	34824
KIA 4117[x]	M35003-4	563.0	Mixed planktic foraminifera	32460	350	32060	35710
KIA 4118[x]	M35003-4	618.0	Mixed planktic foraminifera	36290	560	35890	38443
KIA 6974	M35003-4	650.0	*G ruber* (white)	39680	1090	39280	39230
KIA 4232	M35003-4	680.0	*G ruber* (white)	41200	2030	40800	41300

[x] ^{14}C ages from Rühlemann et al., subm

The benthic foraminiferal Cd/Ca record from the same core displays short-lived maxima at 300, 380, 460, and 650 cm core depth (Stüber, 1999). Similar maxima have been found in mid-depth sediment cores from the northern and mid-latitude North Atlantic during 'Heinrich' meltwater events and have been used to infer ventilation minima during these events (Willamowski, 1999). The Cd maxima in core M35003-4 reflect the ventilation minima during H1 through H4 with radiocarbon ages of 14.78 kyrs (H1 is located between ^{14}C age datums of 290 cm and 310 cm), 19.86 kyrs, 26.18 kyrs (H3

is located 3 cm below a ^{14}C age datum), and 39.28 kyrs. Radiocarbon datings and ^{14}C-ages of the 'Heinrich' events were converted into calendar years by direct comparison with corresponding ages of the stadials in GISP 2 record.

Final tuning of the age scale was done by graphical correlation of the curve structures of total organic carbon (TOC) and carbonate records of core M35003-4 relative to the GISP2 ice core $\delta^{18}O$ record (Figure 7). During stage 3, these proxy-records display rapid fluctuations that resemble concomitant Dansgaard-Oeschger (D-O) variability in the Greenland ice core record. The triplet of TOC maxima between 498 cm - 548 cm core depth and the slightly broader maximum immediately below closely mirror the sequence of interstadials 8 through 5 (37-32 cal. kyrs) in the ice core record. These structures are also seen in the carbonate record, which inversely follows the TOC curve. Likewise, the two broad TOC maxima which run along with two broad carbonate minima at 670 cm- 730 cm and 760 cm - 830 cm core depth mirror interstadials 12 through 9, and 14 to 13. Interstadials 15, 13, 11, 10, and 9 are not well resolved in the proxy records, but I take the sharp changes in the proxy signals at 845 cm, 750 cm, and 620 cm core depth as a clear indication for the abrupt transitions into interstadials 14, 12, and 8.

TOC and carbonate during Termination I also closely track variations in the GISP2 $\delta^{18}O$ record (Figure 7). The early Termination I warming into the Bølling/Allerød is followed in the proxy records by intermittent TOC increases and decreased carbonate contents. Immediately before the onset of the shifts in the proxy records, a short-lived maximum in carbonate contents coincides with a peak in benthic Cd/Ca, which is taken as the correlative with the North Atlantic's 'Heinrich' event H1. The Younger Dryas cold event in the ice core record is displayed in the proxy records as a transient TOC and a salient carbonate maximum. The close fit of the proxy signals in core M35003-4 to the GISP2 $\delta^{18}O$ record during stage 3 and Termination I indicates that a link existed between climate variability in the northern North Atlantic region and climate and ocean variability in the western subtropical Atlantic. I take this as justification for using the structural coherence of the climatic and paleoceanographic signals with the Greenland ice core to derive a fine-tuned age model for core M35003-4. According to the age model, the core reaches 55 cal. kyrs at 940 cm (i.e., oxygen isotope event 3.33 of Martinson et al., 1987). Sedimentation rates vary between 10 and 48 cm/1000 years, yielding a temporal resolution at 5 cm sampling intervals of 300 - 500 years.

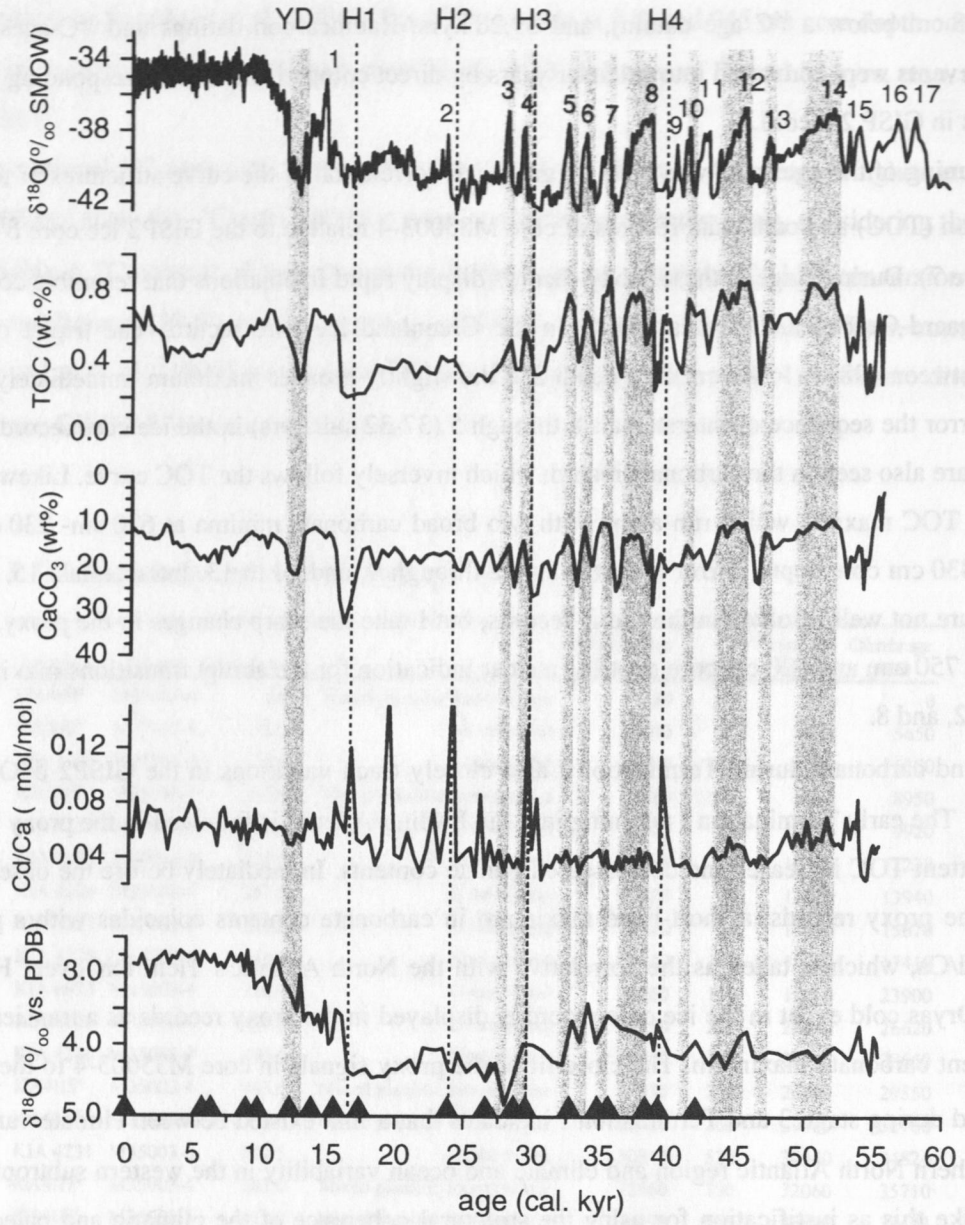

Figure 7. Age model for core M35003-4 and 'calibration' to the GISP 2 ice core. A) $\delta^{18}O$ record of benthic foraminifera (0-400m: *Cibicidoides* sp., converted to *U. peregrina* [+0.64‰], below 400 cm *U. peregrina*, B) Cd/Ca ratio in benthic foraminifera (Stüber, 1999), C + D) carbonate and total organic carbon content (C. Rühlemann, unpubl. data), E) $\delta^{18}O$ ice of GISP 2 (Grootes et al., 1997).

The resulting age control points are summarized in Table 4. By applying this age model to core M35003-4, the age-shifts for converting ^{14}C-ages to calendar years lie within published ranges (e.g. Voelker et al., 1998) (Figure 8).

Table 4: Age control points of M35003-4

Depth (cm)	Event	Age (cal.kyr)
0.0	^{14}C age datum	0.0
98.0	^{14}C age datum	5.7
110.0	^{14}C age datum	6.3
163.0	^{14}C age datum	9.0
190.0	^{14}C age datum	9.9
225.0	^{14}C age datum	12.2
257.5	^{14}C age datum	13.9
290.0	^{14}C age datum	15.7
310.0	^{14}C age datum	17.4
380.0	^{14}C age datum and H-event 2	23.9
420.0	^{14}C age datum	26.6
450.0	TOC maxima, corresponding to end of IS 4	28.7
463.0	^{14}C age datum, immediately before H3	29.6
508.0	^{14}C age datum, TOC minima,stadial between IS 6 and IS	32.8
548.0	^{14}C age datum, TOC maxima, corresponding to IS 7	35.2
563.0	^{14}C age datum, stadial between IS 7 and IS 8	35.7
613.0	TOC maxima, corresponding to begin of IS 8	38.3
650.0	^{14}C age datum and H 4	39.2
693.0	TOC maxima, corresponding to end of IS 12	43.3
728.0	TOC maxima, corresponding to the begin of IS 12	45.3
763.0	TOC maxima, corresponding to IS 13	46.9
828.0	TOC maxima, corresponding to IS 14	51.6
863.0	TOC maxima, corresponding to IS 15	53.5
928.0	TOC maxima, corresponding to the end of IS 16	54.8

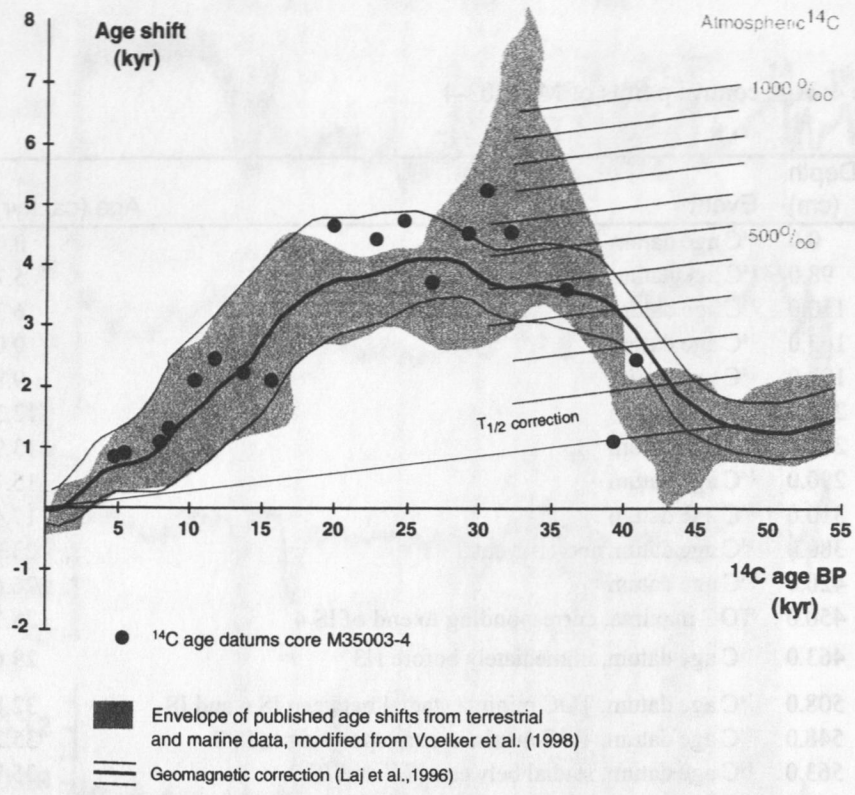

Figure 8. Age shift of ^{14}C-ages to calendar ages, modified from Voelker et al. (1996).

3.1.2 Core M35027-1

According to the benthic oxygen isotope record, core M35027-1 from near the Anegada passage covers the last 3 glacial-interglacial cycles and reaches back into MIS 10 (Figure 9). Ages are assigned by comparison with the SPECMAP stack (Imbrie et al., 1984, 1990) and with the standard curve of Martinson et al. (1987). To compare the data with other paleoceanographic records, age control points <30 kyrs are converted to calendar years using ^{14}C-shifts of Laj et al. (1996) and Voelker et al. (1998).

Sedimentation rates vary between a minimum of 1.2 cm/1000 years at the MIS 4/3 boundary, and 5.2 cm/1000 years during stage 5 and at the 3/2 boundary. The mean sample interval of 2.5 cm for the planktonic foraminiferal census counts between the last Interglacial to Holocene, and 5 cm between MIS 6 to MIS 5, results in a mean time resolution of 790 years and 2 kyrs, resp.

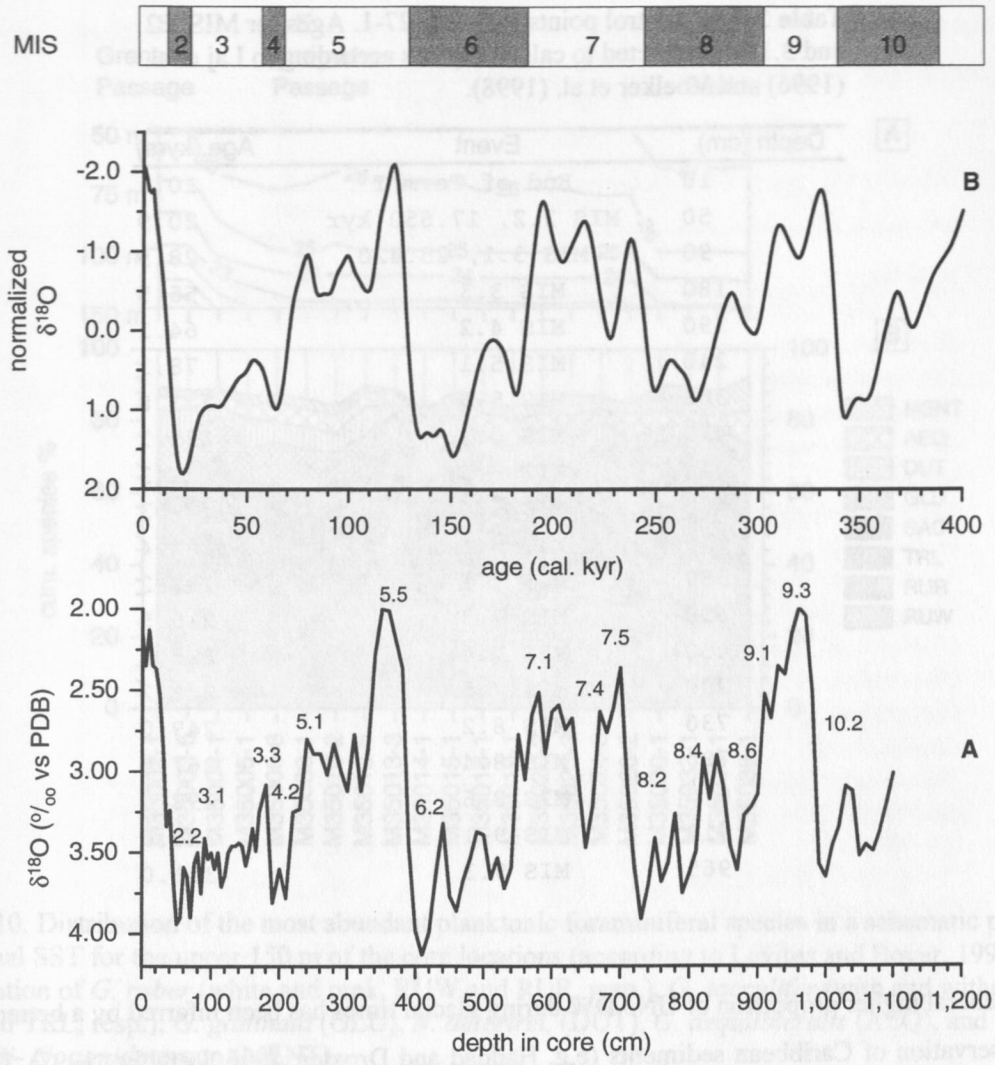

Figure 9. Benthic $\delta^{18}O$ record of M35027-1 (A) compared with the SPECMAP stack (B, Imbrie et al., 1984, 1990).

Benthic $\delta^{18}O$ changes during Terminations I and II are 1.8 ‰ and 2.1 ‰; during Terminations III and IV changes are 1.5 ‰ and 1.6 ‰. These amplitudes exceed the concomitant mean-ocean $\delta^{18}O_w$ –change of Termination I (1.2 ‰, Labeyrie et al., 1987; Fairbanks, 1989) by 0.6 ‰ to 1.0 ‰, and reflect changes in temperature and/or salinity of intermediate depth water masses entering the Caribbean.

Table 5. Age control points for M35027-1. Ages for MIS 2.2 and 3.1 are corrected to calendar years according to Laj et al. (1996) and Voelker et al. (1998).

Depth (cm)	Event	Age (kyrs)
10	End of Term I	10.1
50	MIS 2.2, 17.850 kyr	20.9
90	MIS 3.1, 25.420	28.9
180	MIS 3.3	55.5
190	MIS 4.2	64.1
240	MIS 5.1	78.3
360	MIS 5.5	123.8
410	MIS 6.2	135.1
440	MIS 6.3	141.3
460	MIS 6.4	149.3
530	MIS 6.6	183.4
550	MIS 7.1	193.2
610	MIS 7.3	215.5
650	MIS 7.4	225.2
700	MIS 7.5	241.2
730	MIS 8.2	249.0
790	MIS 8.4	267.5
870	MIS 8.6	298.0
910	MIS 9.1	310.0
965	MIS 9.3	331.0

A general higher proportion of UNADW during glacial times has been inferred by a better carbonate preservation of Caribbean sediments (e.g. Haddad and Droxler, 1996, Lembke, 1997). UNADW may indeed be the source of glacial cooling, as this water mass conceivably forms to the north of the glacial North Atlantic polar front where SST was low (Duplessy et al., 1988; Duplessy et al., 1992; Sarnthein et al., 1994).

3.2 Distribution of modern planktonic foraminiferal assemblages

3.2.1 Planktonic foraminifera in the Caribbean Sea

Planktonic foraminifera have been counted in 21 sediment surface samples from the Caribbean Sea as a supplement to the modern Atlantic reference data set between 65°N and 40°S.

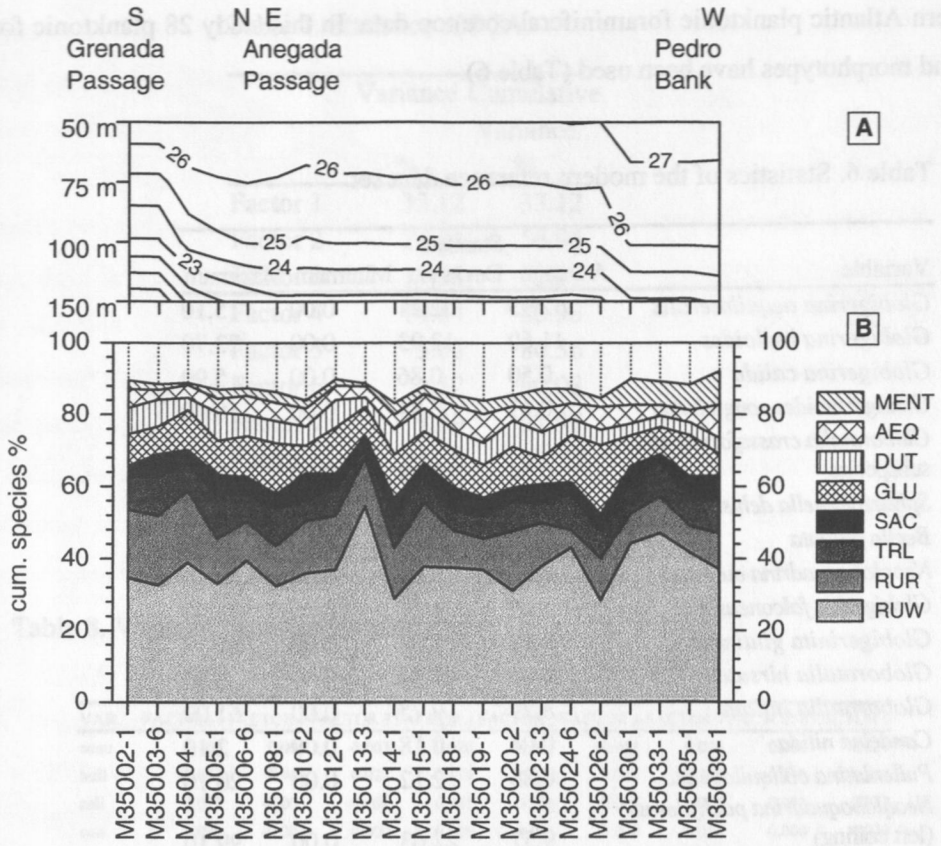

Figure 10. Distribution of the most abundant planktonic foraminiferal species in a schematic profile. A) annual SST for the upper 150 m of the core locations (according to Levitus and Boyer, 1994), B) Distribution of *G. ruber* (white and pink, RUW and RUR, resp.), *G. sacculifer* (with and without sac, SAC and TRL, resp.), *G. glutinata* (GLU), *N. dutertrei,* (DUT), *G. aequilateralis* (AEQ), and *G. menardii- G. tumida* group (MENT).

The distribution of planktonic foraminifera within the Caribbean shows only small faunal variability (Figure 10). As expected, tropical-subtropical species, e.g. *Globigerinoides ruber* (white + pink), *G. sacculifer* (with and without sac-like end-chamber), and *Globorotalia menardii - G. tumida* group, dominate the planktonic foraminiferal assemblage. Within the most abundant species there is no significant trend according to the variations in deep-water SST and the thermal structure of the upper water column.

In 2 surface samples, M35004-1 and M35013-3, the abundance of the species group *Globorotalia menardii - G. tumida* is below 1 %, indicating an age older than Holocene. Therefore, these samples are not included in the modern reference data base.

3.2.2 Factor analysis

Using the CABFAC routine (Klovan and Imbrie, 1971), a Q-mode factor analysis was done on

750 modern Atlantic planktonic foraminiferal core top data. In this study 28 planktonic foraminiferal species and morphotypes have been used (Table 6).

Table 6. Statistics of the modern reference data set.

Variable	Average	Standard Deviation	Minimum	Maximum
Globigerina aequilateralis	2.13	2.21	0.00	15.10
Globigerina bulloides	11.69	12.93	0.00	73.70
Globigerina calida	0.50	0.86	0.00	5.90
Globigerinoides conglobatus	0.41	0.84	0.00	10.00
Globorotalia crassaformis and subspecies	0.54	0.99	0.00	7.60
Sphaeroidinella dehiscens	0.13	0.42	0.00	5.00
Beella digitata	0.25	0.42	0.00	2.40
Neogloboquadrina dutertrei	4.21	7.09	0.00	49.10
Globigerina falconensis	1.85	4.17	0.00	35.90
Globigerinita glutinata	6.10	5.08	0.00	35.70
Globorotalia hirsuta	0.86	1.54	0.00	8.60
Globorotalia inflata	8.29	9.75	0.00	61.00
Candeina nitida	0.04	0.18	0.00	2.10
Pulleniatina obliquiloculata	0.85	2.12	0.00	20.10
Neoqloboquadrina pachyderma (left coiling)	9.57	22.63	0.00	99.10
Turborotalita quinqueloba	2.61	6.20	0.00	44.60
Globigerinoides ruber (r)	2.13	3.97	0.00	21.80
Globigerinoides ruber (w)	15.93	16.67	0.00	78.20
Globigerina rubescens (red + white)	0.69	1.35	0.00	8.30
Globigerinoides sacculifer trilobus	5.06	6.65	0.00	40.00
Globigerinoides sacculifer sacculifer	2.14	3.26	0.00	23.50
Globorotalia scitula	1.02	1.48	0.00	9.30
Globigerinoides tenellus	0.56	1.20	0.00	11.40
Globorotalia truncatulinoides (left + right coiling variety)	2.58	3.42	0.00	19.80
Orbulina universa	1.19	1.87	0.00	19.60
Globorotalia menardii - G. tumida complex	3.44	6.58	0.00	58.60
Neogloboquadrina pachyderma - N. dutertrei intergrades	1.68	4.56	0.00	40.10
Neogloboquadrina pachyderma (right coiling)	4.16	9.25	0.00	81.10

Table 7. Statistics of PCA.

	Variance %	Cumulative Variance %
Factor 1	33.12	33.12
Factor 2	23.84	56.96
Factor 3	13.13	70.09
Factor 4	10.84	80.93
Factor 5	5.63	86.56
Factor 6	3.52	90.08
Factor 7	1.89	91.97
Factor 8	1.76	93.73
Factor 9	1.52	95.25

Table 8. Varimax factor score matrix[x].

VAR.	FACTOR 1	FACTOR 2	FACTOR 3	FACTOR 4	FACTOR 5	FACTOR 6	FACTOR 7	FACTOR 8	FACTOR 9
acqu	0.105	0.004	-0.003	0.020	0.033	-0.001	0.036	0.008	-0.027
bull	-0.042	**0.949**	0.024	-0.119	0.020	0.043	-0.247	-0.018	-0.017
cali	0.022	-0.003	-0.001	0.021	-0.004	0.007	0.027	0.003	0.022
con	0.021	-0.003	0.000	0.005	0.001	0.000	-0.016	0.000	0.023
cras	0.011	-0.005	0.000	0.018	0.070	-0.009	0.006	0.014	0.008
dchi	0.001	-0.002	0.000	0.002	0.028	-0.004	0.000	-0.006	0.018
digi	0.006	0.001	-0.001	0.010	0.012	-0.002	0.003	0.000	0.002
dut	0.031	0.018	-0.009	-0.001	**0.547**	0.024	0.036	**0.762**	0.048
falc	0.025	-0.001	-0.010	0.166	0.035	-0.005	0.015	-0.192	**0.629**
gluti	0.172	0.245	0.009	-0.002	-0.051	0.005	**0.897**	-0.011	0.007
hirs	0.011	0.016	-0.006	0.063	-0.011	-0.003	-0.040	-0.012	0.153
inf	-0.032	0.133	-0.004	**0.922**	0.009	-0.165	-0.016	0.056	-0.162
niti	0.003	0.000	0.000	-0.001	-0.002	0.000	0.004	0.004	-0.006
obl	0.020	-0.003	0.002	-0.016	0.179	-0.004	0.010	-0.115	0.064
pacli	0.007	-0.043	**0.979**	0.022	-0.010	-0.042	-0.049	0.027	-0.018
quin	-0.015	0.103	0.199	-0.082	0.043	0.062	0.216	-0.094	0.157
rur	0.141	-0.014	0.005	-0.005	-0.026	-0.010	0.104	0.126	-0.327
ruw	**0.920**	0.000	-0.003	0.017	-0.178	0.028	-0.170	0.116	0.122
rus	0.033	0.020	-0.001	0.011	-0.026	-0.026	0.026	-0.007	0.010
tril	0.252	0.014	-0.004	-0.020	0.346	0.015	-0.110	-0.399	**-0.413**
sac	0.114	-0.012	0.003	-0.007	0.162	0.004	0.015	-0.175	-0.137
scit	0.011	0.052	-0.007	0.038	0.004	-0.031	0.039	-0.026	0.118
ten	0.030	-0.002	-0.002	0.012	-0.017	0.005	0.021	0.016	0.055
trus	0.051	0.037	-0.014	0.177	-0.011	-0.033	-0.093	-0.046	0.357
univ	0.028	0.024	0.002	0.063	0.011	-0.058	0.021	0.076	-0.104
mentum	0.070	-0.035	0.009	0.012	**0.689**	-0.055	0.042	-0.297	0.168
pdi	-0.009	-0.035	0.014	0.204	-0.028	0.281	0.114	-0.193	-0.161
par	-0.023	-0.018	0.025	0.127	0.033	**0.936**	-0.037	0.045	0.032

[x] bold numbers indicate high factor scores for characteristic foraminiferal species

The factor analysis of the modern planktonic foraminiferal assemblage distribution in the Atlantic yielded 9 factors that explain >95 % of the total variance of the original data (factor model 750-28-9; Table 7, Figure 11). The Atlantic-wide distribution pattern of these 9 factors closely resembles that of earlier factor models (e.g. Imbrie and Kipp, 1971; Kipp, 1976; Molfino et al., 1982).

Factor 1 covers tropical to subtropical waters and is dominated by *G. ruber* (w) (**Tropical/Subtropical Assemblage**; Table 8). Factor 2 represents temperate to cold waters of high northern and southern latitudes, and low-latitude upwelling areas in the eastern Atlantic. *G. bulloides* has highest factor scores on this assemblage (**Subpolar to High Latitude Assemblage**; Table 8). Factors 6 (high loadings of right coiling *N. pachyderma*) and 7 (high factor loadings of *G. glutinata*) according to their geographic distribution may be viewed as subgroups of Factor 2 and were included there. The **Polar Assemblage** (Table 8) is contained in Factor 3, and is characterized by high factor loadings of left coiling *N. pachyderma*. Factor 4 consists mainly of *G. inflata,* and covers oceanic areas between subtropical and boreal waters (**Transitional Assemblage**; Table 8).

Factor 5 is located in restricted areas of the equatorial eastern Atlantic, off NW-Africa and the Gulf of Guinea. The *G. Menardii - tumida* complex and *N. dutertrei* have high factor scores on this factor (**Gyre Margin Assemblage** of Kipp (1976); Table 3). High factor loadings of Factor 8 are limited to the coastal upwelling area off Namibia. *N. dutertrei* has high scores on this factor (**South Atlantic Coastal Upwelling Assemblage**; Table 8). Factor 9 is restricted to the mid-latitude North and South Atlantic at the border of the tropical-subtropical assemblage, with *G. falconensis* as a characteristic species.

From their contribution to the overall variance, and from their geographic distribution, Factors 1 to 6 obviously are of greater (paleo-) oceanographic relevance than the Factors 7 to 9, which display only small and restricted geographic distributions and lower factor loadings. Still, these factors are kept in the computational scheme for SST estimation to enhance the significance of the estimates.

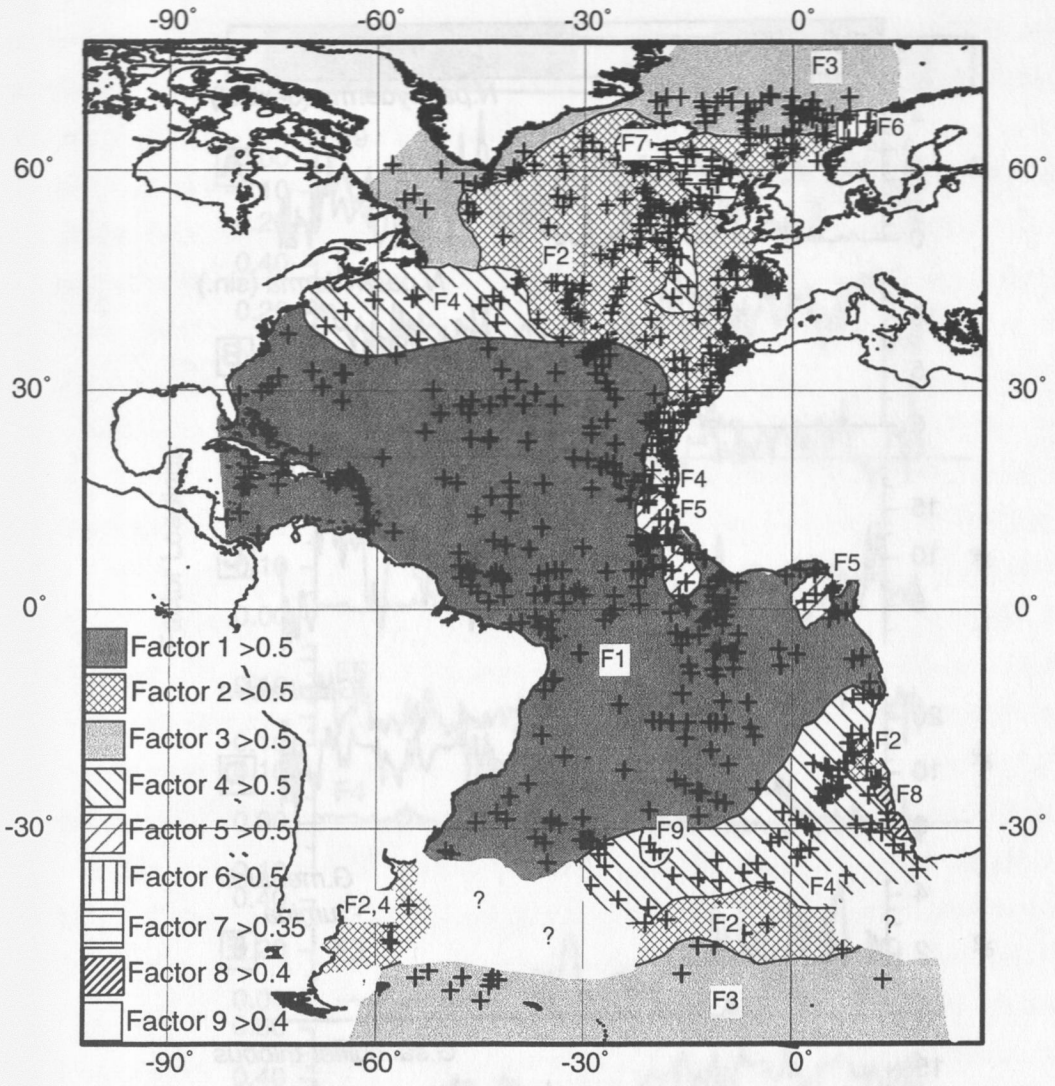

Figure 11. Geographic distribution of 9 varimax assemblages of a Q-Mode Factor Analysis of 750 core tops. Crosses give the location of 750 core tops, compiled from Pflaumann et al. (1996), Imbrie 1990 (SPECMAP Archive # 1), and Caribbean core tops (this thesis).

3.3 Late Pleistocene planktonic foraminiferal assemblages and SST estimates

3.3.1 Tobago Basin: Core M35003-4

Figure 12 shows the down-core distribution of characteristic planktonic foraminiferal species in M35003-4. During glacial times the abundance of warm water species such as *G. ruber* (white) and *G. sacculifer trilobus*, is decreased. Conversely, high-latitudinal 'cold' faunal components, particularly *G. bulloides*, show increased abundances.

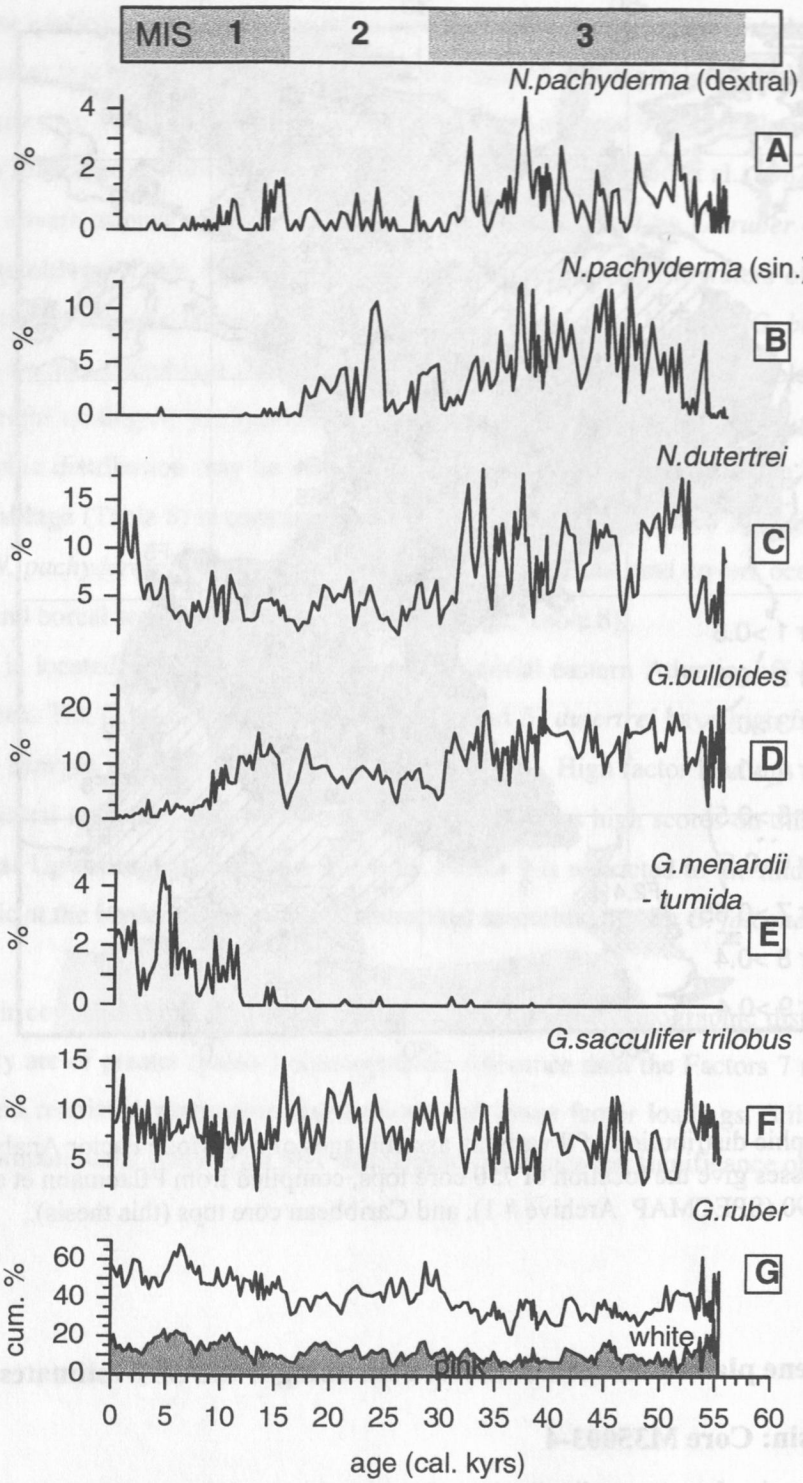

Figure 12. Distribution of characteristic planktonic foraminifera species in core M35003-4; A and B: % right and left *N. pachyderma*, resp., C: % *N. dutertrei*, D:% *G. bulloides*, E: % *G. menardii* and *G. tumida* group, F: % *G. sacculifer trilobus*, G: cumulative % of *G.ruber* pink and white.

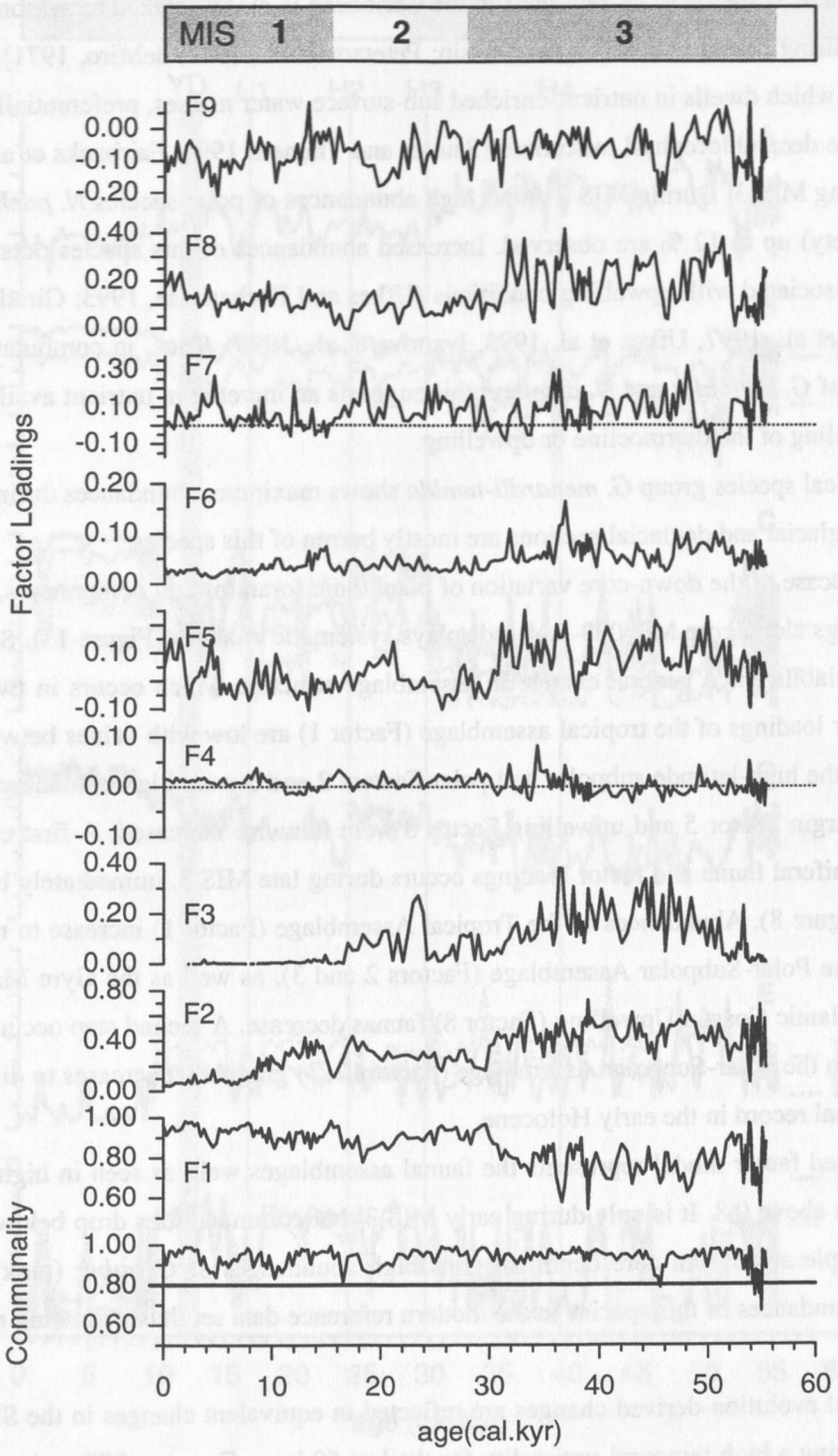

Figure 13. Communality and varimax (factor) assemblages F1 to F9 of Core M35003-4.

Today, the occurrence of *G. bulloides* in the Caribbean is closely linked to seasonal upwelling off Venezuela during boreal winter (Cariaco Basin; Peterson et al., 1991; deMiro, 1971). Abundances of *N. dutertrei*, which dwells in nutrient-enriched sub-surface water masses, preferentially in the thermocline near the deep chlorophyll maximum (Sautter and Thunell, 1991; Fairbanks et al., 1982), are increased during MIS 3. During MIS 2 and 3 high abundances of polar species *N. pachyderma* (left reticulate variety) up to 12 % are observed. Increased abundances of this species outside polar waters have been associated with upwelling conditions (Ufkes and Zachariasse, 1993; Giradeau and Rogers, 1994; Little et al., 1997, Ufkes et al. 1998, Ivanova et al., 1999). Thus, in combination with higher abundances of *G. bulloides* and *N. dutertrei* this suggests an increase in nutrient availability, possibly due to a shoaling of the thermocline or upwelling.

The tropical species group *G. menardii-tumida* shows maximum abundances during the Holocene, whereas the glacial and deglacial sections are mostly barren of this species.

As in the case of the down-core variation of planktonic foraminiferal components, the variation of factor loadings along core M35003-4 also displays systematic changes (Figure 13). Superimposed on the rapid variability is a general change in assemblage structure which occurs in two steps. During MIS 3, factor loadings of the tropical assemblage (Factor 1) are low with values between 0.7 and 0.8. Loadings of the high-latitude subpolar and polar Factors 2 and 3 were higher, loadings of the equatorial Gyre Margin Factor 5 and upwelling Factor 8 were likewise increased. A first change in planktonic foraminiferal fauna and factor loadings occurs during late MIS 3, immediately before 'Heinrich' event H3 (Figure 8). Abundances of the Tropical Assemblage (Factor 1) increase to nearly Holocene levels, and the Polar-Subpolar Assemblage (Factors 2 and 3), as well as the Gyre Margin (Factor 5) and South Atlantic Coastal Upwelling (Factor 8) faunas decrease. A second step occurs during Termination I, when the Polar-Subpolar Assemblage (Factors 2, 3) gradually decreases to disappear entirely from the faunal record in the early Holocene.

The derived factor model represents the faunal assemblages well, as seen in high communalities which remain above 0.8. It is only during early MIS 3 that communalities drop below 0.8. In this interval, a sample at 935 cm core depth contains high abundances of *G. ruber* (pink) which exceed maximum abundances of this species in the modern reference data set thus indicating non-analog conditions.

The faunal evolution-derived changes are reflected in equivalent changes in the SST record (Figure 14), showing a high temporal variability for the last 50 kyrs. Core top SST estimates are close to the modern temperature, within the statistical errors of the method. During glacial stages, similarity values are on average between 0.85 and 0.9, in contrast to Holocene values above 0.95 (Figure 14D).

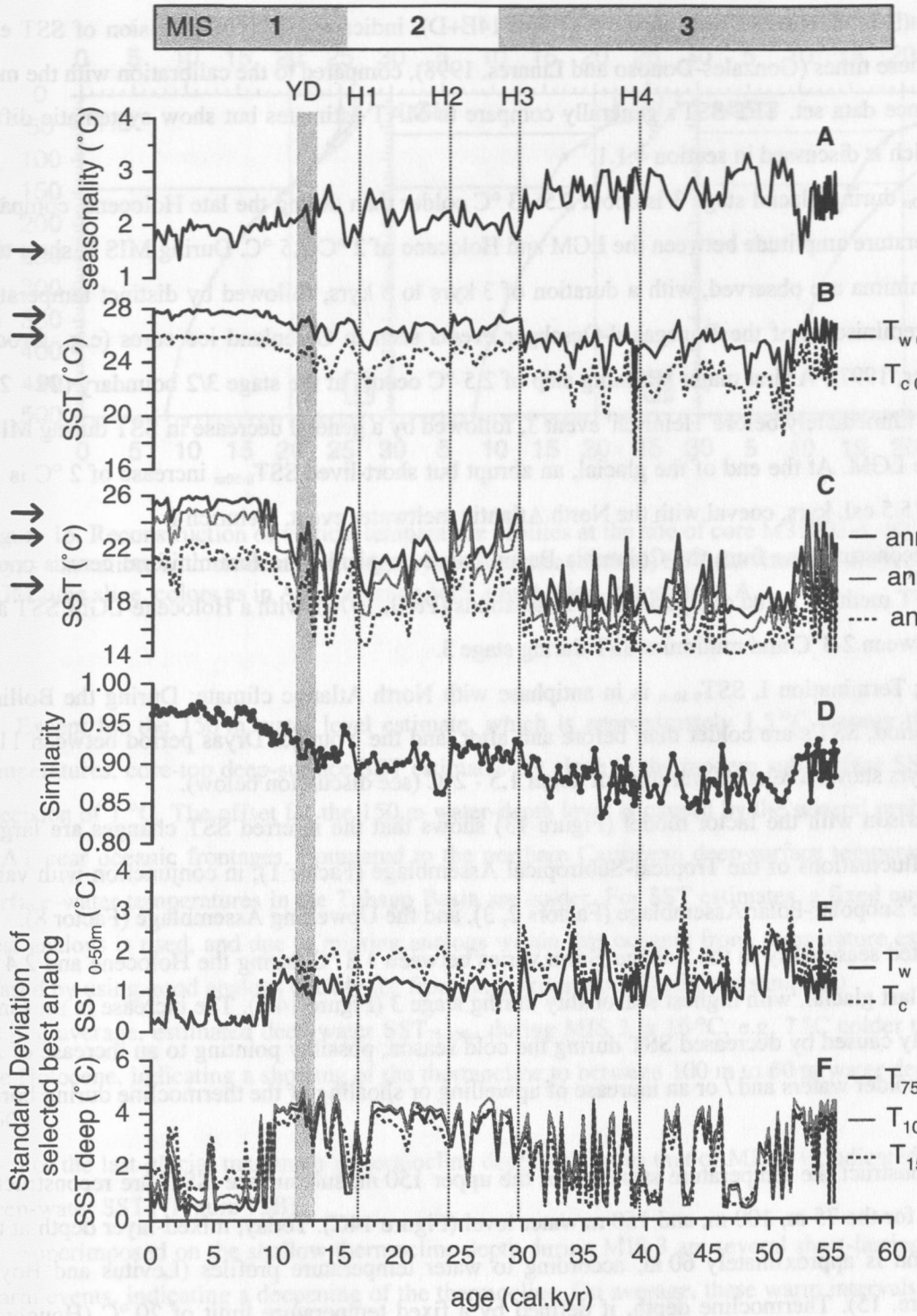

Figure 14. MAT SST estimates for core M35003-4. A) estimated seasonality, B) seasonal $SST_{0\text{-}50m}$ estimates, C) annual $SST_{75\text{-}150m}$ estimates, D) similarity measure, E) standard deviation of selected best analog $SST_{0\text{-}50m}$, F) standard deviation of selected best analog $SST_{75m\text{-}150m}$. Arrows indicate modern SST.

The lower similarity during the last glacial and Termination I is accompanied by increased stan-

dard deviations of selected best analogs (Figure 14E+D), indicating a lower precision of SST estimates at these times (Gonzales-Donoso and Linares, 1998), compared to the calibration with the modern reference data set. TFT-SST's generally compare to MAT estimates but show systematic differences, which is discussed in section 4.1.1.

$SST_{0\text{-}50m}$ during glacial stage 3 is about 2.5 - 3 °C colder than during the late Holocene, compared to a temperature amplitude between the LGM and Holocene of 2 °C-2.5 °C. During MIS 3, short term $SST_{0\text{-}50m}$ minima are observed, with a duration of 3 kyrs to 5 kyrs, followed by distinct temperature maxima, reminiscent of the Dansgaard-Oeschger events seen in Greenland ice cores (e.g., Grootes and Stuiver, 1997). A first major warming step of 2.5 °C occurs at the stage 3/2 boundary (29 - 27.5 cal. kyrs), immediately before 'Heinrich' event 3, followed by a general decrease in SST during MIS 2 toward the LGM. At the end of the glacial, an abrupt but short-lived $SST_{0\text{-}50m}$ increase of 2 °C is observed at 15.5 cal. kyrs, coeval with the North Atlantic meltwater event, Heinrich I.

SST reconstructions from the Columbia Basin, based on planktonic foraminiferal census counts and the TFT method, found comparable SST variations (Prell, 1976), with a Holocene-LGM SST amplitude between 2-3°C and minimum SST during stage 3.

During Termination I, $SST_{0\text{-}50\,m}$ is in antiphase with North Atlantic climate: During the Bølling-Allerød period, SST's are colder than before and after, and the Younger Dryas period between 11 to 12.6 cal. kyrs shows a relative warming of about 1.5 - 2°C (see discussion below).

Comparison with the factor model (Figure 13) shows that the inferred SST changes are largely driven by fluctuations of the Tropical-Subtropical Assemblage (Factor 1), in conjunction with variations of the Subpolar-Polar Assemblage (Factors 2, 3), and the Upwelling Assemblage (Factor 8).

Estimated seasonality in the Tobago Basin varies between 1.8 °C during the Holocene and 2.4 °C during the last glacial, with highest seasonality during stage 3 (Figure 14A). The increase in seasonality is mainly caused by decreased SST during the cold season, possibly pointing to an increase of advection of colder waters and / or an increase of upwelling or shoaling of the thermocline during boreal winter.

To reconstruct the temperature structure of the upper 150 m, sub-surface 'SST' are reconstructed with MAT for the 75 m, 100 m, and 150 m water level (Figure 14C). Today, mixed-layer depth at the core location is approximately 60 m, according to water temperature profiles (Levitus and Boyer, 1994, Figure. 15). Thermocline depth, if defined by a fixed temperature limit of 20 °C (Houghton, 1991), is at 150 m.

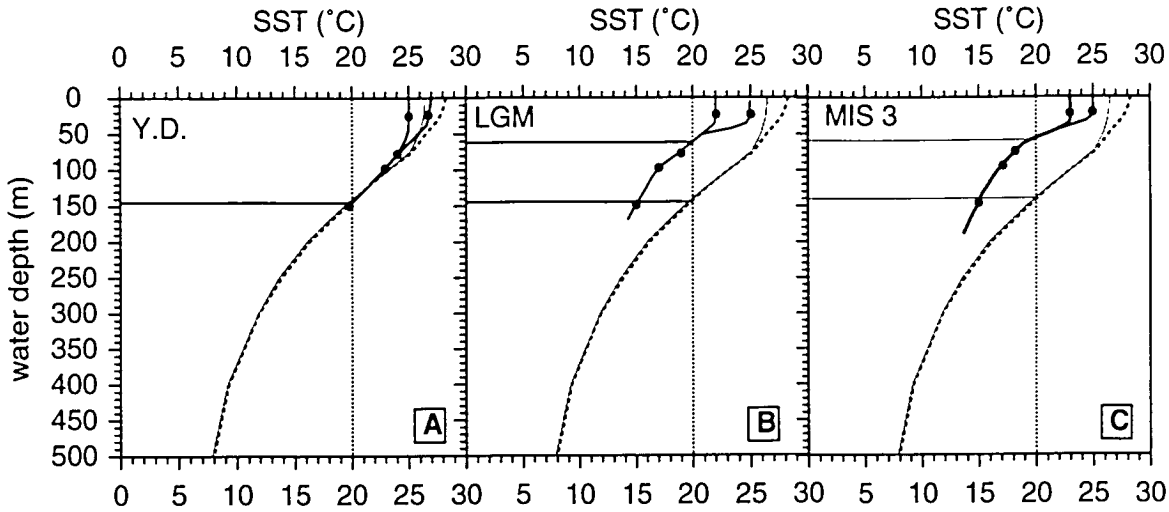

Figure 15. Reconstruction of vertical temperature profiles at the site of core M35003-4, A) Younger Dryas time slice, with modern winter (grey) and summer (dashed) SST (Levitus and Boyer, 1994). B) LGM time slice, colors as in A, C) average MIS 3 time slice, colors as in A.

Except for the 150 m water level estimate, which is approximately 1.5 °C warmer than in situ temperatures, core-top deep-surface SST estimates are close to the modern sub-surface SST within a precision of 1 °C. The offset for the 150 m water-depth level is caused by the general problem of the MAT near oceanic frontages. Compared to the northern Caribbean deep-surface temperatures, deep surface-water temperatures in the Tobago Basin are colder. For SST estimates, a fixed number of 10 best analogs is used, and due to missing analogs within this oceanic front, temperature estimates are biased by using good analogs outside the front (e.g., from inner Caribbean samples.)

On average, estimated deep-water $SST_{75\text{-}150m}$ during MIS 3 is 16 °C, e.g. 7 °C colder than during the Holocene, indicating a shoaling of the thermocline to between 100 m to 60 m water depth (Figure 15C).

For the last glacial maximum a thermocline depth similar to that of MIS 3 is indicated by similar deep-water SSTs (Figure 15B).

Superimposed on the shallow thermocline depth during MIS 3 are several short-lasting (1-2 kyrs) warm events, indicating a deepening of the thermocline. On average, these warm intervals are spaced 2-3 kyrs apart from each other.

Sub-surface temperatures show the same trend as surface temperatures, but with sub-surface SST amplitudes being enhanced over those of surface SST:

- a first warming, concomitant with a deepening of the thermocline to nearly Holocene levels immediately before H3, followed by a stepwise cooling (shoaling of the thermocline again) towards the LGM,

- at the end of the last glacial, a sharp transition from shallow to deeper thermocline depths below 150 m during H1, followed by a shoaling of the thermocline during the Bølling/Allerød,
- during the Younger Dryas, thermocline depth appears to have been the same or slightly shallower compared to the Holocene, indicated by the slightly lower annual SST_{150m} (Figure 15A).

In summary, estimated surface and sub-surface-water SST point to shallower thermocline and mixed-layer depths during the last glacial, which is possibly caused by stronger trade wind intensity during the cold season. Strengthening of trade winds during the last glacial has also been inferred from dust flux rates in the tropical Atlantic (Ruddiman, 1997) and by increased upwelling intensity in the equatorial Atlantic (McIntyre et al., 1989; McIntyre and Molfino, 1996).

3.3.2 Northern Venezuela Basin: Core M35027-1

Planktonic foraminiferal census counts were carried out along core M35027-1 from MIS 6 to the early Holocene. The fauna is dominated by tropical species (Figure 16). Similar to the southern core M35003-4 fluctuations in relative abundance of warm water species *G. ruber* and *G. sacculifer* are opposite to those of colder water species like *G. bulloides* and *N. dutertrei*.

During glacial stages 4-2, abundances of *G. bulloides* and *N. pachyderma* (left and right) are increased, at the expense of the tropical-subtropical species *G. ruber* and *G. sacculifer*.

Similar to M35003-4, *N. dutertrei* shows maximum abundances during MIS 3, during interglacial stage 5, and during glacial-interglacial Terminations II and I. During the last glacial, *N. dutertrei* and *G. bulloides* principally vary in antiphase as is expected from their cold vs. warm habitat preferences (Hilbrecht, 1996).

As has been previously described, the species group *G. menardii-G. tumida* shows a general glacial-interglacial change in abundance, with maxima during interglacial stages (e.g. Ericson and Wollin, 1956; Ericson et al., 1961; Imbrie and Kipp, 1971).

As with core M35003-4, statistical planktonic foraminiferal assemblages are estimated by applying factor model 750-28-9. Three assemblages dominate the planktonic foraminiferal fauna of core M35027-1 (Figure 17): Factor 1 (Tropical-Subtropical Assemblage), Factor 2 in combination with Factor 7 (Subpolar-Temperate Assemblage), and Factor 8 (South Atlantic Coastal Upwelling Assemblage).

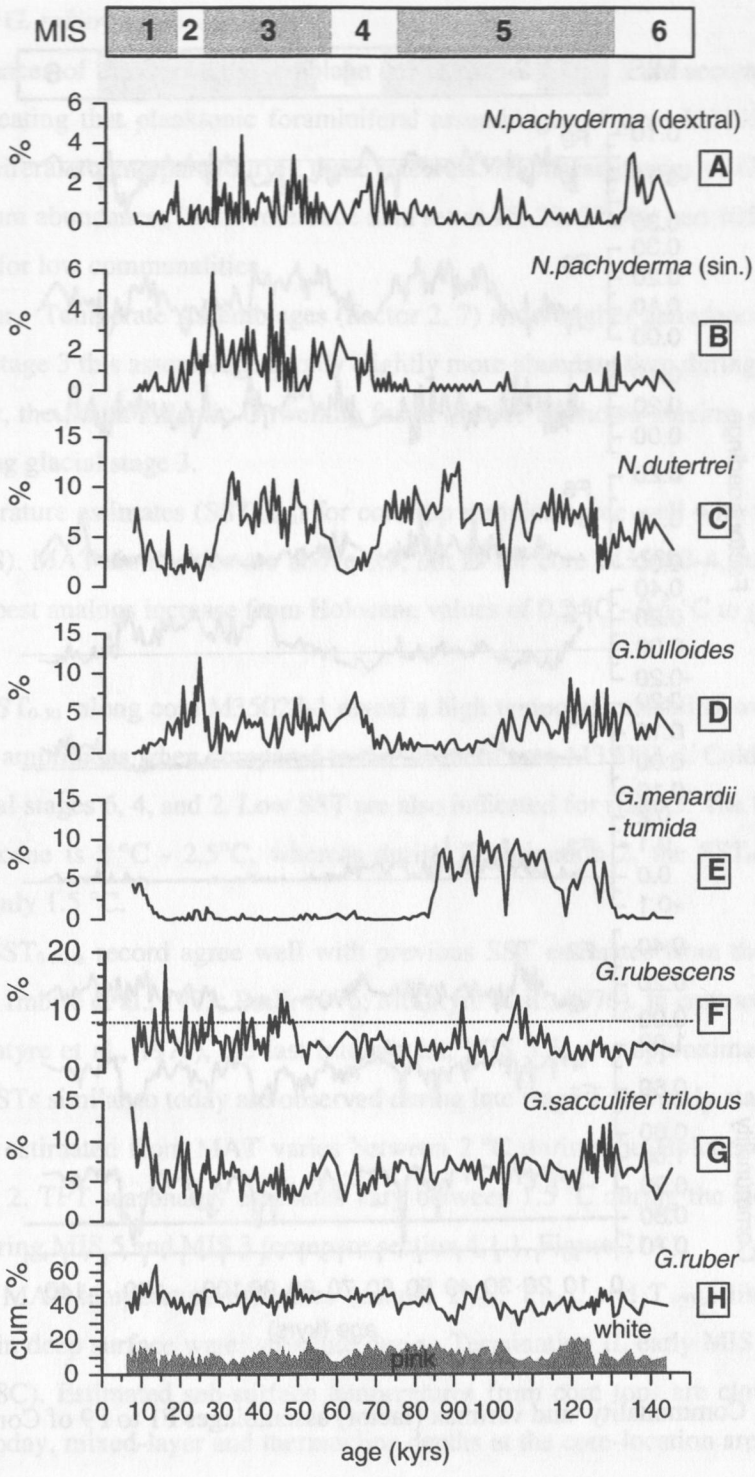

Figure 16. Distribution of characteristic planktonic foraminiferal species in core M35027-1: A and B): % right and left *N. pachyderma*, resp., C): % *N. dutertrei*, D):% *G. bulloides*, E): % *G. menardii* and *G. tumida* group, F) % G. rubescens, dotted line indicates maximum abundance in reference data set, G) % *G. sacculifer trilobus*, H): cummulative % of *G.ruber* pink and white.

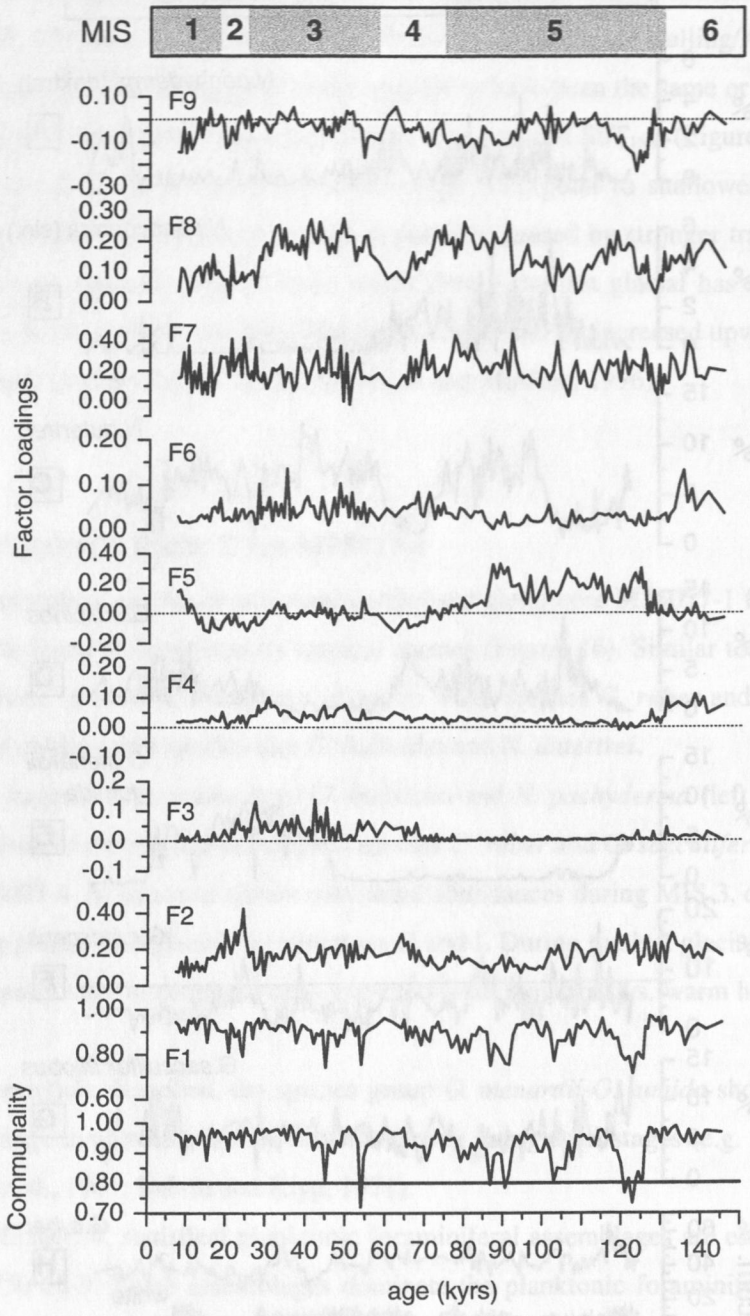

Figure 17. Communality and varimax (factor) assemblages F1 to F9 of Core M35027-1.

The amplitudes of faunal changes in the northern Venezuela Basin are of lesser magnitude than in the Tobago Basin (Figures 12 and 16), indicating only gradual changes of sea-surface conditions at the northern core during the last 150 kyrs. Although time resolution is lower than in the southern core M35003-4, similar high frequency oscillations (4 to 10 kyrs) in the relative abundances, particular for

N. dutertrei and *G. ruber*, are recognized.

Low abundances of the tropical assemblage during stages 5 and 3 are accompanied by low communalities, indicating that planktonic foraminiferal assemblages of core M35027-1 have only poor modern foraminiferal counterparts during these intervals. High abundances of *G. rubescens*, exceeding the maximum abundances in the reference data set at 15, 20, 27, 46, and 105 kyr (Figure 16), are not responsible for low communalities.

The Subpolar - Temperate Assemblages (Factor 2, 7) show higher abundances during MIS 4 and MIS 2. During stage 3 this assemblage is only slightly more abundant than during interglacials.

Interestingly, the South Atlantic Upwelling fauna (Factor 8) shows maxima during early and late MIS 5 and during glacial stage 3.

MAT temperature estimates ($SST_{0\text{-}50m}$) for core top samples agree well with the modern "in situ" SSTs (Figure 18). MAT similarities are above 0.9, but as for core M35003-4, standard deviations of the selected 10 best analogs increase from Holocene values of 0.2 °C - 0.5 °C to glacial values around 1.5 °C.

Estimated $SST_{0\text{-}50}$ along core M35027-1 reveal a high temporal variability over the last 150 kyrs, with lower SST amplitudes when compared to the southern core M35003-4. Coldest surface SSTs occur during glacial stages 6, 4, and 2. Low SST are also indicated for stage 5. The SST change between LGM and Holocene is 2 °C - 2.5°C, whereas during Termination 2, the $SST_{0\text{-}50m}$ change between MIS 5.5-6.2 is only 1.5 °C.

M35027-1 $SST_{0\text{-}50\,m}$ record agree well with previous SST estimates from the Caribbean (Imbrie and Kipp, 1991; Imbrie et al., 1973; Prell, 1976; McIntyre et al., 1976). In contrast to CLIMAP reconstructions (McIntyre et al., 1976), the last Interglacial, MIS 5.5, was approximately 1°C colder than the Holocene. SSTs similar to today are observed during late stage 5 and early stage 4.

Seasonality, estimated from MAT varies between 2 °C during the Holocene and 2.5 °C during MIS 4 and MIS 2. TFT seasonality estimates vary between 1.5 °C during the Holocene and a maximum of 3 °C during MIS 5 and MIS 3 (compare section 4.1.1, Figure 21A).

Sub-surface MAT temperature estimates (annual T_{75m}, T_{100m}, and T_{150m}) likewise reveal a high variability, e.g. in deep surface water structure during Termination II, early MIS 5, and MIS 3 to the LGM (Figure 18C). Estimated sub-surface temperatures from core tops are close to modern *in situ* temperatures. Today, mixed-layer and thermocline depths at the core-location are 80 m and 200 m, as indicated by uniform warm temperatures above 70 m and the continuous temperature decrease below (Figure 19A, B).

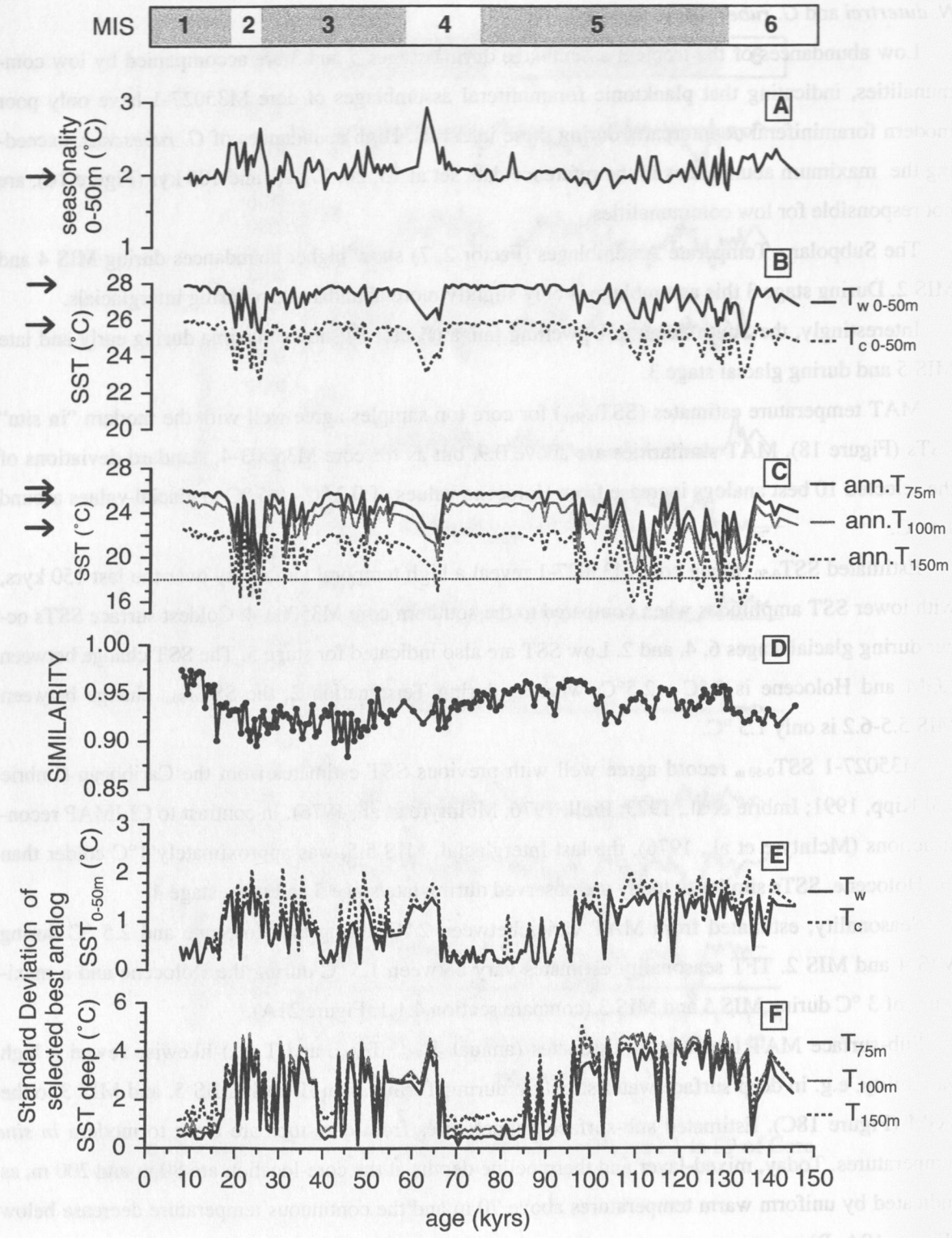

Figure 18. SST estimates from MAT for core M35027-1. A) Estimated seasonality, B) seasonal $SST_{0\text{-}50m}$ estimates, C) annual $SST_{75\text{-}150m}$ estimates, D) similarity measure, E) standard deviations of selected best analog $SST_{0\text{-}50m}$, F) standard deviation of selected best analog $SST_{75m\text{-}150m}$. Arrows indicate modern *in situ* temperatures.

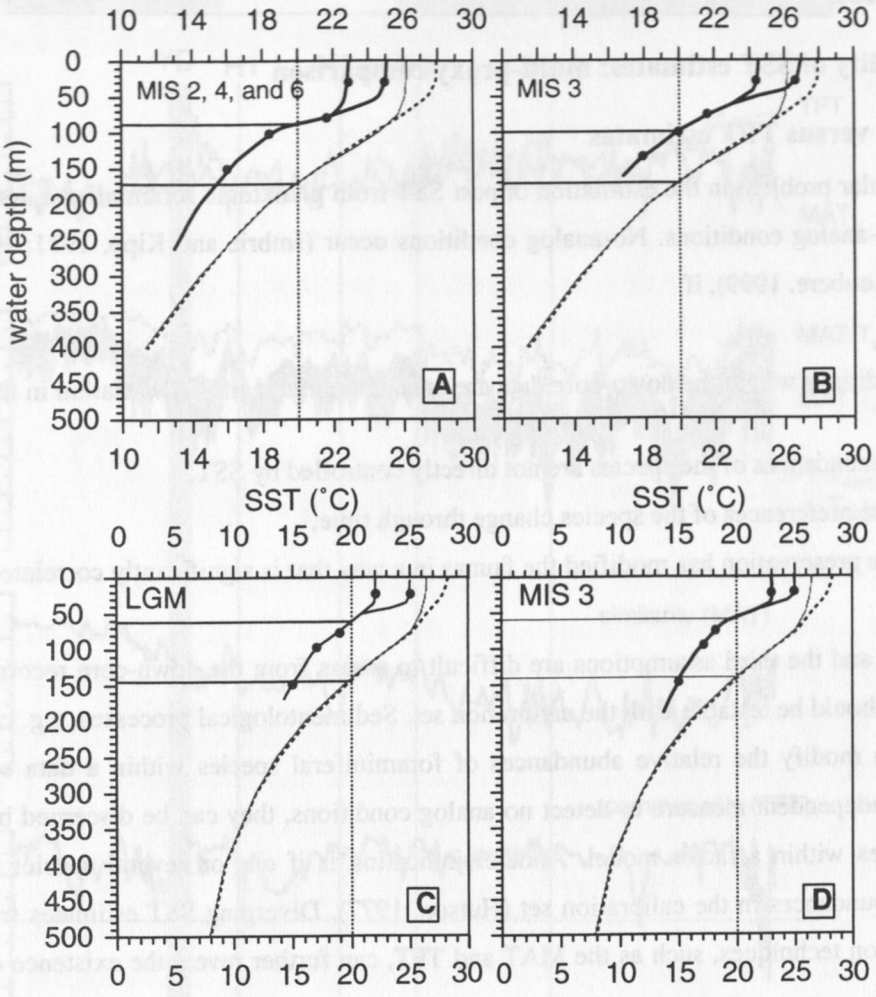

Figure 19. Reconstruction of temperature - water depth profiles, A) M35027-1: glacial cold stage 2 time slice, also representative of MIS 4 and 6 (grey and dashed: modern winter and summer SST; Levitus and Boyer, 1994), B) M35027-1: average MIS 3 time slice, C) M35003-4: LGM time sclice for core M35003-4, D) M35003-4: MIS 3 time slice.

During MIS 6, 5 (at 115 kyrs and 110 kyrs), 4 (65 kyrs) and early MIS 2 (at 25 kyrs), a shoaling of the thermocline approximately to 100-150 m is indicated by lower $SST_{75\text{-}150m}$ sub-surface temperature signals, if a fixed temperature limit such as the 20 °C isotherm for tropical waters is taken (Houghton, 1991). This shoaling is smaller than the inferred shoaling at the southern core location of M35003-4 (Figure 19). Today, the position of M35027-1 is located far away from possible upwelling areas, therefore, the inferred shoaling of the thermocline during the glacial cold stages may indicate a general trend for the tropical Caribbean Sea.

4 Discussion

4.1 Reliability of SST estimates: multi-proxy comparison

4.1.1 MAT versus TFT estimates

A particular problem in the estimation of past SST from planktonic foraminiferal assemblages are so called no-analog conditions. No-analog conditions occur (Imbrie and Kipp, 1971; Hutson, 1977; Mekik and Loubere, 1999), if

1. SST conditions within the down-core data are outside the range of SST variation in the calibration data set;
2. relative abundances of the species are not directly controlled by SST;
3. ecological preferences of the species change through time;
4. carbonate preservation has modified the faunas in a way that is significantly correlated with SST.

The first and the third assumptions are difficult to assess from the down-core record, the second assumption should be testable with the calibration set. Sedimentological processes, e.g. carbonate dissolution, can modify the relative abundances of foraminiferal species within a data set. Although there is no independent measure to detect no-analog conditions, they can be discerned by evaluating communalities within a factor model. Another indication is if one or several species exceed their maximum abundances in the calibration set (Hutson, 1977). Diverging SST estimates from different SST estimation techniques, such as the MAT and TFT, can further reveal the existence of no-analog conditions.

For the interpretation of the SST records from the Tobago Basin and the northern Venezuela Basin, namely the high-frequency oscillations seen in core M35003-4, it is critical to evaluate possible influences of no-analogs on the SST estimates. To check for such artifacts, SST were estimated with MAT and TFT (Figure 20 and 21).

M35003-4

Despite the similarity of SST patterns derived from TFT and MAT, glacial $SST_{0\text{-}50m}$ derived from TFT is systematically colder than MAT estimates by 1.5 °C-3.0 °C. Core-top MAT estimates for the cold (T_c) and warm (T_w) seasons and TFT-derived T_w are close to observed seasonal SSTs of today, whereas TFT-derived T_c estimates are 0.8°C lower than modern T_c.

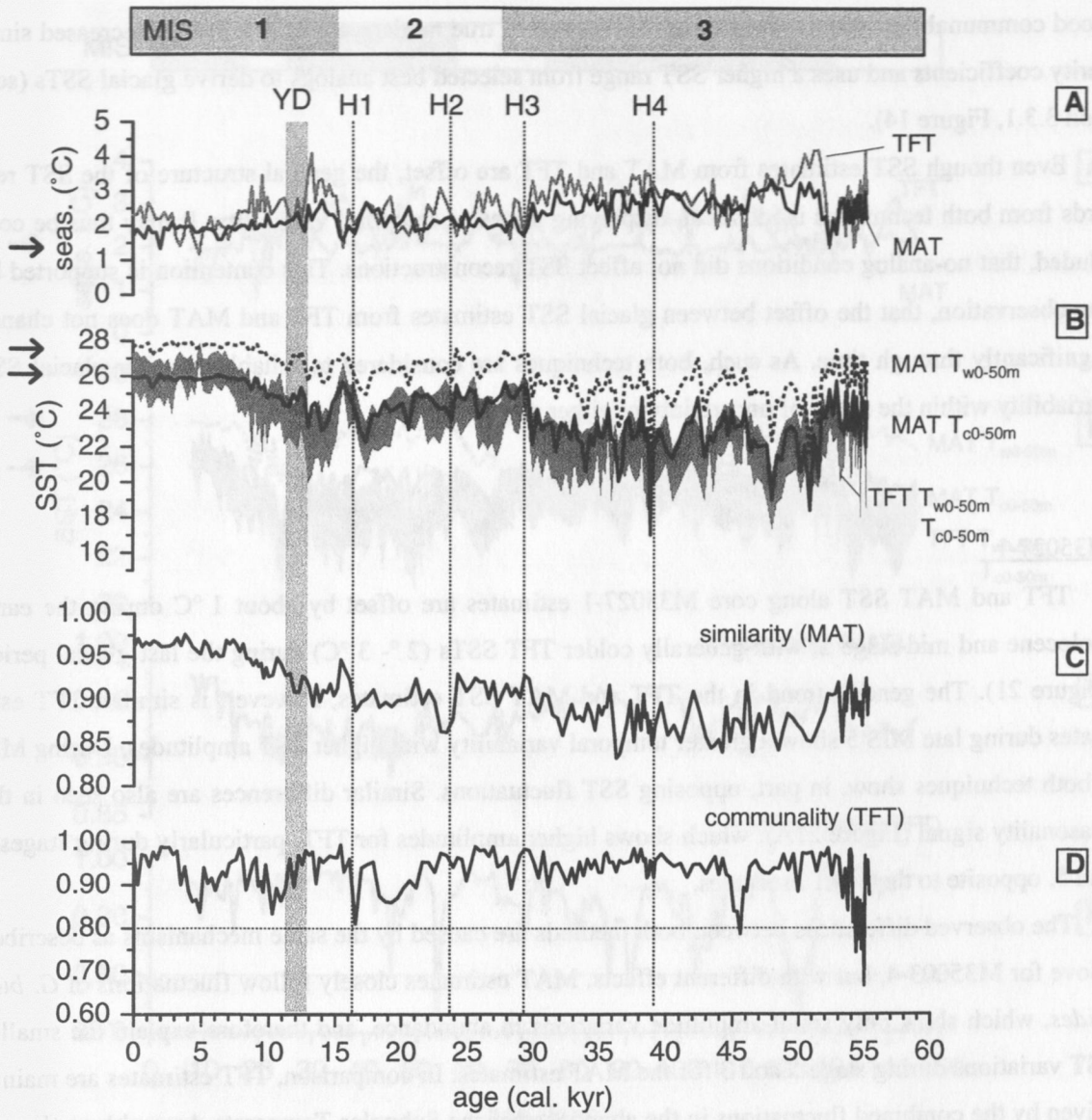

Figure 20. Comparison of MAT and TFT 0-50 m SST estimates for core M35003-4. A) estimated seasonality , B) seasonal MAT (stippled = Tw, black = Tc) and TFT (grey area Tw-Tc), C) similarity measure of MAT, D) communality of the TFT factor model 750-28-9. Black arrows mark modern SST and seasonality levels.

The offset in SST from both techniques may be explained by the observation (from residual analysis of the calibration run) that TFT has a greater tendency to underestimate SST than MAT at the warm end. Furthermore, a co-occurrence of tropical / subtropical faunas with polar / subpolar faunas is observed in glacial samples from core M35003-4 which does not occur in the control data set and, therefore may cause additional 'distortion' of the TFT SST estimates. Still, the factor model yields

good communalities, whereas MAT, in the absence of true modern analogs, displays decreased similarity coefficients and uses a higher SST range from selected best analogs to derive glacial SSTs (section 3.3.1, Figure 14).

Even though SST estimates from MAT and TFT are offset, the general structure of the SST records from both techniques is identical, displaying the same temporal variability. It may thus be concluded, that no-analog conditions did not affect SST reconstructions. This contention is supported by the observation, that the offset between glacial SST estimates from TFT and MAT does not change significantly through time. As such, both techniques are considered to reliably monitor glacial SST variability within the range of uncertainty of either method.

M35027-1

TFT and MAT SST along core M35027-1 estimates are offset by about 1 °C during the early Holocene and mid-stage 5, with generally colder TFT SSTs (2 °- 3 °C) during the last glacial period (Figure 21). The general trend in the TFT and MAT SST estimates, however, is similar. TFT estimates during late MIS 5 show a greater temporal variability with higher SST amplitudes. During MIS 4 both techniques show, in part, opposing SST fluctuations. Similar differences are also seen in the seasonality signal (Figure 21A), which shows higher amplitudes for TFT, particularly during stages 3 and 5, opposite to the MAT estimates.

The observed differences between both methods are caused by the same mechanisms as described above for M35003-4, but with different effects. MAT estimates closely follow fluctuations of *G. bulloides*, which show only small-amplitude variations in abundance, and therefore explain the smaller SST variations during stage 5 and 3 for the MAT estimates. In comparison, TFT estimates are mainly driven by the combined fluctuations in the abundance of the Subpolar-Temperate Assemblage (Factor 2, *G. bulloides*) and the South-Atlantic Upwelling Assemblage (Factor 8, *N. dutertrei*), thus explaining the higher temporal variability of the TFT estimates during MIS 3 and 5.

Compared to the relatively small faunal changes in core M35027-1, the corresponding large TFT SST may overestimate 'true' SST changes. MAT, on the other hand, appears to be relatively insensitive to minor faunal changes, because this method derives SST from averaging environmental information of widely dispersed analogs, in which little faunal changes do not have a great impact on the selection of the analogs, whereas TFT interprets directly SST from the erected factor model and transfer function.

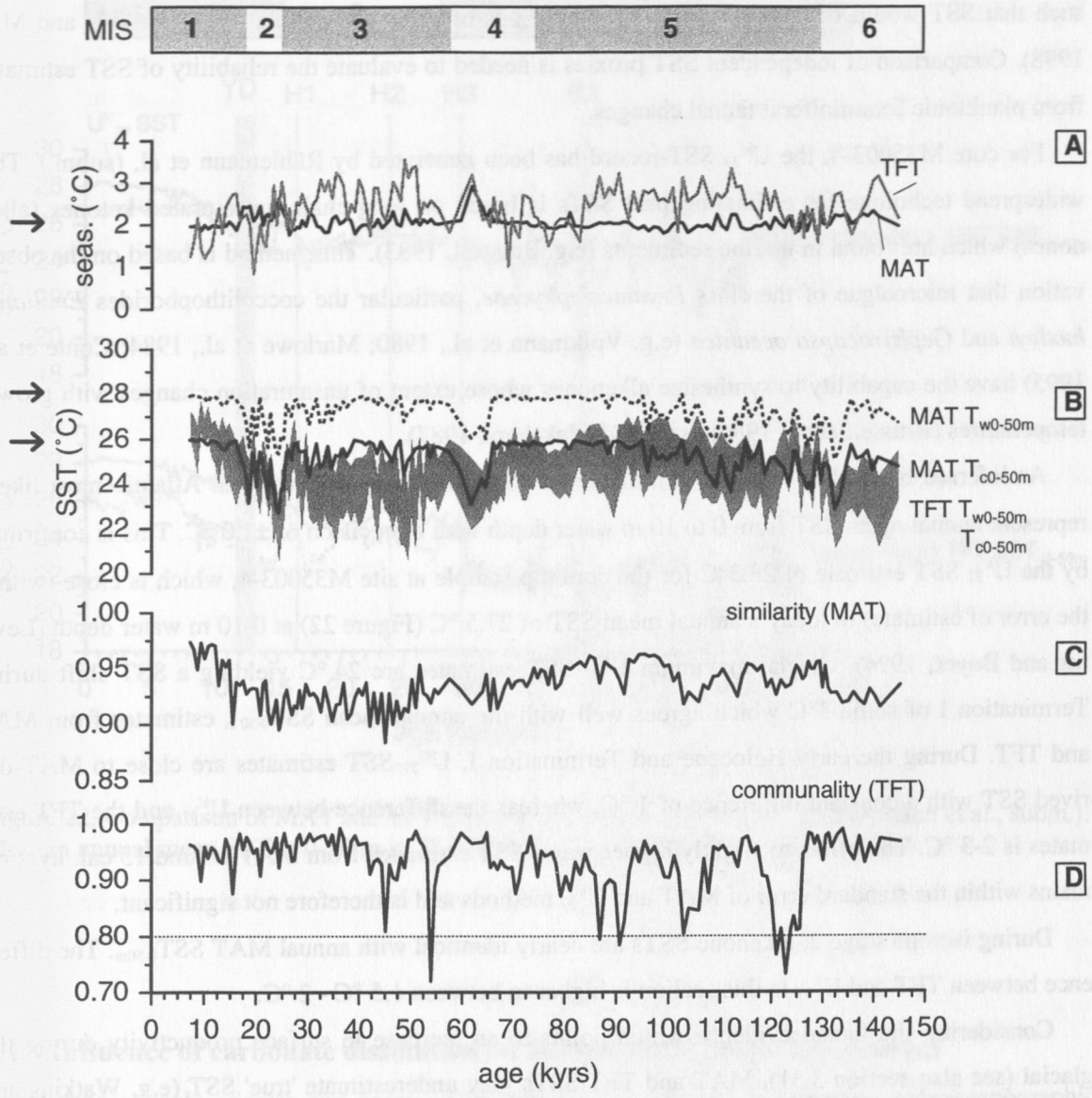

Figure 21. Comparison of MAT and TFT 0-50 m SST estimates for core M35027-1. A) estimated seasonality , B) seasonal MAT (stippled = Tw, black = Tc) and TFT (grey area Tw-Tc), C) similarity measure of the MAT, D) communality of the TFT factor model 750-28-9. Black arrows mark modern SST and seasonality levels.

4.1.2 Organic SST proxy: $U^{k'}_{37}$

Ravelo et al. (1990) and Andreasen and Ravelo (1997) have shown that planktonic foraminiferal assemblages in the tropics are not well correlated to SST, but are more closely related to sea-surface hydrographic parameters like mixed-layer depth, thermocline depth and seasonality. Particularly, planktonic foraminiferal assemblages from planktonic hauls in the equatorial Pacific during an El Niño-La Niña succession show distinctive imprints of primary productivity and mixed-layer depth

such that SST would be overestimated during periods of enhanced productivity (Watkins and Mix, 1998). Comparison of independent SST proxies is needed to evaluate the reliability of SST estimates from planktonic foraminiferal faunal changes.

For core M35003-4, the $U^{k'}_{37}$ SST-record has been generated by Rühlemann et al. (subm.). This widespread technique for estimating past SSTs is based on long-chain, unsaturated ketones (alkenones) which are found in marine sediments (e.g. Brassell, 1983). This method is based on the observation that microalgae of the class *Prymnesiophyceae*, particular the coccolithophorides *Emiliania huxleyi* and *Gephyrocapsa oceanica* (e.g. Volkmann et al., 1980; Marlowe et al., 1984; Conte et al., 1995) have the capability to synthesize alkenones whose extent of unsaturation changes with growth temperatures (Brassell et al., 1986; Prahl and Wakeham, 1987).

As inferred by Müller et al. (1998), alkenone SST-estimates in the tropical Atlantic most likely represent annual mean SST from 0 to 10 m water depth with a precision of ±1.0 °C. This is confirmed by the $U^{k'}_{37}$ SST estimate of 28.3°C for the core top sample at site M35003-4, which is close (within the error of estimate) to today's annual mean SST of 27.5 °C (Figure 22) at 0-10 m water depth (Levitus and Boyer, 1994). Glacial-maximum $U^{k'}_{37}$-SST estimates are 24 °C yielding a SST shift during Termination I of some 3°C which agrees well with the annual mean $SST_{0\text{-}50\,m}$ estimates from MAT and TFT. During the early Holocene and Termination I, $U^{k'}_{37}$-SST estimates are close to MAT-derived SST with a constant difference of 1 °C, whereas the difference between $U^{k'}_{37}$ and the TFT estimates is 2-3 °C. The offset to slightly higher warm SST estimates from MAT around 13 cal. kyrs remains within the standard error of MAT and $U^{k'}_{37}$ methods and is therefore not significant.

During isotope stage 2, alkenone SSTs are nearly identical with annual MAT $SST_{0\text{-}50m}$. The difference between TFT and $U^{k'}_{37}$ in this section is higher to between 1.5 °C - 2 °C.

Considering the faunal evidence which points to an increase in surface productivity during the glacial (see also section 3.31), MAT and TFT SSTs may underestimate 'true' SST (e.g. Watkins and Mix, 1998). Nevertheless, for the last 30 kyrs MAT SSTs are close to alkenone SSTs, thus pointing to MAT as the more 'reliable' SST estimator.

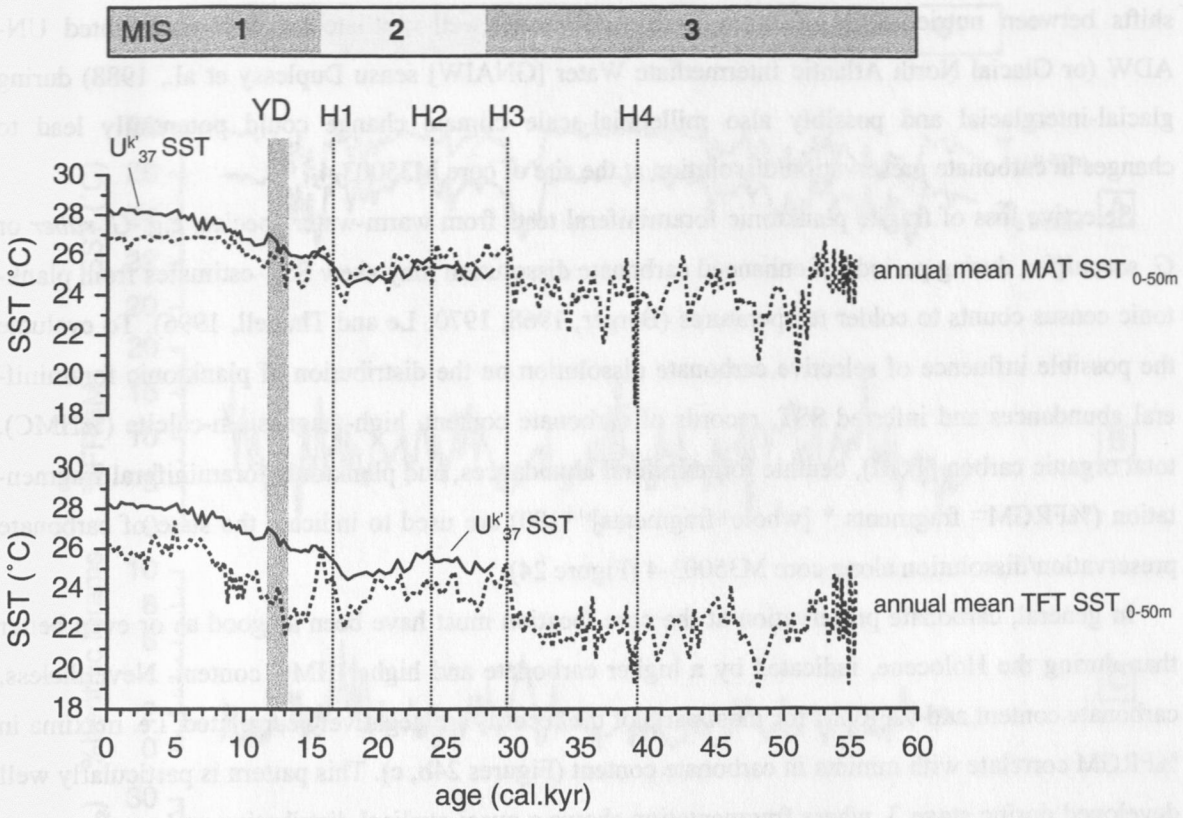

Figure 22. Comparison of MAT and TFT derived SST with SST from $U^{k'}_{37}$ (Rühlemann et al., subm.). Modern annual mean SST at 0-10 m is 27.6 °C and 27.2 °C for 0-50 m water depth.

4.1.3 Influence of carbonate dissolution on foraminiferal faunal assemblages

Millennial-scale climate and ocean variability are documented in numerous paleoceanographic data sets throughout the world's oceans. Rapid changes of deep-ocean circulation resulted in rapid carbonate dissolution cycles at sites where carbonate corrosive AABW alternated with carbonate saturated NADW (e.g. Keigwin and Jones, 1994; Boyle, 1992). During the last glacial, better ventilation of upper deep water and mid-depth levels in the North Atlantic has been inferred from numerous benthic $\delta^{13}C$ and Cd/Ca records (e.g. Marchitto et al., 1998; Oppo et al., 1995; Boyle and Keigwin, 1987). This also caused enhanced carbonate preservation in the Caribbean during the glacial (Haddad and Droxler, 1996). For core M35027-1 enhanced carbonate preservation during glacials is also documented in increased carbonate contents and higher contents of high-magnesium calcite (HMC), a metastable carbonate phase susceptible to dissolution (Lembke, 1997; Figure 23).

Core M35003-4, at a water depth of 1300 m, is influenced today by varying contributions of Upper North Atlantic Deep Water (UNADW) and Antarctic Intermediate Water (AAIW). Systematic

shifts between nutrient-laden CO_2-enriched AAIW and well-ventilated carbonate-saturated UNADW (or Glacial North Atlantic Intermediate Water [GNAIW] sensu Duplessy et al., 1988) during glacial-interglacial and possibly also millennial-scale climate change could potentially lead to changes in carbonate preservation/dissolution at the site of core M35003-4.

Selective loss of fragile planktonic foraminiferal tests from warm-water species, e.g. *G. ruber* or *G. sacculifer*, during periods of enhanced carbonate dissolution may skew SST-estimates from planktonic census counts to colder temperatures (Berger, 1968, 1970; Le and Thunell, 1996). To evaluate the possible influence of selective carbonate dissolution on the distribution of planktonic foraminiferal abundances and inferred SST, records of carbonate content, high-magnesium-calcite (%HMC), total organic carbon (TOC), benthic foraminiferal abundances, and planktonic foraminiferal fragmentation (%FRGM= fragments * [whole+fragments]$^{-1}$*100) are used to indicate the state of carbonate preservation/dissolution along core M35003-4 (Figure 24).

In general, carbonate preservation at the core location must have been as good as or even better than during the Holocene, indicated by a higher carbonate and higher HMC content. Nevertheless, carbonate content and %FRGM for most parts of the records are negatively correlated, i.e. maxima in %FRGM correlate with minima in carbonate content (Figures 24b, c). This pattern is particularly well developed during stage 3, where fragmentation shows a quasi-cyclical distribution and reaches up to 50% in sections with minimum carbonate content. This correlation points to periodically enhanced carbonate dissolution. Conversely, intervals with increased fragmentation of planktonic foraminiferal tests and low carbonate contents correlate with higher proportions of the <63µm size fraction, pointing to increased dilution with terrigenous material.

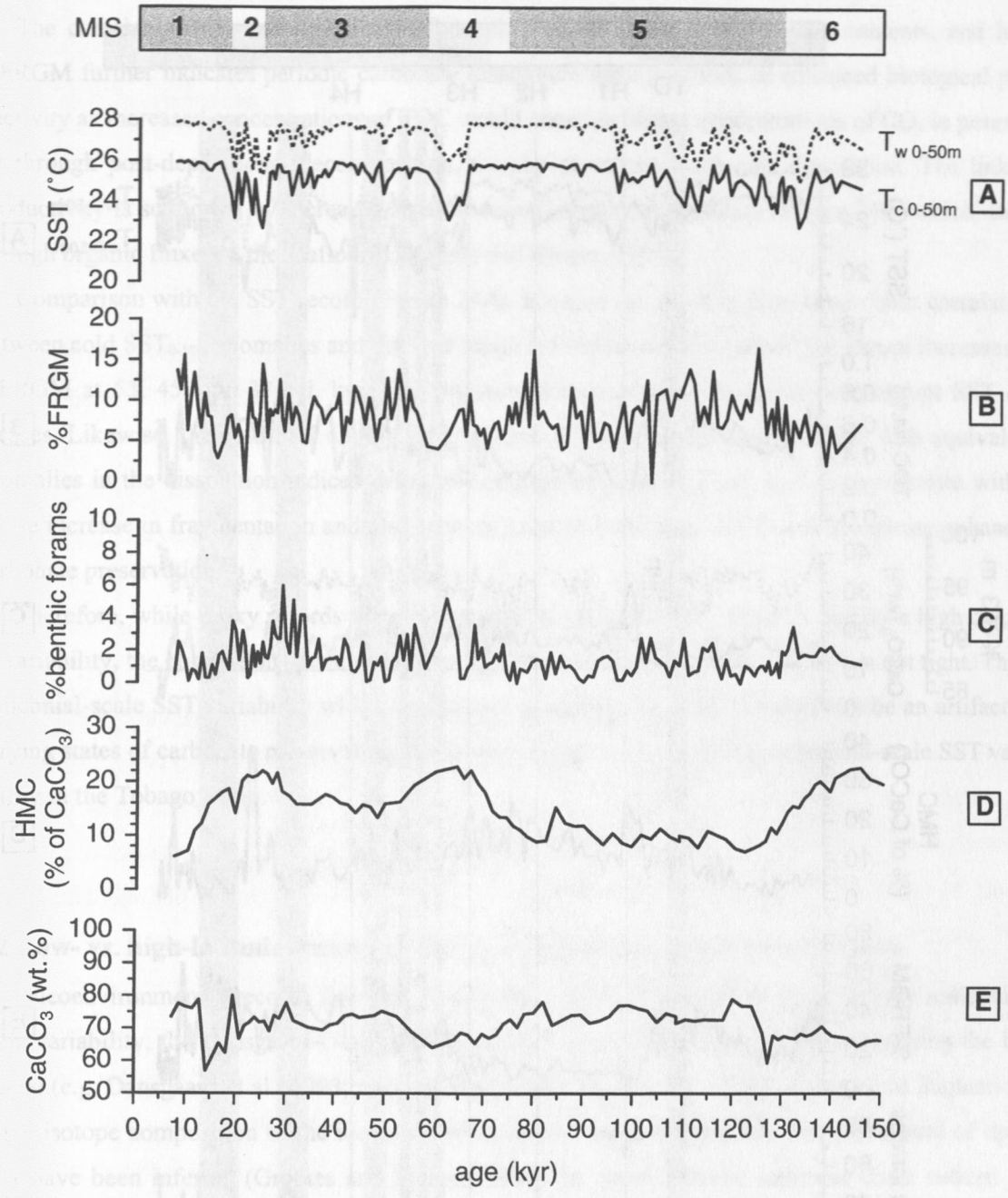

Figure 23. Comparison of carbonate preservation and $SST_{0\text{-}50m}$ for M35027-1. A) cold and warm season MAT $SST_{0\text{-}50m}$, B) fragmentation of planktonic foraminifera, C) relative abunandance of benthic foraminifera, D) HMC content in % of carbonate (modified from Lembke, 1997), E) carbonate content of the sediment (modified from Lembke, 1997).

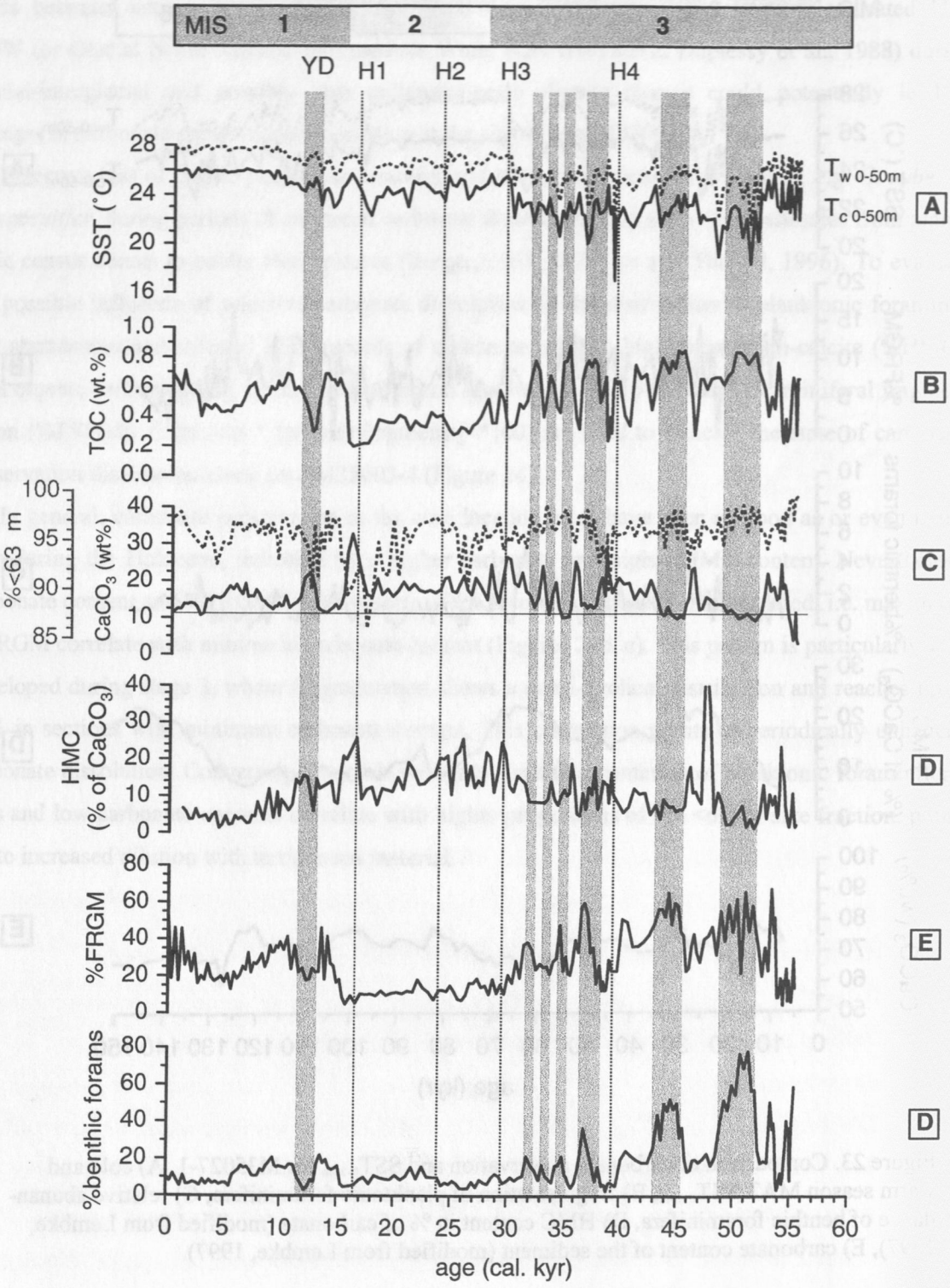

Figure 24. Comparison of carbonate preservation and $SST_{0\text{-}50m}$ for M35003-4. A) cold and warm season MAT $SST_{0\text{-}50m}$, B) Total Organic Carbon (TOC), C) carbonate content of the sediment (black line) and content of <63µm size fraction of the sediment (stippled line), D) HMC content in % of carbonate, E) fragmentation of planktonic foraminifera, F) relative abundance of benthic foraminifera.

The correlation between elevated TOC levels (Figure 24B), low carbonate contents, and high %FRGM further indicates periodic carbonate dissolution during periods of enhanced biological productivity as increased concentrations of TOC would generate higher concentrations of CO_2 in porewater through post-depositional decomposition, thereby promoting carbonate dissolution. The link to productivity is supported by increased abundances of benthic foraminifera (Figure 24E) which dwell on high organic fluxes to the seafloor (Herguera and Berger, 1991).

Comparison with the SST record (Figure 24A), however, shows that there is no direct correlation between cold $SST_{0\text{-}50m}$ anomalies and inferred increased carbonate dissolution. The abrupt increases in %FRGM at 53, 45, and 37 cal. kyrs, for instance, do not correlate with similarly abrupt SST decreases. Likewise, the cold SST anomalies at 42 and 33.5 cal. kyrs do not correlate with equivalent anomalies in the dissolution indices, while the cold anomaly at 47.5 cal. kyrs does correlate with a subtle increase in fragmentation and also with an increase in %HMC which would indicate enhanced carbonate preservation.

Therefore, while proxy records that are susceptible to carbonate dissolution display a high degree of variability, the correlation between enhanced carbonate dissolution and cold SST is not tight. Thus, millennial-scale SST variability which is observed along core M35003-4 should not be an artifact of varying states of carbonate preservation, but is considered to represent true millennial-scale SST variability in the Tobago Basin.

4.2 Low- vs. high-latitude ocean variability - an interhemispheric comparison

Paleoenvironmental records from the Greenland GRIP and GISP2 ice cores display millennial-scale variability, the Dansgaard-Oeschger cycles, with periods of 1.5 kyrs and 3 kyrs during the last glacial (e.g. Dansgaard et al., 1993; Grootes et al., 1993; Taylor et al., 1993). From rapid fluctuations in the isotope composition of the ice cores, mean-annual temperature shifts over Greenland of up to 6 °C have been inferred (Grootes and Stuiver, 1997). In North Atlantic sediment cores sudden increases in the coarse lithic fraction (>150 µm), reduced planktonic foraminifera fluxes, and a lowering of sea-surface salinities have indicated massive iceberg discharges, the so-called 'Heinrich' events (Heinrich, 1988; Bond et al., 1992, 1993; Bond and Lotti; 1995). These Heinrich events, occurring every 5-10 kyr, have been linked to maximally cold stadials recorded in the ice cores (Bond et al., 1993). The sporadic freshwater flux accompanying the iceberg discharges into the North Atlantic may has led to changes in deep water formation by lowering surface water density (Sarnthein et al., 1994; Maslin et al., 1995; Jung, 1996).

Millennial-scale variability is also observed in paleoceanographic records outside the northern North Atlantic region: Records from the mid-latitude North Atlantic and tropical Atlantic display mil-

lennial-scale SST variability, which is linked to rapid changes in thermohaline circulation (e.g. Keigwin and Jones, 1994; Curry and Oppo, 1997; Keigwin and Boyle, 1999). Other records from the low-latitude Atlantic document millennial-scale variability in wind-driven upwelling intensities (e.g. Wang et al., 1995; McIntyre and Molfino, 1996, Little et al., 1997; Martinez et al., 1999). Outside the Atlantic millennial-scale variability has been observed, for example, in Indian Ocean upwelling intensity (Schulz et al., 1998) and in eastern Pacific oceanic oxygen minimum zones (Kennett and Ingram, 1995; Behl and Kennett, 1996).

From the evidence of millennial-scale ocean variability occurring in the high northern North Atlantic, the tropical Atlantic and Indian Ocean, and in the Pacific, teleconnections via the atmosphere and / or ocean thermohaline circulation have been suggested (Stocker, subm.).

Comparison of the isotope records from Greenland and Antarctica reveals that the fast temperature changes over Greenland during the last glacial have an analog in the temperature record from Antarctica, but that Greenland warming events lag behind their Antarctic counterparts in the interval between 50 to 20 kyr (Blunier et al., 1998). A link between the hemispheres through the ocean's thermohaline circulation (THC) has been proposed that the North Atlantic region warms up and the south Atlantic cools down during times of strong THC (Crowley, 1992; Stocker, 1992; Weaver and Hughes, 1994). Numerical models produce convective instabilities in the North Atlantic by advecting salinity anomalies to the convection sites, causing a slow-down of overturning, or, in extreme cases, an abrupt shut-down of convection after salinity anomaly due to freshwater influx have reached a critical threshold value (Rahmsdorf, 1995; Paillard and Labeyrie, 1994). Slow-down and periodic halts of the THC cause the North Atlantic to cool down and, due to a reduced heat export, warming of the South Atlantic (e.g. Manabe and Stouffer, 1997).

Another mechanism for interhemispheric climate coupling involves rapid changes in atmospheric circulation. Combined responses of climate to varying changes in insolation due to precessional forcing have been inferred to drive varying zonality of low-latitude winds, thus causing changes in equatorial and coastal upwelling. Fluctuation in upwelling intensity in the low-latitude North and South Atlantic, and in the equatorial Atlantic, due to changing trade wind intensity have been linked to the North Atlantic Heinrich events due to changes in advection and heat transport from the low-latitude to the high northern Atlantic (McIntyre and Molfino, 1996; Little et al., 1997).

Numerical models which have tested the sensitivity of the climate system to changes in atmospheric greenhouse gases such as methane, carbon dioxide and vapor content, indicate a symmetrical response of SST in the North and South Atlantic (Hansen et al., 1984; Webb et al., 1994; Manabe and Stouffer, 1994).

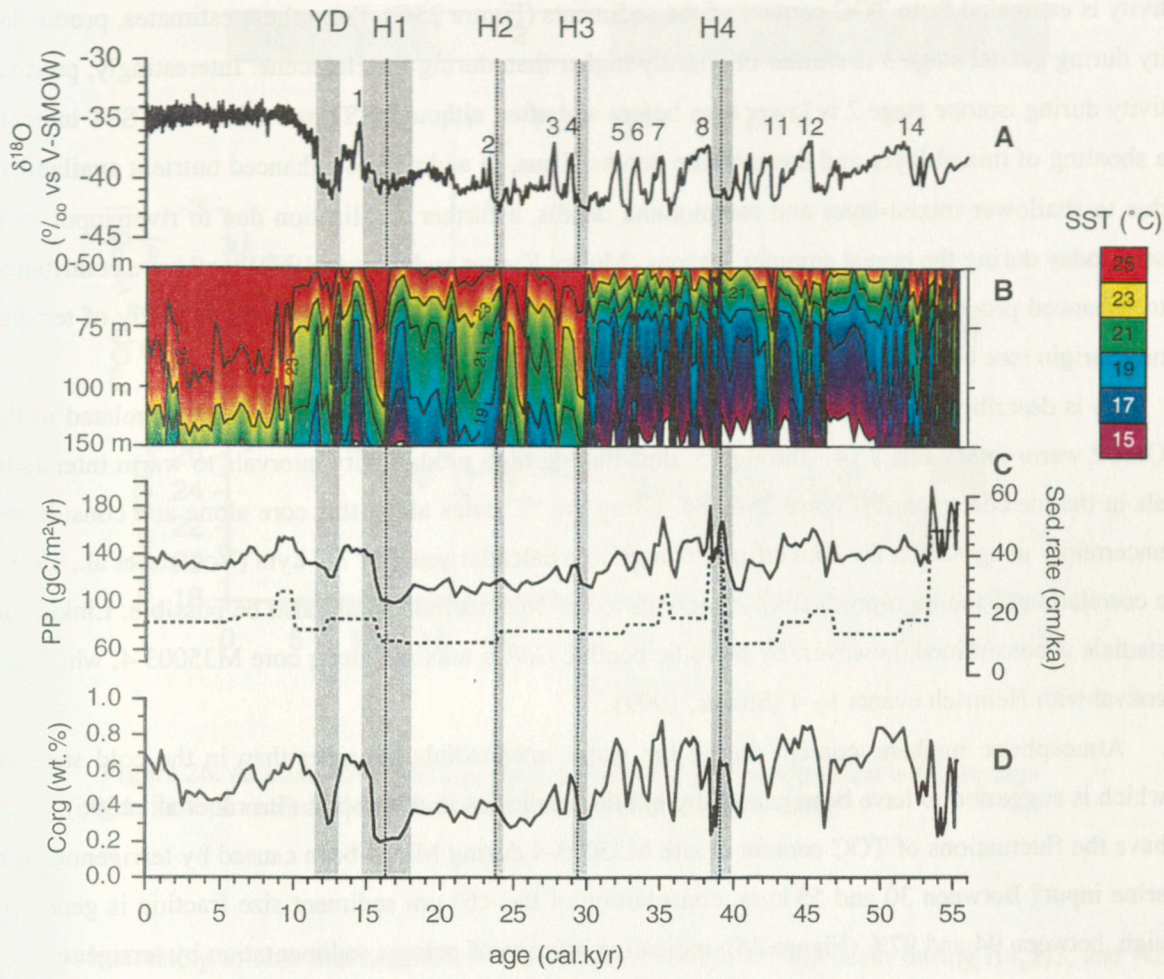

Figure 25. Variation in surface ocean hydrography and productivity at the site of M35003-4 in comparison with $\delta^{18}O$ from GISP 2 (A), B) Evolutionary SST and sub-surface temperature diagram for the upper 150 m, C) Surface productivity, estimated from organic carbon and a paleoproductivity equation (Sarnthein et al., 1992). The dashed line gives the sedimentation rate, D) Organic carbon (unpubl. data, C. Rühlemann).

How does the observed millennial-scale variability from the Caribbean records of M35003-4 and M35027-1 display the effectiveness of these interhemispheric linkages?

Core M35003-4 displays millennial-scale variability in planktonic foraminiferal assemblages and resulting sea-surface temperatures. The time resolution of 300-500 years is sufficiently high to detect the response of the ocean to millennial-scale climate variability such as the 'Heinrich' events and D/O cycles.

During stage 3, between 55 and 30 kyrs, foraminiferal assemblages and SST, in conjunction with organic carbon content of the sediment indicate a shoaling of the thermocline, mixed-layer depths, and enhanced productivity (Figure 25). Using the equation of Sarnthein et al. (1992), primary produc-

tivity is estimated from TOC content of the sediments (Figure 25C). From these estimates, productivity during glacial stage 3 is similar or slightly higher than during the Holocene. Interestingly, productivity during isotope stage 2 is lower than before and after, although SST and subsurface SST indicate a shoaling of mixed-layer and thermocline depths. Thus, in addition to enhanced nutrient availability due to shallower mixed-layer and thermocline depths, a further fertilization due to river input as is seen today during the boreal summer seasons (Muller-Karger and Castro, 1994) may have contributed to enhanced productivity during MIS 3. Alternatively, the TOC of the sediments is partly of terrigenous origin (see below.)

As is described in section 3.1.1, TOC maxima along core M35003-4 have been correlated to the GISP2 warm interstadials 14 - through 5, thus linking high productivity intervals to warm interstadials in the ice core record (Figure 25A, B). Using the ^{14}C dates along this core alone and considering uncertainty in age-shifts for converting ^{14}C ages into calendar years of 3-4 kyrs (Voelker et al., 1998), a correlation of the high-productivity intervals to the cold stadials would also be possible. Linking to stadials is constrained, however, by periodic benthic Cd/Ca maxima along core M35003-4, which are coeval with Heinrich events 1 - 4 (Stüber, 1999).

Atmospheric methane content during the warm interstadials is higher than in the cold stadials, which is suggested to have been caused by humid conditions in the tropics (Brook et al., 1996). If so, have the fluctuations of TOC content at site M35003-4 during MIS 3 been caused by terrigenous riverine input? Between 30 and 55 kyrs, contribution of the <63 µm sediment size fraction is generally high, between 94 and 97% (Figure 24), indicating dilution of pelagic sedimentation by terrigenous input. Low TOC contents at 43 kyrs and 46 kyrs correlate with minima in percent of the <63 µm size fraction, which may indicate a relationship of TOC and terrigenous input. However, carbon isotope measurements from organic carbon and C/N ratios yield no evidence for an input or varying input of organic terrigenous matter (C. Rühlemann, personal communication, 1999).

To evaluate a possible influence of varying freshwater input at the site of core M35003-4 on productivity, MAT $SST_{0\text{-}50m}$ is compared to the oxygen isotope record of the planktonic foraminifera *G. ruber* (pink) (Rühlemann et al., subm., Figure 26). The Glacial-Holocene change is 1.8 ‰, which corresponds to a temperature increase of 3-4 °C, if an ice volume effect of 1-1.2 ‰ (Schrag et al., 1996; Fairbanks, 1989) and a temperature change of 0.2 ‰ per 1 °C are taken into account. This finding is consistent with estimated foraminiferal and $U^{k'}_{37}$ SST changes. During MIS 3, planktonic $\delta^{18}O$ varies coherently with SST fluctuations, except in the time interval between 50 and 53 kyrs, where a negative $\delta^{18}O$ excursion occurs while SST decreases.

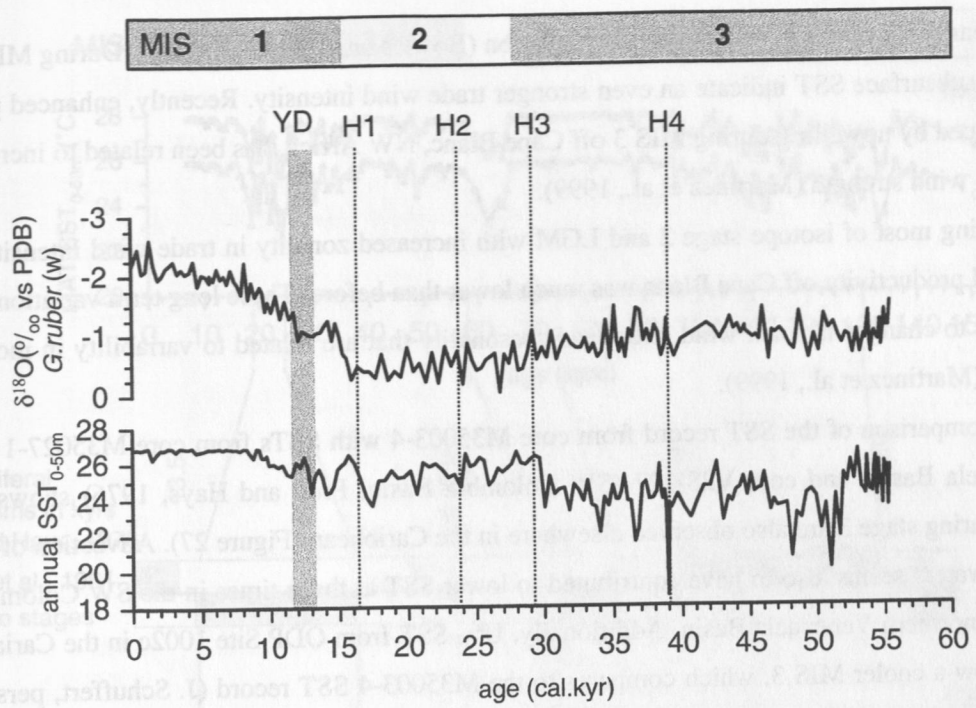

Figure 26. Annual MAT $SST_{0\text{-}50m}$ for core M35003-4 in comparison with the oxygen isotope record of *G. ruber* (pink) (S. Mulitza, unpubl. data).

It is interesting to note that negative $\delta^{18}O$ excursions (Δ 0.2-0.3 ‰) occur during H4, H3, and H2. MAT SST estimations at these times show an inconsistent pattern with decreased SST during H4 and H2, and an increase of SST immediately before H3. Today, the seasonal difference in surface salinity is about 3 PSU (Levitus and Boyer, 1994). The salinity relationship obtained in surface water samples of the eastern and southern Caribbean Sea gives a decrease in $\delta^{18}O$ of 0.3‰ per PSU decrease in salinity (S. Mulitza, personal communication, 1999). Thus, the planktonic $\delta^{18}O$ excursions around H-events are insignificant with respect to the present seasonal and regional salinity variation in the study area.

For the last glacial, a southward dislocation of the ITCZ has been proposed due to equatorward compression of climate zones (Mix et al., 1986a, b). During this time, higher input of eolian sediments into the tropical Atlantic and enhanced productivity in the equatorial Atlantic have been caused by enhanced zonal wind intensity (Ruddiman, 1997; McIntyre et al., 1989; McIntyre and Molfino, 1996). Consistent with this evidence are cooler $SST_{0\text{-}50m}$ and sub-surface SST, indicating a shoaling of mixed-layer and thermocline depths at site M35003-4. Today, enhanced trade wind intensity during boreal winter leads to upwelling along the northern continental margin off Venezuela (Kinder et al., 1985; Muller-Karger and Castrot, 1994). A more southern position of the ITCZ may thus promote an expansion of the upwelling areas further north as has been inferred for the Venezuela Basin in the

Caribbean from enhanced carbonate accumulation (Bowles and Fleischer, 1985). During MIS 3, $SST_{0\text{-}50m}$ and subsurface SST indicate an even stronger trade wind intensity. Recently, enhanced productivity induced by upwelling during MIS 3 off Cape Blanc, NW Africa, has been related to increased meridional wind strength (Martinez et al., 1999).

During most of isotope stage 2 and LGM with increased zonality in trade wind intensity, upwelling and productivity off Cape Blanc was much lower than before. These long term variations were attributed to changes in local wind stress and seasonality that are related to variability in monsoon intensity (Martinez et al., 1999).

A comparison of the SST record from core M35003-4 with SSTs from core M35027-1 (northern Venezuela Basin) and core V28-127 (SW Colombia Basin; Prell and Hays, 1976) shows that low SSTs during stage 3 are also observed elsewhere in the Caribbean (Figure 27). Advection of upwelled cooler waters seems also to have contributed to lower SST at these times in the SW Colombia Basin and the northern Venezuela Basin. Additionally, $U^{k'}_{37}$ SST from ODP Site 1002c in the Cariaco Basin also show a cooler MIS 3, which compares to the M35003-4 SST record (J. Schuffert, pers. comm.; Herbert and Schuffert, subm.). Furthermore, the high variability in SST during stage 5 in M35027-1 is comparable to that in core V28-127. Both cores indicate lower SST for the Caribbean during the last interglacial than for the Holocene.

For the equatorial Atlantic, McIntyre and Molfino (1996) suggest a nonlinear response of climate to precessional forcing to have caused sub-Milankovitch variation in upwelling intensity by changing the equatorial wind field. Higher zonality in the trade winds drives warm water across the equator into the Caribbean and Gulf of Mexico, while equatorial upwelling is enhanced. McIntyre and Molfino (1996) further suggest that at times of maximum monsoon strength and lower trade wind and upwelling intensity, this warm water pool is released into the North Atlantic, producing the rapid melting of ice and hence triggering 'Heinrich' events. To test this conceptual model, the Caribbean SST estimates are compared to SST estimates from the equatorial Atlantic (cores RC24-16 and V30-40; McIntyre et al., 1989), to variations in the abundance of *Florisphaera profunda* of core RC24-08 (McIntyre and Molfino, 1996), to mid-latitude North Atlantic SST from cores SU90-03 (Chapman and Shackleton, 1998) and 15612 (Kiefer, 1998), and to the GISP2 climate record (Figure 28). Except core SU90-03, SSTs for cores RC24-16, V30-40 and 15612 are recalculated with MAT for the 0-50 m water-depth level using published foraminiferal census counts (SPECMAP archive #1; Imbrie at al., 1990; Kiefer, 1998).

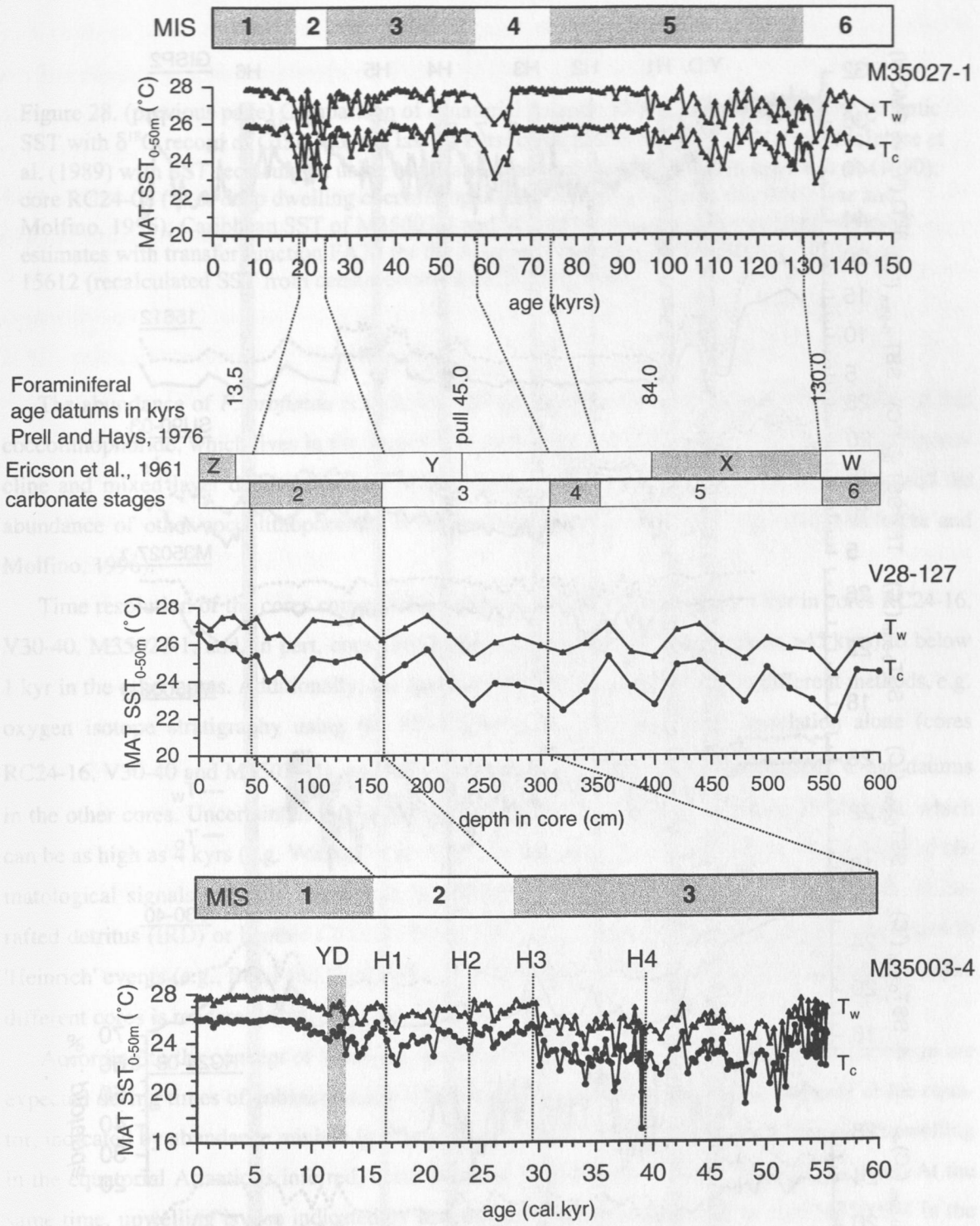

Figure 27. Comparison of SST estimates from core M35003-4 with Caribbean SST of cores M35027-1 and V28-127 (Prell, 1976). For core V28-127, SST was recalculated using the census counts of Prell and Hays (1976; CLIMAP Project Members, 1994) and the MAT. For stratigraphic comparison, the carbonate zonation, which is suggested to compare to the oxygen isotope stages, the planktonic foraminifera zonation of Ericson et al. (1961), and the faunal datums based on ^{14}C and thorium-ionium dates of Broecker and van Donk (1970) are given.

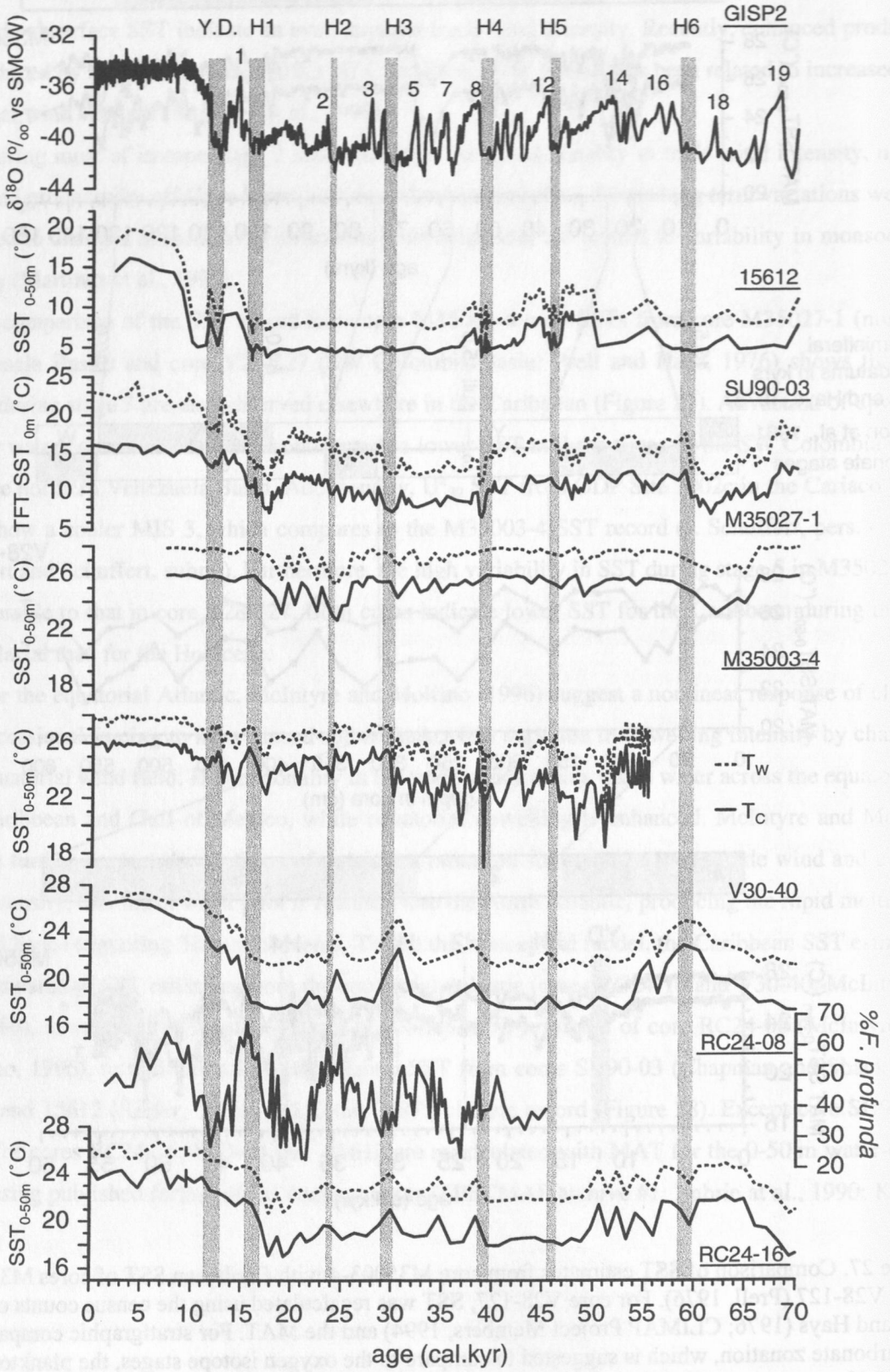
Y.D.
H1
H2
H3
H4
H5
H6
GISP2
1
2
3
5
7
8
12
14
16
18
19
δ18O (‰ vs SMOW)
-32
-36
-40
-44
SST 0-50m (°C)
15612
TFT SST 0m (°C)
SU90-03
M35027-1
SST0-50m (°C)
M35003-4
TW
TC
V30-40
RC24-08
%F. profunda
70
60
50
40
30
20
RC24-16
0
5
10
15
20
25
30
35
40
45
50
55
60
65
70
age (cal.kyr)

Figure 28. (previous page) Comparison of equatorial Atlantic SST, Caribbean and North Atlantic SST with $\delta^{18}O$ record of GISP2 for the last 70 kyrs: cores RC24-16 and V30-40 from McIntyre et al. (1989) with SST recalculated using MAT and census counts published in Imbrie et al. (1990); core RC24-08 (% of deep dwelling coccolithophoride *Florisphaera profunda;* McIntyre and Molfino, 1996); Caribbean SST of M35003-4 and M35027-1 (this thesis); core SU90-03 (SST estimates with transfer function FA20 for the Atlantic, Chapman and Shackleton, 1998); core 15612 (recalculated SST from census counts from Kiefer (1998).

The abundance of *F. profunda* is included into the comparison since abundance variations of this coccolithophoride, which lives in the deeper euphotic zone, are assumed to record changes in thermocline and mixed layer depths. Maxima in abundance occur, when the mixed layer is deep and the abundance of other coccolithophorides is reduced due to lower nutrient availability (McIntyre and Molfino, 1996).

Time resolution of the cores compared is different, ranging from roughly 1 kyr in cores RC24-16, V30-40, M35027-1, and, in part, core 15612 (during Termination I and sections >45 kyrs) to below 1 kyr in the other cores. Additionally, the age models of the cores are based on different methods, e.g. oxygen isotope stratigraphy using the SPECMAP stack to stratigraphic correlation alone (cores RC24-16, V30-40 and M35027-1), and $\delta^{18}O$ stratigraphy in conjunction with detailed ^{14}C-age datums in the other cores. Uncertainties in converting ^{14}C-ages to calendar years between 25- 40 kyrs, which can be as high as 4 kyrs (e.g. Voelker et al., 1998), further make an assessment of lead and lags of climatological signals difficult. Thus, without additional independent age control points such as ice-rafted detritus (IRD) or benthic Cd/Ca ratios as markers for sea-surface and deep-water responses to 'Heinrich' events (e.g., Bond and Lotti, 1995; Willamowski, 1999, Stüber, 1999), a comparison of the different cores is rendered circumstantial at best.

According to the concept of McIntyre and Molfino (1996), higher SSTs within the Caribbean are expected during times of enhanced trade wind intensities. Enhanced trade wind intensity at the equator, indicated by abundance minima in *F. profunda* and low $SST_{0\text{-}50m}$, from which increased upwelling in the equatorial Atlantic is inferred, occur between 35 to 38 cal. kyrs and 20 to 23 cal. kyrs. At the same time, upwelling is also indicated by low surface and sub-surface SST in core M35003-4 in the Tobago Basin, while core M35027-1 still shows high SST and a slight shoaling of mixed-layer and thermocline depths.

For 'Heinrich' event 3, the Caribbean cores exhibit an increase in SST, while in the equatorial Atlantic SST is also elevated. Core RC24-08 at the equator displays a minimum in the abundance of *F. profunda*, indicating increased trade wind intensities. In the North Atlantic, core SU90-03 shows a distinct SST_{om} minimum, while core 15612 still remains at low $SST_{0\text{-}50m}$. However, using a calibration

set with caloric $SST_{0\,m}$, a distinct SST minimum at H3 is seen (Kiefer, 1998).

During H2, equatorial upwelling is low, indicated by high abundances of *F. profunda.* At this time, a decrease from relative high $SST_{0\text{-}50m}$ to low $SST_{0\text{-}50m}$ in core V30-40 coincides with temperature minima in Caribbean cores M35003-4 and M35027-1.

A conspicuous feature of the SST records is the apparent opposite trend in SST between the equatorial and subtropical cores (RC24-16, M35003-4, and M35027-1) on one hand and the North Atlantic cores (SU90-03 and 15612) on the other.

During 'Heinrich' event 1, between 14.5-18 cal. kyrs, core RC24-16 and core M35003-4 display a warming of about 2 °-3 °C. Equatorial upwelling intensity, inferred by increased abundance of *F. profunda* in core RC24-08, is also decreased at this time. However, core V30-40 SST evolution seems to follow more the SST evolution seen in the North Atlantic cores SU90-03 and 15612. In core M35027-1, the increase in SST occurred about 1.5 to 2 kyrs before 'Heinrich' event 1.

During the Bølling-Allerød period, the mid- and high-latitude North Atlantic region exhibits a warming as is inferred from SST estimates of cores SU90-03 and 15612 and GISP2 $\delta^{18}O$, while in the subtropical core M35003-4 a subtle decrease in SST is observed.

During the Younger Dryas period, between 11-12.6 cal. kyrs, SST at the site M35003-4 was warmer than before and after. For the same period, the SST records from equatorial cores RC24-16 and V30-40 also show a warming at these locations. Conversely, equatorial core RC24-08 indicates enhanced upwelling during the Younger Dryas period.

A higher productivity during the Younger Dryas period, caused by enhanced trade wind intensity, is also inferred from productivity records from the Cariaco Basin (Peterson et al, 1991; Hughen et al., 1996 and 1998; Lin et al., 1997). Following the first meltwater pulse Ia (Fairbanks, 1989), the formerly closed Cariaco Basin (sill depth between 120-145 m), was connected again to the open Caribbean circulation. During the Younger Dryas planktonic foraminiferal faunas, stable isotopes of multiple planktonic foraminifera, and laminae-thickness' in the sediments reveal higher productivity induced by upwelling. A cooling event during the Younger Dryas is also inferred by pollen records from the Costa Rican Cordillera, showing a downslope shift of upper forest line by 300-400 m, which indicates a temperature drop of about 2 °-3 °C (La Chonta Stadial, Islebe et al., 1995).

However, Cariaco Basin alkenone SSTs from ODP Site 1002c also show a warming during Younger Dryas (J. Schuffert, pers. com.; Herbert and Schuffert, subm.), and would confirm the SST estimates from nearby Tobago Basin core M35003-4.

Thus, the evidence from the tropic-subtropical SST records is inconclusive, but a warming of the tropical Atlantic during the Younger Dryas is predicted from GCM studies due to the teleconnection of low and high latitudes via the thermohaline circulation (Manabe and Stouffer, 1988; Rahmstorf, 1994). The tropical warming seems to be caused by a slow-down of the thermohaline circulation due to suppressed NADW formation, caused by meltwater-induced instabilities of the sea surface in the

high northern North Atlantic, and, consequently, a reduced heat export to the North Atlantic region.

The equatorial upwelling record of RC24-08, inferred from abundance variations of *F. profunda*, shows cyclic variations in intensity with periods of 7.6 to 8.4 kyrs (McIntyre and Molfino, 1996). On the other hand, sea surface temperatures of the Caribbean sediment cores, particularly those from high-resolution core M35003-4, do not follow these variations in a way expected by McIntyre and Molfino (1996); rather, the M35003-4 SST record seems to show variations in the intensity of the NE trade winds, which causes shoaling and deepening of mixed-layer and thermocline depths at this location with a period of approximately 2-3 kyrs. If the mechanism suggested by McIntyre and Molfino (1996) exists, the warm pool must be located further north in the Gulf of Mexico.

In summary, the comparison of SST records from the equatorial and subtropical Atlantic, the Caribbean Sea and the North Atlantic is inconclusive. The comparison may indicate some connection between the intensity of ocean thermohaline circulation and SST evolution in the tropical-subtropical Atlantic during the Termination I. However, the comparison also reveals the necessity for more high resolution SST records and better areal coverage of the tropical-subtropical Atlantic to resolve the fine-scaled regional variations in hydrography through time. Further, additional stratigraphic information such as benthic $\delta^{13}C$ and Cd/Ca records for fine-scale stratigraphic correlation between cores is needed. Only then paleoceanographic concepts can be tested with greater fidelity that links low- versus high latitude climate variability with changes in ocean thermohaline circulation and interhemispheric marine heat transport.

5 Conclusions

Sea-surface temperature estimates along two sediment cores from the western subtropical North Atlantic are used to reconstruct environmental variability in the area during the late Pleistocene.

Foraminiferal census counts along core M35003-4 from the Tobago Basin reveal a high temporal variability of sea-surface hydrography over the last 55 kyrs. During glacial times, abundances of high-latitude planktonic foraminiferal assemblages increased over those of tropical assemblages. Increased abundances of *N. dutertrei*, *N. pachyderma* (left and right coiling) and *G. bulloides*, all indicate an increase in productivity, possibly due to a northward expansion of Venezuelan upwelling due to increased glacial trade wind intensity. Inferred seasonal SST, estimated with the Transfer-Function Technique (Imbrie and Kipp, 1971) and the Modern Analogue Technique (Prell, 1985), show a glacial-interglacial change of 2.5 ° - 3 °C. Seasonal SST for the upper 0-50 m, annual 'SST' at 75 m, 100 m and 150 m, indicate a shoaling of mixed-layer and thermocline depths during glacial stages due to enhanced wind intensity. For marine isotope stage 3, surface and subsurface temperature estimates are colder than full-glacial stage 2 and also imply shallower thermocline depths, which may indicate stronger trade wind intensities during this period. During MIS 3, inferred surface productivities are equal or slightly higher than during the Holocene, possibly caused by a shallower thermocline in conjunction with higher nutrient supply by river input, while during stage 2 inferred productivity is low. Both faunally derived SST estimates agree well with each other within the uncertainty of the methods, and with independent $U^{k'}_{37}$-SST along the same core.

Planktonic foraminiferal assemblages in the northern Venezuela Basin display a high variability during the last 150,000 years. During the last 50 kyrs, variations in planktonic foraminiferal assemblages follow those seen in core M35003-4, but at lower amplitudes. Estimated SST changes for Terminations I and II are 2 °-2.5 °C and 1.5°C, respectively. During the last interglacial, SST in the northern Venezuela Basin is 1 °C colder than during the Holocene.

SST estimates from MAT and TFT for cores M35003-4 and M35027-1 show comparable SST fluctuations through time, but with generally cooler TFT SST estimates. During the Holocene, a constant offset of 1 °C is observed, which increases during the glacial stages to 2 °-3 °C. A likely explanation of these differences may be the different response of both methods to changes in the planktonic foraminiferal assemblages.

The Caribbean SST estimates are compared to published paleoceanographic records from the equatorial and North Atlantic and the climatic record from GISP 2. The equatorial hydrography during the last glacial is influenced mainly by variations in the zonality of the trade winds, which in turn is driven by precessional forced changes in the monsoon system with periodicities from 7.4-8.6 kyrs (McIntyre and Molfino, 1996). As proposed by McIntyre and Molfino (1996), a higher zonality in the trade winds drives warm water across the equator into the Caribbean and Gulf of Mexico, while equa-

torial upwelling is enhanced. However, located in the Grenada Passage, one of the main gateways for warm surface waters entering the Caribbean Sea, core M35003-4 SSTs mainly display the response of the ocean at this site to varying strength of the NE trade winds. Indicated by periodic SST decreases in core M35003-4, trade wind intensities may have varied with a period of 2-3 kyrs. Enhanced upwelling in the southern Caribbean seems to have compensated for the effects of predicted warming due to the advection of warm surface waters from the equatorial and southern Atlantic.

A conspicuous feature is the opposite direction of SST signals in cores M35003-4, M35027, and RC24-16 from the subtropical / equatorial Atlantic compared to northern hemisphere climatic records such as the GISP 2 isotope record during Termination I. Core M35003-4 SST estimates during Heinrich I and the Younger Dryas period show a warming at the core location, whereas North Atlantic sediment cores and Greenland's GISP2 ice core imply a cooling. During the northern hemisphere warm Bølling-Allerød Period, on the contrary, SST at the core location decrease.

6 Acknowledgments - Danksagung

Für die Vergabe dieser Arbeit, die stimulierenden Anregungen sowie dem steten Interesse am Fortgang der Arbeit, möchte ich Herrn Priv. Doz. Dr. Rainer Zahn recht herzlich danken. Herrn Professor Grootes sei für die Übernahme des Korreferates recht herzlich gedankt, die Diskussionen, insbesondere in der Schlußphase dieser Arbeit, haben sehr zum Gelingen beigetragen.

Herrn Dr. Uwe Pflaumann schulde ich besonderen Dank für die großzügige Bereitstellung eigener Daten, Programme und Quellcodes zur Berechnung von Paläomeeresoberflächentemperaturen. Ohne die geduldige Einführung in die Taxonomie der Planktonforaminiferen sowie die Bereitschaft, Ergebnisse intensiv zu diskutieren und auch zu hinterfragen, wäre diese Arbeit nicht möglich gewesen.

Herrn Dr. Joachim Schönfeld möchte ich für seine Bereitschaft, auch kurzfristig Daten und Probleme bei der Interpretation derselben zu erörtern, recht herzlich danken.

Dr. Carsten Rühlemann und Dr. Stefan Mulitza, Universität Bremen, sei für die Diskussion der paläozeanographischen Relevanz der Daten sowie der Bereitstellung eigener, bisher unveröffentlichter Daten herzlichst gedankt.

Vielen Dank meinen KollegenInnen Dipl.Chem. Arndt Stüber, Dr. C. Willamowski, Dipl.Chem. Anja Müller, Dipl.Geol. Kristina Heilemann, Dipl.Geol. Antje Völker für ihre freundschaftliche Unterstützung und Diskussion der Ergebnisse der vorliegenden Arbeit.

Alexander Konrad, Sven-Oliver Bathke, Oliver Klaus und Holger Kühl sei an dieser Stelle für die zuverlässige und sorgfältige Probenaufbereitung, den Auslesearbeiten zu den Isotopenmessungen sowie dem gewissenhaften und wahrscheinlich langweiligen 'Splitten' recht herzlich gedankt. Herr Dipl.Geol. Lester Lembke führte die Karbonat-, Corg- sowie die Röntgendiffraktrometrie-Messungen durch. Herrn Chris Adamson sei für die Korrektur und kritische Durchsicht des englischen Manuskriptes gedankt.

Gitte, Gerd und Jessika sei an dieser Stelle für die Hilfe bei der Betreuung meiner Kinder während der Schlußphase der Arbeit sehr gedankt.

Mein ganz besonderer Dank gilt meiner lieben Frau Sabine sowie meinen Söhnen Simon und Christoph. Euer Verständnis und Eure Liebe haben mir, insbesondere während der für alle anstrengenden Schlußphase, sehr geholfen.

Diese Arbeit wurde von der Deutschen Forschungsgemeinschaft im Projekt 'Paläo-Karibik' ZA157/13 gefördert.

7 References

Andreasen, D.J., Ravelo, A.C. (1997): Tropical Pacific Ocean thermocline depth reconstructions for the last glacial maximum. - Paleoceanography, Vol. 12, 395-413.

Behl, R. J., Kennett, J. P. (1996): Brief interstadial events in the Santa Barbara basin, NE Pacific, during the past 60 kyr. - Nature, Vol. 379, 243-246.

Bé, A.W.H. (1977): An ecological, zoogeographic, and taxonomic review of recent planktonic foraminifera. - in A.T.S.Ramsay (ed.): Oceanic Micropaleontology, Volume 1, Academic Press, London, 1-100.

Berger, W. H. (1968): Plankton Foraminifera: Selective solution and paleoclimatic interpretation. - Deep Sea Research, Vol. 15, 31-43.

Berger, W.H. (1970): Planktonic foraminifera: Selective solution and the lysocline. - Marine Geology, Vol. 8, 111-138.

Berger, W. H., Wefer, G.(1990): Export production: seasonality and intermittency, and paleoceanographic implications. - Palaeogeography, Palaeoclimatology, Palaeoecology, Vol. 89, 245-254.

Blunier, T., Chappelaz, J., Schwander, J., Dällenbach, A., Stauffer, B., Stocker, T.F., Raynaud, D., Jouzel, J., Clausen, H.B., Hammer, C.U., Johnsen, S.J. (1998): Asynchrony of Antarctic and Greenland climate change during the last glacial period. - Nature, Vol. 394, 739-743.

Bond, G., Heinrich, H., Broecker, W., Labeyrie, L., McManus, J., Andrews, J., Huon, S., Jantschik, R., Clasen, S., Simet, C., Tedesco, K., Klas, M., Bonani, G., Ivy, S. (1992): Evidence for massive discharge of icebergs into the North Atlantic ocean during the last glacial period. - Nature, Vol. 360, 245-249.

Bond, G., Broecker, W.C., Johnsen, S., McManus, J., Labeyrie, L., Jouzel, J., Bonani, G. (1993): Correlations between climate records from North Atlantic sediments and Greenland ice. - Nature, Vol. 365, 143-147.

Bond, G., Lotti, R. (1995): Iceberg discharges into the North Atlantic on millennial time scales during last glaciation. - Science, Vol. 267, 1005-1010.

Bowles, F. A., Fleischer, P. (1985): Orinoco and Amazon river sediment input into the eastern Caribbean Basin. - Marine Geology, Vol. 68, 53-72.

Boyle, E.A., Keigwin, L. (1982): Deep circulation of the North Atlantic over the last 200,000 years: Geochemical evidence. - Science, Vol. 218, 784-787.

Boyle, E. A., Keigwin, L. (1987): North Atlantic thermohaline circulation during the past 20,000 years linked to high-latitude surface temperatures. - Nature, Vol. 330, 35-40.

Boyle, E.A. (1992): Cadmium and $\delta^{13}C$ paleochemical ocean distributions during the glacial stage 2. - Annual Reviews of Earth and Planetary Science, Vol. 20, 245-287.

Brassel, S. C. (1983): Applications of biomarkers for delineating marine paleoclimatic fluctuations during the Pleistocene. - in: M. H. Engel and S. A. Macko (eds.), Organic Geochemistry: Principles and Applications, Plenum Press, pp 699-738.

Brassell, S. C., Eglinton, G., Marlowe, I.T., Pflaumann, U., Sarnthein, M. (1986): Molecular stratigraphy: a new tool for climate assessment. - Nature, Vol. 320, 129-133.

Broecker, W.S., van Donk, J. (1970): Insolation changes, ice volumes and the O^{18} record in deep-sea cores. - Review of Geophysics, Vol. 8, 327-328.

Brook, E. J., Sowers, T., Orchardo, J. (1996): Rapid variations in atmospheric methane concentration during past 110,000 years. - Science, Vol. 273, 1087-1091.

Charles, C. D., Lynch-Stieglitz, J., Ninnemann, U.S., Fairbanks, R.G. (1996): Climate connections between the hemisphere revealed by deep sea sediment core / ice core correlations. - Earth and Planetary Science Letters, Vol. 142, 19-27.

Chang, Y.-M. (1967): Accuracy of fossil percentage estimation. - Journal of Paleontology, Vol. 41, 500-502.

Chapman, M. R., Shackleton, N. J. (1998): Millennial-scale fluctuations in North Atlantic heat flux during the last 150,000 years. - Earth and Planetary Science Letters, Vol. 159, 57-70.

CLIMAP Project Members (1994): CLIMAP 18K Database. - IGBP PAGES/ World Data Center-A for Paleoclimatology Data Contribution Series # 94-001. NOAA/NGDC Paleoclimatology Program, Boulder CO, USA.

Conte, M. H., Thompson, A., Eglinton, G., Green, J.C. (1995): Lipid biomarker diversity in the coccolithophorid Emiliania huxleyi (prymnesiophyceae) and the related species Gephyrocapsa oceanica. - J. Phycol., Vol. 31, 272-281.

Crowley, T. J. (1992): North Atlantic Deep Water cools the southern hemisphere. - Paleoceanography, Vol.7, 489-497.

Curry,W.B., Oppo, D. (1997): Synchronous, high-frequency oscillations in tropical sea surface temperatures and North Atlantic Deep Water production during the last glacial cycle. - Paleoceanography, Vol 12, 1-14.

Dansgaard, W., Johnson, S. J., Clausen, B.H., Dahl-Jensen, D., Gundestrup, N.S., Hammer, C.U., Hvidberg, C.S., Steffensen, J.P., Sveinbjoernsdottir, A.E., Jouzel, J., Bond, G. (1993): Evidence for general instability of past climate from a 250-kyr ice-core record. - Nature, Vol. 339, 532-534.

Davis, J.C. (1986): Statistics and data analysis in geology. - John Wiley, 646 p.

deMiro, M.D. (1971): Los foraminiferos vivos y sedimentados del margen continental de Venezuela (resumen). - Acta Geologica Hispanola, Vol. 6, 102-106.

Dowsett, H.J., Poore, R.Z. (1990): A new planktic foraminifer transfer function for estimating Pliocene-Holocene paleoceanographic conditions in the north Atlantic. - Marine Micropaleontology, Vol. 16, 1-26.

Duplessy, J.-C., Shackleton, N.J., Mathews, R.K., Prell, W., Ruddiman, W.F., Caralp, M., Hendy, C.H. (1984): 13C record of benthic foraminifera in the last Interglacial ocean: Implications for the carbon cycle and the global deep water circulation. - Quaternary Research, Vol. 21, pp 225-243.

Duplessy, J.-C., Shackleton, N. J., Fairbanks, R., Labeyrie, L., Oppo, D., Kallel, N. (1988): Deep water source variations during the last climatic cycle and their impact on the global deepwater circulation. - Paleoceanography, Vol. 3, 343-360.

Duplessy, J.-C., Labeyrie, L., Arnold, M., Paterne, M., Duprat, J., VanWeering, T.C.E. (1992): Changes in surface salinity of the North Atlantic Ocean during the last deglaciation. - Nature, Vol. 358, 485-487.

Ericson, D. B., Wollin, G. (1956): Correlation of six cores from the equatorial Atlantic and the Caribbean. - Deep-Sea Research, Vol. 3, 104-125.

Ericson, D. B., Ewing, M., Wollin, G., Heezen, B.C. (1961): Atlantic deep-sea sediment cores. - Geological Society of America Bulletin, Vol. 72, 193-276.

Fairbanks, R.G., Sverdlove, M., Free, R., Wiebe, P.H., Bé, A.W.H. (1982): Vertical distribution and isotopic fractionation of living planktonic foraminifera from the Panama Basin. - Nature, Vol. 298, 841-844.

Fairbanks, R. (1989): A 17,000-year-glacio-eustatic sea level record, influence of glacial melting rates on the Younger Dryas event and deep ocean circulation. - Nature, Vol. 342, 637-642.

Giradeau, J., Roger, J. (1994): Phytoplankton biomass and sea-surface temperature estimates from sea-bed distribution of nannofossils and plankton foraminifera in the Benguela upwelling system. - Micropaleontology, Vol. 40, 275-285.

Gonzalez-Donoso, J.M., Linares, D. (1998): Evaluation of some numerical techniques for determining paleotemperatures from planktonic foraminiferal assemblages. - Revista Española de Paleontología, Vol.13, 107-129.

Graf, G., Gerlach, S.A., Linke, P., Queisser, W., Ritzrau, W., Scheltz, A., Thomsen, L., Witte, U., (1995): Benthic-pelagic coupling in the Greenland-Norwegian Sea and its effect on the geological record. - Geologische Rundschau, Vol. 84, 49-58.

Grootes, P.M., Stuiver, M., White, J.W.C., Johnsen, S., Jouzel, J. (1993): Comparison of the oxygen isotope records from the GISP2 and GRIP Greenland ice cores. - Nature, Vol. 366, 552-554.

Grootes, P. M., Stuiver, M. (1997): Oxygen 18/16 variability in Greenland snow and ice with 10^{-3} to 10^{5} -year time resolution. - Journal of Geophysical Research, Vol. 102 (C12), 26,455-26,470.

Haddad, G. A., Droxler, A.W. (1996). Metastable $CaCO_3$ dissolution at intermediate water depth of the Caribbean and western North Atlantic: Implication for intermediate water circulation during the past 200,000 years. - Paleoceanography, Vol. 11, 701-716.

Hagelberg, T. K., Bond, G., deMenocal, P. (1994): Milankovitch band forcing of sub-Milankovitch climate variability during the Pleistocene. - Paleoceanography, Vol. 9, 545-558.

Hansen, J., Lacis, A., Rind, D., Russel, G., Stone, P., Fung, I., Ruedy, R., Lerner, J. (1984): Climate sensitivity: analysis of feedback mechanisms. - in: J.E. Hansen and T.Takahashi (eds.), Climate Processes and Climate Sensitivity, Geophysical Monograph Series, Vol.29, 130-163.

Hecht, A.D. (1971): Morphological variation, diversity and stable isotope geochemistry of recent planktonic foraminifera from the North Atlantic. - PhD-thesis, Case Western Reserve University, 222 p.

Heinrich, H. (1988): Origin and consequences of cyclic ice-rafting in the northeast Atlantic Ocean during the past 130,000 years. - Quaternary Research, Vol. 29, 142-152.

Hemleben, C., Spindler, M., Anderson, O.R. (1989): Modern Planktonic Foraminifera. - Springer-Verlag New York-Berlin-Heidelberg-London-Paris-Tokyo, 335 p.

Hemleben, C., Zahn, R., Meischner, D. (1998): Karibik 1996 - Cruise No. 35, 18 April - 3 June 1996. - Meteor Berichte, 98-2, Leitstelle METEOR, Institut für Meereskunde der Universität Hamburg, 208 p.

Herguera, J. C., Berger W. H. (1991): Paleoproductivity from benthic foraminiferal abundance: Glacial to postglacial change in the west-equatorial Pacific. - Geology, Vol. 19, 1173-1176.

Herbert, T. D., Schuffert J. D. (subm.): Alkenone unsaturation estimates of sea-surface temperatures at ODP Site 1002 over a full glacial cycle. - Proceedings of the Ocean Drilling Program, Scientific Results Leg 165.

Hilbrecht, H. (1996): Extant planktic foraminifera and the physical environment in the Atlantic and Indian Oceans. - Mitteilungen aus dem Geologischen Institut der Eidgen. Technischen Hochschule und der Universität Zürich, Neue Folge. No. 300, Zürich, 93 p.

Houghton, R. W. (1991): The relationship of sea surface temperature to thermocline depth at annual and interannual time scales in the tropical Atlantic Ocean. - Journal of Geophysical Research, Vol. 96 (C8), 15,173-15,185.

Hughen, K., A., Overpeck, J.T., Lehman, S.J., Kashgarian, M. , Southon, J., Peterson, L.C., Alley, R., Sigman, D.M. (1996): Rapid climate changes in the tropical Atlantic region during the last deglaciation. - Nature, Vol. 380, 51-54.

Hughen, K.A., Overpeck, J.T., Lehman, S.J., Kashgarian, M., Southon, J., Peterson, L.C., Alley, R., Sigman, D.M. (1998): Deglacial changes in ocean circulation from extended radiocarbon calibration. - Nature , Vol. 391, 65-68.

Hutson, W. H. (1977): Transfer functions under no-analog conditions: Experiments with Indian Ocean planktonic foraminifera. - Quaternary Research, Vol. 8, 355-367.

Imbrie, J., Kipp, N., G. (1971): A new micropaleontological method for quantitative paleoclimatology: Application to a late Pleistocene Caribbean core. - in: Turekian, K.K. (ed.), The late Cenozoic glacial ages, Yale University Press, New Haven, 71-181.

Imbrie, J., van Donk, J., Kipp, N. G. (1973): Paleoclimatic investigation of a Late Pleistocene Caribbean deep-sea core: Comparison of isotopic and faunal methods. - Quaternary Research, Vol. 3, 10-38.

Imbrie, J., Hays, J.D., Martinson, D.G., McIntyre, A., Mix, A.C., Morley, J.J., Pisias, N.G., Prell, W.L., Shackleton, N.J. (1984): The orbital theory of Pleistocene climate: support from a revised chronology of marine $\delta^{18}O$ record. - in A.L. Berger (ed.), Milankovitch and Climate, D. Reidel Publishing Company, 269-305.

Imbrie, J. et al. (1990) : Specmap Archiv #1. - IGBP PAGES / World Data Center-A for Paleoclimatology Data Contribution Series #90-001, NOAA/NGDC Paleoclimatology Program, Boulder CO, USA.

Islebe, G. A., Hooghiemstra, H., van der Borg, K. (1995): A cooling event during the Younger Dryas Chron in Costa Rica. - Palaeogeography, Palaeoclimatology, Palaeoecology, Vol. 117, 73-80.

Ivanova, E. M., Conan, S. M.-H., Peeters, F.J.C., Troelstra, S.R. (1999): Living *Neogloboquadrina pachyderma* sin. and its distribution in the sediments from Oman and Somalia upwelling areas. - Marine Micropaleontology, Vol. 36, 91-107.

Jung, S. J. A. (1996): Wassermassenaustausch zwischen NE-Atlantik und Nordmeer während der letzten 300 000/80 000 Jahre im Abbild stabiler O- und C-Isotope. - Berichte aus dem Sonderforschungsbereich 313 "Sedimentation im Europäischen Nordmeer", Universität Kiel, Nr. 61, 104 p.

Jöreskog, K.G., Klovan, J.E., Rayment, R.A. (1976): Geological Factor Analysis. - Elsevier Scientific Publishing Company, Amsterdam-Oxford-New York, 178 p.

Keigwin, L. D., Jones,G . A. (1994): Western North Atlantic evidence for millennial-scale changes in ocean circulation and climate. - Journal of Geophysical Research, Vol. 99(C6), 12397-12410.

Keigwin, L. D., Boyle, E. A. (1999): Surface and deep ocean variability in the northern Sargasso Sea during marine isotope stage 3. - Paleoceanography, Vol. 14, 164-170.

Kennett, J. P., Ingram, L. (1995): A 20,000 year record of ocean circulation and climate change from the Santa Barbara Basin. - Nature, Vol. 377, 510-514.

Kennett, J.P., Srinivasan, M.S. (1983): Neogene planktonic foraminifera - A phylogenetic atlas. - Hutchinson Ross Publishing Company, 263 p.

Kiefer, T. (1998): Produktivität und Temperaturen im subtropischen Nordatlantik: zyklische und abrupte Veränderungen im späten Quartär (Productivity and temperatures in the subtropical North Atlantic: cyclic and abrupt changes during the Late Quaternary). - Berichte / Reports, Geol.Paläont.Inst.Univ.Kiel, Nr. 90, 127 p.

Kinder , T. H., Heburn, G. W., Green, A.W. (1985): Some aspects of the Caribbean circulation. - Marine Geology, Vol. 68, 25-52.

Kipp, N. (1976): New transfer function for estimating past sea surface conditions from sea bed distribution of planktonic foraminiferal assemblages in the North Atlantic. - in: R. M. Cline and J. D. Hays (eds.), Investigation of Late Quaternary Paleoceanography and Paleoclimatology, Memoirs of the Geological Society of America, 145, 3-41.

Klovan, J. E., Imbrie, J. (1971): An Algorithm and Fortran IV Program for Large-Scale Q-Mode Factor Analysis and Calculation of Factor Scores. - Mathematical Geology, Vol. 3, 61-77.

Labeyrie, L.D., Duplessy, J.C., Blanc, P.L. (1987): Variations in mode of formation and temperature of oceanic deep waters over the past 125,000 years. - Nature, Vol. 327, 477-482.

Laj, C., Mazaud, A., Duplessy, J.C. (1996): Geomagnetic intensity and ^{14}C abundance in the atmosphere and ocean during the past 50 kyr. - Geophysical Research Letters, 23, 2046-2048.

Le, J., Shackleton, N.J. (1992): Carbonate dissolution fluctuations in the western equatorial Pacific during the Late Qaternary. - Paleoceanography, Vol. 7, 21-42.

Le, J., Thunnell, R. C. (1996): Modelling planktic foraminiferal assemblages changes and application to sea surface temperatures estimation in the western equatorial Pacific Ocean. - Marine Micropaleontolgy, Vol. 28, 211-229.

Lebreiro, S.M., Moreno, J.C., McCave, I.N., Weaver, P.P.E. (1996): Evidence for 'Heinrich' layers off Portugal (Torre Seamount: 39°N, 12°W). - Marine Geology, Vol. 131, 47-56.

Lembke, L. (1997): Paläozeanographische Rekonstruktion karibischer Tiefenwassermassen anhand von stabilen Kohlenstoffisotopen aus Benthosforaminiferen und metastabilen Karbonatlösungsindizes. - unpubl. Master Thesis, University of Kiel, 77p.

Levitus, S. and Boyer, T.P.(1994): World Ocean Atlas 1994 Volume 4: Temperature. - NOAA Atlas NESDIS 4, US Department of Commerce, Washington, D.C. 117p.

Lin, H.-L., Peterson, L.C., Overpeck, J.T., Trumbore, S.E., Murray, D.W. (1997): Late Quaternary climate change from $\delta\ ^{18}O$ records of multiple species of planktonic foraminifera: High-resolution records from the anoxic Cariaco Basin, Venezuela. - Paleoceanography, Vol. 12, 415-427.

Little, M.G., Schneider, R.R., Kroon, D., Price, B., Summerhayes, C.P., Segl, M. (1997): Trade wind forcing of upwelling, seasonality, and Heinrich events as a response to sub - Milankovitch climate variability. - Paleoceanography, Vol. 12, 568-576.

Lund, D. C., Mix, A.C. (1998): Millenial-scale deep water oscillations: Reflections of the North Atlantic in deep Pacific from 10 to 60 ka. - Paleoceanography, Vol. 13, 10-19.

Manabe, S., Stouffer, R.J. (1988): Two stable equilibria of a coupled ocean-atmosphere model. - Journal of Climate, Vol. 1, 841-868.

Manabe, S., Stouffer, R.J. (1994): Multiple-century response of a coupled ocean-atmosphere model to an increase of atmospheric carbon dioxide. - Journal of Climatology, Vol. 7, 5-23.

Manabe, S., Stouffer, R. J. (1997): Coupled ocean-atmosphere model response to freshwater input: Comparison to Younger Dryas event. - Paleoceanography, Vol. 12, 321-336.

Marchitto, T.M., Curry, W. B., Oppo, D.W. (1998): Millenial-scale changes in North Atlantic circulation since the last glaciation. - Nature, Vol. 393, 557-561.

Martinez, J. I., Taylor, L., DeDeckker, P., Barrows, T. (1998): Planktonic foraminifera from the eastern Indian Ocean: distribution and ecology in relation to the Western Pacific Warm Pool (WPWP). - Marine Micropaleontology, Vol. 34, 121-151.

Martinez, P., Bertrand, P., Shimmield, G.B., Cochrane, K., Jorissen, F.J., Foster, J., Dignan, M. (1999): Upwelling intensity and ocean productivity changes off Cape Blanc (northwest Africa) during the last 70,000 years: geochemical and micropaleontological evidence. - Marine Geology, Vol. 158, 57-74.

Martinson , D.G., Pisias, N.G., Hays, J.D., Imbrie, J., Moore, T.C., Shackleton, N.J. (1987): Age dating and the orbital theory of the Ice Ages: Development of a high-resolution 0 to 300,000-year chronostratigraphy. - Quaternary Research, Vol. 27, 1-29.

Maslin, M.A., Shackleton, N.J., Pflaumann, U. (1995): Surface water temperature, salinity and density changes in the NE-Atlantic during the last 45,000 years: Heinrich events, deep water formation and climate rebounds. - Paleoceanography, Vol. 10, 527-544.

Marlowe, I. T., Brassell, S. C., Eglinton, G., Green, J.C. (1984): Long-chain alkenones and alkyl alkenoates and the fossil coccolith record of marine sediments. - Chemical Geology, Vol. 88, 349-375.

McAyeal, D.R. (1993): Binge/purge oscillations of the Laurentide ice sheet as a cause of the North Atlantic's 'Heinrich' events. - Paleoceanography, Vol. 8, 775-784.

McIntyre, A., Kipp, N. G., Bé, A.W.H., Crowley, T., Kellogg, T., Gardener, J.V., Prell, W.L., Ruddiman, W.F. (1976): Glacial North Atlantic 18,000 Years ago: A CLIMAP reconstruction. - Geological Society of America Memoir, No. 145, 43-76.

McIntyre, A., Ruddiman, W.F., Karlin, K., Mix, A.C. (1989): Surface water response of the equatorial Atlantic Ocean to orbital forcing. - Paleoceanography, Vol. 4, 19-55.

McIntyre, A., Molfino, B. (1996): Forcing of Atlantic equatorial and subpolar millennial cycles by precession. - Science, Vol. 274, 1867-1870.

Mekik, F., Loubere, P. (1999): Quantitative paleo-estimation: hypothetical experiments with extrapolation and the no-analog problem. - Marine Micropaleontology, Vol. 30, 225-248.

Metcalf, W. G. (1976): Caribbean-Atlantic water exchange through Anegada-Jungfern Passage. - Journal of Geophysical Research, Vol. 81, 6401-6409.

Milliman, J. D. (1974): Marine carbonates. - Springer Verlag, Berlin-Heidelberg-New York, 375 p.

Milliman, J. D., Meade, R. H. (1983): World-delivery of river sediment to the oceans. - Journal of Geology, Vol. 91, 1-21.

Mix, A. C., Ruddiman, W. F., McIntyre, A. (1986a): Quaternary paleoceanography of the tropical Atlantic, 1: Spatial variability of annual mean sea-surface temperatures, 0-20,000 years B.P. - Paleoceanography, Vol. 1, 43-66.

Mix, A. C., Ruddiman, W. F., McIntyre, A. (1986b): Late Quaternary paleoceanography of the Tropical Atlantic, 2: The seasonal cycle of Sea Surface Temperatures, 0-20,000 years B.P. - Paleoceanography, Vol. 1, 339-353.

Molfino, B., Kipp, N. G., Morley, J. J. (1982): Comparison of foraminiferal, coccolithophorid and radiolarian paleotemperature equations: Assemblage coherency and estimate concordancy. - Quaternary Research, Vol. 17, 279-313.

Müller, P. J., Kirst,G., Ruhland, G., von Storch, I., Rosell-Melé, A. (1998): Calibration of the alkenone paleotemperature index $U^{k'}_{37}$ based on core-tops from the eastern South Atlantic and the global ocean (60°N-60°S). - Geochimica et Cosmochimica Acta, Vol. 62, 1757-1772.

Müller-Karger, F. E., Aparicio Castrot, R.(1994): Mesoscale processes affecting phytoplankton abundance in the southern Carribbean Sea. - Continental Shelf Research, Vol. 14, 99-221.

Müller-Karger, F. E., Richardson, P. L., McGillicuddy, D. (1995): On the offshore dispersal of the Amazon's Plume in the North Atlantic: Comments on the paper by A. Longhurst, "Seasonal cooling and blooming in tropical oceans". - Deep-Sea Research, Vol. 42, 2127-2137.

Nadeau, M.-J., Schleicher, M, Grootes, P.M., Erlenkeuser, H., Gottdang, A., Mous, D.J.W., Sarnthein, M., Willkomm, H. (1997): The Leibniz-Labor AMS facility at the Christian-Albrechts University, Kiel, Germany. - Nuclear Instruments and Methods in Physics Research, B123, pp 22-30.

Nürnberg, D., Müller, A., Schneider, R.R. (submitted to Paleoceanography): Paleo-SST calculations in the equatorial East Atlantic from Mg/Ca ratios in planktic foraminifers - A comparison to SST estimates from Uk37 and Transfer Function .

Oppo, D.W., Raymo, M.E., Lohman, G.P., Mix, A.C., Wright, J.D., Prell, W.L. (1995): A $\delta^{13}C$ record of Upper North Atlantic Deep Water during the past 2.6 million years. - Paleoceanography, Vol. 10, 373-394.

Overpeck, J.T., Webb, T., Prentice, I.C. (1985): Quantitative interpretation of fossil pollen spectra: Dissimilarity coefficients and the method of modern analogs. - Quaternary Research, Vol. 23, 87-108.

Paillard, D., Labeyrie, L. (1994): Role of the thermohaline circulation in the abrupt warming after 'Heinrich' events. - Nature, Vol. 372, 162-164.

Peterson, L.C., Overpeck, J.T., Kipp, N.G., Imbrie, J. (1991): A high-resolution Late Quaternary upwelling record from the anoxic Cariaco Basin, Venezuela. - Paleoceanography,Vol. 6, 99-119.

Peterson, R. G., Stramma, L. (1991): Upper-level circulation in the South Atlantic Ocean. - Progress in Oceanography, Vol. 26, 1-73.

Petschick, R. (1996): MacDiff 3.2, Frankfurt a.M., Germany

Pflauman, U., Duprat, J., Pujol, C., Labeyrie, L.D. (1996): SIMMAX: A modern analog technique to deduce Atlantic sea surface temperatures from planktonic foraminifera in deep-sea sediments. - Paleoceanography, Vol. 11, 15-35.

Pflaumann, U., Jian, Z. (1999): Modern distribution patterns of planktonic foraminifera in the South China Sea and western Pacific: a new transfer technique to estimate regional sea-surface temperatures. - Marine Geology, Vol. 156, 41-83.

Prahl, F.G., Wakeham, S.G. (1987): Calibration of unsaturation patterns in long-chain ketone compositions for paleotemperature assessment. - Nature, Vol. 330, 367-369.

Prell, W. L., Hays, J.D. (1976): Late Pleistocene faunal and temperature patterns of the Colombia Basin, Caribbean Sea.- Geological Society of America Memoir, No. 145, 201-220.

Prell, W.L. (1985): The stability of low latitude sea surface temperatures: An evaluation of the CLIMAP reconstruction with emphasis on positive SST anomalies. - U.S. DOE Rep. TR 025, 60 p.

Pujol, C., Vergnaud Grazzini, C. (1995): Distribution patterns of live planktic foraminifers as related to regional hydrography and productive systems of the Mediterranean Sea. - Marine Micropaleontology, Vol. 25, 187-212.

Rahmstorf, S. (1994): Rapid climate transitions in a coupled ocean-atmosphere model. - Nature, Vol. 372, 82-85.

Rahmstorf, S. (1995): Bifurcations of the Atlantic thermohaline circulation in response to changes in the hydrological cycle. - Nature, Vol. 378, 145-149.

Rasmussen, T. L., Thomsen, E., van Weering, T.C.E., Labeyrie, L. (1996): Rapid changes in surface and deep water conditions at the Faeroe Margin during the last 58,000 years. - Paleocenography, Vol. 11, 757-771.

Ravelo, A.C., Fairbanks, R.G., Philander, S.G.H. (1990): Reconstructing tropical Atlantic hydrography using planktonic foraminifera and an ocean model. - Paleoceanography, Vol. 5, 409-431.

Reijmer, J.J.G., Schlager, W.; Droxler, A.W. (1988): ODP Site 632: Pliocene-Pleistocene sedimentation in a Bahamian Basin. - in: Austin, J.A., Schlager, W. et al. (eds.), Proc.ODP Prog., Sc.Res., Vol. 101, 213-220.

Rowe, G. T. (1983): Biomass and production of deep-sea macrobenthos.-in: G. T. Row (ed.): Deep-sea Biology, New York, John Wiley.

Ruddiman, W.F. (1997): Tropical Atlantic terrigeneous fluxes since 25,000 yrs BP. - Marine Geology, Vol. 136, 189-207.

Rühlemann,C., Mulitza, S., Müller, P.J., Wefer, G., Zahn, R. (1999): Tropical Atlantic warming during conveyor slowdown. - Nature, Vol. 402, 511-514.

Saito, T., Thompson, P.R., Breger, D. (1981): Systematic index of recent and Pleistocene planktonic foraminifera. - University of Tokyo Press, 190 p.

Sarnthein, M., Pflaumann, U., Ross, R., Tiedemann, R., Winn, K. (1992): Transfer functions to reconstruct ocean paleoproductivity: a comparison. - in: C.P. Summerhayes, W.L. Prell and K. C. Emeis (eds.), Upwelling Systems: Evolution since the Early Miocene, Geological Society, Special Publication, No. 64, 411-427.

Sarnthein, M., Winn,K., Jung, S.J.A., Duplessy, J.-C., Labeyrie, L., Erlenkeuser, H., Ganssen, G. (1994): Changes in east Atlantic deepwater circulation over the last 30,000 years: Eight time slice reconstructions. - Paleoceanography, Vol. 9, 209-267.

Sarnthein, M., Jansen, E., Weinelt, M., Arnold, M., Duplessy, J.C., Erlenkeuser, H., Flatoy, A., Johannessen, G., Johannessen, T., Jung, S.; Koc, N., Labeyrie, L., Maslin, M., Pflaumann, U., Schulz, H. (1995): Variations in Atlantic surface ocean paleoceanography, 50°-80° N: A time-slice record of the last 30,000 years. - Paleoceanography, Vol. 10, 1063-1094.

Sautter, L. A., Thunell, R. C. (1991): Seasonal Variability in the $\delta\ ^{18}O$ and $\delta\ ^{13}C$ of planktonic foraminifera from an upwelling environment: Sediment trap results from the San Pedro Basin, Southern California Bight. - Paleoceanography, Vol. 6, 307-334.

Schleicher, M., Grootes, P. M., Nadeau, M.-J., Schoon, A. (1998): The carbonate ^{14}C background and its components at the Leibniz AMS facility. - Radiocarbon, Vol. 40, No. 1., 85-94.

Schulz, H., von Rad, U., Erlenkeuser, H. (1998): Correlation between Arabian Sea and Greenland climate oscillations of the past 110,000 years. - Nature, Vol. 393, 54-57.

Schneider, R.R., Müller, P.J., Ruhland, G., Meincke, G., Schmidt, H., Wefer, G. (1996): Late Quaternary surface temperatures and productivity in the East-Equatorial South Atlantic: Response to changes in Trade/Monsoon wind forcing and surface water advection. - in: G. Wefer et al. (eds.), The South Atlantic: Present and past circulation, Springer Verlag, Berlin-Heidelberg, 527-551.

Schrag, D.P., Hampt, G., Murray, D.W. (1996): Pore fluid constraints on the temperature and oxygen isotopic composition of the Glacial Ocean. - Science, Vol. 272, 1930-1932.

Schott, F., Molinari, R. L. (1996): The western boundary circulation of the subtropical warmwatersphere. - in: W. Krauss (ed.), The Warmwatersphere of the North Atlantic Ocean. Berlin, Stuttgart, Gebrüder Borntraeger, 229-252.

Short, D.A., Mengel, J.G., Crowley, T.J., Hyde, W.T., North, G.R. (1991): Filtering of Milankovitch cycles by Earth's geography. - Quaternary Research, Vol. 35, 157-173.

Sikes, E. L., Keigwin, L.D. (1994): Equatorial Atlantic sea surface temperature for the last 30 kyrs: A comparison of $U^{k'}_{37}$, $\delta\ ^{18}O$ and foraminiferal assemblage temperature estimates. - Paleoceanography, Vol. 9, 31-45.

Stalcup, M. C., Metcalf, W. G., Zemanovic, M. (1971): Current measurements in the lesser Antilles. - Woods Hole Oceanographic Institution.

Stocker, T. F., Wright, D.G., Mysak, L. A. (1992): A zonally averaged, coupled ocean-atmosphere model for paleoclimate studies. - Journal of Climatology, Vol. 5, 773-797.

Stocker, T. F. (subm. to Nature): The role of the deep ocean circulation for past and future climate change.

Stramma, L. (1991): Geostrophic transport of the South Equatorial Current in the Atlantic. - Journal of Marine Research, Vol. 49, 281-294.

Stramma, L., Schott, F. (1996): Western equatorial circulation and interhemispheric exchange. - in: W. Krauss (ed.), The warmwatersphere of the North Atlantic Ocean. Berlin, Stuttgart, Gebrüder Borntraeger, 195-227.

Stüber, A. (1999): Spätpleistozäne Variabilität der Zwischenwasserzirkulation im subtropischen Westatlantik auf glazial-interglazialen und suborbitalen Zeitskalen: Reconstruktion anhand stabiler Kohlenstoffisotope und Spurenmetallverhältnissen in kalkschaligen Benthosforaminiferen. - unpubl. PhD Thesis, Christian Albrechts University Kiel.

Stuiver, M., Reimer, P. J. (1993): Extended ^{14}C database and revised CALIB radiocarbon calibration program. - Radiocarbon, Vol. 35, 215-230.

Stuiver, M., Reimer, P.J., Bard, E., Beck, J.W., Burr, G.S., Hughen, K.A., Kromer, B., McCormac, F.G., v. d. Plicht, J., Spurk, M. (1998): INTCAL98 Radiocarbon age calibration 24,000 - 0 cal BP. - Radiocarbon, Vol. 40, 1041-1083.

Sturges, W. (1975): Mixing of renewal water flowing into the Caribbean Sea. - Journal of Marine Research, Vol. 33, 117-130.

Taylor, K.C., Hammer, C.U., Alley, R.B., Clausen, H.B., Dahl-Jensen, D., Gow, A.J., Gundestrup, N.S., Kipfstuhl, J., Moore, J.C., Waddington, E.D. (1993): Electrical conductivity measurements from GISP2 and GRIP Greenland ice cores. - Nature, Vol. 366, 549-552.

Thomas, E., Booth, L., Maslin, M., Shackleton, N.J. (1995): Northeastern benthic foraminifera during the last 45,000 years: Changes in productivity seen from the bottom up. - Paleoceanography, Vol. 10, 545-562.

Thunell, R.C., Honjo, S. (1981): Calcite dissolution and the modification of planktonic foraminiferal assemblage. - Marine Micropaleontology, Vol. 6, 169-182.

Tucker, M. (1996): Methoden der Sedimentologie. - Enke Verlag, Stuttgard, 365 p.

Ufkes, E., Zachariasse, W.J. (1993): Origin of coiling differences in living Neogloboquadrinids in the Walvis Bay region, off Namibia, southwest Africa. - Micropaleontology, Vol. 39, 283-287.

Ufkes, E., Jansen, J.H., Brummer, G.-J.A (1998): Living planktonic foraminifera in the eastern South Atlantic during spring: indicators of water masses, upwelling and the Congo (Zaire) River plume. - Marine Micropaleontology, Vol. 33, 27-53.

van der Plas, L., Tobi, A. C. (1965):A chart for judging the reliability of point counting results. - American Journal of Science, Vol. 263, 87-90.

Vergnaud-Grazzini, C., Vénec-Peryré, M.T., Caulet, J.P., Lerasle, N. (1995): Fertility tracers and monsoon forcing at an equatorial site off Somali Basin (Northwest Indian Ocean). - Marine Micropaleontology, Vol. 26, 137-152.

Voelker, A. H. L., Sarnthein,M., Grootes, P.M., Erlenkeuser, H., Laj, C., Mazaud, A., Nadeau, M.-J., Schleicher, M. (1998): Correlation of marine ^{14}C ages from the Nordic Seas with GISP2 isotope record: Implications for radiocarbon calibration beyond 25 ka BP. - Radiocarbon, Vol. 40, 517-534.

Vogelsang, E. (1990): Paläo-Ozeanographie des Europäischen Nordmeeres an Hand stabiler Kohlenstoff- und Sauerstoffisotope. - Berichte aus dem Sonderforschungsbereich 313 "Sedimentation im Europäischen Nordmeer" / Reports SFB 313, Christian-Albrechts-Universität zu Kiel, No. 23., 136 p.

Volkmann, J. K., Eglinton, G., Corner, E.D.S., Sargent, J.R. (Eds.) (1980): Novel unsaturated straight-chain C_{37}-C_{39} methyl and ethyl ketones in marine sediments and a coccolithophore *Emiliania huxleyi*. - Advances in Organic Geochemistry 1979, Pergamon Press.

Wang, L.,Sarnthein, M., Duplessy, J.C., Erlenkeuser, H., Jung, S., Pflaumann, U. (1995). Paleo sea surface salinities in the low-latitude Atlantic: The $\delta^{18}O$ record of *Globigerinoides ruber* (white). - Paleoceanography, Vol. 10, 749-761.

Watkins, J. A., Mix, A.C. (1998): Testing the effects of tropical temperature, productivity, and mixed-layer depth on foraminiferal transfer functions. - Paleoceanography, Vol. 13, 96-105.

Weaver, A. J., Hughes, T. M.C. (1994): Rapid interglacial climate fluctuations driven by North Atlantic ocean circulation. - Nature, Vol. 367, 447-450.

Webb, R.S., Lehman, S.J., Rind, D.H., Healy, R.J. (1994): Ocean heat transports and LGM cooling (abstract). - EOS Trans. AGU, 75 (44), Fall Meeting Supplement, p. 381.

Willamowski, C. (1999): Verteilungsmuster von Spurenmetallen im glazialen Nordatlantik: Rekonstruktion der Nährstoffbilanz anhand von Cadmiumkonzentrationen in kalkschaligen Foraminiferen. - Geomar Report, No. 79, GEOMAR Research Center for Marine Geosciences, Kiel, 86 p.

Wüst, G. (1964): Stratification and Circulation of the Antillean-Caribbean Basins, Part I, Spreading and Mixing of the Water Types with an Oceanographic Atlas. - New York, Columbia University Press.

Zahn, R., Schönfeld, J., Kudrass, H.-R., Park, Myong-Ho, Erlenkeuser, H., Grootes, P. (1997): Thermohaline instability in the North Atlantic during meltwater events: Stable isotope and ice-rafted detritus records from core So75-26KL, Portuguese margin. - Paleoceanography, Vol. 12, 696-710.

8 Appendix

Appendix I	Core M35003-4, stable isotopes
Appendix II	Core M35003-4, $CaCO_3$ and TOC
Appendix III	Core M35003-4, XRD measurements
Appendix IV	Core M35003-4, planktonic foraminiferal census counts
Appendix V	Core M35003-4, planktonic foraminiferal assemblages (factors) and TFT SST estimates
Appendix VI	Core M35003-4, MAT SST estimates
Appendix VII	Core M35027-1, planktonic foraminiferal census counts
Appendix VIII	Core M35027-1, planktonic foraminiferal assemblages (factors) and TFT SST estimates
Appendix IX	Core M35003-4, MAT SST estimates
Appendix X	Planktonic foraminiferal census counts of Caribbean surface samples

Data available on: http://www.pangaea.de/Projects/GEOMAR/

Abbreviations	species
aeq	*Globigerinella aequilateralis* (Brady) *(Globigerinella siphonifera* (d'Orbigny 1839)
bul	*Globigerina bulloides* (d'Orbigny, 1826)
cal	*Globigerinella calida* (Parker, 1962)
cav	*Globorotalia cavernula* (Bé, 1967)
con	*Globigerinoides conglobatus* (Brady, 1879)
cra	*Globorotalia crassaformis* (Galloway und Whissler 1927).
deh	*Sphaeroidinella dehiscens* (Parker and Jones, 1865)
dig	*Globigerinella (Beella) digitata* (Brady, 1879)
dut	*Neogloboquadrina dutertrei* (d'Orbigny, 1839) = *Globigerina eggeri*
fal	*Globigerina falconensis* (Blow, 1959)
glu	*Globigerinita glutinata* (Egger, 1895)
hirs	*Globorotalia hirsuta* (d'Orbigny, 1839)
humi	*Turborotalita humilis* (Brady, 1884)
inf	*Globorotalia inflata* (d'Orbigny, 1839)
men	*Globorotalia menardii* (d'Orbigny, 1865) = *Globorotalia cultrata*
nit	*Candeina nitita* (d'Orbigny, 1839)
obl	*Pulleniatina obliquiloculata* (Parker and Jones, 1865)
pal	*Neogloboquadrina pachyderma* (sinistral) (Ehrenberg, 1861)
par+	*N. pachyderma* (dextral) + PD/I
qul	left coiling *T. quinqueloba*
qur	right coiling *T. quinqueloba*
qui	*Turborotalita quinqueloba* (Natland 1938) = *Globigerina quinqueloba*
rur	*Globigerinoides ruber* (pink) (d'Orbigny, 1839)
ruw	*Globigerinoides ruber* (white) (d'Orbigny, 1839)
rus	*Globorotalita rubescens* (white + red) (Hofker, 1965) = *Globigerinoides rubescens*
tri	*Globigerinoides sacculifer (*trilobus*)* = *Globigerinoides quadrilobatus* (d'Orbigny), without sac
sac	*Globigerinoides sacculifer* (sacculifer) (Brady, 1877).
sci	*Globorotalia scitula* (Brady, 1882)
ten	*Globoturborotalita tenella* (Parker, 1958) = *Globigerinoides tenellus*
trl	*Globorotalia truncatulinoides* (sinistral) (d'Orbigny, 1839)
trr	*Globorotalia truncatulinoides* (dextral) (d'Orbigny, 1839)
tum	*Globorotalia tumida* (Brady, 1877)
univ	*Orbulina universa* (d'Orbigny, 1839)
mentum	*G.menardii - G.tumida* group
uvu	*Globigerinita uvula* (Ehrenberg, 1861)
pdi	Intergrades between *N. pachyderma* (dextral) and *N. dutertrei.* (Kipp, 1976) .

M35003-4, stable isotopes

	Cibicidoides sp.		*Uvigerina* sp.			*Cibicidoides* sp.		*Uvigerina* sp.	
depth (cm)	$\delta^{13}C$ ‰	$\delta^{18}O$ ‰	$\delta^{13}C$ ‰	$\delta^{18}O$ ‰	depth (cm)	$\delta^{13}C$ ‰	$\delta^{18}O$ ‰	$\delta^{13}C$ ‰	$\delta^{18}O$ ‰
10	1.15	2.23			365	1.14	3.41		
15	0.68	2.25			370	1.14	3.43		
20	1.04	2.10			375	1.15	3.41		
30	0.31	2.43			380	1.29	3.70		
35	1.18	2.20			385	1.23	3.73		
40	1.08	2.18			390	1.24	3.47		
50	0.99	2.07			395	1.37	3.63		
55	0.83	2.24			400	1.22	3.73	-0.940	4.380
60	1.19	2.13			405	1.18	3.36		
65	0.93	2.16			410	1.02	3.98	-0.700	4.260
70	0.91	2.05			415	1.35	3.67		
80	1.20	2.14			420	1.23	3.82	-0.700	4.500
85	1.22	2.12			425	1.31	3.61		
90	1.18	2.07			430	1.32	3.69	-0.750	4.250
95	1.30	2.27			440			-0.890	4.830
100	1.07	2.06			450	1.05	3.27	-1.080	4.400
105	1.12	2.16			460	1.14	3.21	-0.620	3.980
110	1.09	2.21			470			-0.910	3.990
115	0.98	2.11			480			-0.760	4.070
120	1.12	2.27			490			-0.940	4.220
125	0.91	2.21			500			-1.050	4.270
130	1.04	2.29			510			-0.775	3.649
135	0.60	1.32			520			-0.912	3.947
140	0.94	2.07			530			-0.935	3.408
145	0.88	2.18			540	0.91	3.53	-0.108	3.954
150	1.01	2.20			560			-0.765	3.577
155	1.10	2.09			580			-0.998	3.751
160	0.95	2.33			600	0.86	2.92	-1.097	3.804
165	0.84	2.04			620	1.12	3.51	-0.570	3.900
170	0.89	2.39			630	1.16	3.40	-0.690	3.830
175	0.78	2.20			640			-0.920	4.060
180	0.87	2.57			650			-0.810	3.700
185	0.72	2.50			660			-1.060	4.110
195	0.75	2.42			670	1.06	3.22	-1.030	4.170
200	0.68	2.63			680	1.12	3.44	-1.020	3.930
205	0.79	2.29			690			-0.940	4.260
210	0.98	2.13			700			-0.940	4.090
215	0.69	2.41			710			-0.990	4.310
220	0.57	2.52			720			-0.930	4.080
225	0.68	2.62			730			-0.780	3.860
235	0.57	2.89			740	0.87	2.90	-0.920	3.800
240	0.52	2.37			750			-0.970	4.140
245	0.70	3.02			760			-0.910	4.160
250	0.62	2.92			770			-1.150	4.080
255	0.68	2.92			780			-1.110	4.100
260	0.79	3.08			790			-0.990	4.170
265	0.61	2.94			800			-0.950	4.100
270	0.53	3.19			810			-1.260	4.060
275	0.53	2.75			820			-1.080	4.210
275	0.45	2.59			830			-1.030	4.080
280	0.46	3.35			840	0.80	2.82	-1.030	4.010
280	0.43	2.34			850			-1.010	4.090
285	0.95	3.28			860			-1.100	4.190
285	0.41	1.98			870	0.76	3.26	-0.930	4.030
290	0.52	2.87			880	0.58	2.75	-1.170	3.890
295	0.52	2.95			890	0.84	3.47	-0.780	3.720
295	0.36	2.71			900	1.23	3.45	-0.650	4.080
300	1.22	3.72			910	1.03	3.56	-1.220	4.040
305	1.28	3.78			920	0.73	3.18	-1.510	4.270
305	1.03	3.21			930			-0.830	4.400
310	1.25	3.73			940	0.75	2.66	-0.710	3.870
315	1.33	3.70			950			-0.870	3.960
320	1.21	3.82			955			-0.780	4.150
325	1.21	3.80							
330	1.19	3.80							
335	1.31	3.70							
340	1.20	3.70							
350	1.36	3.57							
355	1.10	3.75							
360	1.25	3.40							

depth (cm)	TOC (wt.-%)	CaCO3 (wt.-%)	depth (cm)	TOC (wt.-%)	CaCO3 (wt.-%)	depth (cm)	TOC (wt.-%)	CaCO3 (wt.-%)
5	0.90	11.9	600	0.84	11.6	950	0.66	2.8
15	0.86	11.1	605	0.49	21.8	955	0.71	2.7
25	0.80	9.4	610	0.77	13.7			
35	0.69	9.7	615	0.63	17.5			
45	0.49	7.8	620	0.32	24.5			
55	0.76	11.3	625		21.1			
65	0.92	10.4	630	0.47	20.3			
75	0.67	7.4	635	0.58	14.7			
85	0.81	11.9	640		19.8			
95	0.85	12.3	645	0.90	14.3			
105	0.61	14.3	650	0.58	19.3			
115	0.78	13.9	655	0.38	19.3			
125	0.66	14.8	660	0.69	15.5			
135	0.54	15.8	665	0.77	13.8			
145	0.60	12.6	670	0.61	18.1			
155	0.80	11.0	675	0.71	15.2			
165	0.62	11.9	680	0.46	20.0			
175	0.71	11.4	685	0.60	15.4			
185	0.72	10.9	690	0.80	11.9			
195	0.80	10.2	695	0.79	10.6			
205	0.79	10.7	700	0.75	12.7			
215	0.53	16.7	705	0.75	10.2			
225	0.46	22.0	710	0.69	9.5			
235	0.57	12.4	715	0.73	8.7			
245	0.66	11.2	720	0.83	8.5			
255	0.75	10.1	725	0.80	8.0			
265	1.42	5.6	730	0.79	11.1			
275	0.77	11.4	735	0.76	11.2			
285	0.54	22.0	740	0.69	18.9			
295	0.27	28.1	745	0.34	23.7			
305	0.37	16.4	750	0.25	19.5			
315	0.49	20.6	755	0.61	13.5			
325	0.56	16.3	760	0.62	11.4			
335	0.50	14.8	765	0.62	13.8			
345	1.18	9.2	770	0.65	14.6			
355	0.41	17.2	775	0.65	12.2			
365	0.45	16.6	780	0.67	13.7			
375	0.53	14.5	785	0.64	12.1			
385	0.46	21.7	790	0.67	11.0			
395	0.51	13.4	795	0.74	10.7			
405	0.39	18.1	800	0.75	11.9			
415	0.34	13.8	805	0.78	11.0			
425	0.47	17.0	810	0.75	10.3			
435	0.60	13.9	815	0.76	9.4			
445	0.42	22.9	820	0.70	9.7			
455	0.68	16.0	825	0.79	9.2			
465	0.39	25.0	830	0.67	9.5			
475	0.47	15.0	835	0.50	9.0			
485		20.7	840	0.71	12.1			
495		18.5	845	0.47	20.1			
500		19.2	850	0.50	16.1			
505		19.2	855	0.42	21.0			
510		25.3	860	0.66	14.1			
515		15.2	865	0.64	16.9			
520		18.1	870	0.67	14.6			
525		23.7	875	0.61	14.3			
530		20.5	880	0.33	23.9			
535		14.8	885	0.19	18.6			
540		15.2	890	0.25	18.1			
545	0.88	10.2	895	0.35	15.7			
550	0.47	21.2	900	0.59	16.1			
555	0.70	12.4	905	0.38	16.4			
560	0.45	24.6	910	0.47	9.6			
565	0.41	19.7	915	0.35	10.4			
570	0.65	12.3	920	0.57	6.3			
575	0.77	11.5	925	0.64	6.2			
580	0.83	12.2	930	0.74	6.7			
585	0.88	9.3	935	0.71	2.7			
590	0.93	12.8	940	0.64	10.5			
595	0.92	9.2	945	1.10	-0.8			

Teufe	LMC (% of $CaCO_3$)	HMC (% of $CaCO_3$)	Aragonite (% of $CaCO_3$)	Teufe	LMC (% of $CaCO_3$)	HMC (% of $CaCO_3$)	Aragonite (% of $CaCO_3$)	Teufe	LMC (% of $CaCO_3$)	HMC (% of $CaCO_3$)	Aragonite (% of $CaCO_3$)
20	62.75	6.70	30.55	435	44.21	12.96	42.82	825	69.67	3.94	26.39
25	68.46	5.67	25.87	440	38.97	21.99	39.04	830	46.95	1.45	51.60
30	59.57	3.66	36.78	445	37.03	20.73	42.24	835	76.54	3.00	20.46
35	75.49	3.66	15.74	450	44.46	11.18	44.36	885	57.98	11.79	30.22
40	69.90	6.41	23.68	455	37.78	16.59	45.62	890	49.81	23.59	26.59
45	64.87	4.11	31.02	460	31.03	24.73	44.24	895	49.79	17.35	32.86
55	62.25	4.75	33.00	465	33.89	21.53	44.58	900	45.44	16.57	37.99
60	65.45	3.08	31.47	470	38.14	12.83	49.03	905	50.66	14.25	35.10
65	65.19	4.75	30.06	475	40.60	11.25	48.15	910	56.08	7.68	36.24
70	52.94	5.53	41.53	480	38.88	15.63	45.49	915	57.99	5.09	36.92
75	72.24	1.35	14.28	490	45.29	13.52	41.18	920	48.50	3.36	48.14
80	61.29	2.30	36.40	495	44.48	8.62	46.90	925	47.71	1.86	50.43
85	62.12	4.54	33.33	515	56.60	8.29	35.10	930	56.20	3.79	40.00
90	61.23	2.17	36.60	520	44.51	9.38	46.11	935	40.44	5.07	54.49
95	69.94	2.44	27.61	525	45.73	14.04	40.23	940	51.67	10.94	37.39
100	59.78	4.62	35.60	530	46.12	9.31	44.57	945	42.76	5.62	51.62
105	63.80	3.72	32.48	535	52.72	7.70	39.58	950	42.60	1.75	55.65
110	58.66	4.25	37.09	535	56.54	7.66	35.81	955	39.62	2.34	58.04
120	57.57	2.63	39.80	540	57.86	10.30	31.84				
125	66.07	2.81	31.13	545	48.41	11.89	39.70				
130	60.40	4.69	34.91	550	44.22	10.24	45.54	HMC= High Magnesium Calcite			
135	58.19	4.46	37.35	555	49.85	10.96	39.20	LMC= Low Magnesium Calcite			
140	53.80	8.41	37.79	560	44.03	19.03	36.94	A= Aragonite			
145	59.43	6.03	34.54	565	49.65	14.98	35.38				
150	58.07	3.62	38.31	570	52.85	5.28	41.87				
160	45.69	11.96	42.35	575	51.91	4.77	43.32				
170	65.39	4.14	30.46	580	57.10	10.85	32.05				
175	57.79	6.93	35.28	585	50.39	6.55	43.07				
180	55.31	11.16	33.52	590	51.65	12.50	35.85				
185	58.81	4.58	36.61	595	54.89	10.58	34.53				
190	63.17	9.06	27.76	600	46.98	17.89	35.13				
195	58.51	7.81	33.68	605	60.80	6.60	32.60				
200	55.06	6.13	38.81	610	46.73	10.30	42.98				
205	51.04	7.76	41.20	615	49.58	14.23	36.20				
210	50.16	14.54	35.29	625	45.40	13.34	41.25				
215	45.45	13.23	41.32	630	46.49	13.30	40.20				
220	37.65	15.67	46.68	635	57.82	8.31	33.87				
225	38.06	15.18	46.76	640	52.46	12.73	34.81				
235	51.54	6.01	42.45	645	44.91	16.50	38.58				
240	42.51	14.67	42.82	650	53.02	10.66	36.32				
245	56.28	12.12	31.60	660	53.08	5.65	41.28				
265	47.13	14.07	38.80	665	61.86	7.21	30.93				
270	51.13	8.48	40.39	670	47.34	12.16	40.51				
275	50.12	7.96	41.92	675	51.15	10.70	38.15				
280	40.41	15.98	43.61	680	52.53	11.04	36.43				
285	39.35	20.95	39.69	685	52.11	5.16	42.72				
290	45.01	20.03	34.96	690	60.07	7.68	32.25				
300	42.02	25.93	32.05	695	56.48	3.94	39.59				
305	45.98	9.26	44.76	700	53.28	9.31	37.41				
310	54.07	11.80	34.13	705	52.38	7.91	39.71				
315	44.02	12.49	43.49	710	51.71	7.11	41.18				
320	50.91	7.64	41.45	715	49.58	7.36	43.06				
325	42.53	12.09	45.38	720	49.30	6.01	44.69				
335	43.52	11.23	45.25	725	50.12	6.54	43.34				
340	40.23	15.11	44.66	730	40.77	6.47	52.76				
345	45.82	11.80	42.38	735	44.58	7.58	47.84				
350	41.41	19.21	39.38	740	47.40	14.98	37.62				
355	43.74	17.01	39.26	745	48.16	18.11	33.72				
360	47.35	13.18	39.47	750	50.62	11.12	38.26				
365	43.44	13.40	43.16	755	55.80	11.39	32.81				
370	43.12	14.99	41.89	760	53.11	9.71	37.18				
375	44.55	15.86	39.59	765	55.77	8.17	36.06				
380	37.53	20.50	41.97	770	35.69	48.98	15.33				
385	37.69	20.17	42.15	775	38.32	34.66	27.01				
390	36.33	21.16	42.50	780	58.76	5.68	35.55				
395	43.61	10.54	45.84	785	62.15	11.18	26.66				
400	38.75	21.33	39.92	790	60.90	8.09	31.01				
405	39.21	22.23	38.56	795	59.20	2.45	38.35				
410	36.30	25.66	38.04	800	60.45	2.53	37.02				
415	41.39	12.96	45.65	805	60.83	4.23	34.94				
420	36.97	18.28	44.74	810	58.89	5.65	35.46				
425	39.75	12.40	47.85	815	60.16	7.54	32.29				
430	39.22	14.28	46.50	820	59.60	1.80	38.60				

depth (cm)	Lat	Long	water depth (m)	counted	aeq	bul	cal	cav	con	cra	deh	dig	dut	fat	glu	hir	hum	inf
0	12.0830	-61.2330	1299	358	4.8	0.0	0.0	0.0	1.0	0.0	0.2	0.0	8.8	0.0	7.2	0.0	0.0	0.0
5	12.0830	-61.2330	1299	508	4.3	0.6	0.3	0.0	0.9	0.0	0.0	0.0	9.4	0.0	5.7	0.0	0.0	0.0
10	12.0830	-61.2330	1299	439	6.2	0.2	0.0	0.0	0.5	0.0	0.2	0.0	13.7	0.0	5.9	0.0	0.0	0.0
15	12.0830	-61.2330	1299	441	1.8	0.7	0.5	0.0	0.2	0.0	0.0	0.0	9.8	0.0	6.3	0.0	0.0	0.0
20	12.0830	-61.2330	1299	526	7.3	0.3	0.5	0.0	0.7	0.0	0.0	0.3	9.0	0.0	9.2	0.0	0.0	0.0
25	12.0830	-61.2330	1299	593	3.7	0.5	0.5	0.0	1.3	0.3	0.0	0.2	13.3	0.0	8.9	0.0	0.0	0.0
30	12.0830	-61.2330	1299	710	4.1	1.0	0.0	0.0	0.0	0.0	0.0	0.3	9.2	0.1	7.7	0.1	0.0	0.0
35	12.0830	-61.2330	1299	495	3.6	1.0	0.4	0.0	0.4	0.6	0.0	0.0	6.3	0.0	7.9	0.0	0.2	0.0
40	12.0830	-61.2330	1299	432	6.3	1.8	0.1	0.0	0.1	0.1	0.0	0.0	4.7	0.0	12.0	0.0	0.0	0.0
45	12.0830	-61.2330	1299	509	2.8	0.6	0.0	0.0	0.2	0.2	0.0	0.0	6.1	0.0	10.0	0.0	0.0	0.0
50	12.0830	-61.2330	1299	532	6.6	3.4	0.3	0.0	0.4	0.3	0.1	0.0	6.3	0.0	9.1	0.0	0.0	0.0
55	12.0830	-61.2330	1299	485	3.5	0.4	0.2	0.0	1.2	0.8	0.2	0.0	4.7	0.2	9.1	0.0	0.0	0.0
60	12.0830	-61.2330	1299	403	6.0	0.5	0.0	0.0	0.2	0.5	0.0	0.0	4.7	0.0	10.9	0.0	0.0	0.0
65	12.0830	-61.2330	1299	660	2.7	0.4	1.3	0.0	0.5	0.0	0.2	0.2	5.2	0.2	10.6	0.2	0.0	0.0
70	12.0830	-61.2330	1299	380	5.0	1.8	1.1	0.0	0.3	0.3	0.3	0.0	7.1	0.0	8.4	0.0	0.0	0.0
75	12.0830	-61.2330	1299	704	4.4	1.6	0.4	0.0	0.0	0.3	0.3	0.0	6.7	0.0	8.5	0.0	0.0	0.0
80	12.0830	-61.2330	1299	483	5.2	3.3	1.0	0.0	0.2	0.6	0.2	0.0	3.7	0.0	15.1	0.0	0.0	0.2
85	12.0830	-61.2330	1299	386	3.6	1.0	0.0	0.0	1.0	0.3	0.0	0.0	3.4	0.0	9.3	0.0	0.0	0.0
90	12.0830	-61.2330	1299	489	5.7	1.6	0.8	0.0	0.4	0.4	0.2	0.0	2.7	0.0	10.4	0.0	0.0	0.0
95	12.0830	-61.2330	1299	385	3.0	2.8	0.8	0.0	0.9	0.0	0.2	0.0	3.2	0.0	7.6	0.0	0.0	0.4
100	12.0830	-61.2330	1299	520	2.1	2.1	1.7	0.0	1.0	0.0	0.0	0.2	3.5	0.0	6.7	0.0	0.0	0.0
105	12.0830	-61.2330	1299	392	2.0	2.3	0.3	0.0	1.0	0.0	0.0	0.0	3.1	0.0	7.7	0.0	0.0	0.0
110	12.0830	-61.2330	1299	533	1.7	1.5	1.1	0.0	0.4	0.0	0.0	0.2	2.1	0.0	5.6	0.0	0.0	0.0
115	12.0830	-61.2330	1299	387	3.0	2.2	0.4	0.0	0.2	0.2	0.0	0.0	1.8	0.0	8.2	0.0	0.0	0.0
120	12.0830	-61.2330	1299	588	2.3	0.8	1.8	0.0	0.7	0.0	0.0	0.2	4.3	0.0	8.7	0.0	0.0	0.0
125	12.0830	-61.2330	1299	454	4.8	2.2	0.4	0.0	0.2	0.0	0.0	0.2	3.5	0.0	8.6	0.0	0.0	0.0
130	12.0830	-61.2330	1299	606	1.9	2.2	0.7	0.0	0.3	0.3	0.0	0.0	4.5	0.0	8.9	0.0	0.0	0.0
135	12.0830	-61.2330	1299	647	7.6	2.5	1.7	0.0	0.4	0.8	0.0	0.0	3.5	0.1	7.8	0.0	0.0	0.0
140	12.0830	-61.2330	1299	612	4.3	2.4	2.7	0.0	0.8	0.0	0.0	0.0	2.9	0.0	10.8	0.0	0.0	0.0
145	12.0830	-61.2330	1299	394	5.8	3.3	0.3	0.0	1.3	0.0	0.0	0.3	3.6	0.0	7.1	0.0	0.0	0.0
150	12.0830	-61.2330	1299	642	4.4	3.7	1.2	0.0	0.3	0.0	0.0	0.5	5.3	0.0	9.8	0.0	0.0	0.0
155	12.0830	-61.2330	1299	352	4.8	2.0	0.0	0.0	1.2	0.0	0.0	0.0	7.6	0.0	7.6	0.0	0.0	0.0
160	12.0830	-61.2330	1299	636	5.6	8.9	1.3	0.0	0.4	0.0	0.0	0.2	5.4	0.0	8.1	0.0	0.0	0.0
165	12.0830	-61.2330	1299	315	3.8	3.2	1.0	0.0	0.6	0.0	0.0	0.4	3.0	0.0	13.8	0.0	0.0	0.0
170	12.0830	-61.2330	1299	433	4.6	7.1	3.4	0.0	0.4	0.0	0.0	0.6	5.2	0.0	7.6	0.0	0.0	0.0
175	12.0830	-61.2330	1299	432	8.1	6.3	0.9	0.0	0.2	0.0	0.0	0.2	5.8	0.2	7.6	0.0	0.0	0.0
180	12.0830	-61.2330	1299	525	7.6	9.3	2.3	0.0	0.4	0.0	0.0	0.0	6.1	0.0	6.1	0.0	0.0	0.0
185	12.0830	-61.2330	1299	368	5.0	5.6	1.5	0.0	0.9	0.6	0.0	0.0	2.2	0.0	9.0	0.0	0.0	0.0
190	12.0830	-61.2330	1299	582	3.6	9.8	1.7	0.0	0.2	0.9	0.0	0.2	2.6	0.3	8.4	0.0	0.0	0.0
195	12.0830	-61.2330	1299	389	4.6	6.9	0.5	0.0	0.3	0.5	0.3	0.0	7.2	0.0	8.2	0.0	0.3	0.0
200	12.0830	-61.2330	1299	453	4.6	6.6	0.2	0.0	0.4	0.7	0.0	0.2	6.0	0.2	8.2	0.0	0.0	0.0
205	12.0830	-61.2330	1299	596	7.1	6.7	0.5	0.0	0.1	0.2	0.0	0.0	4.9	0.2	5.1	0.0	0.0	0.0
210	12.0830	-61.2330	1299	554	2.9	11.4	1.8	0.0	0.0	0.2	0.0	0.0	4.7	0.0	7.2	0.0	0.0	0.0
215	12.0830	-61.2330	1299	642	5.0	11.4	0.9	0.0	0.2	1.6	0.0	0.0	2.5	0.2	6.4	0.0	0.0	0.0
220	12.0830	-61.2330	1299	412	8.5	9.9	0.1	0.0	1.3	0.5	0.0	0.0	2.6	0.9	15.6	0.0	0.0	0.0
225	12.0830	-61.2330	1299	444	6.7	11.6	0.0	0.0	0.5	1.7	0.0	0.0	2.5	0.0	9.5	0.4	0.0	0.0
230	12.0830	-61.2330	1299	418	6.5	9.1	0.0	0.0	0.5	1.7	0.0	0.0	2.6	0.0	9.1	0.0	0.0	0.0
235	12.0830	-61.2330	1299	612	3.9	12.1	0.8	0.0	0.1	1.6	0.0	0.0	2.9	0.0	8.5	0.0	0.4	0.0
240	12.0830	-61.2330	1299	405	3.5	15.8	0.7	0.0	0.6	0.9	0.0	0.4	4.3	0.0	8.9	0.0	0.0	0.4
245	12.0830	-61.2330	1299	572	2.1	11.6	0.3	0.0	0.3	1.6	0.0	0.0	4.6	0.0	11.0	0.0	0.0	0.0
250	12.0830	-61.2330	1299	366	6.3	11.6	0.6	0.0	0.6	1.1	0.0	0.0	4.6	0.6	10.3	0.0	0.0	0.0
255	12.0830	-61.2330	1299	615	1.4	11.9	0.2	0.0	0.8	2.4	0.0	0.0	4.6	0.2	7.4	0.0	0.2	0.0
260	12.0830	-61.2330	1299	336	4.5	13.7	0.0	0.0	0.3	1.8	0.0	0.0	4.8	0.1	7.3	0.0	0.0	0.1
265	12.0830	-61.2330	1299	736	1.6	12.5	0.3	0.0	0.4	2.3	0.0	0.0	4.1	1.2	8.0	0.1	0.1	0.1
270	12.0830	-61.2330	1299	592	3.8	11.9	1.4	0.0	0.5	2.4	0.0	0.0	4.6	0.6	9.5	0.0	0.0	0.0
275	12.0830	-61.2330	1299	668	2.3	11.1	0.5	0.0	0.2	1.5	0.0	0.2	3.1	0.2	6.4	0.0	0.4	0.0
280	12.0830	-61.2330	1299	404	6.1	6.8	0.6	0.0	0.5	2.4	0.0	0.0	4.0	1.0	8.1	0.0	0.0	0.0
285	12.0830	-61.2330	1299	503	7.1	4.1	0.6	0.0	0.5	0.6	0.0	0.8	2.5	0.8	9.4	0.0	0.3	0.0
290	12.0830	-61.2330	1299	339	12.3	2.1	0.4	0.0	1.5	0.3	0.0	0.7	2.6	0.1	9.1	0.0	0.0	0.0
295	12.0830	-61.2330	1299	455	10.2	5.0	0.3	0.0	1.3	1.9	0.0	0.1	2.5	1.2	9.7	0.0	0.0	0.0
300	12.0830	-61.2330	1299	316	15.4	6.7	0.0	0.0	0.7	2.1	0.0	0.8	1.5	0.8	10.3	0.0	0.0	0.4
305	12.0830	-61.2330	1299	712	8.8	10.5	0.7	0.0	1.1	2.4	0.0	0.0	2.4	1.8	10.0	0.0	0.0	0.3
310	12.0830	-61.2330	1299	301	6.5	13.8	0.7	0.0	0.6	3.8	0.0	0.0	2.3	1.1	14.1	0.0	0.0	0.4
315	12.0830	-61.2330	1299	501	4.4	9.4	0.5	0.0	1.5	2.4	0.0	0.0	4.5	3.5	12.0	0.0	0.0	0.0
320	12.0830	-61.2330	1299	561	6.1	9.4	2.7	0.0	1.1	2.6	0.0	0.1	3.6	1.4	15.4	0.2	0.0	0.5
325	12.0830	-61.2330	1299	532	4.0	9.8	0.5	0.0	1.9	2.0	0.0	0.0	6.2	2.5	9.3	0.0	0.3	0.0
330	12.0830	-61.2330	1299	442	5.4	9.8	2.5	0.0	1.1	4.9	0.0	0.3	5.8	0.9	5.8	0.0	0.0	0.0
335	12.0830	-61.2330	1299	391	3.0	8.0	0.0	0.0	1.4	3.5	0.0	0.0	4.5	1.4	10.1	0.0	0.0	0.0
340	12.0830	-61.2330	1299	323	6.2	6.8	0.6	0.0	0.6	4.0	0.0	0.0	5.3	1.5	7.1	0.0	0.0	0.6
345	12.0830	-61.2330	1299	401	8.5	7.9	0.3	0.0	1.0	4.0	0.0	0.0	5.0	0.3	14.2	0.0	0.0	0.5
350	12.0830	-61.2330	1299	444	9.2	5.9	1.4	0.0	0.7	2.5	0.0	0.0	7.0	1.6	10.4	0.0	0.0	0.0
355	12.0830	-61.2330	1299	420	4.7	8.0	0.0	0.0	1.7	2.6	0.0	0.0	2.1	0.3	13.0	0.0	0.0	0.0
360	12.0830	-61.2330	1299	366	5.2	9.2	1.2	0.0	0.7	0.3	0.0	0.0	4.4	3.0	8.7	0.0	0.0	0.0
365	12.0830	-61.2330	1299	448	3.6	9.8	0.6	0.0	0.7	0.8	0.0	0.1	4.2	0.9	9.2	0.0	0.0	0.2
370	12.0830	-61.2330	1299	501	1.0	8.8	1.1	0.0	1.0	1.4	0.0	0.0	6.2	1.2	11.3	0.2	0.0	0.1

depth (cm)	men	nit	obl	pal	par+	qul	qur	qui	rur	ruw	rus	tri	sac	sci	ten	trl	trr	trus	tum	univ
0	1.6	0.0	0.8	0.0	0.8	0.0	0.0	0.0	15.4	42.7	0.4	8.8	5.8	0.4	0.0	0.0	0.0	0.0	0.6	0.6
5	2.5	0.7	1.5	0.0	0.1	0.0	0.0	0.0	20.4	34.1	0.9	8.9	5.5	0.0	0.0	0.0	1.6	1.6	0.0	1.9
10	1.4	0.0	0.9	0.0	0.0	0.0	0.0	0.0	13.4	37.4	0.9	10.0	6.6	0.0	0.0	0.0	0.5	0.5	0.9	1.1
15	1.6	0.2	0.2	0.0	0.0	0.0	0.0	0.0	15.0	41.5	1.1	13.6	4.3	0.5	0.0	0.0	0.0	0.0	0.0	2.5
20	2.6	1.3	0.7	0.0	0.0	0.0	0.0	0.0	12.1	33.4	4.3	4.6	7.4	4.3	0.0	0.0	0.1	0.1	0.0	1.2
25	2.0	0.2	1.0	0.0	0.0	0.0	0.0	0.0	12.6	35.2	0.3	10.3	5.9	0.5	0.2	0.0	0.0	0.0	0.0	2.5
30	2.4	0.4	0.3	0.0	0.0	0.0	0.0	0.0	15.6	36.7	0.7	9.8	6.2	0.5	0.0	0.0	1.0	1.0	0.3	3.5
35	1.4	0.2	0.6	0.0	0.0	0.0	0.0	0.0	11.9	47.9	0.0	10.7	5.1	0.0	0.0	0.0	0.2	0.2	0.0	1.6
40	0.3	0.1	0.1	0.0	0.1	0.0	0.0	0.0	12.8	46.8	1.3	6.9	4.3	0.4	0.4	0.0	0.0	0.0	0.0	1.4
45	1.2	0.2	1.0	0.0	0.2	0.0	0.0	0.0	11.6	46.6	1.2	10.2	4.1	0.0	0.0	0.0	0.0	0.0	0.0	3.7
50	0.4	1.6	0.4	0.0	0.3	0.0	0.0	0.0	10.2	36.7	3.5	6.8	7.9	0.5	0.1	0.0	0.3	0.3	0.1	4.2
55	0.8	1.6	1.0	0.0	0.0	0.0	0.0	0.0	13.0	38.1	1.9	11.1	5.6	0.0	1.2	0.8	0.2	1.0	0.2	3.7
60	1.0	2.2	1.7	0.0	0.0	0.0	0.0	0.0	16.1	28.5	4.7	7.4	9.4	0.5	0.7	0.5	0.0	0.5	0.2	3.2
65	1.1	1.2	0.0	0.7	0.3	0.0	0.0	0.0	16.2	34.2	4.8	8.7	4.8	0.4	0.9	0.5	0.0	0.5	0.4	3.7
70	3.4	1.3	1.1	0.0	0.0	0.0	0.0	0.0	18.9	31.6	5.3	5.0	5.5	0.5	0.8	0.0	0.3	0.3	0.3	1.3
75	4.1	1.0	1.7	0.0	0.1	0.0	0.0	0.0	19.6	26.4	5.0	9.4	4.3	0.3	2.1	0.1	0.0	0.1	0.4	3.0
80	3.9	1.2	1.7	0.0	0.0	0.0	0.0	0.0	20.3	26.9	4.1	5.8	3.3	0.2	0.6	0.0	0.0	0.0	0.0	2.1
85	3.6	2.1	1.8	0.0	0.0	0.0	0.0	0.0	23.6	29.0	1.3	11.4	5.4	0.3	2.1	0.0	0.0	0.0	0.3	0.5
90	0.8	1.8	1.4	0.0	0.0	0.0	0.0	0.0	17.6	37.4	2.9	7.2	3.3	0.4	1.8	0.2	0.0	0.2	0.2	1.6
95	2.8	1.3	0.6	0.0	0.8	0.0	0.0	0.0	21.0	38.4	1.1	7.9	3.4	0.0	1.3	0.4	0.0	0.4	0.2	1.3
100	1.2	1.5	1.2	0.0	0.2	0.0	0.0	0.0	21.2	42.9	2.9	8.1	3.1	0.0	0.2	0.0	0.0	0.0	0.0	0.0
105	1.8	0.5	2.6	0.0	0.0	0.0	0.0	0.0	23.0	38.8	1.8	9.2	5.1	0.0	0.5	0.3	0.0	0.3	0.0	0.3
110	1.9	0.6	1.7	0.0	0.0	0.0	0.0	0.0	21.8	46.2	1.1	7.9	5.4	0.0	0.0	0.0	0.0	0.0	0.0	0.2
115	0.7	0.5	1.6	0.0	0.4	0.0	0.0	0.0	21.0	45.2	0.4	8.6	3.9	0.0	0.0	0.0	0.0	0.0	0.2	1.3
120	1.7	0.6	0.9	0.0	0.0	0.0	0.0	0.0	21.1	40.5	1.4	8.5	4.3	0.0	0.5	0.0	0.0	0.0	0.1	1.3
125	1.1	1.1	2.2	0.0	0.2	0.0	0.0	0.0	17.4	38.3	0.9	11.2	4.0	0.0	0.7	0.2	0.4	0.7	0.2	1.8
130	1.5	0.6	0.3	0.0	0.1	0.0	0.0	0.0	17.4	41.8	2.3	9.7	5.2	0.0	0.7	0.0	0.5	0.5	0.0	1.1
135	0.3	0.2	1.3	0.0	0.2	0.0	0.0	0.0	15.3	38.8	2.4	8.6	4.6	0.6	0.0	0.0	1.5	1.5	0.1	1.7
140	0.1	0.9	0.4	0.0	0.0	0.0	0.0	0.0	10.8	41.8	3.9	7.5	3.3	2.2	0.0	0.0	3.5	3.5	0.2	0.9
145	0.5	0.5	0.5	0.0	0.3	0.0	0.0	0.0	15.2	41.4	3.6	7.6	3.6	0.5	0.3	0.0	2.0	2.0	0.0	2.0
150	0.5	0.0	1.2	0.0	0.0	0.0	0.0	0.0	17.6	30.1	3.9	6.9	4.4	2.0	0.3	0.0	5.9	5.9	0.2	1.4
155	1.0	0.0	0.8	0.0	0.2	0.0	0.0	0.0	15.3	32.9	1.0	10.6	5.0	0.8	0.2	0.0	7.8	7.8	0.4	0.4
160	0.3	0.3	1.9	0.0	0.2	0.0	0.0	0.0	13.0	34.3	4.0	4.7	4.0	1.3	0.6	0.3	3.0	3.3	0.5	1.3
165	0.0	0.0	1.2	0.0	0.8	0.0	0.0	0.0	13.2	34.5	1.6	9.0	4.0	2.8	0.0	0.0	4.8	4.8	0.4	1.2
170	1.5	0.0	0.4	0.0	0.6	0.0	0.0	0.0	16.6	30.7	1.7	5.9	4.6	1.3	0.6	0.2	5.0	5.2	0.8	0.8
175	0.5	0.0	1.2	0.0	0.5	0.0	0.0	0.0	16.2	31.0	2.5	9.7	1.4	0.7	0.0	0.2	3.9	4.2	1.2	1.2
180	0.6	0.0	1.0	0.0	0.2	0.0	0.0	0.0	17.1	31.6	2.7	3.2	4.4	0.8	0.0	0.0	4.8	4.8	0.2	1.1
185	0.2	0.2	0.9	0.0	0.6	0.0	0.0	0.0	16.4	39.6	0.4	8.0	1.5	1.5	1.5	0.0	3.6	3.6	0.6	0.2
190	0.3	0.2	0.7	0.0	0.3	0.0	0.0	0.0	16.8	33.7	3.4	4.6	4.8	3.1	0.0	0.0	2.7	2.7	0.9	0.3
195	0.3	0.0	1.0	0.0	1.0	0.0	0.0	0.3	20.6	26.0	1.8	10.3	4.6	0.0	0.3	0.0	4.4	4.4	0.5	0.0
200	0.9	0.2	1.8	0.0	1.5	0.0	0.0	0.2	18.1	30.2	3.5	6.8	3.8	0.9	0.0	0.0	2.4	2.4	1.3	0.7
205	0.0	0.0	0.9	0.0	0.5	0.0	0.0	0.0	21.8	34.6	2.8	7.4	2.2	0.5	0.0	0.6	2.3	2.9	0.9	0.6
210	0.5	0.0	1.8	0.0	0.0	0.0	0.0	0.0	18.2	31.6	3.8	6.0	4.7	0.2	0.0	0.2	2.0	2.2	1.4	0.5
215	0.0	0.2	0.9	0.2	0.2	0.0	0.0	0.0	14.6	37.1	2.2	10.1	3.6	0.2	0.0	0.5	0.8	1.2	0.3	1.2
220	0.0	0.0	0.3	0.0	0.0	0.0	0.0	0.0	14.3	27.3	8.6	6.8	1.5	0.0	0.0	0.1	0.5	0.6	0.0	0.5
225	0.0	0.2	0.7	0.0	0.0	0.0	0.0	0.0	11.3	39.1	5.8	7.3	2.0	0.0	0.0	0.0	0.3	0.3	0.0	0.4
230	0.0	0.5	0.5	0.0	0.2	0.0	0.0	0.0	14.8	34.7	5.0	9.3	2.2	0.7	0.0	0.0	0.5	0.5	0.0	1.7
235	0.0	0.0	1.0	0.0	0.0	0.0	0.0	0.0	10.5	38.8	3.7	7.3	5.8	0.7	0.2	0.1	0.9	1.0	0.0	0.8
240	0.0	0.0	0.7	0.0	0.4	0.0	0.0	0.0	9.4	34.3	4.9	5.3	2.2	4.1	0.9	0.2	0.4	0.7	0.0	0.7
245	0.0	0.2	0.7	0.6	2.3	0.0	0.0	0.0	5.6	48.4	2.3	2.2	0.6	1.3	0.3	0.0	3.0	3.0	0.0	0.7
250	0.0	0.3	1.6	0.0	0.0	0.0	0.0	0.0	14.7	25.4	4.0	7.9	2.2	2.3	0.6	0.0	3.2	3.2	0.0	1.6
255	0.0	0.2	1.1	0.6	1.3	0.0	0.0	0.0	12.9	40.1	3.4	6.4	2.0	0.2	0.0	0.0	2.5	2.5	0.0	0.0
260	0.6	0.1	1.6	0.0	0.8	0.0	0.0	1.1	8.9	30.9	6.8	6.4	1.8	3.4	0.0	0.1	2.4	2.5	0.0	0.6
265	0.0	0.0	1.1	0.3	1.6	0.0	0.0	0.0	12.1	34.1	2.9	9.6	1.5	1.4	0.1	0.0	3.0	3.0	0.0	1.2
270	0.6	0.0	1.5	0.0	1.4	0.0	0.0	0.0	10.0	32.3	4.2	6.4	2.2	3.2	0.0	0.1	2.4	2.5	0.0	0.6
275	0.1	0.0	1.6	1.2	2.5	0.0	0.0	0.4	11.3	37.3	5.4	8.3	1.8	1.6	0.2	0.0	2.4	2.4	0.0	0.1
280	0.0	0.0	1.6	0.0	0.8	0.0	0.0	0.3	10.0	35.7	5.8	7.2	2.6	2.9	0.0	0.0	3.1	3.1	0.0	0.2
285	0.0	0.0	0.0	0.0	0.1	0.0	0.0	0.0	9.0	42.4	1.5	11.5	3.7	0.8	0.8	0.1	1.4	1.5	0.0	0.9
290	0.0	0.3	0.1	0.0	0.0	0.0	0.0	0.0	10.3	34.3	2.6	15.5	1.6	1.1	0.5	0.0	3.3	3.3	0.0	0.3
295	0.0	0.0	0.0	0.3	0.7	0.0	0.0	0.0	8.2	35.1	3.2	8.7	3.5	0.6	0.6	0.0	5.6	5.6	0.0	0.6
300	0.0	0.0	0.0	0.0	0.0	0.0	0.0	0.0	7.0	24.8	9.3	10.5	2.1	2.5	0.0	0.0	2.6	2.6	0.0	0.6
305	0.0	0.0	0.0	2.8	0.7	0.0	0.0	0.0	6.9	26.4	4.2	11.5	4.0	1.8	0.6	0.2	2.9	3.1	0.0	0.1
310	0.0	0.0	0.0	1.7	0.7	0.0	0.0	0.0	12.0	28.1	0.6	6.6	2.8	1.7	0.0	0.0	1.0	1.0	0.0	0.1
315	0.3	0.0	0.0	1.9	0.5	0.0	0.0	0.0	10.8	29.0	3.5	9.6	3.7	0.5	0.3	0.0	1.6	1.6	0.0	0.4
320	0.0	0.0	0.0	3.6	0.3	0.0	0.0	0.0	14.4	19.5	2.7	5.9	4.2	2.3	0.5	0.1	1.6	1.7	0.0	0.1
325	0.0	0.0	0.0	3.0	0.4	0.0	0.0	0.0	17.1	24.4	0.5	8.8	4.3	0.8	0.5	0.1	2.6	2.8	0.0	0.5
330	0.0	0.0	0.0	2.2	0.8	0.0	0.0	0.0	15.8	25.0	2.5	6.8	4.5	2.2	1.8	0.0	1.8	1.8	0.0	0.0
335	0.0	0.0	0.0	2.8	0.5	0.0	0.0	0.0	17.5	25.7	0.3	12.4	4.0	2.8	0.3	0.0	1.2	1.2	0.0	0.3
340	0.0	0.3	0.0	4.3	2.5	0.0	0.0	0.3	13.9	24.5	3.1	11.8	4.3	0.3	0.0	0.0	1.2	1.2	0.0	0.6
345	0.0	0.0	0.0	4.5	0.6	0.0	0.0	0.0	13.2	23.3	1.6	9.5	3.1	0.6	0.3	0.0	0.6	0.6	0.0	0.2
350	0.2	0.2	0.0	0.2	0.2	0.0	0.0	0.9	10.6	21.8	2.5	11.0	5.2	2.3	0.7	0.0	2.0	2.0	0.0	1.8
355	0.0	0.0	0.0	4.5	1.5	0.0	0.0	0.0	12.6	29.4	1.5	13.0	2.7	0.0	0.3	0.0	0.9	0.9	0.0	0.5
360	0.0	0.0	0.0	0.0	0.3	0.0	0.0	1.0	12.8	32.4	1.7	9.1	3.9	2.0	0.7	0.0	2.0	2.0	0.0	0.0
365	0.0	0.2	0.0	4.9	0.8	0.0	0.0	0.0	16.0	31.2	0.4	10.5	2.2	0.0	0.0	0.0	2.1	2.1	0.0	0.6
370	0.0	0.0	0.0	9.9	0.5	0.0	0.0	0.0	9.0	34.0	0.2	4.3	3.6	2.5	0.5	0.0	2.1	2.1	0.0	0.2

depth (cm)	uvu		ment	pdi	par
0	0.0	2.2	0.6	0.2
5	0.0	2.5	0.1	0.0
10	0.0	2.3	0.0	0.0
15	0.0	1.6	0.0	0.0
20	0.0	2.6	0.0	0.0
25	0.0	2.0	0.0	0.0
30	0.0	2.8	0.0	0.0
35	0.0	1.4	0.0	0.0
40	0.0	0.3	0.1	0.0
45	0.0	1.2	0.0	0.2
50	0.0	0.5	0.0	0.3
55	0.0	1.0	0.0	0.0
60	0.0	1.2	0.0	0.0
65	0.0	1.5	0.1	0.2
70	0.0	3.7	0.0	0.0
75	0.0	4.5	0.1	0.0
80	0.0	3.9	0.0	0.0
85	0.0	3.9	0.0	0.0
90	0.0	1.0	0.0	0.0
95	0.0	3.0	0.8	0.0
100	0.0	1.2	0.0	0.2
105	0.0	1.8	0.0	0.0
110	0.0	1.9	0.0	0.0
115	0.0	0.9	0.0	0.4
120	0.0	1.8	0.0	0.0
125	0.0	1.3	0.0	0.2
130	0.0	1.5	0.0	0.1
135	0.0	0.4	0.0	0.2
140	0.0	0.3	0.0	0.0
145	0.0	0.5	0.0	0.3
150	0.0	0.6	0.0	0.0
155	0.0	1.4	0.0	0.2
160	0.0	0.8	0.2	0.0
165	0.0	0.4	0.0	0.8
170	0.0	2.3	0.4	0.2
175	0.0	1.6	0.2	0.2
180	0.0	0.8	0.0	0.2
185	0.0	0.7	0.0	0.6
190	0.0	1.2	0.2	0.2
195	0.0	0.8	0.0	1.0
200	0.0	2.2	0.7	0.9
205	0.0	0.9	0.2	0.2
210	0.0	2.0	0.0	0.0
215	0.0	0.3	0.2	0.0
220	0.0	0.1	0.0	0.0
225	0.0	0.0	0.0	0.0
230	0.0	0.0	0.0	0.2
235	0.0	0.0	0.0	0.0
240	0.0	0.0	0.4	0.0
245	0.0	0.0	0.8	1.5
250	0.0	0.0	0.0	0.0
255	0.0	0.0	0.0	1.3
260	0.0	0.6	0.3	0.6
265	0.0	0.0	0.0	1.6
270	0.0	0.6	0.0	1.4
275	0.0	0.1	0.8	1.7
280	0.0	0.0	0.2	0.6
285	0.0	0.0	0.1	0.0
290	0.0	0.0	0.0	0.0
295	0.0	0.0	0.4	0.3
300	0.0	0.0	0.0	0.0
305	0.0	0.0	0.2	0.6
310	0.0	0.0	0.0	0.7
315	0.0	0.3	0.0	0.5
320	0.0	0.0	0.1	0.2
325	0.0	0.0	0.4	0.0
330	0.0	0.0	0.5	0.3
335	0.0	0.0	0.5	0.0
340	0.0	0.0	1.9	0.6
345	0.0	0.0	0.2	0.5
350	0.0	0.2	0.2	0.0
355	0.0	0.0	0.3	1.2
360	0.0	0.0	0.3	0.0
365	0.1	0.0	0.3	0.4
370	0.0	0.0	0.5	0.0

depth (cm)	Lat	Long	water depth (m)	counted	aeq	bul	cal	cav	con	cra	deh	dig	dut	fal	glu	hir	hum	inf
375	12.0830	-61.2330	1299	547	1.7	7.5	0.0	0.0	2.6	0.5	0.0	0.0	4.3	0.2	11.2	0.0	0.0	0.5
380	12.0830	-61.2330	1299	403	4.6	10.0	0.9	0.0	0.9	2.2	0.0	0.0	2.8	0.0	9.7	0.0	0.0	0.2
385	12.0830	-61.2330	1299	472	7.6	6.7	0.6	0.0	1.0	1.3	0.0	0.0	2.6	0.0	16.6	0.0	0.0	0.0
390	12.0830	-61.2330	1299	453	4.5	8.0	1.3	0.0	1.3	3.2	0.0	0.0	2.9	0.6	10.4	0.0	0.3	0.1
395	12.0830	-61.2330	1299	355	7.5	7.5	0.0	0.0	1.3	1.8	0.0	0.0	2.0	0.7	14.3	0.0	0.0	0.2
400	12.0830	-61.2330	1299	322	4.7	5.0	0.3	0.0	2.8	3.4	0.0	0.0	1.6	0.0	11.5	0.0	0.0	0.0
405	12.0830	-61.2330	1299	285	4.1	3.2	0.0	0.0	2.0	0.5	0.0	0.0	1.1	0.6	18.2	0.0	0.0	0.0
410	12.0830	-61.2330	1299	297	8.1	7.3	0.6	0.0	1.4	2.3	0.0	0.0	4.0	0.6	14.7	0.0	0.0	0.2
415	12.0830	-61.2330	1299	387	3.4	7.8	0.5	0.0	2.1	1.5	0.0	0.0	2.6	1.3	14.0	0.0	0.0	0.6
420	12.0830	-61.2330	1299	374	2.1	8.7	0.4	0.0	1.1	2.0	0.0	0.0	3.7	1.4	9.0	0.2	0.0	0.2
425	12.0830	-61.2330	1299	357	3.2	7.4	0.2	0.0	2.1	1.0	0.0	0.0	3.8	0.4	13.1	0.0	0.0	0.8
430	12.0830	-61.2330	1299	608	1.9	8.9	0.4	0.0	2.1	1.6	0.0	0.2	6.2	2.0	10.8	0.0	0.0	0.6
435	12.0830	-61.2330	1299	456	2.5	9.4	0.4	0.0	1.7	1.4	0.0	0.0	6.5	0.0	10.9	0.0	0.3	0.1
440	12.0830	-61.2330	1299	411	3.6	5.9	1.0	0.0	1.6	0.1	0.0	0.3	3.9	0.9	12.7	0.0	0.0	0.0
445	12.0830	-61.2330	1299	582	3.6	6.2	0.0	0.0	1.8	0.7	0.0	0.7	4.0	0.4	13.0	0.0	0.0	0.4
450	12.0830	-61.2330	1299	428	1.5	7.5	0.6	0.0	0.9	1.3	0.0	0.0	3.5	0.3	7.3	0.3	0.0	0.3
455	12.0830	-61.2330	1299	600	1.3	5.4	0.0	0.0	1.0	1.8	0.0	0.0	6.7	0.0	9.5	0.0	0.0	0.8
460	12.0830	-61.2330	1299	309	2.1	3.8	0.9	0.0	0.6	2.5	0.0	0.4	2.3	0.8	16.3	0.0	0.0	0.0
465	12.0830	-61.2330	1299	394	1.8	4.7	0.0	0.0	1.0	2.1	0.0	0.0	3.7	0.0	12.2	0.0	0.0	0.5
470	12.0830	-61.2330	1299	345	2.4	12.7	0.4	0.0	1.3	1.3	0.0	0.7	4.2	4.0	7.8	0.4	0.0	0.4
475	12.0830	-61.2330	1299	466	0.3	12.4	0.0	0.0	1.1	3.4	0.0	0.0	5.1	0.3	9.0	0.0	0.0	0.0
480	12.0830	-61.2330	1299	374	2.5	16.0	0.3	0.0	0.5	1.2	0.0	0.3	4.5	2.0	10.6	0.0	0.0	0.0
485	12.0830	-61.2330	1299	428	1.4	13.6	0.5	0.0	1.9	1.9	0.0	0.0	10.3	0.0	6.1	0.0	0.0	0.7
490	12.0830	-61.2330	1299	459	2.2	15.2	0.0	0.0	1.4	1.0	0.0	0.0	8.6	2.3	5.7	0.0	0.0	0.1
495	12.0830	-61.2330	1299	538	0.4	10.0	0.0	0.0	0.5	1.6	0.0	0.0	16.8	1.6	9.5	0.0	0.0	1.2
500	12.0830	-61.2330	1299	392	0.8	14.3	0.3	0.0	1.7	0.8	0.0	0.0	9.7	2.7	11.1	0.0	0.0	0.0
505	12.0830	-61.2330	1299	541	1.1	12.9	0.0	0.0	0.7	2.1	0.0	0.0	7.1	1.9	12.7	0.0	0.0	0.1
510	12.0830	-61.2330	1299	647	3.3	17.0	0.4	0.0	1.5	2.6	0.0	0.0	10.4	0.4	8.6	0.4	0.0	0.4
515	12.0830	-61.2330	1299	414	2.2	9.7	0.2	0.0	1.9	1.0	0.0	0.2	18.4	0.7	6.5	0.0	0.0	0.5
520	12.0830	-61.2330	1299	498	2.6	19.3	0.6	0.0	0.6	0.6	0.0	0.0	10.2	1.0	7.2	0.2	0.0	0.2
525	12.0830	-61.2330	1299	444	7.0	19.9	1.6	0.0	1.6	1.3	0.0	0.3	6.3	2.1	7.2	0.0	0.0	0.1
530	12.0830	-61.2330	1299	371	3.4	14.3	0.5	0.0	0.7	1.9	0.0	0.0	3.8	2.1	13.4	0.7	0.0	0.7
535	12.0830	-61.2330	1299	402	1.8	10.1	2.3	0.0	0.8	0.7	0.0	0.0	12.4	3.3	9.2	0.0	0.0	2.3
540	12.0830	-61.2330	1299	498	3.4	13.1	2.2	0.0	1.0	2.0	0.0	0.0	9.4	1.0	10.4	0.0	0.2	1.0
545	12.0830	-61.2330	1299	401	4.0	7.4	0.4	0.0	0.9	2.1	0.0	0.0	12.7	1.8	9.5	0.0	0.0	0.5
550	12.0830	-61.2330	1299	530	5.3	13.2	1.0	0.0	0.4	1.6	0.0	0.0	9.7	1.5	11.1	0.0	0.0	0.9
555	12.0830	-61.2330	1299	407	4.1	12.1	0.7	0.0	0.3	2.2	0.0	0.3	7.8	1.0	11.3	0.0	0.0	0.5
560	12.0830	-61.2330	1299	985	5.6	13.4	0.3	0.0	0.6	1.2	0.0	0.0	5.5	0.5	15.4	0.0	0.0	0.3
565	12.0830	-61.2330	1299	449	5.4	6.5	0.3	0.0	1.0	0.6	0.0	0.0	6.5	1.7	18.2	0.0	0.0	0.7
570	12.0830	-61.2330	1299	360	2.8	15.3	0.0	0.0	1.1	0.6	0.0	0.0	13.9	0.6	12.2	0.0	0.0	0.6
575	12.0830	-61.2330	1299	609	2.1	10.4	0.3	0.0	0.9	0.3	0.0	0.0	11.1	0.6	16.6	0.0	0.2	0.2
580	12.0830	-61.2330	1299	609	2.3	18.2	0.5	0.0	0.3	0.7	0.0	0.0	12.5	0.8	11.0	0.0	0.0	0.5
585	12.0830	-61.2330	1299	364	1.1	15.4	0.3	0.0	1.1	0.5	0.0	0.3	17.9	0.0	6.6	0.0	0.0	1.4
590	12.0830	-61.2330	1299	374	6.7	11.6	1.0	0.0	0.9	0.1	0.0	0.0	10.9	1.2	10.4	0.0	0.0	0.1
595	12.0830	-61.2330	1299	319	2.1	9.3	0.4	0.0	1.5	0.6	0.0	0.0	11.2	0.8	10.3	0.0	0.0	0.6
600	12.0830	-61.2330	1299	400	3.6	17.8	0.0	0.0	0.4	0.7	0.0	0.0	6.3	0.0	10.3	0.0	0.0	0.3
605	12.0830	-61.2330	1299	465	8.5	14.2	0.3	0.0	0.9	0.3	0.0	0.3	3.0	0.3	9.7	0.0	0.0	1.1
610	12.0830	-61.2330	1299	774	3.6	15.6	1.2	0.0	0.5	0.3	0.0	0.0	9.3	0.1	8.3	0.1	0.0	0.0
615	12.0830	-61.2330	1299	557	10.2	8.3	0.4	0.0	1.3	0.4	0.0	0.3	7.2	0.4	12.1	0.0	0.0	0.1
620	12.0830	-61.2330	1299	494	4.9	15.4	1.0	0.0	1.1	1.0	0.0	0.3	5.1	0.0	15.9	0.0	0.0	0.4
625	12.0830	-61.2330	1299	500	5.0	18.8	0.0	0.0	0.9	0.9	0.0	0.0	8.6	0.5	8.9	0.0	0.0	0.1
630	12.0830	-61.2330	1299	552	7.1	17.3	0.9	0.0	0.6	1.0	0.0	0.2	6.4	0.0	14.2	0.5	0.0	0.0
635	12.0830	-61.2330	1299	451	4.8	15.6	0.9	0.0	0.9	0.7	0.0	0.0	7.9	1.2	11.7	0.0	0.0	0.3
640	12.0830	-61.2330	1299	486	1.4	24.2	0.8	0.0	0.9	0.1	0.0	0.0	7.8	1.1	13.7	0.0	0.0	0.4
645	12.0830	-61.2330	1299	517	3.0	16.1	0.4	0.0	0.8	1.0	0.0	0.3	11.4	1.9	6.8	0.0	0.0	0.3
650	12.0830	-61.2330	1299	516	4.9	17.2	0.2	0.0	0.2	1.1	0.0	0.5	5.4	0.7	11.5	0.2	0.2	0.1
655	12.0830	-61.2330	1299	378	3.6	15.9	1.8	0.0	0.5	0.7	0.0	0.5	5.7	0.0	12.0	0.0	0.5	0.6
660	12.0830	-61.2330	1299	397	2.7	15.5	0.5	0.0	0.3	1.5	0.0	0.6	8.6	0.0	9.9	0.0	0.0	0.2
665	12.0830	-61.2330	1299	385	2.7	15.8	0.4	0.0	0.7	0.7	0.0	0.0	13.7	0.0	13.9	0.4	0.0	0.7
670	12.0830	-61.2330	1299	370	2.3	16.2	0.4	0.0	0.2	0.9	0.0	0.0	11.7	0.4	12.9	0.0	0.0	0.0
675	12.0830	-61.2330	1299	410	4.4	14.2	0.3	0.0	0.5	1.1	0.0	0.0	11.4	0.3	8.5	0.3	0.0	0.0
680	12.0830	-61.2330	1299	527	6.1	11.5	0.4	0.0	0.3	0.7	0.0	0.0	5.7	0.7	13.5	0.0	0.0	0.1
685	12.0830	-61.2330	1299	535	3.4	12.6	0.7	0.0	0.5	0.0	0.0	0.0	8.2	0.5	14.3	0.0	0.0	0.0
690	12.0830	-61.2330	1299	353	2.4	19.2	0.4	0.0	0.6	0.2	0.0	0.0	8.7	0.4	13.0	0.0	0.4	0.0
695	12.0830	-61.2330	1299	328	2.0	12.6	0.0	0.0	1.2	0.8	0.0	0.0	13.0	1.2	9.3	0.0	0.0	0.0
700	12.0830	-61.2330	1299	519	2.4	17.1	0.4	0.0	0.4	1.1	0.0	0.0	10.2	1.9	13.1	0.0	0.0	0.0
705	12.0830	-61.2330	1299	466	2.1	11.7	0.7	0.0	0.3	0.8	0.0	0.0	12.0	0.3	13.7	0.0	0.0	0.0
710	12.0830	-61.2330	1299	441	3.1	12.8	0.6	0.0	0.6	0.0	0.0	0.0	11.3	0.6	15.3	0.3	0.0	0.0
715	12.0830	-61.2330	1299	374	3.2	8.6	0.3	0.0	1.3	0.8	0.0	0.0	12.6	0.8	8.6	0.0	0.0	0.3
720	12.0830	-61.2330	1299	459	1.3	11.4	0.0	0.0	0.3	0.6	0.0	0.0	11.4	1.2	11.3	0.0	0.0	0.1
725	12.0830	-61.2330	1299	340	1.5	7.4	0.0	0.0	0.7	1.1	0.0	0.0	15.3	0.9	7.0	0.0	0.0	0.0
730	12.0830	-61.2330	1299	439	2.1	12.8	0.0	0.0	0.5	0.7	0.0	0.0	11.4	0.7	8.0	0.0	0.0	0.0
735	12.0830	-61.2330	1299	461	2.9	14.0	0.3	0.0	0.4	0.1	0.0	0.0	9.6	0.6	8.7	0.0	0.0	0.3
740	12.0830	-61.2330	1299	434	6.3	15.3	0.3	0.0	0.6	0.3	0.0	0.0	5.3	0.3	12.6	0.3	0.0	0.0
745	12.0830	-61.2330	1299	484	8.2	9.1	0.4	0.0	1.0	0.4	0.0	0.0	3.3	0.7	14.8	0.0	0.0	0.4

depth (cm)	men	nit	obl	pal	par+	qul	qur	qui	rur	ruw	rus	tri	sac	sci	ten	trl	trr	trus	tum	univ
375	0.0	0.0	0.0	10.7	1.8	0.0	0.0	0.0	10.2	31.9	0.2	7.8	2.9	2.4	0.2	0.0	3.3	3.3	0.0	0.1
380	0.0	0.0	0.0	7.6	0.1	0.0	0.0	0.0	13.3	28.5	0.0	11.8	2.1	1.3	0.8	0.1	2.1	2.2	0.0	0.0
385	0.3	0.0	0.0	0.5	0.4	0.0	0.0	0.0	11.8	30.8	2.6	9.7	2.5	1.3	0.0	0.0	2.8	2.8	0.0	0.5
390	0.0	0.0	0.0	0.9	0.1	0.0	0.0	0.0	12.1	31.4	2.6	9.1	3.5	1.8	0.9	0.0	3.4	3.4	0.0	0.6
395	0.0	0.0	0.0	1.5	0.6	0.0	0.0	0.0	13.9	24.8	3.7	7.0	5.5	2.2	0.4	0.0	2.8	2.8	0.0	1.1
400	0.0	0.6	0.0	0.3	0.0	0.0	0.0	0.6	13.0	34.5	0.6	8.1	4.0	1.6	0.3	0.6	5.6	6.2	0.0	0.9
405	0.0	0.3	0.0	0.6	0.2	0.0	0.0	0.0	6.5	44.4	2.4	8.6	0.9	2.0	0.0	0.0	2.7	2.7	0.0	0.9
410	0.0	0.2	0.0	1.2	0.0	0.0	0.0	0.0	5.2	36.1	4.3	6.4	2.1	1.8	0.6	0.0	1.8	1.8	0.0	0.5
415	0.0	0.0	0.0	1.3	0.0	0.0	0.0	0.0	9.1	34.3	4.5	8.6	2.3	2.6	0.6	0.0	1.6	1.6	0.0	1.0
420	0.0	0.2	0.0	3.2	0.5	0.0	0.0	0.0	12.2	38.8	3.5	5.3	3.5	1.4	0.0	0.0	2.0	2.0	0.0	0.2
425	0.0	0.0	0.0	0.4	1.3	0.0	0.0	0.0	8.2	38.6	2.7	7.4	4.6	3.0	0.0	0.2	1.1	1.3	0.0	0.2
430	0.0	0.0	0.0	3.8	0.0	0.0	0.0	0.0	10.1	27.8	3.4	6.2	7.1	3.4	0.0	0.0	2.0	2.0	0.0	0.7
435	0.0	0.1	0.0	4.1	0.4	0.0	0.0	0.0	11.4	27.5	4.6	10.6	2.6	1.2	0.3	0.0	2.7	2.7	0.0	1.0
440	0.0	0.6	0.0	4.0	0.0	0.0	0.0	0.0	11.8	31.0	3.8	8.8	4.0	2.3	0.3	0.0	1.9	1.9	0.0	0.4
445	0.0	0.2	0.0	4.5	0.0	0.0	0.0	0.0	17.2	25.9	2.0	11.0	2.7	1.3	0.0	0.0	3.1	3.1	0.0	0.6
450	0.0	0.0	0.0	0.6	1.6	0.0	0.0	0.0	18.0	41.5	0.6	7.4	2.8	0.0	0.0	0.0	3.3	3.3	0.0	0.3
455	0.0	0.0	0.0	4.9	0.4	0.0	0.0	0.2	11.8	36.5	3.1	8.4	2.6	0.7	0.2	0.2	4.1	4.3	0.0	0.4
460	0.0	0.0	0.0	0.8	0.0	0.0	0.0	0.0	9.1	38.3	3.4	11.6	2.8	1.1	0.0	0.2	1.3	1.5	0.0	0.4
465	0.0	0.2	0.0	0.6	0.3	0.0	0.0	0.0	11.8	43.6	1.0	8.8	2.1	0.6	0.0	0.0	3.9	3.9	0.0	0.5
470	0.0	0.0	0.0	1.8	0.5	0.0	0.0	0.0	12.0	32.7	2.5	7.1	3.3	0.7	0.2	0.0	3.3	3.3	0.0	0.2
475	0.0	0.0	0.0	1.1	0.6	0.0	0.0	0.3	14.3	29.0	1.4	10.6	3.3	1.4	0.0	0.3	4.6	4.9	0.0	0.6
480	0.3	0.0	0.0	2.0	0.7	0.0	0.0	0.0	8.8	30.0	2.4	9.1	3.5	2.0	0.3	0.2	1.9	2.0	0.0	0.2
485	0.0	0.0	0.0	1.2	0.5	0.0	0.0	0.0	12.4	22.4	2.8	14.3	5.4	0.5	0.2	0.2	3.5	3.7	0.0	0.5
490	0.0	0.0	0.0	2.9	0.7	0.0	0.0	0.0	9.2	27.5	3.4	7.3	5.5	2.0	0.3	0.1	3.7	3.9	0.0	0.3
495	0.0	0.0	0.0	3.7	3.4	0.0	0.0	0.0	9.5	26.9	2.1	6.4	2.2	0.3	0.0	0.1	3.5	3.7	0.0	0.4
500	0.0	0.2	0.0	5.0	0.8	0.0	0.0	0.0	12.6	26.1	2.0	4.0	1.8	2.4	0.0	0.0	2.7	2.7	0.0	0.5
505	0.2	0.0	0.0	5.6	0.9	0.0	0.0	0.0	14.5	24.1	3.9	6.4	1.9	1.2	0.0	0.0	2.1	2.1	0.0	0.6
510	0.0	0.5	0.0	2.5	1.5	0.0	0.0	0.0	11.1	22.1	2.5	6.5	3.1	0.7	0.5	0.6	2.3	3.0	0.0	1.2
515	0.0	0.2	0.0	3.6	1.2	0.0	0.0	0.0	11.8	23.2	1.2	8.7	3.1	0.2	0.0	0.0	4.6	4.6	0.0	0.0
520	0.0	0.0	0.2	5.0	0.8	0.0	0.0	0.2	10.0	24.3	0.8	7.4	3.4	0.8	0.0	0.0	3.0	3.0	0.0	1.4
525	0.0	0.7	0.0	2.7	0.6	0.0	0.0	0.0	8.4	19.4	1.8	10.9	2.8	0.3	0.0	1.3	1.6	3.0	0.0	1.3
530	0.0	0.3	0.0	3.1	1.0	0.0	0.0	0.3	6.4	23.4	3.8	10.7	3.3	0.7	0.3	0.3	2.6	2.9	0.0	1.5
535	0.0	0.2	0.0	3.9	2.1	0.0	0.0	0.0	9.3	23.7	3.3	6.5	2.1	1.6	0.0	0.5	1.5	2.0	0.0	1.5
540	0.0	0.4	0.0	8.0	1.6	0.0	0.0	0.0	8.8	23.3	2.0	3.2	2.4	1.4	0.0	0.6	2.4	3.0	0.0	1.8
545	0.0	0.2	0.0	4.7	1.4	0.0	0.0	0.4	12.8	26.0	0.7	8.6	1.8	0.4	0.0	0.0	3.2	3.2	0.0	0.7
550	0.0	0.5	0.0	4.2	1.6	0.0	0.0	0.0	9.2	20.8	3.5	5.0	3.6	1.2	0.2	1.2	3.1	4.3	0.0	0.7
555	0.0	0.3	0.0	4.6	2.3	0.0	0.0	0.0	8.3	26.0	1.7	9.1	3.2	0.0	0.0	0.5	2.2	2.7	0.0	0.8
560	0.0	0.3	0.0	5.7	1.1	0.0	0.0	0.0	5.1	25.4	3.0	8.1	3.4	0.9	0.2	0.3	1.7	2.0	0.0	1.1
565	0.0	0.4	0.0	2.5	0.6	0.0	0.0	0.0	7.4	25.2	2.8	12.4	2.4	0.6	0.6	0.1	1.3	1.4	0.0	2.2
570	0.0	0.3	0.0	4.4	1.7	0.0	0.0	0.0	7.5	19.7	2.8	7.2	3.6	0.8	0.0	0.3	2.2	2.5	0.0	2.5
575	0.0	0.0	0.0	12.1	4.1	0.0	0.0	0.2	6.4	15.9	3.2	5.8	3.0	3.2	0.4	0.1	2.2	2.3	0.0	0.5
580	0.0	0.0	0.0	12.5	3.6	0.0	0.0	0.3	5.4	16.7	3.9	3.9	2.1	1.6	0.3	0.3	1.3	1.6	0.0	0.8
585	0.0	0.0	0.3	7.4	6.9	0.0	0.0	0.0	7.7	21.4	1.9	4.1	1.4	1.1	0.3	0.0	3.0	3.0	0.0	0.0
590	0.0	0.1	0.0	4.6	3.3	0.0	0.0	0.6	8.1	23.8	1.2	7.8	0.9	0.6	0.0	0.9	2.6	3.5	0.0	1.9
595	0.0	0.0	0.0	4.2	2.1	0.0	0.0	0.0	11.4	28.5	3.8	7.2	1.3	2.1	0.4	0.2	1.1	1.3	0.0	0.6
600	0.0	0.0	0.0	11.9	1.1	0.0	0.0	0.4	5.4	29.7	2.2	4.0	2.5	2.2	0.4	0.0	0.6	0.6	0.0	0.2
605	0.0	0.1	0.0	3.8	2.8	0.0	0.0	0.0	9.9	30.3	1.4	4.7	2.0	3.8	0.3	0.1	1.3	1.4	0.0	0.6
610	0.1	0.0	0.0	7.6	2.2	0.0	0.0	0.0	7.6	31.1	3.0	4.3	1.8	1.0	0.0	0.1	1.6	1.7	0.0	0.1
615	0.0	0.1	0.0	4.2	0.7	0.0	0.0	0.0	9.2	29.9	2.9	6.3	1.9	1.3	0.9	0.0	1.3	1.3	0.0	0.4
620	0.0	0.1	0.0	5.3	2.0	0.0	0.0	0.3	8.3	21.7	3.8	6.5	2.5	1.0	0.3	0.0	2.6	2.6	0.0	0.3
625	0.0	0.1	0.0	2.7	0.9	0.0	0.0	0.0	14.8	25.0	1.1	6.2	1.6	0.0	0.3	0.3	2.7	3.0	0.0	0.1
630	0.0	0.0	0.0	4.5	1.4	0.0	0.0	0.0	11.3	20.6	2.9	3.1	1.8	3.4	0.0	0.1	2.1	2.3	0.0	0.5
635	0.0	0.1	0.0	4.7	2.9	0.0	0.0	0.0	9.5	24.0	1.5	5.6	1.9	2.0	0.0	0.6	3.1	3.7	0.0	0.1
640	0.0	0.0	0.4	10.4	1.4	0.0	0.0	0.4	7.8	16.8	1.8	3.4	1.7	1.4	0.0	0.1	3.9	4.0	0.0	0.1
645	0.0	0.1	0.0	7.6	2.7	0.0	0.0	0.0	9.4	18.9	3.3	6.8	2.9	2.4	0.0	0.0	3.3	3.3	0.0	0.3
650	0.0	0.1	0.0	7.4	1.8	0.0	0.0	0.0	6.8	20.9	3.3	7.7	2.3	3.8	0.5	0.4	1.2	1.6	0.0	0.5
655	0.0	0.0	0.0	4.6	0.0	0.0	0.0	0.0	8.3	25.7	2.3	10.2	2.2	2.3	0.5	0.3	1.5	1.8	0.0	0.5
660	0.0	0.0	0.0	9.7	2.8	0.0	0.0	0.0	7.2	21.0	0.9	7.9	4.6	0.5	1.9	0.3	3.2	3.6	0.0	0.1
665	0.0	0.0	0.0	5.7	1.4	0.0	0.0	0.0	7.3	19.4	2.1	8.0	2.0	0.7	0.0	0.0	4.3	4.3	0.0	0.4
670	0.0	0.4	0.0	8.6	1.3	0.0	0.0	0.0	7.4	19.6	2.9	5.9	2.9	2.9	0.4	0.0	2.7	2.7	0.0	0.2
675	0.0	0.0	0.0	5.7	0.3	0.0	0.0	0.0	14.8	25.1	2.2	6.2	1.1	1.9	0.3	0.0	1.4	1.4	0.0	0.0
680	0.0	0.2	0.0	2.7	1.1	0.0	0.0	0.0	13.3	27.9	1.3	7.8	2.3	2.7	0.3	0.0	1.1	1.1	0.0	0.2
685	0.0	0.4	0.0	4.1	0.6	0.0	0.0	0.0	11.9	25.4	0.7	7.5	2.9	1.7	0.0	0.1	3.6	3.7	0.0	0.7
690	0.0	0.0	0.0	6.4	0.2	0.0	0.0	0.0	10.9	18.6	2.3	7.2	2.3	2.6	0.4	0.0	3.6	3.6	0.0	0.4
695	0.0	0.0	0.0	10.5	2.0	0.0	0.0	0.0	9.1	23.7	0.8	6.3	2.0	0.8	0.4	0.2	3.8	4.0	0.0	0.2
700	0.0	0.2	0.0	8.0	1.2	0.0	0.0	0.0	8.0	24.3	1.9	4.6	2.0	0.0	0.0	0.0	2.7	2.7	0.0	0.4
705	0.0	0.0	0.0	10.3	1.7	0.0	0.0	0.0	10.9	19.2	0.6	7.3	2.5	0.8	0.8	0.1	3.5	3.6	0.0	0.7
710	0.0	0.2	0.3	11.9	0.9	0.0	0.0	0.0	6.3	22.2	1.8	5.5	2.0	0.6	0.0	0.0	3.2	3.2	0.0	0.6
715	0.0	0.0	0.3	5.3	0.5	0.0	0.0	0.0	12.3	26.2	1.3	9.1	2.4	0.8	0.0	0.5	4.5	5.1	0.0	0.3
720	0.0	0.0	1.6	11.9	1.3	0.0	0.0	0.0	13.1	22.3	0.9	3.6	3.4	0.9	0.3	0.3	2.1	2.4	0.0	0.1
725	0.0	0.0	0.9	5.2	1.1	0.0	0.0	0.0	17.5	22.5	1.7	9.6	3.1	0.4	0.0	0.2	3.9	4.1	0.0	0.0
730	0.0	0.0	1.8	4.3	1.4	0.0	0.0	0.0	15.9	19.4	0.9	8.7	5.5	1.1	0.0	0.2	4.6	4.8	0.0	0.2
735	0.0	0.3	1.0	5.8	0.3	0.0	0.0	0.0	18.8	16.7	0.9	11.6	2.8	0.3	0.0	0.0	3.8	3.8	0.0	0.1
740	0.0	0.0	1.9	8.8	0.6	0.0	0.0	0.0	13.1	18.0	2.6	6.7	3.4	2.3	0.0	0.0	1.0	1.0	0.0	0.1
745	0.0	0.2	1.6	1.4	0.0	0.0	0.0	0.0	15.9	22.5	2.5	11.7	2.4	0.7	0.4	0.0	1.0	1.0	0.0	1.0

depth (cm)	uvu	ment	pdi	par
375	0.0	0.0	0.4	1.4
380	0.0	0.0	0.0	0.1
385	0.0	0.3	0.0	0.4
390	0.3	0.0	0.1	0.0
395	0.0	0.0	0.2	0.4
400	0.0	0.0	0.0	0.0
405	0.0	0.0	0.2	0.0
410	0.0	0.0	0.0	0.0
415	0.0	0.0	0.0	0.0
420	0.0	0.0	0.5	0.0
425	0.0	0.0	0.2	1.1
430	0.2	0.0	0.0	0.0
435	0.0	0.0	0.1	0.3
440	0.0	0.0	0.0	0.0
445	0.0	0.0	0.0	0.0
450	0.0	0.0	0.4	1.2
455	0.0	0.0	0.0	0.4
460	0.0	0.0	0.0	0.0
465	0.0	0.0	0.3	0.0
470	0.0	0.0	0.0	0.5
475	0.0	0.0	0.0	0.6
480	0.0	0.3	0.3	0.3
485	0.0	0.0	0.0	0.5
490	0.0	0.0	0.1	0.6
495	0.0	0.0	0.3	3.1
500	0.0	0.0	0.0	0.8
505	0.0	0.2	0.4	0.5
510	0.0	0.0	0.1	1.4
515	0.0	0.0	1.0	0.2
520	0.0	0.0	0.8	0.0
525	0.0	0.0	0.3	0.3
530	0.0	0.0	0.3	0.7
535	0.0	0.0	1.1	1.0
540	0.0	0.0	0.8	0.8
545	0.0	0.0	0.0	1.4
550	0.0	0.0	1.0	0.6
555	0.0	0.0	0.5	1.8
560	0.0	0.0	0.0	1.1
565	0.0	0.0	0.0	0.6
570	0.0	0.0	0.0	1.7
575	0.0	0.0	0.9	3.2
580	0.0	0.0	0.2	3.4
585	0.0	0.0	2.5	4.4
590	0.0	0.0	0.4	2.9
595	0.0	0.0	0.4	1.7
600	0.0	0.0	0.0	1.1
605	0.0	0.0	0.8	2.0
610	0.0	0.1	0.1	2.1
615	0.0	0.0	0.0	0.7
620	0.0	0.0	0.3	1.8
625	0.0	0.0	0.1	0.8
630	0.0	0.0	0.0	1.4
635	0.0	0.0	0.7	2.2
640	0.0	0.0	0.0	1.4
645	0.0	0.0	0.8	1.9
650	0.0	0.0	0.1	1.7
655	0.0	0.0	0.0	0.0
660	0.0	0.0	0.0	2.8
665	0.0	0.0	0.0	1.4
670	0.0	0.0	0.2	1.1
675	0.0	0.0	0.0	0.3
680	0.0	0.0	0.1	1.0
685	0.0	0.0	0.0	0.6
690	0.0	0.0	0.2	0.0
695	0.0	0.0	0.0	2.0
700	0.0	0.0	0.0	1.2
705	0.0	0.0	0.3	1.4
710	0.0	0.0	0.0	0.9
715	0.0	0.0	0.5	0.0
720	0.0	0.0	0.0	1.3
725	0.0	0.0	0.7	0.4
730	0.0	0.0	0.0	1.4
735	0.0	0.0	0.0	0.3
740	0.0	0.0	0.3	0.3
745	0.0	0.0	0.0	0.0

Appendix IV: M35003-4, foraminiferal census counts

depth (cm)	Lat	Long	water depth (m)	counted	aeq	bul	cal	cav	con	cra	deh	dig	dut	fal	glu	hir	hum	inf
750	12.0830	-61.2330	1299	645	5.7	13.8	0.1	0.0	0.8	0.2	0.0	0.8	4.0	0.0	9.7	0.0	0.0	0.4
755	12.0830	-61.2330	1299	431	1.0	17.5	0.5	0.0	0.5	0.5	0.0	0.0	6.5	0.4	10.2	0.4	0.0	0.3
760	12.0830	-61.2330	1299	537	1.6	15.2	0.5	0.0	0.9	0.5	0.0	0.0	8.0	1.2	14.8	0.0	0.0	0.5
765	12.0830	-61.2330	1299	509	4.0	16.1	0.8	0.0	0.7	0.6	0.0	0.0	5.1	1.1	10.5	0.0	0.0	0.3
770	12.0830	-61.2330	1299	537	3.1	16.1	0.3	0.0	0.7	1.0	0.0	0.0	5.4	0.3	16.8	0.3	0.0	0.2
775	12.0830	-61.2330	1299	480	1.7	16.0	0.0	0.0	0.6	0.6	0.0	0.0	13.0	1.2	11.8	0.0	0.0	0.1
780	12.0830	-61.2330	1299	403	2.5	18.6	0.0	0.0	0.2	0.6	0.0	0.0	5.3	0.4	21.6	0.4	0.0	0.1
785	12.0830	-61.2330	1299	478	1.9	16.9	0.0	0.0	0.7	0.7	0.0	0.0	11.5	1.4	14.7	0.0	0.0	0.6
790	12.0830	-61.2330	1299	757	1.2	19.2	0.3	0.0	0.3	0.4	0.0	0.0	13.1	0.7	9.5	0.0	0.0	0.4
795	12.0830	-61.2330	1299	299	1.0	12.4	0.3	0.0	1.0	0.3	0.0	0.0	13.7	0.7	7.4	0.0	0.0	1.0
800	12.0830	-61.2330	1299	430	1.3	14.1	0.0	0.0	0.8	0.2	0.0	0.0	9.7	0.3	10.3	0.0	0.0	0.2
805	12.0830	-61.2330	1299	299	1.0	12.7	0.7	0.0	1.3	0.7	0.0	0.0	16.4	0.0	5.0	0.0	0.0	0.3
810	12.0830	-61.2330	1299	542	0.2	18.0	0.2	0.0	0.1	0.2	0.0	0.0	11.8	0.0	10.7	0.0	0.0	0.7
815	12.0830	-61.2330	1299	170	0.4	15.7	0.0	0.0	1.6	0.0	0.0	0.0	14.1	0.0	2.4	0.0	0.0	0.4
820	12.0830	-61.2330	1299	462	0.8	19.6	0.6	0.0	0.4	0.1	0.0	0.0	13.9	0.3	7.6	0.3	0.0	0.6
825	12.0830	-61.2330	1299	321	0.3	16.5	0.0	0.0	1.2	0.6	0.0	0.0	17.4	0.6	5.3	0.0	0.3	0.0
830	12.0830	-61.2330	1299	443	0.4	17.0	0.6	0.0	0.1	0.3	0.0	0.0	11.1	0.0	10.1	0.0	0.0	0.0
835	12.0830	-61.2330	1299	522	1.4	8.5	0.1	0.0	2.3	0.8	0.0	0.0	17.1	0.6	6.8	0.0	0.0	0.0
840	12.0830	-61.2330	1299	634	2.3	10.4	0.6	0.0	0.5	0.7	0.0	0.0	4.8	0.3	16.5	0.0	0.0	0.1
845	12.0830	-61.2330	1299	448	2.8	11.4	0.6	0.0	0.8	0.6	0.0	0.0	3.1	0.0	14.3	0.0	0.0	0.0
850	12.0830	-61.2330	1299	509	5.6	10.1	0.2	0.0	0.6	0.6	0.0	0.2	4.0	0.0	14.1	0.0	0.0	0.0
855	12.0830	-61.2330	1299	559	6.5	8.8	1.6	0.0	1.3	0.1	0.0	0.0	5.4	0.2	12.4	0.0	0.0	0.0
860	12.0830	-61.2330	1299	401	2.7	16.2	0.3	0.0	0.6	0.5	0.0	0.0	7.2	0.3	11.2	0.0	0.3	0.0
865	12.0830	-61.2330	1299	356	2.4	13.5	0.4	0.0	0.5	0.7	0.0	0.0	7.1	0.4	10.2	0.0	0.0	0.4
870	12.0830	-61.2330	1299	511	3.4	15.2	0.3	0.0	0.6	0.1	0.0	0.0	4.7	0.0	15.5	0.0	0.0	0.3
875	12.0830	-61.2330	1299	531	1.9	7.3	0.6	0.0	1.1	0.9	0.0	0.0	2.6	1.2	11.4	0.2	0.0	0.1
880	12.0830	-61.2330	1299	382	8.3	4.4	3.0	0.0	0.6	0.2	0.0	0.0	2.4	0.0	9.5	0.0	0.0	1.1
885	12.0830	-61.2330	1299	382	6.0	2.7	0.8	0.0	1.6	0.0	0.0	0.0	2.5	0.4	3.8	0.0	0.0	0.8
890	12.0830	-61.2330	1299	414	7.1	13.5	1.2	0.0	1.8	0.8	0.0	0.0	3.3	0.0	12.6	0.0	0.0	0.1
895	12.0830	-61.2330	1299	547	8.0	18.1	1.3	0.0	1.5	1.0	0.0	0.6	4.8	1.0	9.0	0.0	0.0	0.3
900	12.0830	-61.2330	1299	398	6.1	15.8	1.8	0.0	2.7	0.7	0.0	0.0	3.6	0.0	8.8	0.0	0.0	0.0
905	12.0830	-61.2330	1299	526	8.0	6.3	2.0	0.0	2.3	1.1	0.0	0.0	5.2	0.8	15.6	0.0	0.0	0.0
910	12.0830	-61.2330	1299	327	6.5	14.3	1.4	0.0	1.5	1.2	0.0	0.5	2.0	1.4	20.8	0.0	0.0	0.1
915	12.0830	-61.2330	1299	407	6.9	10.7	2.0	0.0	1.3	0.3	0.0	0.0	4.0	0.9	13.3	0.0	0.0	0.1
920	12.0830	-61.2330	1299	332	7.9	16.1	4.0	0.0	0.8	0.8	0.0	0.0	2.5	0.0	15.6	0.0	0.0	0.1
925	12.0830	-61.2330	1299	472	4.3	12.3	1.4	0.0	0.1	2.2	0.0	0.0	6.6	0.0	10.6	0.0	0.0	0.0
930	12.0830	-61.2330	1299	361	3.5	20.9	1.3	0.0	0.7	2.9	0.0	0.0	5.5	0.7	14.4	0.0	0.0	0.0
935	12.0830	-61.2330	1299	356	5.4	6.2	3.0	0.0	1.0	0.8	0.0	0.4	6.6	0.0	8.0	0.0	0.0	0.0
940	12.0830	-61.2330	1299	529	7.4	9.2	0.9	0.0	0.9	0.0	0.0	0.0	1.2	4.6	10.1	0.0	0.0	0.0
945	12.0830	-61.2330	1299	342	3.1	7.6	0.4	0.0	0.4	2.2	0.0	0.0	10.2	0.0	11.0	0.0	0.0	0.0
950	12.0830	-61.2330	1299	329	4.1	20.9	1.6	0.0	0.2	3.3	0.0	0.0	8.7	0.2	10.2	0.0	0.0	0.0
955	12.0830	-61.2330	1299	492	0.4	5.5	0.0	0.0	0.9	3.9	0.0	0.0	8.8	1.2	10.8	0.0	0.0	0.0

Appendix IV: M35003-4, foraminiferal census counts

depth (cm)	men	nit	obl	pal	par+	qul	qur	qui	rur	ruw	rus	tri	sac	sci	ten	trl	trr	trus	tum	univ
750	0.0	0.3	1.8	4.8	0.2	0.0	0.0	0.0	9.1	22.3	2.1	10.7	4.2	3.5	0.3	0.1	3.3	3.4	0.0	1.2
755	0.0	0.2	1.2	12.5	1.1	0.0	0.0	0.0	9.5	23.7	4.1	6.6	0.5	0.8	0.0	0.0	1.4	1.4	0.0	0.5
760	0.0	0.0	3.0	9.2	1.2	0.0	0.0	0.0	6.9	23.4	4.4	3.6	1.7	0.2	0.2	0.0	1.8	1.8	0.2	0.5
765	0.0	0.1	2.4	5.4	3.1	0.0	0.0	0.0	11.0	22.6	2.9	8.2	1.9	0.0	0.7	0.0	2.1	2.1	0.0	0.4
770	0.0	0.1	1.1	8.7	1.8	0.0	0.0	0.0	11.1	18.4	1.0	6.4	1.7	2.6	0.0	0.0	2.7	2.7	0.0	0.4
775	0.0	0.0	2.3	2.3	1.9	0.0	0.0	0.0	11.4	20.7	2.9	6.2	3.2	0.6	0.3	0.1	2.6	2.7	0.0	0.6
780	0.0	0.2	0.3	5.4	2.9	0.0	0.0	0.0	8.8	18.0	0.8	4.8	2.1	2.1	0.0	0.1	4.6	4.7	0.0	0.2
785	0.0	0.0	1.8	8.9	1.4	0.0	0.0	0.0	9.7	19.8	3.3	2.9	1.1	0.0	0.0	0.1	2.5	2.6	0.0	0.0
790	0.0	0.3	1.8	6.1	1.7	0.0	0.0	0.3	6.3	27.3	1.3	3.7	1.7	0.7	0.1	0.1	3.4	3.6	0.0	0.1
795	0.0	0.0	1.3	4.0	3.3	0.0	0.0	0.0	8.4	24.4	2.7	8.0	2.7	0.3	0.7	0.0	5.4	5.4	0.0	1.0
800	0.0	0.0	1.1	6.0	2.5	0.0	0.0	0.0	7.1	28.2	1.9	8.3	2.7	0.6	0.6	0.0	3.6	3.6	0.0	0.0
805	0.0	0.0	2.3	2.3	2.3	0.0	0.0	0.0	12.4	22.4	2.3	6.7	4.0	0.3	0.0	0.0	6.4	6.4	0.0	0.0
810	0.0	0.0	1.5	6.5	1.6	0.0	0.0	0.0	5.8	29.2	2.2	5.1	1.9	0.7	0.0	0.1	3.0	3.1	0.0	0.2
815	0.0	0.0	0.0	2.4	3.2	0.0	0.0	0.0	9.2	38.2	1.6	3.6	2.0	0.0	0.0	0.0	4.8	4.8	0.0	0.4
820	0.0	0.0	0.6	6.8	1.7	0.0	0.0	0.0	5.6	28.5	2.5	3.5	0.4	2.3	0.0	0.0	3.9	3.9	0.0	0.0
825	0.0	0.0	0.9	0.9	2.8	0.0	0.0	0.3	13.1	29.6	2.8	3.4	2.8	0.3	0.0	0.0	2.5	2.5	0.0	0.0
830	0.0	0.0	1.6	1.4	1.0	0.0	0.0	0.0	2.4	42.2	2.0	5.4	0.9	1.1	0.0	0.0	2.4	2.4	0.0	0.0
835	0.0	0.0	0.0	0.3	1.9	0.0	0.0	0.0	6.0	36.9	1.0	8.6	3.1	0.0	0.1	0.0	4.1	4.1	0.0	0.0
840	0.0	0.1	0.6	1.7	1.9	0.0	0.0	0.0	6.9	36.0	1.4	9.5	1.2	1.2	0.0	0.0	2.9	2.9	0.0	0.1
845	0.0	0.3	0.8	0.3	0.1	0.0	0.0	0.0	15.2	27.1	0.3	14.6	3.8	0.3	0.0	0.0	3.2	3.2	0.0	0.0
850	0.0	0.0	1.0	2.9	1.0	0.0	0.0	0.0	12.2	31.3	0.5	9.3	2.8	1.2	0.0	0.1	2.1	2.2	0.0	0.1
855	0.0	0.3	1.1	1.8	0.8	0.0	0.0	0.0	9.9	27.6	2.3	11.3	4.3	1.1	0.0	0.1	2.4	2.5	0.0	0.3
860	0.0	0.6	0.6	7.1	2.2	0.0	0.0	0.6	13.6	16.7	2.9	7.5	2.4	0.6	0.0	0.2	4.7	4.8	0.0	0.6
865	0.0	0.4	1.1	0.4	1.6	0.0	0.0	0.4	13.7	27.9	1.8	9.5	3.5	0.4	0.0	0.0	3.6	3.6	0.0	0.0
870	0.0	0.0	0.6	2.3	1.3	0.0	0.0	0.0	15.0	19.8	0.5	11.2	1.5	2.8	0.0	0.1	3.7	3.8	0.0	0.8
875	0.0	0.0	1.4	0.2	2.1	0.0	0.0	0.0	20.3	27.1	1.2	10.9	3.0	0.5	0.0	0.0	4.7	4.7	0.0	0.5
880	0.0	0.0	0.6	0.4	0.5	0.0	0.0	0.0	7.1	43.9	0.4	7.5	0.6	0.4	0.4	0.1	6.1	6.2	0.0	0.5
885	0.0	0.0	1.8	0.0	0.4	0.0	0.0	0.0	3.3	59.0	0.4	7.4	2.0	0.4	0.0	0.4	5.3	5.7	0.0	0.0
890	0.0	0.0	0.8	0.0	0.9	0.0	0.0	0.0	10.7	30.2	0.0	9.8	1.7	1.2	0.0	0.7	2.0	2.7	0.0	0.9
895	0.0	0.0	1.0	0.3	1.0	0.0	0.0	0.0	15.5	16.7	4.5	7.7	3.1	0.0	0.0	0.1	3.9	4.0	0.0	0.5
900	0.0	0.2	0.8	0.0	0.3	0.0	0.0	0.3	15.1	21.1	1.3	10.9	2.3	1.7	0.3	0.0	5.0	5.0	0.0	0.2
905	0.0	0.0	0.8	0.0	1.7	0.0	0.0	0.0	21.7	16.3	1.5	9.5	2.8	0.5	0.0	0.4	2.2	2.6	0.0	1.3
910	0.0	0.0	1.1	0.0	2.5	0.0	0.0	0.0	15.5	16.2	0.9	8.7	0.9	0.0	0.9	0.1	1.4	1.5	0.0	0.9
915	0.0	0.0	0.8	0.4	0.7	0.0	0.0	0.0	20.0	19.1	1.8	10.3	1.2	0.0	0.4	0.6	4.3	4.9	0.0	0.4
920	0.0	0.0	0.6	0.5	0.5	0.0	0.0	0.5	13.2	15.9	2.0	10.3	2.0	0.0	1.0	1.0	2.5	3.5	0.0	0.5
925	0.0	0.0	1.1	0.6	1.7	0.0	0.0	0.0	21.5	18.0	3.6	9.4	1.5	0.0	0.6	1.7	2.0	3.6	0.0	0.8
930	0.0	0.0	0.2	0.4	2.7	0.0	0.0	0.0	14.9	14.0	5.1	5.3	1.6	1.1	1.8	1.5	0.9	2.4	0.0	0.7
935	0.0	0.0	0.6	0.0	1.2	0.0	0.0	0.0	30.0	23.7	0.8	8.0	1.0	0.0	0.0	1.2	1.6	2.8	0.0	0.2
940	0.0	0.0	0.8	0.9	1.5	0.0	0.0	0.0	10.6	37.9	0.3	9.2	1.7	0.3	0.3	0.1	0.1	0.2	0.0	1.6
945	0.0	0.0	1.4	0.0	0.4	0.0	0.0	0.0	18.2	29.6	3.1	6.9	1.4	0.0	1.2	0.2	2.0	2.2	0.0	0.2
950	0.0	0.0	0.2	0.0	0.6	0.0	0.0	0.0	10.0	27.8	4.5	4.9	0.2	0.0	0.0	0.4	1.0	1.4	0.0	0.4
955	0.0	0.0	1.3	0.0	0.5	0.0	0.0	0.0	21.0	33.6	2.0	5.7	1.3	0.0	0.4	0.1	0.5	0.6	0.0	1.9

depth (cm)	uvu		ment	pdi	par
750	0.0	0.0	0.1	0.1	
755	0.0	0.0	0.7	0.4	
760	0.0	0.2	0.2	1.0	
765	0.0	0.0	0.5	2.6	
770	0.0	0.0	0.1	1.7	
775	0.0	0.0	0.4	1.4	
780	0.0	0.0	0.1	2.8	
785	0.0	0.0	0.3	1.1	
790	0.0	0.0	0.9	0.8	
795	0.0	0.0	2.0	1.3	
800	0.0	0.0	0.9	1.6	
805	0.0	0.0	1.0	1.3	
810	0.0	0.0	0.6	1.0	
815	0.0	0.0	0.0	3.2	
820	0.0	0.0	0.0	1.7	
825	0.0	0.0	0.9	1.9	
830	0.0	0.0	0.3	0.7	
835	0.0	0.0	1.4	0.5	
840	0.0	0.0	0.1	1.8	
845	0.0	0.0	0.1	0.0	
850	0.0	0.0	0.2	0.7	
855	0.0	0.0	0.6	0.2	
860	0.0	0.0	1.3	1.0	
865	0.0	0.0	0.9	0.7	
870	0.0	0.0	0.0	1.3	
875	0.0	0.0	1.4	0.7	
880	0.0	0.0	0.5	0.0	
885	0.0	0.0	0.0	0.4	
890	0.0	0.0	0.1	0.8	
895	0.0	0.0	1.0	0.0	
900	0.0	0.0	0.0	0.3	
905	0.0	0.0	1.4	0.3	
910	0.0	0.0	0.6	1.9	
915	0.0	0.0	0.7	0.0	
920	0.0	0.0	0.0	0.5	
925	0.0	0.0	1.4	0.3	
930	0.0	0.0	1.3	1.5	
935	0.0	0.0	0.8	0.4	
940	0.0	0.0	0.1	1.4	
945	0.0	0.0	0.4	0.0	
950	0.0	0.0	0.2	0.4	
955	0.0	0.0	0.0	0.5	

Appendix V: M35003-4, planktonic foraminiferal assemblages (factors) and TFT SST estimates

depth (cm)	age (cal.kyr)	COMM.	factor 1	factor 2	Factor 3	Factor 4	Factor 5	Factor 6	Factor 7	Factor 8	Factor 9	Est. Tc0-50 (°C)	Est. Tw0-50 (°C)	seasonality
0	0.00	0.969	0.964	0.036	-0.001	0.015	0.047	0.033	0.013	0.170	-0.074	25.0	27.3	2.3
5	0.29	0.901	0.913	0.046	-0.001	0.016	0.101	0.020	0.022	0.193	-0.133	25.1	27.4	2.3
10	0.58	0.971	0.939	0.040	-0.003	0.013	0.150	0.027	0.002	0.237	-0.086	24.5	27.1	2.6
15	0.87	0.968	0.959	0.050	-0.002	0.009	0.081	0.026	-0.018	0.158	-0.115	25.1	27.2	2.1
20	1.15	0.943	0.936	0.070	-0.002	0.019	0.077	0.018	0.109	0.204	-0.039	24.2	26.9	2.7
25	1.44	0.977	0.938	0.066	-0.002	0.011	0.152	0.027	0.069	0.236	-0.095	24.2	26.7	2.5
30	1.73	0.960	0.950	0.067	-0.001	0.016	0.098	0.021	0.039	0.171	-0.104	24.7	26.9	2.2
35	2.02	0.989	0.984	0.057	-0.001	0.011	0.000	0.028	-0.014	0.120	-0.053	24.8	27.0	2.2
40	2.31	0.987	0.974	0.092	0.000	0.011	-0.061	0.028	0.069	0.136	-0.036	24.3	26.7	2.4
45	2.59	0.988	0.982	0.062	-0.001	0.014	-0.008	0.028	0.030	0.127	-0.054	24.8	27.0	2.2
50	2.88	0.971	0.961	0.134	0.001	0.012	0.012	0.031	0.052	0.148	-0.065	23.8	26.2	2.4
55	3.17	0.979	0.976	0.063	-0.001	0.018	0.018	0.021	0.051	0.090	-0.099	25.4	27.1	1.7
60	3.46	0.901	0.910	0.084	0.001	0.015	0.050	0.015	0.170	0.103	-0.151	26.0	27.4	1.4
65	3.75	0.943	0.945	0.074	0.017	0.019	0.015	0.021	0.119	0.128	-0.115	25.4	27.1	1.7
70	4.04	0.886	0.905	0.092	0.001	0.011	0.070	0.016	0.101	0.181	-0.102	24.6	27.0	2.4
75	4.32	0.862	0.876	0.096	0.002	0.009	0.146	0.012	0.126	0.127	-0.179	25.4	27.2	1.8
80	4.61	0.866	0.854	0.173	0.005	0.008	0.043	0.012	0.268	0.109	-0.142	24.9	26.4	1.5
85	4.90	0.837	0.873	0.072	0.002	0.003	0.086	0.016	0.121	0.050	-0.210	26.8	27.9	1.2
90	5.19	0.941	0.949	0.092	0.001	0.011	-0.046	0.021	0.095	0.107	-0.097	25.2	27.0	1.8
95	5.48	0.904	0.932	0.095	0.002	0.018	-0.010	0.024	0.032	0.102	-0.118	25.0	27.0	2.0
100	5.76	0.916	0.940	0.071	0.001	0.006	-0.045	0.028	-0.001	0.120	-0.101	25.0	27.2	2.3
105	6.03	0.888	0.923	0.082	0.002	0.003	-0.009	0.022	0.032	0.090	-0.139	25.5	27.4	1.8
110	6.30	0.916	0.945	0.049	0.001	0.006	-0.050	0.023	-0.027	0.091	-0.095	25.3	27.4	2.1
115	6.55	0.931	0.949	0.076	0.001	0.007	-0.064	0.031	0.014	0.091	-0.103	25.2	27.1	2.0
120	6.80	0.920	0.941	0.057	0.001	0.009	-0.015	0.022	0.052	0.123	-0.117	25.5	27.4	1.9
125	7.05	0.950	0.958	0.093	0.001	0.008	0.005	0.028	0.038	0.078	-0.126	25.4	27.0	1.6
130	7.30	0.956	0.962	0.088	0.001	0.008	-0.011	0.027	0.032	0.108	-0.099	25.0	26.9	1.9
135	7.55	0.959	0.964	0.098	0.000	0.015	-0.028	0.028	0.022	0.102	-0.085	24.7	26.7	2.0
140	7.80	0.985	0.977	0.114	-0.001	0.024	-0.070	0.023	0.056	0.096	-0.007	23.9	26.3	2.4
145	8.05	0.964	0.965	0.108	0.000	0.016	-0.050	0.029	-0.008	0.120	-0.060	24.1	26.5	2.4
150	8.30	0.889	0.908	0.161	0.000	0.029	0.010	0.017	0.103	0.143	-0.076	23.7	26.1	2.4
155	8.55	0.920	0.937	0.101	-0.003	0.038	0.079	0.025	0.026	0.135	-0.065	24.2	26.5	2.4
160	8.80	0.952	0.925	0.264	0.003	0.005	-0.012	0.029	0.013	0.158	-0.026	21.8	24.9	3.1
165	9.02	0.964	0.951	0.162	0.001	0.027	-0.027	0.039	0.149	0.073	-0.052	24.1	26.0	1.9
170	9.20	0.898	0.906	0.227	0.003	0.019	0.031	0.030	0.032	0.137	-0.060	22.7	25.4	2.8
175	9.38	0.909	0.915	0.205	0.001	0.015	0.053	0.029	0.025	0.127	-0.096	23.3	25.7	2.4
180	9.56	0.884	0.879	0.264	0.003	0.010	-0.004	0.030	-0.011	0.195	-0.043	21.7	25.1	3.5
185	9.74	0.948	0.950	0.168	0.002	0.014	-0.061	0.038	0.020	0.094	-0.052	23.5	25.9	2.4
190	9.92	0.910	0.902	0.280	0.005	0.001	-0.044	0.031	0.025	0.107	-0.055	22.1	25.0	2.8
195	10.25	0.834	0.847	0.229	0.005	0.006	0.097	0.050	0.065	0.144	-0.168	23.5	25.9	2.3
200	10.58	0.893	0.898	0.215	0.005	0.009	0.054	0.050	0.060	0.147	-0.103	23.2	25.7	2.5
205	10.91	0.864	0.893	0.176	0.002	0.008	-0.007	0.029	-0.026	0.149	-0.113	23.5	26.2	2.7
210	11.23	0.891	0.876	0.311	0.006	-0.014	0.022	0.028	-0.002	0.128	-0.098	22.1	25.0	2.8
215	11.56	0.961	0.927	0.284	0.009	-0.012	-0.024	0.034	-0.059	0.067	-0.103	22.6	24.9	2.3
220	11.89	0.897	0.844	0.346	0.007	-0.011	-0.040	0.026	0.214	0.088	-0.094	22.3	24.4	2.2
225	12.22	0.969	0.929	0.299	0.005	-0.015	-0.066	0.033	-0.003	0.094	-0.048	21.9	24.7	2.8
230	12.49	0.948	0.925	0.263	0.004	-0.009	-0.036	0.033	0.025	0.086	-0.112	23.0	25.2	2.2
235	12.75	0.981	0.934	0.309	0.005	-0.015	-0.045	0.035	-0.028	0.084	-0.048	21.8	24.5	2.7
240	13.01	0.970	0.876	0.426	0.007	-0.014	-0.043	0.036	-0.017	0.130	-0.019	20.0	23.5	3.5
245	13.28	0.978	0.926	0.269	0.015	0.008	-0.105	0.065	-0.014	0.160	0.083	20.4	24.5	4.1
250	13.54	0.904	0.849	0.389	0.006	-0.006	0.025	0.027	0.088	0.115	-0.099	21.3	24.1	2.7
255	13.81	0.963	0.922	0.290	0.018	-0.005	-0.049	0.060	-0.053	0.141	-0.022	21.4	24.7	3.3
260	14.07	0.953	0.878	0.405	0.012	-0.010	0.005	0.049	-0.029	0.119	-0.011	20.5	23.8	3.4
265	14.34	0.961	0.908	0.344	0.013	0.001	-0.008	0.069	-0.035	0.094	-0.047	21.4	24.2	2.9
270	14.61	0.968	0.905	0.360	0.006	-0.001	-0.006	0.065	0.021	0.122	-0.010	20.8	24.0	3.2
275	14.87	0.965	0.927	0.289	0.034	0.001	-0.041	0.074	-0.065	0.088	-0.037	21.8	24.6	2.9
280	15.14	0.964	0.950	0.217	0.003	0.017	-0.030	0.041	0.007	0.106	0.000	22.4	25.2	2.9
285	15.40	0.994	0.984	0.137	0.000	0.013	-0.042	0.030	0.006	0.052	-0.043	24.1	26.1	2.0
290	15.67	0.931	0.951	0.109	-0.002	0.021	0.015	0.025	0.037	0.013	-0.108	25.4	26.8	1.4
295	16.11	0.961	0.959	0.183	0.007	0.034	-0.038	0.034	0.038	0.057	0.004	23.0	25.5	2.5
300	16.54	0.810	0.850	0.266	0.001	0.025	0.008	0.017	0.104	-0.002	-0.072	23.6	25.6	2.1
305	16.98	0.940	0.891	0.361	0.082	0.015	0.033	0.044	0.046	-0.005	-0.060	21.8	24.2	2.4
310	17.41	0.948	0.849	0.437	0.053	-0.008	-0.033	0.049	0.139	0.076	-0.068	20.8	23.4	2.7
315	17.87	0.954	0.909	0.322	0.055	0.007	0.029	0.043	0.105	0.072	-0.041	21.9	24.5	2.6
320	18.34	0.875	0.777	0.391	0.116	0.013	0.017	0.026	0.287	0.098	-0.111	21.8	23.8	2.1
325	18.80	0.862	0.840	0.326	0.088	0.005	0.067	0.030	0.078	0.131	-0.118	22.1	24.6	2.6
330	19.26	0.860	0.847	0.312	0.067	0.001	0.050	0.039	-0.001	0.156	-0.114	22.0	24.8	2.9
335	19.73	0.871	0.860	0.273	0.078	-0.002	0.064	0.029	0.094	0.065	-0.180	23.6	25.4	1.8
340	20.19	0.894	0.877	0.240	0.129	0.031	0.092	0.053	0.036	0.074	-0.175	23.4	25.4	2.0
345	20.66	0.911	0.842	0.314	0.132	0.007	0.057	0.038	0.215	0.106	-0.157	23.1	24.8	1.7
350	21.12	0.894	0.868	0.266	0.013	0.013	0.141	0.028	0.156	0.102	-0.122	23.0	25.2	2.2
355	21.58	0.954	0.907	0.276	0.120	-0.003	0.008	0.058	0.119	0.020	-0.153	23.9	25.5	1.6
360	22.05	0.953	0.928	0.285	0.008	0.005	0.003	0.037	0.026	0.085	-0.039	22.1	24.8	2.6
365	22.51	0.930	0.897	0.287	0.125	0.002	0.005	0.039	0.025	0.098	-0.124	22.6	25.0	2.3
370	22.97	0.975	0.898	0.270	0.244	0.013	-0.029	0.026	0.062	0.174	0.018	22.2	25.3	3.1

Appendix V: M35003-4, planktonic foraminiferal assemblages (factors) and TFT SST estimates

depth (cm)	age (cal.kyr)	COMM.	factor 1	factor 2	Factor 3	Factor 4	Factor 5	Factor 6	Factor 7	Factor 8	Factor 9	Est. Tc0-50 (°C)	Est. Tw0-50 (°C)	seasonality
375	23.44	0.969	0.901	0.248	0.271	0.028	-0.021	0.053	0.063	0.114	-0.041	23.1	25.8	2.7
380	23.90	0.942	0.884	0.311	0.202	-0.003	0.012	0.027	0.034	0.051	-0.139	22.9	25.1	2.2
385	24.24	0.964	0.914	0.267	0.016	0.007	-0.021	0.036	0.211	0.058	-0.083	23.4	25.1	1.7
390	24.58	0.960	0.933	0.271	0.026	0.011	-0.018	0.027	0.064	0.070	-0.067	22.6	24.9	2.3
395	24.92	0.910	0.866	0.306	0.047	0.015	-0.019	0.031	0.220	0.056	-0.105	23.1	24.8	1.8
400	25.26	0.950	0.947	0.192	0.011	0.025	-0.056	0.023	0.088	0.061	-0.036	23.5	25.6	2.2
405	25.60	0.990	0.962	0.157	0.012	0.020	-0.102	0.026	0.157	0.055	0.023	23.7	26.0	2.3
410	25.94	0.980	0.938	0.259	0.030	0.013	-0.050	0.028	0.132	0.109	0.023	21.8	24.8	3.0
415	26.28	0.982	0.938	0.275	0.035	0.019	-0.049	0.024	0.125	0.068	-0.026	22.3	24.7	2.4
420	26.62	0.967	0.939	0.240	0.075	0.012	-0.068	0.030	0.004	0.126	-0.005	21.8	24.9	3.1
425	26.96	0.990	0.953	0.242	0.012	0.022	-0.047	0.053	0.086	0.097	-0.014	22.2	24.8	2.6
430	27.30	0.943	0.893	0.319	0.109	0.021	0.035	0.023	0.096	0.137	-0.030	21.4	24.3	2.9
435	27.64	0.949	0.889	0.325	0.115	0.000	0.058	0.034	0.080	0.128	-0.109	22.1	24.5	2.4
440	27.98	0.966	0.933	0.231	0.105	0.009	-0.013	0.023	0.134	0.090	-0.070	23.3	25.5	2.1
445	28.32	0.891	0.868	0.247	0.122	0.017	0.025	0.018	0.168	0.083	-0.160	24.0	25.6	1.6
450	28.66	0.936	0.935	0.188	0.015	0.016	-0.063	0.054	-0.029	0.125	-0.061	22.9	25.6	2.8
455	29.00	0.970	0.945	0.182	0.115	0.035	-0.004	0.029	0.027	0.162	-0.036	22.7	25.4	2.7
460	29.35	0.984	0.960	0.174	0.019	0.011	-0.042	0.027	0.157	0.040	-0.049	24.4	26.1	1.7
465	29.69	0.981	0.967	0.159	0.013	0.026	-0.063	0.028	0.053	0.106	-0.021	23.2	25.7	2.5
470	30.05	0.953	0.900	0.357	0.049	0.017	-0.019	0.043	-0.031	0.100	0.012	20.6	23.9	3.3
475	30.41	0.917	0.869	0.371	0.035	-0.004	0.038	0.046	0.008	0.097	-0.098	21.6	24.2	2.7
480	30.77	0.978	0.865	0.465	0.059	-0.017	0.020	0.046	0.016	0.072	-0.033	20.3	23.3	3.0
485	31.13	0.897	0.788	0.419	0.039	-0.003	0.204	0.047	-0.051	0.142	-0.181	21.5	24.1	2.6
490	31.49	0.950	0.837	0.444	0.084	-0.002	0.086	0.051	-0.083	0.169	-0.006	20.2	23.6	3.4
495	31.85	0.953	0.807	0.328	0.101	0.045	0.178	0.109	0.051	0.369	0.002	20.2	23.4	3.2
500	32.21	0.929	0.796	0.448	0.141	-0.004	0.050	0.051	0.080	0.252	0.009	19.5	23.1	3.6
505	32.57	0.903	0.795	0.429	0.162	-0.004	0.044	0.041	0.140	0.178	-0.072	20.6	23.5	2.9
510	32.90	0.940	0.747	0.538	0.081	-0.012	0.127	0.074	0.012	0.244	-0.073	19.3	22.8	3.5
515	33.20	0.905	0.765	0.310	0.099	0.021	0.252	0.045	0.003	0.378	-0.069	21.1	24.0	2.9
520	33.49	0.955	0.749	0.554	0.145	-0.022	0.116	0.043	-0.054	0.208	-0.060	19.7	23.0	3.3
525	33.79	0.922	0.705	0.617	0.089	-0.027	0.129	0.049	-0.053	0.073	-0.094	19.9	22.8	2.9
530	34.08	0.961	0.822	0.503	0.099	0.012	0.053	0.050	0.121	0.024	-0.054	20.3	23.0	2.8
535	34.38	0.939	0.817	0.372	0.119	0.082	0.144	0.056	0.075	0.288	-0.011	19.8	23.1	3.3
540	34.68	0.959	0.781	0.452	0.242	0.032	0.065	0.049	0.084	0.267	-0.003	20.2	23.2	3.1
545	34.97	0.930	0.852	0.267	0.132	0.029	0.146	0.063	0.080	0.282	-0.060	21.7	24.4	2.7
550	35.23	0.930	0.770	0.483	0.135	0.033	0.110	0.050	0.120	0.235	-0.018	19.1	22.5	3.4
555	35.41	0.970	0.858	0.409	0.135	0.013	0.086	0.083	0.076	0.154	-0.064	20.8	23.7	2.9
560	35.60	0.976	0.830	0.464	0.165	-0.005	0.039	0.058	0.166	0.103	-0.040	20.5	23.4	3.0
565	35.81	0.953	0.868	0.302	0.071	0.025	0.082	0.039	0.281	0.084	-0.090	22.6	24.6	2.0
570	36.08	0.954	0.709	0.528	0.136	-0.002	0.201	0.078	0.121	0.299	-0.061	19.0	22.0	3.1
575	36.34	0.931	0.642	0.431	0.379	0.018	0.153	0.115	0.299	0.246	-0.038	21.5	23.3	1.8
580	36.60	0.958	0.577	0.591	0.378	-0.007	0.156	0.119	0.078	0.298	-0.008	20.3	22.4	2.1
585	36.86	0.951	0.663	0.466	0.215	0.043	0.212	0.165	-0.026	0.417	-0.015	20.6	22.9	2.4
590	37.12	0.953	0.818	0.407	0.142	0.015	0.128	0.115	0.080	0.248	-0.027	20.3	23.4	3.1
595	37.38	0.956	0.867	0.314	0.116	0.018	0.086	0.073	0.077	0.266	-0.053	21.1	24.0	2.9
600	37.64	0.985	0.789	0.487	0.306	-0.021	-0.008	0.054	-0.003	0.171	0.004	20.5	24.0	3.5
605	37.90	0.954	0.861	0.421	0.106	0.022	-0.051	0.080	0.024	0.116	-0.032	20.0	23.4	3.4
610	38.16	0.984	0.834	0.428	0.198	-0.014	0.029	0.084	-0.034	0.240	0.005	20.4	23.8	3.5
615	38.37	0.956	0.898	0.290	0.112	0.005	0.019	0.045	0.118	0.187	-0.036	21.7	24.5	2.8
620	38.49	0.962	0.759	0.541	0.164	-0.007	0.029	0.080	0.204	0.117	-0.062	19.6	22.5	2.9
625	38.62	0.917	0.755	0.530	0.080	-0.028	0.063	0.058	0.002	0.212	-0.084	19.4	23.0	3.6
630	38.74	0.924	0.705	0.576	0.139	-0.023	0.022	0.066	0.174	0.194	-0.044	18.3	21.7	3.5
635	38.86	0.957	0.787	0.510	0.141	0.006	0.056	0.096	0.086	0.193	-0.015	19.2	22.7	3.5
640	38.98	0.951	0.541	0.721	0.297	-0.028	0.065	0.064	0.097	0.178	0.002	17.5	20.9	3.5
645	39.11	0.918	0.692	0.529	0.239	0.005	0.172	0.089	-0.023	0.251	-0.040	20.4	23.2	2.9
650	39.23	0.957	0.737	0.576	0.228	-0.021	0.060	0.077	0.074	0.105	-0.056	19.8	23.0	3.2
655	39.70	0.973	0.822	0.503	0.132	-0.014	0.055	0.032	0.066	0.099	-0.092	20.3	23.1	2.8
660	40.18	0.956	0.741	0.508	0.294	-0.007	0.125	0.107	0.031	0.175	-0.065	21.1	23.9	2.8
665	40.65	0.944	0.691	0.541	0.170	0.002	0.191	0.069	0.148	0.281	-0.049	18.9	21.9	3.0
670	41.13	0.951	0.689	0.548	0.257	-0.020	0.144	0.061	0.131	0.260	-0.033	19.8	22.5	2.8
675	41.60	0.918	0.782	0.423	0.158	-0.022	0.100	0.039	0.028	0.284	-0.090	20.6	23.6	3.0
680	42.08	0.948	0.864	0.380	0.077	-0.008	0.018	0.056	0.144	0.140	-0.089	21.3	23.9	2.6
685	42.55	0.949	0.826	0.428	0.117	-0.007	0.064	0.046	0.160	0.184	-0.065	20.4	23.3	2.9
690	43.03	0.927	0.664	0.620	0.192	-0.033	0.107	0.033	0.118	0.180	-0.079	18.9	22.0	3.1
695	43.42	0.952	0.765	0.401	0.297	0.005	0.142	0.079	0.032	0.300	-0.010	21.8	24.2	2.4
700	43.70	0.966	0.747	0.529	0.224	-0.016	0.075	0.064	0.099	0.241	0.012	19.4	22.7	3.4
705	43.99	0.924	0.713	0.423	0.305	-0.001	0.158	0.064	0.185	0.271	-0.082	21.6	23.6	1.9
710	44.27	0.962	0.734	0.444	0.335	-0.004	0.107	0.047	0.185	0.257	-0.003	21.4	23.8	2.4
715	44.55	0.925	0.849	0.291	0.145	0.022	0.146	0.030	0.040	0.265	-0.063	21.7	24.4	2.7
720	44.83	0.917	0.737	0.377	0.338	0.000	0.104	0.055	0.121	0.296	-0.042	22.3	24.3	2.0
725	45.11	0.840	0.770	0.244	0.142	0.011	0.213	0.041	0.043	0.317	-0.132	22.3	24.8	2.5
730	45.37	0.838	0.729	0.419	0.131	-0.006	0.193	0.067	0.041	0.231	-0.133	21.0	23.8	2.8
735	45.61	0.786	0.667	0.446	0.172	-0.014	0.182	0.033	0.061	0.172	-0.214	21.1	23.6	2.5
740	45.84	0.894	0.695	0.523	0.270	-0.031	0.070	0.034	0.157	0.118	-0.138	20.9	23.4	2.5
745	46.07	0.885	0.821	0.345	0.045	-0.003	0.050	0.024	0.222	0.042	-0.191	23.5	24.8	1.3

Appendix V: M35003-4, planktonic foraminiferal assemblages (factors) and TFT SST estimates

depth (cm)	age (cal.kyr)	COMM.	factor 1	factor 2	Factor 3	Factor 4	Factor 5	Factor 6	Factor 7	Factor 8	Factor 9	Est. Tc0-50 (°C)	Est. Tw0-50 (°C)	seasonality
750	46.31	0.941	0.819	0.475	0.149	-0.005	0.078	0.028	0.041	0.037	-0.117	21.0	23.6	2.6
755	46.54	0.950	0.729	0.517	0.346	-0.019	0.037	0.039	0.023	0.156	-0.064	20.9	24.0	3.0
760	46.77	0.957	0.746	0.508	0.265	-0.004	0.049	0.052	0.164	0.201	0.014	19.8	23.1	3.3
765	47.06	0.939	0.778	0.519	0.166	-0.009	0.058	0.106	0.054	0.103	-0.089	20.2	23.3	3.0
770	47.42	0.928	0.678	0.561	0.260	-0.015	0.048	0.070	0.237	0.125	-0.082	19.9	22.6	2.7
775	47.78	0.927	0.716	0.526	0.075	-0.018	0.172	0.078	0.115	0.281	-0.057	18.7	22.3	3.5
780	48.14	0.939	0.626	0.629	0.159	-0.013	0.025	0.100	0.320	0.117	-0.020	17.3	20.6	3.2
785	48.50	0.938	0.659	0.556	0.259	-0.004	0.102	0.058	0.178	0.288	-0.003	18.8	21.7	2.9
790	48.86	0.971	0.746	0.536	0.165	-0.011	0.101	0.064	-0.012	0.291	0.040	19.1	22.8	3.7
795	49.22	0.935	0.800	0.403	0.118	0.042	0.178	0.079	-0.012	0.281	-0.030	20.3	23.5	3.2
800	49.59	0.972	0.842	0.430	0.165	0.000	0.089	0.081	0.020	0.191	-0.026	20.5	23.7	3.2
805	49.95	0.885	0.738	0.387	0.068	0.014	0.227	0.075	-0.050	0.352	-0.050	20.7	24.1	3.4
810	50.31	0.974	0.785	0.504	0.170	-0.005	0.080	0.063	0.006	0.256	0.016	19.4	23.0	3.6
815	50.67	0.973	0.840	0.347	0.057	0.008	0.054	0.103	-0.171	0.315	0.044	20.6	24.7	4.1
820	51.03	0.976	0.739	0.524	0.176	-0.005	0.094	0.074	-0.069	0.318	0.059	19.4	23.1	3.7
825	51.39	0.932	0.761	0.418	0.030	-0.016	0.141	0.091	-0.067	0.382	-0.013	20.0	24.2	4.2
830	51.72	0.974	0.873	0.391	0.033	-0.017	0.012	0.058	-0.049	0.219	0.070	19.7	23.9	4.2
835	51.99	0.967	0.892	0.231	0.006	0.013	0.136	0.059	-0.048	0.304	0.021	21.6	25.2	3.6
840	52.26	0.986	0.918	0.328	0.044	0.003	-0.020	0.073	0.134	0.097	-0.010	21.3	24.1	2.8
845	52.53	0.922	0.856	0.367	0.014	-0.017	0.048	0.035	0.137	0.009	-0.178	23.3	24.7	1.4
850	52.80	0.968	0.905	0.328	0.077	-0.006	-0.004	0.049	0.130	0.089	-0.088	22.2	24.5	2.3
855	53.07	0.962	0.906	0.318	0.052	-0.001	0.062	0.041	0.121	0.074	-0.109	22.5	24.6	2.1
860	53.34	0.870	0.664	0.557	0.229	-0.012	0.105	0.065	0.116	0.151	-0.122	20.0	22.8	2.8
865	53.54	0.938	0.854	0.412	0.020	-0.002	0.065	0.060	0.046	0.135	-0.101	20.9	23.8	2.8
870	53.64	0.884	0.730	0.517	0.074	-0.013	0.070	0.062	0.197	0.070	-0.160	20.7	23.0	2.3
875	53.75	0.841	0.857	0.253	0.010	0.021	0.006	0.050	0.122	0.045	-0.151	23.9	25.6	1.7
880	53.85	0.980	0.969	0.146	0.007	0.052	-0.086	0.026	-0.003	0.089	0.038	22.6	25.5	2.9
885	53.95	0.983	0.967	0.065	-0.003	0.041	-0.099	0.032	-0.131	0.088	0.084	23.0	26.2	3.2
890	54.06	0.967	0.882	0.411	0.007	-0.011	-0.003	0.056	0.079	0.068	-0.080	21.3	23.7	2.5
895	54.16	0.813	0.658	0.583	0.020	-0.016	0.080	0.039	0.058	0.087	-0.146	19.9	22.9	3.0
900	54.26	0.864	0.763	0.501	0.010	-0.020	0.062	0.042	0.025	0.047	-0.149	21.2	23.7	2.5
905	54.37	0.744	0.699	0.280	0.006	0.012	0.082	0.037	0.326	0.101	-0.230	23.7	25.1	1.4
910	54.47	0.869	0.653	0.522	0.014	-0.015	0.021	0.083	0.372	0.025	-0.154	20.8	22.3	1.5
915	54.57	0.774	0.739	0.382	0.018	0.005	0.053	0.029	0.201	0.073	-0.181	22.4	24.4	2.0
920	54.68	0.864	0.669	0.571	0.030	-0.028	0.058	0.047	0.233	0.011	-0.168	20.7	22.7	1.9
925	54.78	0.751	0.696	0.408	0.025	-0.009	0.096	0.044	0.142	0.144	-0.219	21.6	24.2	2.6
930	54.88	0.855	0.554	0.682	0.028	-0.034	0.062	0.084	0.198	0.128	-0.123	17.6	20.9	3.3
935	54.98	0.666	0.731	0.187	0.004	0.005	0.037	0.034	0.102	0.186	-0.223	23.7	26.5	2.8
940	55.09	0.968	0.944	0.257	0.024	0.013	-0.060	0.063	0.019	0.038	-0.004	22.3	24.8	2.6
945	55.19	0.902	0.863	0.254	0.003	-0.002	0.061	0.033	0.116	0.251	-0.104	22.0	24.9	3.0
950	55.29	0.958	0.761	0.570	0.011	-0.040	0.037	0.054	0.008	0.216	-0.031	18.5	22.7	4.2
955	55.40	0.877	0.874	0.183	0.003	0.005	0.013	0.036	0.107	0.240	-0.092	22.8	25.8	3.0

depth (cm)	age (cal.kyr)	DSML	STDEV	mean analog Tc0-50m (°C)	STDEV	mean analog Tw0-50m (°C)	STDEV	mean analog annual T75m (°C)	STDEV	mean analog annual T100m (°C)	STDEV	mean analog annual T150m (°C)	STDEV	SIM
0	0.0	0.075	0.009	26.0	0.2	27.6	0.4	25.2	1.0	23.8	1.5	20.7	2.0	0.962
5	0.3	0.058	0.009	25.9	0.2	27.8	0.2	25.6	0.5	24.4	1.0	21.6	1.7	0.971
10	0.6	0.076	0.006	25.9	0.3	27.7	0.4	25.3	1.0	24.0	1.5	21.0	2.0	0.962
15	0.9	0.066	0.013	26.0	0.3	27.7	0.2	25.4	0.5	24.0	1.0	20.9	1.7	0.967
20	1.2	0.072	0.012	25.9	0.1	27.9	0.2	25.8	0.4	24.8	0.7	22.2	1.2	0.964
25	1.4	0.063	0.010	25.4	1.2	27.2	1.0	24.1	2.5	22.3	3.2	19.2	3.6	0.969
30	1.7	0.068	0.009	25.7	1.0	27.5	0.8	24.9	2.0	23.4	2.7	20.3	3.0	0.966
35	2.0	0.077	0.008	26.1	0.5	27.5	0.4	25.0	1.0	22.9	2.1	18.5	3.5	0.962
40	2.3	0.076	0.014	25.8	0.3	27.8	0.4	25.8	0.4	24.8	0.7	22.1	1.1	0.962
45	2.6	0.075	0.009	26.0	0.2	27.9	0.3	25.8	0.6	24.7	1.0	22.0	1.6	0.963
50	2.9	0.070	0.009	25.9	0.1	27.9	0.1	26.0	0.1	25.1	0.1	22.7	0.3	0.965
55	3.2	0.056	0.011	25.7	0.5	27.7	0.5	25.7	0.6	24.7	0.9	22.0	1.5	0.972
60	3.5	0.074	0.009	25.9	0.3	27.9	0.2	25.9	0.5	24.9	0.8	22.4	1.2	0.963
65	3.7	0.048	0.009	25.9	0.1	27.9	0.2	25.8	0.4	24.8	0.7	22.1	1.2	0.976
70	4.0	0.061	0.010	25.9	0.2	27.9	0.2	25.8	0.4	24.8	0.7	22.1	1.2	0.970
75	4.3	0.077	0.011	25.9	0.2	27.9	0.2	25.9	0.5	25.0	0.8	22.4	1.2	0.962
80	4.6	0.086	0.011	25.8	0.5	27.6	0.9	24.9	2.8	23.9	2.9	21.3	2.6	0.957
85	4.9	0.094	0.009	25.8	1.0	27.6	0.9	25.2	2.2	23.9	2.8	21.0	3.2	0.953
90	5.2	0.063	0.015	25.8	0.3	27.7	0.3	25.7	0.4	24.7	0.7	22.0	1.1	0.968
95	5.5	0.075	0.013	25.9	0.2	27.8	0.2	25.7	0.5	24.5	0.9	21.8	1.4	0.963
100	5.8	0.100	0.019	25.9	0.2	27.8	0.2	25.7	0.5	24.5	0.9	21.8	1.4	0.950
105	6.0	0.089	0.013	26.0	0.2	27.8	0.2	25.6	0.5	24.3	1.0	21.4	1.7	0.956
110	6.3	0.100	0.013	26.1	0.4	27.7	0.2	25.5	0.5	24.0	1.0	20.5	1.9	0.950
115	6.6	0.098	0.014	26.0	0.5	27.6	0.3	25.5	0.5	24.2	0.9	20.8	1.9	0.951
120	6.8	0.062	0.018	26.0	0.2	27.8	0.2	25.6	0.5	24.4	1.0	21.4	1.7	0.969
125	7.1	0.071	0.010	25.9	0.2	27.9	0.2	25.8	0.4	24.8	0.7	22.1	1.2	0.965
130	7.3	0.060	0.015	25.9	0.4	27.8	0.4	25.8	0.5	24.8	0.8	22.2	1.3	0.970
135	7.6	0.072	0.013	25.9	0.2	27.8	0.3	25.5	0.9	24.2	1.7	21.2	2.9	0.964
140	7.8	0.089	0.014	25.8	0.4	27.7	0.4	25.7	0.5	24.6	0.8	21.9	1.4	0.956
145	8.1	0.069	0.013	25.9	0.2	27.9	0.2	25.8	0.4	24.8	0.7	22.2	1.2	0.965
150	8.3	0.103	0.016	25.9	0.2	27.9	0.2	25.8	0.4	24.8	0.7	22.2	1.2	0.948
155	8.6	0.105	0.015	25.6	0.5	27.5	0.6	25.4	0.7	24.2	1.1	21.4	1.8	0.948
160	8.8	0.120	0.012	25.3	1.4	27.4	0.9	24.1	3.6	22.8	4.0	20.4	3.6	0.940
165	9.0	0.108	0.011	25.9	0.2	27.8	0.2	25.7	0.5	24.6	0.9	21.8	1.5	0.946
170	9.2	0.122	0.017	25.9	0.2	27.8	0.2	25.6	0.5	24.5	0.9	21.8	1.5	0.939
175	9.4	0.115	0.013	25.3	1.2	27.4	1.0	24.2	3.2	23.0	3.7	20.4	3.7	0.943
180	9.6	0.149	0.014	25.3	1.2	27.4	1.1	24.1	3.5	23.0	3.7	20.5	3.4	0.925
185	9.7	0.125	0.018	25.5	0.5	27.5	0.6	25.4	0.6	24.3	0.9	21.5	1.6	0.938
190	9.9	0.146	0.019	24.8	1.8	27.1	1.2	23.1	4.1	22.0	4.4	19.6	3.9	0.927
195	10.2	0.142	0.013	25.0	1.6	27.0	1.3	23.0	4.1	21.8	4.1	19.5	3.6	0.929
200	10.6	0.102	0.005	24.8	1.9	26.8	1.6	23.0	4.2	21.8	4.3	19.4	3.7	0.949
205	10.9	0.118	0.016	24.9	1.8	27.0	1.2	23.1	4.0	21.9	4.0	19.4	3.5	0.941
210	11.2	0.144	0.012	24.4	1.8	26.5	1.4	21.6	4.2	20.3	4.4	18.0	3.9	0.928
215	11.6	0.138	0.015	24.3	1.9	26.4	1.2	20.8	4.2	19.3	4.3	17.1	3.7	0.931
220	11.9	0.182	0.019	25.0	1.5	27.2	1.0	23.2	4.1	22.0	4.4	19.6	4.0	0.909
225	12.2	0.181	0.018	24.7	1.7	27.0	1.2	22.5	4.6	21.3	5.0	19.1	4.6	0.909
230	12.5	0.145	0.017	25.4	1.1	27.4	0.9	24.0	3.7	23.0	3.8	20.5	3.5	0.928
235	12.7	0.152	0.015	24.9	1.8	26.7	1.0	21.8	4.1	19.9	4.5	17.2	3.9	0.924
240	13.0	0.171	0.022	23.1	1.5	25.7	0.8	18.9	2.9	17.2	3.3	15.3	2.6	0.915
245	13.3	0.214	0.012	24.3	1.7	26.5	1.4	22.7	3.6	21.3	4.3	18.7	3.8	0.893
250	13.5	0.164	0.020	24.5	1.8	26.9	1.2	22.3	4.4	21.1	4.6	18.8	4.1	0.918
255	13.8	0.204	0.013	24.0	1.9	26.5	1.3	21.5	4.4	20.2	4.8	18.2	4.3	0.898
260	14.1	0.178	0.014	23.0	1.7	25.7	1.0	18.3	2.9	16.5	3.1	14.9	2.8	0.911
265	14.3	0.182	0.019	23.2	1.9	25.7	1.0	18.4	2.7	16.6	2.8	14.9	2.3	0.909
270	14.6	0.162	0.013	23.7	2.1	26.0	1.4	20.3	3.8	18.5	4.1	16.2	3.5	0.919
275	14.9	0.191	0.012	24.5	2.1	26.9	1.2	22.2	4.4	20.9	4.7	18.6	4.1	0.905
280	15.1	0.173	0.012	24.8	1.6	27.0	1.0	22.9	3.9	21.5	4.3	19.0	3.8	0.914
285	15.4	0.106	0.009	25.2	1.0	26.9	1.0	24.1	2.2	22.6	3.0	19.5	3.5	0.947
290	15.7	0.125	0.009	25.7	0.7	27.3	0.6	25.1	1.0	23.5	1.9	19.9	3.2	0.938
295	16.1	0.153	0.009	25.0	1.0	27.0	1.0	25.0	1.0	24.0	1.1	21.1	1.6	0.923
300	16.5	0.226	0.015	24.3	1.9	26.0	1.1	20.9	3.4	18.7	3.7	15.5	3.1	0.887
305	17.0	0.204	0.019	23.0	1.5	25.3	0.7	19.0	2.1	17.2	2.4	14.9	1.6	0.898
310	17.4	0.195	0.017	22.3	0.8	25.0	0.8	18.5	2.2	17.1	2.4	14.8	1.6	0.902
315	17.9	0.176	0.012	23.8	1.8	26.2	1.3	21.1	4.0	19.5	4.4	17.1	4.0	0.912
320	18.3	0.217	0.018	23.8	2.0	26.3	1.4	20.9	4.2	19.4	4.4	17.1	3.9	0.891
325	18.8	0.205	0.021	24.6	1.8	26.6	1.2	21.6	4.1	20.1	4.2	17.8	3.7	0.898
330	19.3	0.216	0.021	24.0	1.9	26.3	1.3	20.7	4.2	19.4	4.3	17.3	3.7	0.892

depth (cm)	STEV	Est. Tc0-50m (°C)	Est. Tw0-50m (°C)	Est. annual T75m (°C)	Est. annual T100m (°C)	Est. annual T150m (°C)	#best Ana
0	0.005	26.0	27.6	25.2	23.8	20.7	10
5	0.005	25.9	27.8	25.6	24.4	21.6	10
10	0.003	25.9	27.7	25.3	24.0	21.0	10
15	0.007	26.0	27.7	25.4	24.0	20.9	10
20	0.006	25.9	27.9	25.8	24.8	22.2	10
25	0.005	25.4	27.2	24.1	22.3	19.2	10
30	0.005	25.7	27.5	24.9	23.4	20.3	10
35	0.004	26.1	27.5	25.0	22.9	18.5	10
40	0.007	25.8	27.8	25.8	24.8	22.1	10
45	0.005	26.0	27.9	25.8	24.7	22.0	10
50	0.004	25.9	27.9	26.0	25.1	22.6	10
55	0.005	25.7	27.7	25.7	24.7	22.0	10
60	0.004	25.9	27.9	25.9	24.9	22.4	10
65	0.005	25.9	27.9	25.8	24.8	22.1	10
70	0.005	25.9	27.9	25.8	24.8	22.1	10
75	0.006	25.9	27.9	25.9	24.9	22.4	10
80	0.005	25.8	27.6	24.9	23.9	21.3	10
85	0.004	25.8	27.6	25.2	23.9	21.0	10
90	0.007	25.8	27.7	25.7	24.7	22.0	10
95	0.007	25.9	27.8	25.7	24.5	21.8	10
100	0.010	25.9	27.8	25.7	24.5	21.8	10
105	0.006	26.0	27.8	25.6	24.4	21.4	10
110	0.007	26.1	27.7	25.5	24.0	20.5	10
115	0.007	26.0	27.6	25.5	24.2	20.8	10
120	0.009	26.0	27.8	25.6	24.4	21.4	10
125	0.005	25.9	27.9	25.8	24.8	22.1	10
130	0.008	25.9	27.8	25.8	24.8	22.2	10
135	0.007	25.9	27.8	25.5	24.2	21.3	10
140	0.007	25.8	27.7	25.7	24.6	21.9	10
145	0.007	25.9	27.9	25.8	24.8	22.2	10
150	0.008	25.9	27.9	25.8	24.8	22.2	10
155	0.008	25.6	27.5	25.4	24.2	21.4	10
160	0.006	25.3	27.4	24.1	22.9	20.4	10
165	0.005	25.9	27.8	25.7	24.6	21.8	10
170	0.008	25.9	27.8	25.6	24.5	21.8	10
175	0.006	25.3	27.4	24.2	23.0	20.4	10
180	0.007	25.3	27.4	24.1	23.0	20.5	10
185	0.009	25.5	27.5	25.4	24.3	21.5	10
190	0.009	24.8	27.1	23.2	22.0	19.6	10
195	0.006	25.0	27.0	23.0	21.8	19.5	10
200	0.003	24.8	26.8	23.0	21.8	19.4	10
205	0.008	24.9	27.0	23.1	21.9	19.4	10
210	0.006	24.4	26.5	21.6	20.3	18.0	10
215	0.008	24.3	26.4	20.8	19.3	17.1	10
220	0.010	25.0	27.2	23.2	22.0	19.6	10
225	0.009	24.7	27.0	22.5	21.2	19.1	10
230	0.009	25.4	27.4	24.0	23.0	20.5	10
235	0.007	24.9	26.7	21.8	19.9	17.2	10
240	0.011	23.1	25.7	18.8	17.2	15.3	10
245	0.006	24.3	26.5	22.7	21.3	18.7	10
250	0.010	24.5	26.9	22.3	21.0	18.8	10
255	0.006	24.0	26.5	21.5	20.2	18.2	10
260	0.007	23.0	25.7	18.3	16.5	14.9	10
265	0.009	23.2	25.7	18.4	16.6	14.9	10
270	0.006	23.6	26.0	20.3	18.5	16.2	10
275	0.006	24.5	26.9	22.2	20.9	18.6	10
280	0.006	24.8	27.0	22.9	21.5	19.0	10
285	0.005	25.2	26.9	24.1	22.6	19.5	10
290	0.005	25.7	27.3	25.1	23.5	19.9	10
295	0.005	25.0	27.0	25.0	24.0	21.1	10
300	0.007	24.3	26.0	20.9	18.7	15.5	10
305	0.010	23.0	25.3	19.0	17.2	14.9	10
310	0.009	22.3	25.0	18.5	17.1	14.8	10
315	0.006	23.8	26.2	21.1	19.5	17.1	10
320	0.009	23.8	26.3	20.9	19.4	17.1	10
325	0.010	24.6	26.6	21.6	20.1	17.7	10
330	0.011	24.0	26.3	20.7	19.4	17.3	10

depth (cm)	age (cal.kyr)	DSML	STDEV	mean analog Tc0-50m (°C)	STDEV	mean analog Tw0-50m (°C)	STDEV	mean analog annual T75m (°C)	STDEV	mean analog annual T100m (°C)	STDEV	mean analog annual T150m (°C)	STDEV	SIM
335	19.7	0.201	0.022	24.2	2.0	26.2	1.4	20.8	4.0	19.1	4.1	16.7	3.5	0.900
340	20.2	0.200	0.018	24.5	2.1	26.7	1.2	22.0	4.2	20.7	4.1	18.2	3.4	0.900
345	20.7	0.193	0.024	23.0	1.8	25.5	1.3	19.2	3.4	17.7	3.3	15.5	2.6	0.904
350	21.1	0.150	0.008	25.1	1.6	26.9	1.2	22.7	4.0	21.2	4.4	18.8	4.0	0.925
355	21.6	0.209	0.018	24.9	1.7	26.8	1.1	22.3	4.0	20.7	4.4	18.1	4.3	0.895
360	22.0	0.178	0.016	25.0	1.3	26.9	0.9	23.0	3.7	21.5	4.1	18.9	3.6	0.911
365	22.5	0.204	0.017	24.6	1.8	26.8	1.3	22.2	4.2	21.0	4.3	18.6	3.8	0.898
370	23.0	0.274	0.012	24.2	1.9	26.2	1.2	21.1	3.8	19.7	4.1	17.3	3.4	0.863
375	23.4	0.276	0.012	24.3	2.1	26.5	1.2	21.3	4.0	19.7	4.2	17.4	3.4	0.862
380	23.9	0.245	0.019	23.5	1.8	25.8	1.0	19.5	3.5	18.1	3.5	16.0	2.7	0.878
385	24.2	0.140	0.012	25.5	0.9	27.5	0.8	24.8	2.8	23.7	2.9	21.1	2.8	0.930
390	24.6	0.158	0.014	24.8	1.2	26.8	1.2	22.8	3.7	21.5	3.9	18.9	3.6	0.921
395	24.9	0.180	0.018	24.7	1.8	27.1	1.2	23.1	4.1	21.9	4.4	19.7	3.9	0.910
400	25.3	0.168	0.017	25.3	0.8	27.3	0.8	24.6	2.7	23.5	2.8	20.9	2.7	0.916
405	25.6	0.149	0.015	25.1	1.2	27.1	1.2	25.2	1.3	24.2	1.3	21.5	1.8	0.926
410	25.9	0.159	0.014	23.7	1.6	25.9	1.3	21.3	3.5	19.7	4.0	17.1	3.5	0.921
415	26.3	0.158	0.012	24.0	1.6	26.1	1.4	22.0	3.3	20.4	3.7	17.6	3.3	0.921
420	26.6	0.198	0.016	24.7	1.5	26.7	1.1	22.2	3.8	20.7	4.2	18.3	3.7	0.901
425	27.0	0.157	0.011	24.5	1.8	26.5	1.3	21.4	3.9	19.5	4.4	17.0	4.0	0.922
430	27.3	0.215	0.015	24.7	1.8	26.7	1.2	21.8	4.1	20.2	4.6	18.0	4.1	0.893
435	27.6	0.186	0.019	24.9	1.7	26.9	1.2	22.5	4.2	21.2	4.4	18.8	4.0	0.907
440	28.0	0.163	0.017	25.7	0.4	27.5	0.7	24.9	2.2	23.7	2.8	21.0	2.8	0.918
445	28.3	0.191	0.020	24.9	1.7	27.1	1.1	23.0	4.1	21.8	4.1	19.3	3.6	0.905
450	28.7	0.174	0.014	24.8	1.7	27.0	1.2	23.0	3.9	21.8	4.0	19.5	3.6	0.913
455	29.0	0.195	0.014	25.3	1.7	27.1	1.1	23.3	3.8	22.0	4.1	19.5	3.8	0.903
460	29.3	0.143	0.014	25.5	0.5	27.2	0.7	24.6	2.1	23.3	2.7	20.6	2.7	0.929
465	29.7	0.151	0.012	25.2	0.9	27.2	0.8	24.5	2.7	23.5	2.8	20.9	2.7	0.924
470	30.1	0.206	0.018	22.1	2.6	24.8	2.0	19.0	3.1	17.5	3.2	15.5	2.5	0.897
475	30.4	0.227	0.023	24.2	2.0	26.3	1.2	20.7	4.0	19.2	4.0	17.0	3.3	0.887
480	30.8	0.185	0.016	23.0	1.5	25.5	0.6	18.5	2.0	16.6	2.2	14.6	1.5	0.908
485	31.1	0.191	0.037	23.4	1.6	25.7	0.9	18.3	2.8	16.9	2.9	15.3	2.7	0.905
490	31.5	0.235	0.026	23.4	1.7	25.8	0.9	18.8	2.8	17.1	3.0	15.4	2.7	0.883
495	31.8	0.242	0.030	21.8	1.2	24.8	0.9	17.0	0.5	15.6	0.6	14.2	0.6	0.879
500	32.2	0.283	0.018	23.4	1.9	26.1	1.2	19.7	4.0	18.3	4.1	16.4	3.4	0.859
505	32.6	0.242	0.027	23.1	1.8	25.7	1.2	18.8	3.4	17.4	3.4	15.5	2.6	0.879
510	32.9	0.209	0.032	22.5	1.7	25.2	0.8	17.3	1.0	15.7	0.6	14.2	0.6	0.895
515	33.2	0.244	0.028	23.8	1.9	26.2	1.3	20.8	4.0	19.6	4.0	17.4	3.4	0.878
520	33.5	0.238	0.024	22.4	2.3	24.8	1.7	17.6	1.0	16.0	0.6	14.5	0.8	0.881
525	33.8	0.249	0.027	22.3	2.7	24.7	1.8	18.4	2.2	16.7	2.1	14.7	1.5	0.876
530	34.1	0.208	0.018	20.6	3.1	23.5	2.5	17.7	1.4	16.5	1.2	14.9	1.1	0.896
535	34.4	0.231	0.023	22.7	1.8	25.3	1.0	18.4	2.6	16.8	2.4	14.8	1.6	0.885
540	34.7	0.270	0.024	22.1	1.1	25.0	0.8	17.4	1.3	16.0	1.1	14.2	0.6	0.865
545	35.0	0.212	0.022	23.5	1.9	25.9	1.3	19.5	3.9	18.2	3.8	16.2	3.1	0.894
550	35.2	0.234	0.027	22.6	1.2	25.2	0.7	17.7	1.3	16.1	1.1	14.3	0.5	0.883
555	35.4	0.215	0.019	22.5	1.2	25.3	0.7	17.7	1.3	16.0	1.1	14.2	0.5	0.892
560	35.6	0.217	0.017	23.1	1.5	25.6	0.6	18.0	1.3	16.0	1.1	14.1	0.4	0.892
565	35.8	0.166	0.015	24.2	1.7	26.4	1.5	21.8	4.0	20.4	4.5	17.9	4.3	0.917
570	36.1	0.235	0.024	22.5	1.7	25.2	0.8	17.3	1.0	15.7	0.6	14.2	0.6	0.882
575	36.3	0.336	0.018	22.3	1.6	25.3	1.3	18.3	3.0	16.8	3.2	15.0	2.8	0.832
580	36.6	0.325	0.020	20.1	2.3	23.1	2.4	17.2	0.7	16.2	0.9	14.9	1.1	0.838
585	36.9	0.291	0.042	20.8	2.2	23.8	2.1	17.0	0.5	15.8	0.6	14.4	0.7	0.855
590	37.1	0.254	0.014	23.4	1.9	26.0	1.3	20.0	3.7	18.5	3.8	16.2	3.1	0.873
595	37.4	0.201	0.018	23.7	1.9	26.1	1.2	19.9	3.9	18.4	4.0	16.4	3.4	0.900
600	37.6	0.298	0.015	22.5	1.4	25.4	0.7	17.3	0.7	15.7	0.6	14.2	0.5	0.851
605	37.9	0.212	0.017	22.6	1.2	25.3	0.5	18.3	1.9	16.8	2.1	14.8	1.5	0.894
610	38.2	0.270	0.010	22.9	1.6	25.6	1.0	18.7	2.9	17.0	3.1	15.1	2.7	0.865
615	38.4	0.187	0.010	24.8	1.6	26.9	1.4	22.9	3.9	21.4	4.4	18.8	4.2	0.906
620	38.5	0.242	0.019	23.0	1.6	25.7	1.0	18.6	2.9	17.0	3.1	15.1	2.8	0.879
625	38.6	0.230	0.037	22.5	1.6	25.4	1.2	17.9	2.8	16.6	3.0	15.1	2.8	0.885
630	38.7	0.276	0.018	23.1	1.7	25.7	1.4	19.3	3.7	17.8	3.8	15.7	3.4	0.862
635	38.9	0.249	0.020	22.2	1.1	25.2	0.7	17.5	1.2	16.0	1.1	14.3	0.5	0.875
640	39.0	0.305	0.013	17.0	1.5	20.1	0.9	17.0	1.3	16.5	1.2	15.7	1.0	0.847
645	39.1	0.289	0.034	22.1	1.1	25.2	0.8	17.1	0.5	15.6	0.6	14.2	0.6	0.855
650	39.2	0.260	0.013	22.0	2.2	24.8	1.7	17.6	1.3	16.0	1.1	14.3	0.7	0.870
655	39.7	0.207	0.027	23.0	1.5	25.3	0.6	18.6	2.0	16.9	2.0	14.8	1.4	0.897
660	40.2	0.283	0.022	21.9	2.2	24.9	1.6	17.2	0.7	15.7	0.6	14.3	0.7	0.859
665	40.7	0.259	0.022	21.4	2.0	24.3	2.1	17.3	0.7	16.1	1.0	14.8	1.1	0.871

depth (cm)	STEV	Est. Tc0-50m (°C)	Est. Tw0-50m (°C)	Est. annual T75m (°C)	Est. annual T100m (°C)	Est. annual T150m (°C)	#best Ana
335	0.011	24.2	26.2	20.8	19.1	16.7	10
340	0.009	24.5	26.7	21.9	20.7	18.2	10
345	0.012	23.0	25.5	19.1	17.7	15.5	10
350	0.004	25.1	26.9	22.7	21.2	18.8	10
355	0.009	24.9	26.8	22.3	20.7	18.1	10
360	0.008	25.0	26.9	23.0	21.5	18.8	10
365	0.009	24.6	26.8	22.2	21.0	18.6	10
370	0.006	24.2	26.2	21.1	19.7	17.3	10
375	0.006	24.3	26.5	21.3	19.7	17.4	10
380	0.010	23.5	25.8	19.5	18.0	16.0	10
385	0.006	25.5	27.5	24.8	23.7	21.1	10
390	0.007	24.8	26.8	22.8	21.5	18.9	10
395	0.009	24.7	27.1	23.1	21.9	19.7	10
400	0.009	25.3	27.3	24.6	23.5	20.9	10
405	0.007	25.1	27.1	25.2	24.2	21.5	10
410	0.007	23.7	25.9	21.3	19.7	17.0	10
415	0.006	24.0	26.1	21.9	20.4	17.5	10
420	0.008	24.7	26.7	22.2	20.7	18.3	10
425	0.006	24.5	26.5	21.4	19.5	17.0	10
430	0.007	24.7	26.7	21.8	20.2	18.0	10
435	0.009	24.9	26.9	22.5	21.2	18.8	10
440	0.008	25.7	27.5	25.0	23.7	21.0	10
445	0.010	24.9	27.1	23.0	21.8	19.3	10
450	0.007	24.8	27.0	23.0	21.8	19.5	10
455	0.007	25.2	27.1	23.3	22.0	19.5	10
460	0.007	25.5	27.2	24.6	23.3	20.6	10
465	0.006	25.2	27.3	24.5	23.5	20.9	10
470	0.009	22.2	24.8	19.0	17.5	15.5	10
475	0.011	24.2	26.3	20.7	19.2	17.0	10
480	0.008	23.0	25.5	18.5	16.6	14.6	10
485	0.019	23.3	25.7	18.3	16.9	15.3	10
490	0.013	23.4	25.8	18.8	17.1	15.3	10
495	0.015	21.8	24.8	17.0	15.6	14.2	10
500	0.009	23.4	26.1	19.7	18.3	16.4	10
505	0.013	23.1	25.7	18.8	17.3	15.5	10
510	0.016	22.5	25.2	17.3	15.8	14.2	10
515	0.014	23.8	26.2	20.8	19.5	17.3	10
520	0.012	22.4	24.8	17.6	16.0	14.5	10
525	0.014	22.3	24.7	18.3	16.7	14.7	10
530	0.009	20.6	23.6	17.7	16.5	14.9	10
535	0.012	22.7	25.3	18.4	16.8	14.8	10
540	0.012	22.1	25.0	17.4	16.0	14.2	10
545	0.011	23.5	25.9	19.5	18.2	16.2	10
550	0.014	22.6	25.2	17.7	16.1	14.3	10
555	0.009	22.5	25.3	17.7	16.0	14.2	10
560	0.009	23.1	25.6	18.0	16.0	14.1	10
565	0.008	24.2	26.4	21.8	20.4	17.9	10
570	0.012	22.5	25.2	17.3	15.7	14.2	10
575	0.009	22.3	25.3	18.3	16.8	15.0	10
580	0.010	20.1	23.1	17.2	16.2	14.9	10
585	0.021	20.8	23.8	17.0	15.8	14.4	10
590	0.007	23.4	26.0	20.0	18.5	16.2	10
595	0.009	23.7	26.1	19.9	18.4	16.4	10
600	0.007	22.5	25.4	17.3	15.7	14.2	10
605	0.009	22.6	25.3	18.3	16.8	14.8	10
610	0.005	22.9	25.6	18.7	17.0	15.1	10
615	0.005	24.8	26.9	22.9	21.4	18.8	10
620	0.010	23.0	25.7	18.6	17.0	15.1	10
625	0.018	22.5	25.4	17.9	16.6	15.1	10
630	0.009	23.1	25.7	19.3	17.8	15.7	10
635	0.010	22.2	25.2	17.5	16.0	14.3	10
640	0.006	17.0	20.1	17.0	16.5	15.7	10
645	0.017	22.1	25.2	17.1	15.6	14.2	10
650	0.007	22.0	24.8	17.6	16.0	14.3	10
655	0.014	23.0	25.3	18.6	16.9	14.8	10
660	0.011	21.9	24.9	17.2	15.7	14.3	10
665	0.011	21.4	24.3	17.3	16.1	14.7	10

depth (cm)	age (cal.kyr)	DSML	STDEV	mean analog Tc0-50m (°C)	STDEV	mean analog Tw0-50m (°C)	STDEV	mean analog annual T75m (°C)	STDEV	mean analog annual T100m (°C)	STDEV	mean analog annual T150m (°C)	STDEV	SIM
670	41.1	0.299	0.016	22.3	1.5	25.3	0.8	17.2	0.7	15.6	0.5	14.1	0.5	0.851
675	41.6	0.243	0.028	23.4	2.0	25.9	1.4	19.7	4.0	18.3	4.1	16.3	3.4	0.878
680	42.1	0.181	0.014	23.4	1.7	25.8	1.1	19.4	3.3	17.7	3.3	15.4	2.6	0.910
685	42.6	0.229	0.011	24.8	1.9	27.1	1.2	23.1	4.1	21.8	4.3	19.4	3.8	0.885
690	43.0	0.287	0.028	21.5	3.5	23.9	2.7	17.5	1.1	16.1	0.5	14.7	0.8	0.856
695	43.4	0.312	0.024	22.6	1.2	25.4	0.6	17.4	0.6	15.7	0.5	14.2	0.6	0.844
700	43.7	0.305	0.016	22.3	0.9	25.2	0.7	17.6	1.2	16.0	1.1	14.2	0.6	0.847
705	44.0	0.293	0.021	23.1	1.7	25.7	1.2	18.8	3.5	17.4	3.5	15.6	3.0	0.854
710	44.3	0.322	0.012	23.3	1.8	25.8	1.4	19.4	3.7	17.8	4.0	15.8	3.7	0.839
715	44.5	0.217	0.017	24.0	2.1	26.3	1.2	20.8	4.0	19.2	4.2	17.1	3.6	0.892
720	44.8	0.298	0.022	22.7	1.4	25.6	1.1	18.3	2.8	16.7	3.0	15.0	2.8	0.851
725	45.1	0.246	0.020	24.1	2.0	26.4	1.3	21.5	4.1	20.1	4.2	17.8	3.7	0.877
730	45.4	0.246	0.027	23.1	1.7	25.5	0.9	18.4	2.5	16.6	2.3	14.7	1.7	0.877
735	45.6	0.255	0.033	23.2	1.7	25.7	1.1	18.7	3.2	17.3	3.0	15.3	2.1	0.873
740	45.8	0.280	0.023	23.2	1.7	25.8	1.1	18.8	3.4	17.2	3.4	15.4	2.7	0.860
745	46.1	0.159	0.025	24.2	1.9	26.5	1.4	21.8	4.2	20.4	4.5	18.0	4.1	0.921
750	46.3	0.213	0.023	23.0	1.5	25.5	0.6	17.6	1.0	15.6	0.5	14.0	0.4	0.894
755	46.5	0.322	0.019	21.7	1.8	24.8	1.7	17.2	0.4	15.8	0.7	14.4	0.8	0.839
760	46.8	0.267	0.022	22.4	1.2	25.3	0.8	17.7	1.2	15.9	1.1	14.1	0.6	0.867
765	47.1	0.233	0.022	22.0	1.2	25.0	1.1	17.5	1.2	15.9	1.1	14.2	0.5	0.883
770	47.4	0.279	0.017	22.0	1.1	25.1	0.8	17.4	1.3	15.8	1.1	14.1	0.5	0.861
775	47.8	0.217	0.026	22.1	1.1	25.2	0.8	17.1	0.5	15.6	0.6	14.2	0.6	0.892
780	48.1	0.283	0.009	19.0	3.1	22.3	2.9	16.8	0.4	15.9	0.5	14.9	0.7	0.859
785	48.5	0.317	0.019	21.5	1.7	24.6	1.7	17.1	0.5	15.7	0.7	14.4	0.8	0.841
790	48.9	0.270	0.014	21.3	1.9	24.3	2.1	17.3	0.7	16.0	1.0	14.7	1.1	0.865
795	49.2	0.232	0.028	22.9	2.1	25.5	1.0	18.6	2.8	16.8	2.6	14.8	1.8	0.884
800	49.6	0.244	0.019	23.2	1.9	25.6	0.8	18.3	2.3	16.4	2.3	14.7	1.8	0.878
805	49.9	0.259	0.031	22.9	2.6	25.2	2.1	19.1	3.4	17.6	3.4	15.9	2.9	0.870
810	50.3	0.272	0.014	20.6	2.4	23.8	2.5	17.2	0.7	15.9	1.0	14.7	1.1	0.864
815	50.7	0.295	0.019	22.1	2.4	25.0	2.0	18.7	3.8	17.7	4.0	16.2	3.6	0.853
820	51.0	0.298	0.009	18.4	2.0	21.7	2.3	17.1	0.7	16.3	0.9	15.3	1.0	0.851
825	51.4	0.273	0.030	22.7	1.9	25.6	1.3	18.7	3.5	17.3	3.6	15.6	3.0	0.864
830	51.7	0.247	0.013	20.3	3.0	23.3	2.6	17.1	1.0	15.7	1.0	14.6	1.1	0.876
835	52.0	0.225	0.014	24.2	2.0	26.4	1.2	20.9	4.0	19.4	4.5	17.4	4.1	0.888
840	52.3	0.186	0.015	23.7	1.9	26.0	1.4	20.2	3.8	18.4	4.2	16.1	3.6	0.907
845	52.5	0.189	0.019	25.3	1.2	26.8	1.1	22.1	3.9	20.3	4.0	17.5	3.8	0.906
850	52.8	0.187	0.014	23.9	2.0	26.0	1.3	19.9	3.9	18.2	4.1	16.2	3.5	0.907
855	53.1	0.159	0.009	25.8	0.9	27.5	0.7	24.8	2.7	23.5	2.8	20.4	3.0	0.921
860	53.3	0.299	0.027	23.2	2.2	25.8	1.5	19.5	4.1	18.2	4.1	16.3	3.4	0.851
865	53.5	0.182	0.021	23.0	1.8	25.7	1.2	18.8	3.4	17.3	3.4	15.4	2.6	0.909
870	53.6	0.226	0.029	22.7	1.5	25.5	0.9	18.0	2.4	16.4	2.3	14.7	1.7	0.887
875	53.7	0.177	0.018	25.2	1.6	27.3	1.0	23.9	3.6	22.7	3.6	20.2	3.3	0.912
880	53.9	0.157	0.013	23.6	1.6	26.0	1.2	21.9	3.3	20.4	3.8	17.8	3.4	0.922
885	54.0	0.144	0.020	23.0	1.4	25.7	0.8	22.7	1.3	21.8	1.3	19.1	1.8	0.928
890	54.1	0.183	0.016	23.4	1.8	25.5	1.1	19.3	3.0	17.6	3.2	15.3	2.6	0.909
895	54.2	0.243	0.039	23.0	2.5	25.5	2.3	20.2	4.0	19.0	4.3	17.0	4.0	0.879
900	54.3	0.218	0.029	24.5	1.9	26.7	1.1	21.5	4.1	20.0	4.4	17.6	3.8	0.891
905	54.4	0.175	0.012	25.2	1.6	27.3	1.1	23.9	3.6	22.7	3.6	20.2	3.3	0.912
910	54.5	0.225	0.028	22.7	1.4	25.5	1.4	19.9	3.3	18.7	3.6	16.4	3.3	0.888
915	54.6	0.205	0.023	24.9	1.7	27.1	1.2	23.1	4.2	22.1	4.2	19.8	3.9	0.898
920	54.7	0.238	0.032	23.1	1.7	26.1	1.3	19.9	3.8	18.4	4.1	16.4	3.7	0.881
925	54.8	0.205	0.030	23.9	1.8	26.2	1.4	20.5	4.4	19.3	4.4	17.2	3.9	0.897
930	54.9	0.260	0.037	22.1	1.1	25.0	0.8	17.4	1.3	16.0	1.1	14.3	0.5	0.870
935	55.0	0.176	0.020	24.9	1.8	27.0	1.2	23.1	4.0	21.9	4.0	19.4	3.5	0.912
940	55.1	0.193	0.011	23.9	1.8	26.3	1.2	22.2	3.5	20.7	4.1	18.3	3.9	0.904
945	55.2	0.149	0.013	24.6	1.8	26.8	1.3	22.3	4.3	21.2	4.4	18.9	3.9	0.925
950	55.3	0.236	0.028	22.0	1.1	25.0	0.8	17.5	1.3	16.0	1.1	14.2	0.6	0.882
955	55.4	0.173	0.011	24.6	1.8	26.8	1.3	22.3	4.3	21.2	4.4	18.9	3.9	0.914

depth (cm)	STEV	Est. Tc0-50m (°C)	Est. Tw0-50m (°C)	Est. annual T75m (°C)	Est. annual T100m (°C)	Est. annual T150m (°C)	#best Ana
670	0.008	22.3	25.3	17.2	15.6	14.1	10
675	0.014	23.3	25.9	19.6	18.3	16.3	10
680	0.007	23.4	25.8	19.4	17.7	15.4	10
685	0.005	24.8	27.1	23.1	21.8	19.4	10
690	0.014	21.5	24.0	17.5	16.1	14.6	10
695	0.012	22.6	25.4	17.4	15.7	14.2	10
700	0.008	22.3	25.2	17.6	16.0	14.2	10
705	0.011	23.1	25.7	18.8	17.4	15.6	10
710	0.006	23.3	25.8	19.4	17.8	15.8	10
715	0.009	24.0	26.3	20.7	19.2	17.1	10
720	0.011	22.7	25.5	18.3	16.7	15.0	10
725	0.010	24.1	26.4	21.5	20.1	17.7	10
730	0.014	23.1	25.5	18.4	16.6	14.7	10
735	0.017	23.2	25.7	18.6	17.3	15.3	10
740	0.011	23.2	25.8	18.8	17.2	15.3	10
745	0.013	24.2	26.5	21.8	20.4	18.0	10
750	0.012	23.0	25.5	17.6	15.6	14.0	10
755	0.010	21.7	24.8	17.2	15.8	14.4	10
760	0.011	22.4	25.3	17.7	15.9	14.1	10
765	0.011	22.0	25.0	17.5	15.9	14.2	10
770	0.008	22.1	25.1	17.4	15.8	14.1	10
775	0.013	22.1	25.2	17.1	15.6	14.2	10
780	0.004	19.0	22.3	16.8	15.9	14.9	10
785	0.010	21.6	24.6	17.1	15.7	14.4	10
790	0.007	21.3	24.3	17.3	16.0	14.7	10
795	0.014	22.9	25.5	18.6	16.8	14.8	10
800	0.010	23.2	25.6	18.3	16.4	14.7	10
805	0.016	22.9	25.2	19.0	17.6	15.9	10
810	0.007	20.6	23.8	17.2	15.9	14.7	10
815	0.010	22.1	25.0	18.7	17.7	16.2	10
820	0.004	18.4	21.7	17.1	16.3	15.3	10
825	0.015	22.7	25.6	18.7	17.3	15.6	10
830	0.006	20.3	23.3	17.1	15.7	14.5	10
835	0.007	24.2	26.4	20.9	19.4	17.4	10
840	0.008	23.7	26.0	20.1	18.3	16.1	10
845	0.010	25.3	26.8	22.1	20.3	17.4	10
850	0.007	23.9	26.0	19.9	18.2	16.2	10
855	0.005	25.8	27.5	24.8	23.5	20.4	10
860	0.013	23.2	25.8	19.4	18.2	16.3	10
865	0.011	23.0	25.7	18.8	17.3	15.4	10
870	0.015	22.7	25.5	17.9	16.4	14.7	10
875	0.009	25.2	27.3	23.9	22.7	20.2	10
880	0.007	23.6	26.0	21.9	20.4	17.8	10
885	0.010	23.0	25.7	22.7	21.8	19.1	10
890	0.008	23.4	25.5	19.3	17.6	15.3	10
895	0.020	23.0	25.5	20.2	19.0	17.0	10
900	0.014	24.5	26.7	21.5	19.9	17.6	10
905	0.006	25.2	27.3	23.9	22.7	20.2	10
910	0.014	22.7	25.4	19.9	18.7	16.4	10
915	0.011	24.9	27.1	23.1	22.0	19.7	10
920	0.016	23.1	26.1	19.8	18.4	16.4	10
925	0.015	23.9	26.2	20.5	19.3	17.2	10
930	0.019	22.1	25.0	17.4	16.0	14.3	10
935	0.010	24.9	27.0	23.1	21.9	19.4	10
940	0.006	23.9	26.3	22.2	20.7	18.3	10
945	0.006	24.6	26.8	22.3	21.2	18.9	10
950	0.014	22.0	25.0	17.5	16.0	14.2	10
955	0.005	24.6	26.8	22.3	21.2	18.9	10

depth (cm)	LAT	LON	water depth (cm)	counted	aeq	bul	cal	cav	con	cra	deh	dig	dut	fal	glu	hir	hum	inf	men	nit
0.0	17.6483	-67.1667	1814	719	4.9	0.0	0.1	0.0	0.3	0.1	0.4	0.0	5.5	0.0	11.7	0.0	0.0	0.0	4.1	0.4
2.5	17.6483	-67.1667	1814	410	4.7	0.0	0.0	0.0	0.8	0.0	0.0	0.0	7.9	0.0	11.3	0.0	0.0	0.0	2.9	1.7
5.0	17.6483	-67.1667	1814	747	4.3	0.3	0.0	0.0	0.2	0.3	0.2	0.0	5.8	0.0	16.5	0.0	0.0	0.3	3.8	1.1
7.5	17.6483	-67.1667	1814	399	4.0	0.0	0.9	0.0	1.1	0.0	0.0	0.0	4.4	0.0	8.7	0.0	0.0	0.0	3.8	0.8
10.0	17.6483	-67.1667	1814	707	6.5	1.0	1.5	0.0	0.4	0.1	0.2	0.1	1.7	0.1	21.0	0.0	0.0	0.0	2.8	0.7
12.5	17.6483	-67.1667	1814	349	5.2	0.0	0.0	0.0	0.2	0.0	0.1	0.0	3.9	0.0	8.0	0.0	0.6	0.0	2.0	0.6
15.0	17.6483	-67.1667	1814	684	5.8	1.3	0.3	0.0	0.5	0.5	0.0	0.0	4.7	0.0	14.2	0.0	0.0	0.0	1.4	0.9
17.5	17.6483	-67.1667	1814	384	2.7	1.2	1.8	0.0	0.6	0.1	0.0	0.1	3.7	0.0	10.2	0.0	0.0	0.0	1.3	0.1
20.0	17.6483	-67.1667	1814	586	2.1	1.0	0.6	0.0	0.7	0.4	0.1	0.0	3.2	0.4	16.6	0.0	0.9	0.0	0.2	0.0
22.5	17.6483	-67.1667	1814	315	5.2	1.3	0.6	0.0	0.4	0.3	0.0	0.0	2.1	0.0	7.8	0.0	0.0	0.0	0.1	0.1
25.0	17.6483	-67.1667	1814	434	4.5	1.8	0.0	0.0	0.1	0.0	0.0	0.2	2.1	0.6	14.5	0.0	0.0	0.3	0.0	0.0
27.5	17.6483	-67.1667	1814	332	4.0	1.7	0.0	0.0	0.6	0.2	0.0	0.0	1.9	0.4	9.9	0.0	0.0	0.3	0.3	0.0
30.0	17.6483	-67.1667	1814	487	3.4	1.1	0.1	0.0	0.4	0.4	0.0	0.0	1.2	0.0	23.6	0.0	0.0	0.1	0.0	0.1
32.5	17.6483	-67.1667	1814	341	3.1	3.9	1.6	0.0	1.3	0.1	0.0	0.0	5.6	0.0	8.3	0.0	0.0	0.7	0.0	0.0
35.0	17.6483	-67.1667	1814	459	4.1	3.4	0.2	0.0	0.6	0.5	0.0	0.5	1.8	0.0	15.0	0.0	0.0	0.4	0.0	0.0
37.5	17.6483	-67.1667	1814	339	6.2	2.3	1.6	0.0	0.8	0.2	0.0	0.5	1.8	0.5	14.5	0.0	0.5	0.1	0.0	0.0
40.0	17.6483	-67.1667	1814	602	8.3	3.7	0.0	0.0	1.1	0.3	0.0	0.0	1.3	0.7	22.1	0.0	0.7	0.2	0.1	0.0
42.5	17.6483	-67.1667	1814	346	7.5	4.4	1.8	0.0	1.3	1.5	0.0	1.1	2.1	2.7	18.1	0.0	0.0	1.4	0.1	0.0
45.0	17.6483	-67.1667	1814	439	7.2	1.9	0.0	0.0	1.9	0.8	0.0	0.5	2.2	0.0	18.0	0.0	0.0	0.7	0.0	0.0
47.5	17.6483	-67.1667	1814	321	8.1	8.4	0.5	0.0	1.2	0.4	0.0	0.0	1.4	0.5	13.7	0.0	0.5	0.3	0.3	0.0
50.0	17.6483	-67.1667	1814	467	2.5	3.4	6.1	0.0	0.3	0.5	0.0	0.0	4.2	0.0	23.2	0.0	0.0	0.5	0.0	0.1
52.5	17.6483	-67.1667	1814	330	7.0	3.4	0.5	0.0	0.5	0.8	0.0	1.0	2.0	1.0	15.0	0.0	0.0	0.2	0.0	0.0
55.0	17.6483	-67.1667	1814	434	7.5	4.9	0.8	0.0	2.3	1.0	0.0	0.0	2.9	0.0	17.0	0.0	0.0	0.6	0.8	0.0
57.5	17.6483	-67.1667	1814	369	7.1	6.4	0.0	0.0	2.3	0.1	0.0	0.9	2.1	0.9	17.7	0.0	0.0	0.7	0.1	0.0
60.0	17.6483	-67.1667	1814	611	4.5	3.9	0.1	0.0	0.2	0.0	0.0	0.1	1.6	2.6	19.0	0.0	0.0	0.7	0.0	0.1
62.5	17.6483	-67.1667	1814	328	2.9	8.4	0.0	0.0	1.2	1.0	0.0	0.0	2.3	0.7	14.0	0.0	0.0	0.2	0.4	0.0
65.0	17.6483	-67.1667	1814	511	5.2	6.6	0.3	0.0	1.2	0.9	0.0	0.0	1.9	1.1	24.8	0.0	0.0	1.4	1.2	0.0
67.5	17.6483	-67.1667	1814	312	2.9	12.0	0.0	0.0	0.7	1.0	0.0	0.0	0.7	0.8	19.5	0.0	0.0	1.2	0.9	0.0
70.0	17.6483	-67.1667	1814	506	6.3	8.4	0.0	0.0	0.3	0.1	0.0	0.1	1.5	1.0	17.5	0.0	0.0	0.3	0.0	0.0
72.5	17.6483	-67.1667	1814	321	1.7	6.2	0.9	0.0	1.2	0.8	0.0	0.6	2.3	0.6	16.4	0.0	0.0	1.0	0.0	0.0
75.0	17.6483	-67.1667	1814	445	2.1	2.8	0.4	0.0	0.8	0.5	0.0	1.0	3.3	0.8	15.0	0.0	0.0	0.9	0.0	0.0
77.5	17.6483	-67.1667	1814	321	3.6	4.6	1.5	0.0	0.0	1.5	0.0	0.0	2.8	0.7	12.7	0.0	0.7	0.6	1.5	0.0
80.0	17.6483	-67.1667	1814	716	1.1	1.8	0.0	0.0	1.9	0.1	0.0	0.0	3.0	0.9	22.0	0.0	0.0	0.9	0.9	0.0
82.5	17.6483	-67.1667	1814	352	1.0	0.3	0.1	0.0	0.8	0.4	0.0	0.0	2.6	0.0	14.4	0.0	0.0	0.8	0.9	0.0
85.0	17.6483	-67.1667	1814	413	1.5	0.8	0.0	0.0	1.4	1.5	0.0	0.7	3.9	0.0	13.5	0.0	0.0	1.5	0.7	0.0
87.5	17.6483	-67.1667	1814	360	2.9	1.8	0.0	0.0	0.7	0.2	0.0	0.0	4.6	0.0	13.9	0.0	0.0	1.4	0.1	0.0
90.0	17.6483	-67.1667	1814	720	1.5	5.1	0.0	0.0	1.5	0.3	0.0	0.0	6.1	1.9	15.8	0.0	0.0	2.1	0.1	0.0
92.5	17.6483	-67.1667	1814	319	4.3	0.0	2.8	0.0	0.4	0.4	0.0	0.0	6.8	0.7	9.2	0.0	0.0	1.4	0.1	0.0
95.0	17.6483	-67.1667	1814	393	4.6	3.7	0.2	0.0	0.3	0.2	0.0	0.0	6.7	1.0	11.9	0.0	0.0	3.1	0.0	0.2
97.5	17.6483	-67.1667	1814	365	4.4	3.2	0.2	0.0	0.8	1.0	0.0	0.0	7.9	0.6	15.1	0.0	0.0	2.0	0.0	0.0
100.0	17.6483	-67.1667	1814	460	5.0	1.6	0.1	0.0	0.4	0.1	0.0	0.0	10.7	0.4	14.5	0.0	0.0	1.7	0.0	0.0
102.5	17.6483	-67.1667	1814	384	5.2	2.7	0.0	0.0	0.3	0.5	0.0	0.9	11.5	1.3	14.5	0.0	0.0	1.1	0.2	0.0
105.0	17.6483	-67.1667	1814	355	2.6	1.6	0.0	0.0	0.3	1.0	0.0	0.3	8.8	0.8	17.8	0.0	0.0	0.4	0.2	0.0
107.5	17.6483	-67.1667	1814	384	4.5	2.9	0.8	0.0	1.3	0.0	0.0	0.3	10.6	0.6	9.9	0.0	0.0	1.0	0.0	0.0
110.0	17.6483	-67.1667	1814	483	4.5	4.2	0.1	0.0	0.4	0.4	0.0	0.4	6.2	0.4	14.6	0.0	0.0	0.6	0.0	0.0
112.5	17.6483	-67.1667	1814	356	6.0	5.4	0.7	0.0	1.4	0.4	0.0	0.1	6.7	0.0	14.1	0.0	0.0	1.6	0.7	0.0
115.0	17.6483	-67.1667	1814	333	4.3	3.2	0.0	0.0	1.1	0.3	0.0	0.5	7.3	1.1	11.2	0.0	0.5	0.3	0.1	0.0
117.5	17.6483	-67.1667	1814	408	4.4	4.2	0.4	0.0	1.3	0.3	0.0	0.0	7.0	0.0	12.8	0.0	0.0	0.8	0.1	0.0
120.0	17.6483	-67.1667	1814	388	5.1	3.3	0.0	0.0	2.0	1.8	0.0	0.2	5.4	0.7	18.9	0.0	0.0	0.2	0.1	0.0
122.5	17.6483	-67.1667	1814	319	4.3	3.9	0.0	0.0	0.7	2.4	0.0	1.0	8.5	0.0	16.3	0.0	0.0	0.0	0.0	0.0
125.0	17.6483	-67.1667	1814	424	3.1	3.4	1.0	0.0	0.2	0.3	0.0	0.7	6.1	0.5	16.3	0.0	0.0	1.0	0.0	0.0
127.5	17.6483	-67.1667	1814	295	4.0	4.4	0.2	0.0	0.0	0.0	0.0	0.9	9.3	0.0	11.1	0.0	0.0	0.2	0.4	0.0
130.0	17.6483	-67.1667	1814	413	5.9	1.8	0.0	0.0	0.7	0.9	0.0	0.5	10.0	0.0	13.6	0.0	0.0	0.2	0.0	0.0
132.5	17.6483	-67.1667	1814	380	4.0	1.3	1.3	0.0	0.3	1.2	0.0	0.8	7.7	0.0	17.0	0.0	0.0	0.5	0.0	0.0
135.0	17.6483	-67.1667	1815	321	2.3	0.8	0.0	0.0	0.5	0.2	0.0	0.2	6.5	0.0	17.9	0.0	1.3	0.2	0.0	0.0
137.5	17.6483	-67.1667	1816	395	2.8	2.4	0.6	0.0	0.7	0.7	0.0	0.0	10.8	0.6	12.2	0.0	0.0	0.0	0.0	0.1
140.0	17.6483	-67.1667	1817	478	2.6	4.6	0.0	0.0	0.1	0.0	0.0	0.2	7.7	0.0	14.9	0.0	0.0	1.2	0.2	0.0
142.5	17.6483	-67.1667	1818	395	1.9	0.7	0.0	0.0	0.0	0.3	0.0	0.1	9.1	0.0	12.7	0.0	0.0	1.4	0.0	0.0
145.0	17.6483	-67.1667	1818	381	2.9	2.2	1.3	0.0	0.4	0.6	0.0	0.0	4.9	2.2	19.1	0.0	1.1	0.0	0.0	0.0
147.5	17.6483	-67.1667	1818	412	3.2	4.5	0.5	0.0	0.5	0.1	0.0	0.7	7.9	0.0	12.2	0.0	0.0	1.1	0.0	0.0
150.0	17.6483	-67.1667	1818	347	6.4	4.9	0.0	0.0	0.5	0.8	0.0	0.2	4.1	0.8	14.0	0.0	0.0	0.5	0.0	0.0
152.5	17.6483	-67.1667	1818	383	1.7	2.9	0.0	0.0	1.6	0.7	0.0	0.2	8.0	0.7	11.9	0.0	0.0	1.6	0.0	0.0
155.0	17.6483	-67.1667	1818	490	1.8	2.3	0.6	0.0	1.2	0.3	0.0	0.0	7.8	0.0	19.6	0.0	0.3	1.1	0.1	0.0
157.5	17.6483	-67.1667	1818	284	3.0	6.9	0.0	0.0	1.1	0.2	0.0	0.0	10.7	0.0	5.9	0.0	0.0	1.9	0.0	0.0
160.0	17.6483	-67.1667	1818	331	3.5	3.5	0.0	0.0	0.5	0.9	0.0	0.0	8.5	0.5	19.3	0.0	0.0	1.5	0.0	0.0
162.5	17.6483	-67.1667	1818	393	4.6	3.0	0.4	0.0	1.0	0.4	0.0	0.0	8.0	0.0	6.4	0.2	0.0	1.7	0.5	0.0
165.0	17.6483	-67.1667	1818	553	5.0	6.0	0.5	0.0	0.8	0.0	0.0	0.0	8.0	0.0	13.9	0.2	0.0	0.4	0.0	0.0
167.5	17.6483	-67.1667	1818	312	7.5	1.5	0.2	0.0	0.7	0.9	0.0	0.0	4.4	0.0	16.6	0.0	0.0	0.2	0.7	0.2
170.0	17.6483	-67.1667	1818	410	3.5	5.1	0.0	0.0	0.6	0.2	0.0	0.2	6.2	0.0	18.3	0.0	0.0	0.4	0.5	0.1

depth (cm)	obl	pal	par+	qul	qur	qui	rur	ruw	rus	tri	sac	sci	ten	trl	trr	trus	tum	univ	uvu	ment	pdi	par
0.0	0.6	0.0	0.8	0.0	0.0	0.0	11.7	30.2	5.6	14.3	4.4	0.2	0.2	0.3	0.4	0.7	0.4	2.8	0.0	4.4	0.4	0.5
2.5	0.4	0.0	0.1	0.0	0.0	0.0	12.4	29.6	1.3	11.1	8.4	0.9	0.0	0.1	0.0	0.1	0.5	4.9	0.0	3.5	0.1	0.0
5.0	0.6	0.3	0.2	0.0	0.0	2.6	9.0	27.3	8.5	6.8	3.8	0.7	2.0	0.4	0.3	0.7	0.8	2.8	0.0	4.5	0.1	0.1
7.5	0.9	0.0	0.9	0.0	0.0	0.0	18.3	30.1	4.4	9.0	7.4	1.3	0.0	0.7	0.0	0.7	0.7	1.4	0.0	4.5	0.9	0.0
10.0	0.7	0.5	0.3	0.0	0.0	0.0	9.3	28.8	7.6	8.3	2.7	0.5	0.5	0.4	0.7	1.1	0.4	1.8	0.0	3.2	0.3	0.0
12.5	0.6	0.0	0.0	0.0	0.0	0.0	17.1	34.6	3.4	12.3	4.7	1.1	1.1	0.0	1.9	1.9	1.1	1.2	0.0	3.2	0.0	0.0
15.0	0.9	0.3	0.0	0.0	0.0	0.0	14.8	32.0	2.8	9.7	4.3	0.6	0.0	0.3	2.2	2.5	0.4	1.9	0.0	1.8	0.0	0.0
17.5	0.5	0.6	0.3	0.0	0.0	0.0	15.5	37.6	5.3	8.0	3.8	1.2	0.0	0.4	2.1	2.4	0.4	1.6	0.0	1.8	0.3	0.0
20.0	0.9	0.9	0.7	0.0	0.0	2.2	11.3	34.2	10.6	4.6	1.6	0.9	0.9	0.2	2.1	2.2	0.6	1.3	0.0	0.8	0.3	0.4
22.5	1.1	0.0	0.7	0.0	0.0	0.0	15.6	34.6	5.4	8.4	5.9	0.6	3.6	0.1	3.8	3.9	0.8	0.6	0.0	0.9	0.1	0.6
25.0	0.9	0.2	0.3	0.0	0.0	0.0	14.1	45.3	4.3	4.9	1.7	0.6	1.2	0.0	0.9	0.9	0.3	0.8	0.0	0.3	0.3	0.0
27.5	0.0	0.0	1.1	0.0	0.0	0.0	16.9	46.9	3.8	4.1	3.3	0.0	2.1	0.4	0.5	0.9	0.1	1.2	0.0	0.4	0.6	0.4
30.0	0.3	0.0	0.1	0.0	0.0	1.1	3.6	38.0	17.9	3.7	1.1	0.0	0.1	0.3	0.1	0.4	0.1	0.8	0.0	0.1	0.0	0.1
32.5	1.7	0.0	1.5	0.0	0.0	0.0	11.4	36.5	7.4	6.4	3.0	1.7	1.7	0.2	2.0	2.2	0.0	1.2	0.0	0.0	0.7	0.9
35.0	0.9	1.2	1.8	0.0	0.0	0.2	10.8	38.1	5.2	6.4	2.4	1.0	2.2	0.2	1.2	1.4	0.0	1.5	0.0	0.0	0.6	1.2
37.5	1.0	0.0	1.2	0.0	0.0	0.0	11.7	35.2	7.0	4.6	2.1	1.6	4.8	0.0	0.4	0.4	0.0	0.6	0.0	0.0	0.7	0.5
40.0	0.3	0.0	2.2	0.0	0.0	0.0	7.1	36.8	5.0	4.3	2.1	0.0	1.4	0.0	0.5	0.5	0.0	0.4	0.0	0.1	0.1	2.1
42.5	0.1	0.5	0.3	0.0	0.0	0.0	9.8	29.9	4.4	6.5	1.5	1.1	1.1	0.0	0.5	0.5	0.1	0.5	0.0	0.1	0.3	0.0
45.0	1.1	1.4	0.2	0.0	0.0	0.0	14.9	29.7	2.9	8.7	2.7	0.0	2.9	0.0	0.1	0.2	0.0	0.9	0.0	0.0	0.0	0.2
47.5	0.1	0.5	0.0	0.0	0.0	0.0	9.8	28.6	5.8	10.6	3.5	1.1	2.1	0.0	0.2	0.2	0.0	0.9	0.0	0.3	0.0	0.0
50.0	0.0	0.0	0.1	0.0	0.0	0.0	11.8	28.1	11.1	3.0	1.3	0.0	1.0	0.0	0.2	0.2	0.0	0.4	0.0	0.0	0.1	0.0
52.5	0.0	1.5	0.0	0.0	0.0	0.0	12.8	32.1	2.6	8.2	2.9	1.0	1.5	0.0	1.7	1.7	0.0	1.3	0.0	0.0	0.0	0.0
55.0	0.1	0.8	0.9	0.0	0.0	0.0	10.3	30.1	2.3	9.9	2.3	0.8	3.8	0.1	0.3	0.4	0.0	0.5	0.0	0.8	0.0	0.9
57.5	0.0	1.8	0.2	0.0	0.0	0.0	8.9	27.2	4.4	6.4	2.3	4.4	3.5	0.0	1.0	1.0	0.0	0.7	0.0	0.1	0.2	0.0
60.0	0.0	2.6	0.7	0.0	0.0	1.1	10.9	29.6	7.9	5.4	1.4	2.6	1.6	0.0	1.1	1.1	0.0	0.4	0.0	0.0	0.1	0.6
62.5	0.0	1.4	1.4	0.0	0.0	0.0	9.5	31.9	6.3	4.4	1.5	4.2	2.1	0.0	1.6	1.6	0.7	0.4	0.0	1.1	0.7	0.7
65.0	0.0	1.1	1.4	0.0	0.0	0.6	7.8	27.7	3.7	4.6	1.7	0.3	4.0	0.0	0.6	0.6	0.0	0.7	0.0	1.2	0.6	0.9
67.5	0.0	1.5	0.9	0.0	0.0	0.0	14.1	25.9	5.3	2.2	2.5	1.5	2.3	0.0	1.9	1.9	0.0	0.3	0.0	0.9	0.9	0.0
70.0	0.0	0.0	0.1	0.0	0.0	1.0	6.9	38.8	9.1	3.7	2.0	1.0	1.0	0.0	0.5	0.5	0.0	0.3	0.0	0.0	0.0	0.1
72.5	0.0	1.8	0.6	0.0	0.0	0.0	6.3	40.2	4.8	5.9	3.4	0.6	3.6	0.0	0.5	0.5	0.0	0.5	0.0	0.0	0.0	0.6
75.0	0.0	1.2	1.2	0.0	0.0	0.0	12.4	33.7	6.5	7.2	3.4	0.8	3.2	0.0	1.2	1.2	0.0	0.5	0.0	0.0	0.4	0.8
77.5	0.0	3.0	2.3	0.0	0.0	0.0	10.8	34.9	6.0	6.0	0.7	0.7	3.0	0.0	1.2	1.2	0.0	0.3	0.0	1.5	2.2	0.1
80.0	0.1	4.3	0.1	0.0	0.0	0.0	6.4	29.4	9.5	8.9	2.2	1.8	1.7	0.0	1.6	1.6	0.0	0.4	0.0	0.9	0.0	0.1
82.5	0.0	5.9	0.6	0.0	0.0	0.0	10.3	37.4	11.3	6.3	2.7	0.6	1.8	0.0	0.7	0.7	0.0	0.3	0.0	0.9	0.6	0.0
85.0	0.0	3.3	4.8	0.0	0.0	0.0	10.7	38.3	4.7	4.2	1.8	0.8	2.7	0.3	2.3	2.6	0.0	0.5	0.0	0.7	1.0	3.8
87.5	0.6	3.0	1.0	0.0	0.0	0.0	8.8	40.6	6.0	5.6	3.0	0.0	3.0	0.3	1.3	1.6	0.0	0.4	0.0	0.1	1.0	0.0
90.0	0.0	1.0	1.5	0.0	0.0	0.0	12.7	35.4	4.9	5.0	1.2	0.0	1.0	0.3	1.1	1.3	0.0	0.4	0.0	0.1	0.2	1.3
92.5	0.7	2.8	2.0	0.0	0.0	0.0	12.1	36.5	5.1	5.3	2.9	0.0	2.8	0.0	1.1	1.1	0.0	1.1	0.0	0.1	1.1	0.9
95.0	0.0	1.2	3.1	0.0	0.0	0.5	10.4	32.3	2.0	8.8	2.5	2.0	2.0	0.5	1.0	1.5	0.0	1.1	0.0	0.0	1.1	2.0
97.5	0.0	1.2	0.6	0.0	0.0	0.0	10.9	31.6	6.1	5.4	2.4	1.2	2.4	0.5	1.5	2.0	0.0	1.0	0.0	0.0	0.6	0.0
100.0	0.0	1.7	2.7	0.0	0.0	0.0	9.3	32.4	5.9	6.2	2.1	0.4	1.7	0.3	2.1	2.3	0.0	0.6	0.0	0.0	1.3	1.5
102.5	0.1	2.5	1.3	0.0	0.0	0.6	7.3	30.1	1.9	5.7	3.0	2.5	2.5	0.2	3.5	3.7	0.0	0.5	0.0	0.2	1.3	0.0
105.0	0.2	0.8	2.3	0.0	0.0	0.0	5.4	34.6	4.8	7.4	2.4	0.8	2.4	0.1	2.3	2.3	0.0	0.5	0.0	0.2	1.3	1.0
107.5	0.0	1.8	0.9	0.0	0.0	0.0	7.9	31.5	6.8	6.2	3.8	1.2	2.5	0.8	2.8	3.6	0.0	0.5	0.0	0.0	0.9	0.0
110.0	0.0	2.6	5.2	0.0	0.0	0.0	9.3	31.3	2.1	6.5	1.4	2.6	2.6	0.6	2.3	3.0	0.0	0.6	0.0	0.0	0.8	4.4
112.5	0.0	1.2	0.6	0.0	0.0	0.6	7.6	32.7	9.9	2.6	2.3	1.7	1.2	0.0	1.5	1.5	0.0	0.5	0.0	0.7	0.4	0.1
115.0	0.0	3.2	1.1	0.0	0.0	0.5	5.6	39.1	3.7	5.8	3.9	1.6	0.5	0.7	2.3	3.0	0.0	0.3	0.0	0.1	0.0	1.1
117.5	0.0	0.8	0.4	0.0	0.0	0.0	9.9	38.4	7.2	5.2	2.1	0.8	1.3	0.2	1.4	1.6	0.0	0.3	0.0	0.1	0.4	0.0
120.0	0.0	3.0	0.8	0.0	0.0	0.0	9.6	25.9	9.0	5.0	2.2	1.5	3.7	0.4	0.6	0.9	0.0	0.7	0.0	0.1	0.1	0.7
122.5	0.2	1.6	1.2	0.0	0.0	0.8	11.2	29.8	3.9	5.4	2.4	0.0	3.1	0.4	1.9	2.3	0.0	0.3	0.0	0.0	1.0	0.2
125.0	0.1	1.0	3.2	0.0	0.0	0.5	9.4	33.7	5.4	6.8	3.2	1.0	0.0	1.2	1.3	2.5	0.0	0.4	0.0	0.0	1.9	1.2
127.5	0.4	0.7	3.5	0.0	0.0	0.0	13.2	35.0	2.9	3.8	2.7	2.2	1.5	0.5	1.7	2.3	0.0	0.7	0.0	0.4	2.0	1.5
130.0	0.0	1.8	2.0	0.0	0.0	0.0	11.4	31.8	5.6	3.7	2.0	1.4	1.1	0.0	3.2	3.2	0.0	1.8	0.0	0.0	0.9	1.1
132.5	0.2	0.0	1.5	0.0	0.0	0.0	13.6	31.7	2.0	5.1	2.3	2.6	2.6	1.6	1.3	2.8	0.0	0.6	0.0	0.0	0.2	1.3
135.0	0.5	5.1	0.8	0.0	0.0	1.3	14.1	27.7	9.5	4.5	1.7	2.5	0.0	0.3	1.1	1.4	0.0	0.5	0.0	0.0	0.2	0.6
137.5	0.7	1.2	0.1	0.0	0.0	0.0	12.6	28.5	6.5	5.8	3.4	2.4	3.5	0.0	2.8	2.8	0.0	0.5	0.0	0.0	0.1	0.0
140.0	0.3	2.9	2.7	0.0	0.0	0.2	9.5	29.7	9.3	4.1	2.5	2.7	1.0	0.0	2.8	2.8	0.0	0.4	0.0	0.2	0.5	2.2
142.5	0.3	0.5	2.5	0.0	0.0	0.0	14.9	31.1	5.9	6.7	4.2	1.8	0.5	0.1	3.9	4.0	0.0	0.4	0.0	0.0	2.0	0.5
145.0	0.6	3.9	0.7	0.0	0.0	0.0	14.4	20.5	12.9	3.1	1.2	2.8	0.6	0.0	1.3	1.3	0.0	0.4	0.0	0.0	0.7	0.0
147.5	1.3	0.0	1.5	0.0	0.0	0.0	12.5	29.9	8.5	7.2	1.6	2.6	0.5	0.0	0.9	0.9	0.0	0.7	0.0	0.0	1.5	0.0
150.0	1.0	1.6	2.7	0.0	0.0	0.0	10.7	31.6	11.7	2.7	1.2	1.2	1.2	0.0	1.4	1.4	0.0	0.5	0.0	0.0	0.6	2.1
152.5	0.7	0.0	0.7	0.0	0.0	0.0	16.9	32.3	8.2	4.5	1.7	1.4	0.0	0.2	2.0	2.2	0.0	0.6	0.0	0.0	0.0	0.7
155.0	1.0	2.2	4.3	0.0	0.0	0.3	9.6	27.1	8.7	2.3	2.7	1.4	0.6	0.3	2.2	2.6	0.0	1.2	0.0	0.1	0.9	3.4
157.5	0.7	0.0	1.9	0.0	0.0	1.0	13.5	31.5	6.7	4.4	3.0	1.0	1.0	0.0	4.8	4.8	0.0	1.0	0.0	0.0	1.0	1.0
160.0	0.2	0.0	2.9	0.0	0.0	0.5	8.9	29.7	3.3	3.3	4.4	0.9	0.9	0.5	5.4	5.8	0.0	0.5	0.0	0.0	0.8	2.1
162.5	0.9	0.4	1.1	0.0	0.0	0.0	11.6	45.4	3.4	3.2	2.5	1.7	0.4	0.0	2.0	2.0	0.0	0.2	0.0	0.5	1.1	0.0
165.0	0.1	0.7	2.5	0.0	0.0	0.0	8.1	35.9	3.6	4.4	1.8	3.3	1.1	0.0	2.8	2.8	0.0	0.1	0.0	0.0	0.2	2.4
167.5	1.0	0.0	0.2	0.0	0.0	0.0	13.4	35.9	1.4	5.7	2.5	2.7	2.1	0.3	1.8	2.2	0.0	0.2	0.0	0.7	0.2	0.0
170.0	0.1	0.6	1.8	0.0	0.0	0.0	12.2	30.5	4.9	4.1	2.3	4.1	1.2	0.1	1.9	1.9	0.0	0.4	0.0	0.5	0.8	1.0

depth (cm)	LAT	LON	water depth (cm)	counted	aeq	bul	cal	cav	con	cra	deh	dig	dut	fal	glu	hir	hum	inf	men	nit
172.5	17.6483	-67.1667	1818	375	5.2	2.8	0.3	0.0	0.9	0.0	0.0	0.0	5.4	0.6	11.3	0.0	0.0	0.0	0.0	0.0
175.0	17.6483	-67.1667	1818	369	5.5	3.5	0.0	0.0	1.3	0.7	0.0	0.0	8.6	0.0	8.8	0.0	0.0	0.7	0.6	0.3
177.5	17.6483	-67.1667	1818	348	6.0	2.9	0.6	0.0	1.4	0.2	0.0	1.0	7.7	0.0	10.6	0.0	0.0	0.2	0.1	0.0
180.0	17.6483	-67.1667	1818	408	6.7	5.5	0.5	0.0	0.9	0.1	0.0	0.0	5.3	0.0	11.7	0.0	0.0	0.4	0.1	0.0
182.5	17.6483	-67.1667	1818	361	10.2	2.8	0.0	0.0	1.9	0.7	0.0	0.6	4.8	0.0	14.1	0.0	0.0	0.8	0.2	0.0
185.0	17.6483	-67.1667	1818	526	7.2	4.3	0.0	0.0	0.8	0.6	0.0	0.5	1.8	0.3	13.3	0.0	0.0	0.2	0.7	0.0
187.5	17.6483	-67.1667	1818	311	7.7	5.0	0.8	0.0	2.3	0.1	0.0	0.1	1.3	1.6	11.5	0.0	0.0	1.0	0.0	0.0
190.0	17.6483	-67.1667	1818	400	5.2	7.6	0.7	0.0	1.0	0.5	0.0	0.1	1.8	0.5	14.7	0.0	0.0	1.3	1.0	0.0
192.5	17.6483	-67.1667	1818	359	7.8	5.9	0.8	0.0	0.4	0.9	0.0	0.3	2.9	0.8	12.6	0.0	0.0	1.0	0.1	0.1
195.0	17.6483	-67.1667	1818	435	9.2	5.3	0.0	0.0	0.5	0.6	0.0	0.0	1.7	0.0	18.2	0.0	0.0	1.1	0.1	0.1
197.5	17.6483	-67.1667	1818	301	8.2	3.3	2.3	0.0	0.7	0.2	0.0	0.0	3.4	0.0	11.7	0.0	0.0	0.0	0.2	0.0
200.0	17.6483	-67.1667	1818	427	11.4	4.7	0.0	0.0	0.7	0.7	0.0	0.0	2.1	0.0	17.6	0.0	0.0	0.3	0.0	0.0
202.5	17.6483	-67.1667	1818	349	13.5	2.5	1.7	0.0	0.3	0.2	0.0	0.0	3.0	0.0	13.3	0.0	0.0	0.0	0.1	0.0
205.0	17.6483	-67.1667	1818	491	5.5	3.6	1.0	0.0	1.5	0.1	0.0	0.6	3.9	1.6	16.2	0.0	0.0	0.2	0.0	0.0
207.5	17.6483	-67.1667	1818	327	5.1	0.6	0.6	0.0	0.8	0.3	0.0	0.0	3.9	0.6	22.2	0.0	0.0	0.2	0.0	0.0
210.0	17.6483	-67.1667	1818	571	7.2	1.7	0.0	0.0	0.8	0.9	0.0	0.3	4.1	0.0	13.4	0.0	0.0	0.5	0.0	0.0
212.5	17.6483	-67.1667	1818	392	11.4	0.6	1.3	0.0	0.5	1.3	0.1	0.4	6.1	0.0	13.0	0.0	0.0	0.0	0.0	0.0
215.0	17.6483	-67.1667	1818	516	5.7	2.2	0.5	0.0	0.8	0.5	0.0	0.0	6.3	0.3	16.1	0.0	0.0	0.0	0.0	0.0
217.5	17.6483	-67.1667	1818	369	5.3	1.8	0.0	0.0	2.2	1.3	0.0	0.0	8.6	0.6	11.7	0.6	0.0	0.0	0.0	0.0
220.0	17.6483	-67.1667	1818	539	9.2	1.2	0.3	0.0	0.9	0.8	0.1	0.8	8.3	0.6	12.5	0.0	0.0	0.2	0.0	0.0
222.5	17.6483	-67.1667	1818	391	7.9	0.0	0.8	0.0	0.7	1.9	0.0	0.0	6.9	0.8	15.5	0.0	0.0	0.0	0.0	0.0
225.0	17.6483	-67.1667	1818	581	4.1	0.2	0.9	0.0	1.6	1.8	0.0	0.0	9.6	0.0	14.1	0.0	0.0	0.0	0.0	0.0
227.5	17.6483	-67.1667	1818	394	7.0	1.2	1.7	0.0	1.1	3.4	0.1	0.0	6.9	0.5	11.0	0.2	0.0	0.0	0.0	0.0
230.0	17.6483	-67.1667	1818	441	5.2	2.5	0.3	0.0	1.4	1.0	0.0	0.3	6.8	0.0	15.9	0.0	0.0	0.0	0.0	0.0
232.5	17.6483	-67.1667	1818	393	5.8	0.5	0.8	0.0	0.6	1.9	0.1	0.0	8.7	0.0	17.8	0.0	0.0	0.0	0.1	0.0
235.0	17.6483	-67.1667	1818	544	4.9	1.3	0.4	0.0	0.6	3.1	0.0	0.3	6.5	0.6	20.9	0.0	0.0	0.0	0.0	0.0
237.5	17.6483	-67.1667	1818	308	3.5	0.5	2.0	0.0	0.5	1.3	0.1	0.2	9.0	0.0	19.8	0.0	0.0	0.0	0.1	0.0
240.0	17.6483	-67.1667	1818	500	6.8	1.8	1.1	0.0	0.8	3.5	0.0	0.5	6.3	0.4	16.3	0.0	0.0	0.0	0.0	0.0
242.5	17.6483	-67.1667	1818	367	6.3	0.3	0.6	0.0	0.8	2.7	0.2	0.0	10.1	0.0	15.6	0.0	0.0	0.0	0.4	0.0
245.0	17.6483	-67.1667	1818	496	4.3	1.3	1.3	0.0	1.1	3.0	0.1	0.3	8.8	0.0	13.9	0.0	0.0	0.0	0.3	0.0
247.5	17.6483	-67.1667	1818	366	9.5	0.9	1.3	0.0	0.5	0.5	0.0	0.4	8.0	0.9	18.5	0.0	0.0	0.0	0.7	0.0
250.0	17.6483	-67.1667	1818	567	8.6	0.9	0.5	0.0	1.8	2.7	0.2	0.7	6.8	0.0	15.2	0.0	0.0	0.2	0.8	0.0
252.5	17.6483	-67.1667	1818	349	4.2	0.9	0.9	0.0	1.3	2.6	0.1	0.9	7.7	0.0	14.5	0.0	0.0	0.0	0.3	0.0
255.0	17.6483	-67.1667	1818	471	4.8	0.9	2.3	0.0	2.3	2.3	0.0	0.8	8.4	0.4	11.7	0.0	0.0	0.0	2.1	0.0
257.5	17.6483	-67.1667	1818	342	3.3	0.5	0.7	0.0	2.0	0.8	0.1	0.7	7.3	0.0	14.1	0.0	0.0	0.0	4.0	0.0
260.0	17.6483	-67.1667	1818	554	7.0	1.4	1.4	0.0	1.3	0.5	0.0	0.1	7.7	0.0	10.8	0.0	0.0	0.0	8.1	0.0
262.5	17.6483	-67.1667	1818	385	6.0	0.0	1.1	0.0	2.9	0.2	0.0	0.5	11.7	0.0	9.9	0.0	0.0	0.0	8.8	0.0
265.0	17.6483	-67.1667	1818	654	8.1	1.0	1.5	0.0	1.7	0.1	0.0	0.3	9.6	0.0	11.8	0.0	0.0	0.0	5.0	0.0
267.5	17.6483	-67.1667	1818	304	6.5	1.6	1.1	0.0	2.1	0.7	0.0	0.5	11.3	0.0	10.4	0.0	0.0	0.0	8.2	0.0
270.0	17.6483	-67.1667	1818	584	6.3	1.7	1.2	0.0	1.6	0.3	0.0	0.3	11.1	0.0	14.0	0.3	0.0	0.1	4.8	0.1
272.5	17.6483	-67.1667	1818	328	13.2	0.5	1.5	0.0	1.7	0.7	0.0	0.2	12.5	0.5	7.3	0.0	0.0	0.0	4.4	0.1
275.0	17.6483	-67.1667	1818	543	6.9	0.3	1.1	0.0	1.8	0.6	0.0	0.0	5.9	0.9	17.2	0.0	0.3	0.0	3.7	0.0
277.5	17.6483	-67.1667	1818	314	7.5	0.5	0.5	0.0	3.7	0.5	0.0	0.5	6.6	0.0	14.0	0.0	0.0	0.0	5.4	0.0
280.0	17.6483	-67.1667	1818	601	5.8	1.1	2.9	0.0	1.9	0.4	0.0	0.1	6.9	0.0	10.9	0.0	0.0	0.0	3.9	0.2
282.5	17.6483	-67.1667	1818	360	6.8	0.0	0.7	0.0	0.9	0.5	0.0	0.7	7.3	0.7	10.7	0.0	0.0	0.0	2.5	0.0
285.0	17.6483	-67.1667	1818	460	3.5	1.5	1.8	0.0	1.2	0.3	0.0	0.5	8.3	0.5	13.2	0.0	0.0	0.0	2.3	0.1
287.5	17.6483	-67.1667	1818	372	4.8	1.3	0.4	0.0	1.1	0.6	0.0	0.4	8.3	0.4	9.7	0.0	0.0	0.0	6.3	0.0
290.0	17.6483	-67.1667	1818	664	3.3	1.3	1.3	0.0	0.5	0.7	0.0	0.0	6.2	0.0	12.2	0.0	0.0	0.0	5.0	0.0
292.5	17.6483	-67.1667	1818	404	3.0	1.7	0.4	0.0	1.0	1.0	0.0	0.0	6.3	0.0	10.2	0.0	0.0	0.0	7.0	0.0
295.0	17.6483	-67.1667	1818	677	5.0	1.1	0.7	0.0	0.8	1.8	0.0	0.0	6.2	0.2	12.3	0.0	0.0	0.0	6.1	0.2
297.5	17.6483	-67.1667	1818	389	4.6	0.8	0.0	0.0	2.5	1.6	0.0	0.6	8.5	0.0	10.7	0.0	0.0	0.0	4.4	0.1
300.0	17.6483	-67.1667	1818	583	1.2	3.0	1.7	0.0	1.5	1.5	0.0	0.4	3.7	0.4	12.5	0.0	0.0	0.0	4.7	0.1
302.5	17.6483	-67.1667	1818	319	2.7	4.2	1.4	0.0	1.4	0.7	0.0	0.0	4.2	0.0	13.0	0.0	0.0	0.0	4.0	0.0
305.0	17.6483	-67.1667	1818	602	6.6	1.3	1.5	0.0	0.9	0.7	0.0	0.0	6.1	0.0	17.3	0.1	0.0	0.0	2.6	0.0
307.5	17.6483	-67.1667	1818	353	1.4	5.3	0.0	0.0	0.6	0.7	0.0	0.0	5.1	0.7	11.4	0.0	0.0	0.0	5.4	0.0
312.5	17.6483	-67.1667	1818	302	3.3	1.8	0.8	0.0	1.6	2.0	0.0	0.8	9.1	0.0	4.9	0.0	0.0	0.0	4.1	0.2
315.0	17.6483	-67.1667	1818	550	2.9	1.5	1.6	0.0	2.7	2.7	0.0	0.2	7.2	0.0	11.6	0.0	0.0	0.0	5.4	0.0
317.5	17.6483	-67.1667	1818	314	6.6	4.2	0.7	0.0	2.3	1.1	0.1	0.7	5.1	0.7	13.3	0.0	0.0	0.0	4.4	0.0
320.0	17.6483	-67.1667	1818	668	4.0	5.5	1.7	0.0	3.4	4.0	0.1	0.0	4.6	0.0	10.4	0.0	0.0	0.0	4.1	0.0
322.5	17.6483	-67.1667	1818	360	4.6	3.9	1.3	0.0	2.2	2.4	0.1	0.7	6.6	0.0	12.8	0.0	0.0	0.0	5.2	0.0
325.0	17.6483	-67.1667	1818	529	3.3	2.8	1.1	0.0	2.9	2.6	0.1	0.1	7.3	0.0	9.7	0.0	0.0	0.0	6.2	0.1
327.5	17.6483	-67.1667	1818	334	3.4	4.6	0.9	0.0	1.6	3.8	0.1	0.0	7.0	0.0	9.6	0.0	0.0	0.1	4.1	0.0
330.0	17.6483	-67.1667	1818	570	5.3	4.1	1.6	0.0	3.0	4.5	0.0	0.3	8.4	0.0	11.7	0.0	0.0	0.0	6.3	0.0
332.5	17.6483	-67.1667	1818	354	4.0	3.4	2.9	0.0	3.3	4.3	0.2	0.0	7.1	0.0	13.9	0.0	0.0	0.0	3.0	0.0
335.0	17.6483	-67.1667	1818	631	3.4	1.8	1.8	0.0	2.8	4.2	0.0	0.3	9.8	0.0	11.9	0.0	0.0	0.0	4.1	0.0
337.5	17.6483	-67.1667	1818	366	7.6	2.7	2.2	0.0	1.1	2.8	0.0	0.0	5.7	0.6	11.6	0.0	0.0	0.0	2.6	0.3
340.0	17.6483	-67.1667	1818	673	6.2	2.4	1.7	0.0	2.9	3.3	0.2	0.2	9.2	0.0	13.6	0.0	0.0	0.0	2.8	0.5
342.5	17.6483	-67.1667	1818	408	6.4	5.1	1.1	0.0	1.8	1.4	0.3	0.0	6.3	0.0	14.3	0.0	0.0	0.0	2.9	0.3
345.0	17.6483	-67.1667	1818	496	4.3	1.3	1.3	0.0	1.1	3.0	0.1	0.3	8.8	0.0	13.9	0.0	0.0	0.0	0.3	0.0

depth (cm)	obl	pal	par+	qul	qur	qui	rur	ruw	rus	tri	sac	sci	ten	trl	trr	trus	tum	univ	uvu	ment	pdi	par
172.5	0.4	2.6	0.6	0.0	0.0	0.6	14.7	31.7	4.5	5.1	3.6	3.2	2.6	0.2	2.3	2.5	0.0	0.5	0.0	0.0	0.6	0.0
175.0	0.1	1.2	2.9	0.0	0.0	0.0	22.1	19.7	4.1	7.2	3.0	2.9	1.2	0.0	5.2	5.2	0.0	0.2	0.0	0.6	1.5	1.5
177.5	0.2	1.9	0.0	0.0	0.0	0.0	17.4	28.2	5.2	5.7	3.0	2.6	1.3	0.8	2.7	3.5	0.0	0.3	0.0	0.1	0.0	0.0
180.0	0.1	2.4	1.3	0.0	0.0	0.0	14.7	29.0	4.4	6.4	2.8	2.0	2.0	0.7	2.8	3.5	0.0	0.4	0.0	0.1	0.3	1.0
182.5	0.1	0.6	0.0	0.0	0.0	0.0	13.8	32.2	2.8	8.8	1.4	1.1	0.6	0.1	1.5	1.6	0.0	0.5	0.0	0.2	0.0	0.0
185.0	0.3	2.7	1.1	0.0	0.0	0.0	7.3	37.9	4.9	6.9	1.9	0.3	2.4	0.6	2.3	2.9	0.0	0.4	0.0	0.7	0.0	1.1
187.5	1.0	1.6	1.6	0.0	0.0	0.0	7.1	38.5	6.6	2.5	1.8	0.8	2.5	0.2	1.7	1.9	0.0	1.4	0.0	0.0	1.6	0.0
190.0	0.1	1.6	1.4	0.0	0.0	0.0	11.2	31.2	5.2	6.8	3.5	0.0	1.0	0.9	1.4	2.2	0.0	0.5	0.0	1.0	0.3	1.2
192.5	0.2	0.0	0.8	0.0	0.0	0.8	9.7	35.6	1.6	8.3	3.1	1.6	1.6	0.1	0.7	0.8	0.0	0.6	0.0	0.1	0.0	0.8
195.0	0.2	1.6	1.6	0.0	0.0	0.0	14.6	29.3	4.1	3.3	1.2	0.5	4.1	0.6	0.9	1.5	0.1	0.6	0.0	0.1	0.0	1.6
197.5	0.2	0.8	1.6	0.0	0.0	0.0	14.9	35.2	6.2	3.2	1.6	0.8	1.6	0.1	0.8	0.9	0.0	0.6	0.0	0.2	0.0	1.6
200.0	0.6	1.0	1.7	0.0	0.0	0.0	12.4	29.5	6.2	4.8	1.2	1.0	1.6	0.6	1.4	2.0	0.0	0.5	0.0	0.0	0.1	1.6
202.5	0.3	2.5	3.3	0.0	0.0	0.0	10.7	35.4	2.5	3.5	1.9	0.8	2.5	0.1	0.5	0.7	0.0	0.5	0.0	0.1	0.8	2.5
205.0	0.1	0.6	1.1	0.0	0.0	0.0	15.8	29.6	5.5	5.0	1.1	1.0	1.6	0.4	1.8	2.2	0.0	1.5	0.0	0.0	0.5	0.6
207.5	0.0	0.0	1.8	0.0	0.0	0.0	18.3	28.8	5.4	5.7	1.3	1.2	1.2	0.3	0.9	1.2	0.0	0.5	0.0	0.0	1.8	0.0
210.0	0.6	0.6	2.4	0.0	0.0	0.0	15.8	31.3	5.4	4.0	1.9	2.5	2.5	0.2	1.5	1.6	0.0	1.0	0.0	0.0	0.8	1.6
212.5	0.6	0.0	2.5	0.0	0.0	0.0	14.2	25.3	6.7	8.0	3.0	0.0	1.7	0.9	1.0	1.9	0.0	0.9	0.0	0.0	0.0	2.5
215.0	0.1	0.6	2.8	0.0	0.0	0.0	17.3	26.5	5.4	5.4	2.5	1.9	1.3	1.2	0.2	1.4	0.0	0.9	0.0	0.0	1.9	0.9
217.5	0.3	0.0	0.0	0.0	0.0	0.0	14.3	31.8	4.7	5.8	2.3	2.3	1.8	0.4	1.1	1.5	0.0	1.1	0.0	0.0	0.0	0.0
220.0	0.3	0.9	1.7	0.0	0.0	0.3	13.5	33.3	3.9	4.4	1.3	1.8	2.1	0.1	0.5	0.6	0.0	0.6	0.0	0.0	0.6	1.1
222.5	1.1	0.0	1.1	0.0	0.0	0.0	11.2	39.0	3.8	4.8	0.8	1.5	0.8	0.0	0.0	0.0	0.0	0.8	0.0	0.0	1.1	0.0
225.0	0.2	0.4	2.8	0.0	0.0	0.0	15.1	30.4	4.5	5.0	3.3	0.9	0.9	0.1	0.9	0.9	0.0	2.0	0.0	0.0	1.7	1.1
227.5	0.6	0.0	1.0	0.0	0.0	0.0	17.0	29.1	1.4	7.4	1.6	2.4	0.5	0.0	1.5	1.5	0.0	1.6	0.0	0.0	0.5	0.5
230.0	0.6	0.3	0.7	0.0	0.0	0.0	16.0	31.5	2.0	6.2	2.6	1.4	2.0	0.3	0.3	0.6	0.0	1.4	0.0	0.0	0.2	0.5
232.5	0.6	0.0	0.5	0.0	0.0	0.0	14.7	27.2	1.0	7.6	2.1	0.5	3.6	1.0	1.5	2.5	0.0	2.2	0.0	0.1	0.0	0.5
235.0	0.3	0.6	0.6	0.0	0.0	0.6	11.6	23.4	5.6	7.3	3.0	2.8	0.6	0.5	0.5	1.0	0.3	2.2	0.0	0.3	0.3	0.3
237.5	0.6	0.0	0.5	0.0	0.0	0.0	14.3	25.8	2.9	7.2	3.5	2.4	2.0	0.7	0.7	1.5	0.0	1.7	0.0	0.1	0.5	0.0
240.0	0.7	0.0	1.8	0.0	0.0	0.0	14.4	27.2	2.2	6.2	2.0	2.9	0.0	0.2	2.6	2.9	0.0	1.6	0.0	0.0	0.9	0.9
242.5	1.9	0.0	1.2	0.0	0.0	0.0	18.4	22.7	0.6	6.1	2.1	1.8	1.2	0.5	2.1	2.6	0.0	3.7	0.0	0.4	0.0	1.2
245.0	0.9	0.0	1.1	0.0	0.0	0.0	15.9	25.5	5.6	6.1	3.3	2.2	0.5	0.0	1.5	1.5	0.1	1.9	0.0	0.3	0.5	0.5
247.5	0.5	0.0	0.4	0.0	0.0	0.0	17.9	24.2	3.5	4.7	1.4	1.3	0.0	0.2	1.5	1.7	0.0	1.1	0.0	0.7	0.0	0.4
250.0	0.6	0.0	0.9	0.0	0.0	0.0	13.5	26.2	3.7	6.7	3.6	1.9	0.0	0.2	0.9	1.2	0.0	1.9	0.0	0.8	0.0	0.9
252.5	0.6	0.0	1.3	0.0	0.0	0.0	17.5	27.4	3.5	9.5	1.9	0.4	0.4	0.3	1.2	1.5	0.0	1.0	0.0	0.3	0.9	0.4
255.0	0.5	0.4	1.1	0.0	0.0	0.0	12.6	29.9	5.3	5.3	1.4	1.9	0.4	0.2	0.6	0.8	1.1	0.8	0.0	3.3	0.4	0.8
257.5	0.4	0.0	0.2	0.0	0.0	0.0	17.8	31.6	1.9	4.6	1.5	1.0	1.5	0.5	1.3	1.9	0.1	0.9	0.0	4.1	0.2	0.0
260.0	0.3	0.3	0.1	0.0	0.0	0.0	14.8	27.9	4.7	6.1	1.4	1.1	0.6	0.0	0.4	0.4	0.0	1.4	0.0	8.1	0.1	0.0
262.5	0.7	0.0	0.0	0.0	0.0	0.0	19.4	18.5	3.3	6.2	2.5	2.2	1.6	0.3	2.0	2.3	0.0	1.0	0.0	8.8	0.0	0.0
265.0	0.3	0.3	0.7	0.0	0.0	0.0	15.0	22.8	4.1	6.5	2.2	2.1	0.6	0.1	0.5	0.6	2.0	1.0	0.0	7.0	0.4	0.3
267.5	0.3	0.0	0.3	0.0	0.0	0.0	14.6	21.0	3.8	8.1	3.0	0.5	1.6	0.1	0.8	1.0	0.3	1.4	0.0	8.5	0.3	0.0
270.0	0.6	0.3	1.7	0.0	0.0	0.0	12.5	18.7	7.2	7.2	3.6	1.2	0.9	0.4	1.0	1.4	0.0	1.6	0.0	4.8	1.2	0.6
272.5	0.2	0.0	0.0	0.0	0.0	0.0	15.4	18.5	3.9	6.5	2.8	2.4	1.0	0.1	1.6	1.7	1.5	2.0	0.0	5.9	0.0	0.0
275.0	0.6	0.3	0.6	0.0	0.0	1.3	11.3	17.4	11.7	6.3	1.8	1.9	0.3	0.3	0.7	1.1	2.2	1.1	0.0	5.9	0.3	0.3
277.5	0.5	0.0	0.0	0.0	0.0	0.0	14.6	25.6	4.0	7.6	3.9	0.5	0.0	0.1	1.1	1.2	1.9	0.7	0.0	7.2	0.0	0.0
280.0	0.6	0.3	0.0	0.0	0.0	0.3	9.5	28.3	3.9	6.2	3.9	3.3	1.4	0.0	1.6	1.6	4.6	1.2	0.0	8.5	0.0	0.0
282.5	0.1	0.0	0.0	0.0	0.0	0.0	16.0	31.6	1.3	7.3	2.9	2.6	2.0	0.0	1.2	1.2	3.0	0.8	0.0	5.4	0.0	0.0
285.0	0.4	0.5	0.5	0.0	0.0	0.0	11.1	35.2	5.9	5.2	2.4	1.8	0.5	0.1	0.3	0.4	1.9	0.7	0.0	4.2	0.0	0.5
287.5	0.5	0.0	0.6	0.0	0.0	0.0	12.0	29.6	2.5	7.6	2.2	2.2	1.8	0.2	0.5	0.7	4.7	1.3	0.0	11.1	0.2	0.4
290.0	0.6	0.0	0.0	0.0	0.0	0.0	11.1	39.9	4.2	4.0	2.6	0.4	2.1	0.0	0.7	0.7	3.3	0.5	0.0	8.3	0.0	0.0
292.5	0.5	0.0	0.0	0.0	0.0	0.0	14.9	38.8	0.4	5.2	3.2	0.0	1.9	0.0	0.8	0.8	2.8	0.5	0.0	9.8	0.0	0.0
295.0	0.8	0.0	0.8	0.0	0.0	0.2	15.4	28.0	2.0	4.9	3.1	1.8	2.3	0.0	1.5	1.5	3.3	0.2	0.0	9.4	0.6	0.2
297.5	0.7	0.0	1.3	0.0	0.0	0.0	15.8	25.6	2.5	6.7	4.2	1.3	2.5	0.1	0.5	0.5	4.3	0.5	0.0	8.7	0.6	0.6
300.0	0.2	0.4	2.2	0.0	0.0	0.0	8.8	35.2	5.2	4.7	1.4	1.3	0.9	0.0	2.0	2.0	4.6	0.6	0.4	9.3	0.5	1.7
302.5	0.3	0.0	0.0	0.0	0.0	0.0	14.2	25.7	6.1	10.2	3.0	0.0	0.7	0.2	3.0	3.1	2.4	0.3	0.0	6.3	0.0	0.0
305.0	0.3	0.0	0.9	0.0	0.0	0.4	12.3	20.6	13.0	3.1	1.8	2.2	0.0	0.5	3.4	3.9	3.1	0.3	0.0	5.8	0.0	0.9
307.5	0.3	0.0	0.0	0.0	0.0	0.0	15.8	25.4	7.7	7.1	1.5	2.1	3.5	0.0	1.8	1.8	2.5	0.2	0.0	7.9	0.0	0.0
312.5	1.5	0.0	0.0	0.0	0.0	0.0	9.7	25.6	12.6	8.3	1.6	0.8	2.4	0.3	0.9	1.2	5.9	0.2	0.0	10.0	0.0	0.0
315.0	0.6	0.0	1.5	0.0	0.0	0.0	8.7	27.7	5.4	5.9	1.7	2.5	1.1	0.1	1.1	1.3	5.3	0.3	0.0	10.7	0.2	1.3
317.5	1.2	0.0	0.2	0.0	0.0	0.0	7.3	20.9	10.5	7.8	2.7	0.0	1.4	0.1	0.8	0.9	3.7	0.5	0.0	8.0	0.0	0.2
320.0	0.7	0.0	0.7	0.0	0.0	0.0	7.5	28.6	4.4	7.9	2.9	1.3	0.9	0.1	0.6	0.7	3.9	0.5	0.0	8.1	0.2	0.4
322.5	0.7	0.0	0.0	0.0	0.0	0.0	8.7	27.7	5.6	7.5	1.3	0.6	2.8	0.0	0.1	0.1	3.2	0.6	0.0	8.4	0.0	0.0
325.0	0.8	0.0	0.6	0.0	0.0	0.0	9.9	33.2	4.4	7.3	1.7	0.4	1.8	0.3	0.3	0.6	2.0	0.3	0.0	8.2	0.6	0.0
327.5	0.8	0.0	0.5	0.0	0.0	0.0	7.2	31.3	7.8	6.7	2.9	0.0	0.9	0.0	0.2	0.2	4.1	0.8	0.0	8.2	0.5	0.0
330.0	0.3	0.0	0.5	0.0	0.0	0.3	6.9	26.8	3.9	5.3	2.5	1.0	1.6	0.0	0.2	0.2	3.9	0.3	0.0	10.2	0.2	0.3
332.5	0.5	0.0	0.7	0.0	0.0	0.0	10.2	25.0	6.2	4.9	1.5	0.0	1.4	0.0	0.0	0.0	3.6	1.0	0.0	6.5	0.0	0.7
335.0	0.5	0.0	1.3	0.0	0.0	0.0	7.8	26.7	2.8	7.5	2.2	1.0	1.3	0.0	0.0	0.0	2.9	1.6	0.0	7.0	1.0	0.3
337.5	0.5	0.0	0.3	0.0	0.0	0.0	8.4	33.1	3.2	6.7	2.9	0.0	1.3	0.0	0.0	0.0	1.4	1.1	0.0	4.0	0.2	0.2
340.0	0.9	0.0	0.5	0.0	0.0	0.0	12.2	24.7	2.4	6.3	3.0	0.5	0.7	0.0	0.1	0.1	1.7	1.1	0.2	4.5	0.0	0.5
342.5	0.3	0.0	0.0	0.0	0.0	0.0	12.0	27.8	3.5	6.1	2.4	0.5	2.0	0.0	0.0	0.0	0.6	0.3	0.0	3.4	0.0	0.0
345.0	0.9	0.0	1.1	0.0	0.0	0.0	15.9	25.5	5.6	6.1	3.3	2.2	0.5	0.0	1.5	1.5	0.1	1.9	0.0	0.3	0.5	0.5

Appendix VII: M35027-1, planktonic foraminiferal census counts

depth (cm)	LAT	LON	water depth (cm)	counted	aeq	bul	cal	cav	con	cra	deh	dig	dut	fal	glu	hir	hum	inf	men	nit
347.5	17.6483	-67.1667	1818	356	5.6	9.3	2.0	0.0	3.7	1.5	0.4	0.0	6.1	0.0	11.0	0.0	0.0	0.0	3.2	0.5
350.0	17.6483	-67.1667	1818	556	5.0	3.8	1.1	0.0	4.6	1.7	0.1	0.0	7.6	0.6	14.3	0.0	0.0	0.0	4.1	0.6
352.5	17.6483	-67.1667	1818	319	3.8	8.0	0.2	0.0	5.0	1.0	0.1	0.0	6.9	0.0	10.5	0.0	0.0	0.0	2.7	1.2
355.0	17.6483	-67.1667	1818	541	3.1	3.1	1.4	0.0	5.5	2.0	0.1	0.2	8.3	0.5	12.0	0.0	0.0	0.2	5.2	1.1
357.5	17.6483	-67.1667	1818	406	4.6	4.3	0.0	0.0	4.0	0.9	0.2	0.2	6.8	0.4	10.5	0.0	0.0	0.0	6.7	1.3
360.0	17.6483	-67.1667	1818	651	3.9	5.7	1.0	0.0	3.6	1.2	0.2	0.6	5.1	0.3	11.2	0.0	0.0	0.0	7.0	0.6
362.5	17.6483	-67.1667	1818	370	4.8	1.3	0.4	0.0	3.3	1.7	0.3	0.0	8.9	0.0	9.5	0.0	0.0	0.0	4.8	0.4
365.0	17.6483	-67.1667	1818	603	4.2	1.9	0.5	0.0	1.9	0.1	0.2	0.6	4.9	0.0	15.1	0.0	0.0	0.2	7.5	0.7
367.5	17.6483	-67.1667	1818	387	3.2	2.0	0.9	0.0	3.7	0.1	0.1	0.4	7.8	0.4	13.3	0.0	0.0	0.2	2.8	0.0
370.0	17.6483	-67.1667	1818	476	4.9	7.8	1.0	0.0	1.8	0.0	0.2	0.1	1.4	0.0	12.2	0.0	0.0	0.8	3.7	0.1
372.5	17.6483	-67.1667	1818	380	4.5	4.2	1.1	0.0	3.4	0.7	0.0	0.7	4.1	0.0	14.7	0.0	0.0	0.6	0.1	0.0
375.0	17.6483	-67.1667	1818	755	4.3	2.1	0.8	0.0	3.4	0.0	0.1	0.7	2.7	1.4	14.5	0.0	0.0	1.4	4.1	0.0
377.5	17.6483	-67.1667	1818	380	4.4	3.3	0.6	0.0	1.7	0.3	0.1	1.7	4.9	0.0	10.0	0.0	0.0	0.7	3.6	0.0
380.0	17.6483	-67.1667	1818	646	3.9	8.0	0.7	0.0	0.8	0.0	0.1	1.0	1.8	0.0	9.9	0.0	0.0	1.0	4.2	0.1
382.5	17.6483	-67.1667	1818	393	5.1	2.1	1.2	0.0	1.5	0.2	0.2	0.5	2.7	0.0	16.2	0.0	0.0	0.7	1.3	0.3
385.0	17.6483	-67.1667	1818	510	4.5	3.1	0.0	0.0	2.4	1.5	0.0	0.5	4.0	0.0	8.5	0.0	0.0	0.1	2.1	0.1
387.5	17.6483	-67.1667	1818	340	3.1	5.6	0.1	0.0	1.2	0.0	0.0	0.7	5.2	0.0	12.9	0.0	0.0	1.1	0.9	0.1
390.0	17.6483	-67.1667	1818	464	7.0	4.9	1.9	0.0	2.6	0.6	0.1	0.1	3.9	0.0	11.9	0.0	0.0	1.2	1.1	0.1
392.5	17.6483	-67.1667	1818	381	5.9	1.5	2.1	0.0	1.7	1.7	0.0	0.0	4.0	0.0	11.8	0.0	0.0	3.3	0.0	0.1
395.0	17.6483	-67.1667	1818	532	6.1	3.2	0.9	0.0	3.0	3.0	0.0	0.0	6.4	1.1	16.2	0.0	0.0	1.5	0.1	0.0
400.0	17.6483	-67.1667	1818	582	4.7	6.0	1.9	0.0	3.6	2.0	0.0	0.5	4.6	0.4	16.8	0.0	0.0	2.0	0.4	0.0
405.0	17.6483	-67.1667	1818	365	3.3	5.6	0.5	0.0	0.7	1.6	0.0	0.5	5.0	0.0	14.9	0.0	0.0	2.7	0.0	0.0
410.0	17.6483	-67.1667	1818	501	2.8	4.5	2.3	0.0	0.4	0.7	0.0	0.5	4.0	0.3	12.6	0.0	0.0	1.3	0.2	0.2
415.0	17.6483	-67.1667	1818	381	5.8	1.6	2.3	0.0	0.7	0.4	0.0	0.6	7.4	1.6	19.6	0.0	0.0	1.2	0.0	0.0
420.0	17.6483	-67.1667	1818	521	6.9	3.1	0.7	0.0	1.4	0.4	0.0	0.7	4.8	0.3	19.7	0.0	0.0	1.3	0.0	0.1
425.0	17.6483	-67.1667	1818	319	7.0	1.7	1.5	0.0	1.8	0.2	0.0	0.0	7.1	0.7	10.9	0.0	0.0	2.7	0.0	0.3
430.0	17.6483	-67.1667	1818	509	9.1	3.5	1.2	0.0	0.5	0.5	0.0	0.0	5.4	0.0	12.5	0.0	0.0	1.6	0.0	0.0
435.0	17.6483	-67.1667	1818	352	10.9	2.3	0.7	0.0	0.7	0.8	0.0	0.7	6.7	0.7	11.1	0.0	0.0	2.2	0.7	0.0
440.0	17.6483	-67.1667	1818	433	8.8	5.0	1.0	0.0	2.5	0.0	0.0	0.0	6.1	0.0	16.3	0.5	0.0	1.0	0.1	0.0
450.0	17.6483	-67.1667	1818	512	6.4	2.3	2.1	0.0	1.8	1.5	0.0	0.8	3.7	0.4	13.2	0.0	0.0	1.3	0.1	0.1

depth (cm)	obl	pal	par+	qul	qur	qui	rur	ruw	rus	tri	sac	sci	ten	trl	trr	trus	tum	univ	uvu	ment	pdi	par
347.5	0.7	0.0	0.0	0.0	0.0	0.0	15.8	28.5	2.0	4.6	1.7	0.5	0.0	0.1	0.6	0.6	0.7	0.5	0.0	3.9	0.0	0.0
350.0	1.2	0.3	1.1	0.0	0.0	0.0	16.2	19.6	2.0	6.2	2.1	1.4	0.8	0.0	0.3	0.3	0.8	1.8	0.0	4.9	0.4	0.7
352.5	0.1	0.0	0.0	0.0	0.0	0.0	21.7	22.4	4.2	3.8	4.3	0.7	0.0	0.0	1.4	1.4	1.0	0.7	0.0	3.7	0.0	0.0
355.0	0.8	0.0	0.5	0.0	0.0	0.0	18.8	19.9	1.9	6.6	3.0	0.5	0.9	0.0	0.1	0.1	0.2	0.8	0.0	5.4	0.5	0.0
357.5	0.1	0.0	0.0	0.0	0.0	0.0	21.1	15.8	4.1	10.1	2.7	1.5	0.4	0.0	0.2	0.2	0.0	1.2	0.0	6.7	0.0	0.0
360.0	0.4	0.8	1.1	0.0	0.0	0.0	18.2	20.2	2.8	6.3	3.4	2.0	0.8	0.0	0.1	0.1	0.5	0.6	0.1	7.4	0.4	0.7
362.5	0.9	0.0	0.4	0.0	0.0	0.4	18.1	19.9	1.7	11.7	1.7	3.0	1.3	0.0	0.2	0.2	2.3	0.9	0.0	7.0	0.4	0.0
365.0	0.7	0.0	0.5	0.0	0.0	0.0	20.1	20.7	5.0	5.9	3.1	0.9	1.2	0.0	0.6	0.6	0.0	1.2	0.0	7.5	0.5	0.0
367.5	0.6	0.0	0.0	0.0	0.0	0.0	19.4	19.0	3.9	8.2	2.9	2.2	1.3	0.0	0.6	0.6	2.3	1.4	0.4	5.1	0.0	0.0
370.0	0.3	0.0	1.2	0.0	0.0	0.0	12.1	32.1	4.5	4.7	1.4	0.5	1.5	0.0	0.2	0.2	0.6	1.1	0.0	4.3	0.7	0.6
372.5	0.3	0.0	0.0	0.0	0.0	0.0	8.5	25.7	5.6	9.9	3.5	0.6	4.5	0.0	1.0	1.0	1.9	1.0	0.0	2.1	0.0	0.0
375.0	0.9	0.0	0.8	0.0	0.0	0.0	3.4	39.3	2.4	8.5	1.5	0.3	2.1	0.0	1.5	1.5	0.0	1.4	0.0	4.1	0.8	0.0
377.5	1.0	1.1	0.6	0.0	0.0	0.0	5.8	33.1	3.9	11.9	1.4	0.0	1.1	0.6	1.3	1.9	3.3	1.0	0.0	7.0	0.6	0.0
380.0	0.2	0.0	0.1	0.0	0.0	0.0	11.1	38.3	4.2	6.8	2.1	0.5	1.6	0.0	0.2	0.2	1.4	0.3	0.0	5.7	0.0	0.1
382.5	0.5	0.0	0.1	0.0	0.0	0.0	10.5	33.5	2.1	6.0	2.1	1.6	4.3	0.0	0.4	0.4	1.8	0.6	0.0	3.1	0.0	0.1
385.0	0.3	0.0	0.5	0.0	0.0	0.0	13.8	34.2	1.9	12.1	2.7	1.4	2.8	0.1	0.3	0.4	0.0	0.7	0.0	2.2	0.5	0.0
387.5	1.3	0.0	0.3	0.0	0.0	0.0	11.8	30.1	2.3	5.5	0.9	0.6	8.2	0.0	1.0	1.0	0.4	1.3	0.0	1.3	0.0	0.3
390.0	0.3	0.0	0.6	0.0	0.0	0.0	9.2	33.7	4.0	8.3	1.5	0.8	1.2	0.0	0.7	0.7	0.2	0.4	0.4	1.3	0.2	0.4
392.5	1.0	1.9	0.5	0.0	0.0	0.0	9.5	34.8	2.8	9.4	0.8	0.9	1.4	0.1	2.1	2.1	0.1	0.3	0.0	0.1	0.5	0.0
395.0	0.1	0.4	0.7	0.0	0.0	0.0	8.5	24.2	3.7	7.6	2.1	1.1	0.4	0.0	1.2	1.2	0.0	1.1	0.0	0.1	0.4	0.4
400.0	0.2	0.4	1.6	0.0	0.0	0.4	6.4	28.3	3.3	5.3	2.2	0.4	1.5	0.5	2.7	3.2	0.0	0.7	0.0	0.4	0.9	0.7
405.0	0.0	0.0	4.1	0.0	0.0	0.0	8.8	37.8	1.0	6.3	0.6	0.5	2.0	0.5	2.5	3.1	0.0	0.4	0.0	0.0	0.9	3.2
410.0	0.2	0.3	6.0	0.0	0.0	0.0	11.5	29.0	4.6	6.5	1.7	0.7	5.0	0.2	1.4	1.6	0.2	0.7	0.0	0.4	2.5	3.5
415.0	0.0	0.5	2.3	0.0	0.0	0.0	14.2	24.7	4.2	6.0	2.2	0.5	2.1	0.2	1.3	1.5	0.0	0.6	0.0	0.0	0.9	1.4
420.0	0.0	0.3	4.0	0.0	0.0	0.3	7.3	28.8	4.2	6.7	1.7	0.7	1.7	0.0	3.0	3.1	0.0	1.3	0.3	0.0	1.6	2.4
425.0	0.0	0.7	1.3	0.0	0.0	0.0	7.8	26.1	4.7	9.7	1.0	0.7	6.0	0.0	2.7	2.8	0.0	1.5	0.0	0.0	0.3	1.0
430.0	0.1	0.4	2.8	0.0	0.0	0.0	10.3	32.5	4.1	4.4	1.6	1.2	1.2	0.0	2.3	2.3	0.0	1.3	0.0	0.0	1.5	1.2
435.0	0.0	0.0	3.0	0.0	0.0	0.0	9.9	31.4	3.5	4.0	1.3	0.7	3.5	0.0	3.9	3.9	0.0	0.6	0.0	0.7	0.9	2.1
440.0	0.1	1.0	2.9	0.0	0.0	0.0	7.0	33.9	4.4	2.6	1.0	1.0	1.5	0.0	1.2	1.2	0.0	0.8	0.0	0.1	0.5	2.4
450.0	0.1	0.0	1.7	0.0	0.0	0.0	9.3	29.8	3.3	6.4	2.7	1.7	4.6	0.1	3.4	3.4	0.0	1.6	0.0	0.1	1.3	0.3

depth (cm)	age (kyrs)	COMM.	Factor 1	Factor 2	Factor 3	Factor 4	Factor 5	Factor 6	Factor 7	Factor 8	Factor 9	Est. Tc 0-50m (°C)	Est. Tw 0-50m (°C)	seasonality
0.0	7.4	0.963	0.944	0.077	0.000	0.019	0.144	0.029	0.149	0.034	-0.145	26.0	27.2	1.3
2.5	8.1	0.960	0.933	0.075	0.000	0.017	0.157	0.016	0.158	0.111	-0.146	25.4	27.0	1.6
5.0	8.8	0.952	0.899	0.132	0.024	0.023	0.096	0.015	0.322	0.101	-0.036	24.4	26.6	2.2
7.5	9.4	0.898	0.920	0.052	0.001	0.020	0.095	0.018	0.114	0.066	-0.150	26.3	27.7	1.4
10.0	10.1	0.959	0.892	0.158	0.015	0.020	0.005	0.014	0.366	0.019	-0.058	25.7	26.9	1.2
12.5	10.8	0.939	0.954	0.048	-0.001	0.019	0.060	0.016	0.054	0.055	-0.133	26.1	27.5	1.4
15.0	11.4	0.958	0.940	0.120	0.008	0.020	0.035	0.018	0.195	0.093	-0.105	25.2	26.7	1.5
17.5	12.1	0.952	0.960	0.086	0.013	0.023	-0.021	0.019	0.083	0.103	-0.068	24.9	26.8	2.0
20.0	12.8	0.935	0.914	0.132	0.033	0.023	-0.071	0.028	0.249	0.115	0.005	24.0	26.4	2.4
22.5	13.5	0.930	0.953	0.080	-0.001	0.028	-0.027	0.032	0.043	0.063	-0.080	25.2	27.0	1.8
25.0	14.1	0.974	0.959	0.107	0.005	0.023	-0.111	0.024	0.123	0.116	-0.010	24.0	26.4	2.4
27.5	14.8	0.956	0.957	0.078	0.001	0.025	-0.115	0.032	0.043	0.126	-0.027	24.1	26.7	2.6
30.0	15.5	0.876	0.855	0.152	0.006	0.016	-0.125	0.018	0.314	0.074	0.048	23.6	26.4	2.7
32.5	16.2	0.958	0.952	0.148	0.000	0.037	-0.028	0.046	0.032	0.155	-0.028	23.0	25.8	2.8
35.0	16.8	0.983	0.954	0.162	0.030	0.027	-0.091	0.050	0.159	0.089	-0.029	23.7	25.8	2.1
37.5	17.5	0.955	0.936	0.142	0.002	0.023	-0.100	0.037	0.190	0.102	-0.020	24.0	26.2	2.2
40.0	18.2	0.977	0.909	0.201	0.004	0.021	-0.108	0.069	0.296	0.082	0.018	23.1	25.3	2.3
42.5	18.9	0.965	0.905	0.232	0.016	0.052	-0.061	0.020	0.285	0.070	-0.016	23.1	25.1	2.0
45.0	19.5	0.948	0.902	0.157	0.037	0.024	-0.038	0.023	0.291	0.073	-0.127	25.6	26.5	0.9
47.5	20.2	0.956	0.907	0.309	0.018	-0.002	-0.013	0.027	0.155	0.011	-0.111	23.4	24.9	1.5
50.0	20.9	0.908	0.811	0.224	0.004	0.018	-0.075	0.018	0.411	0.152	-0.034	22.7	24.7	2.0
52.5	21.4	0.967	0.938	0.177	0.039	0.022	-0.053	0.021	0.199	0.070	-0.071	24.4	26.0	1.6
55.0	21.9	0.969	0.918	0.230	0.024	0.018	-0.005	0.046	0.241	0.060	-0.092	24.0	25.5	1.5
57.5	22.4	0.955	0.880	0.295	0.052	0.027	-0.052	0.020	0.286	0.066	-0.031	22.6	24.7	2.1
60.0	22.9	0.949	0.883	0.225	0.074	0.038	-0.088	0.030	0.314	0.071	0.003	23.2	25.3	2.2
62.5	23.4	0.958	0.907	0.303	0.041	0.015	-0.070	0.044	0.157	0.096	0.012	21.4	24.3	3.0
65.0	23.9	0.976	0.827	0.316	0.037	0.039	-0.060	0.044	0.422	0.066	-0.004	21.9	23.9	2.0
67.5	24.4	0.922	0.792	0.426	0.049	0.022	-0.094	0.024	0.305	0.079	-0.040	20.5	22.9	2.4
70.0	24.9	0.965	0.912	0.278	0.009	0.005	-0.117	0.030	0.178	0.089	0.037	21.6	24.6	3.0
72.5	25.4	0.984	0.945	0.223	0.042	0.026	-0.093	0.038	0.146	0.089	0.015	22.4	25.1	2.7
75.0	25.9	0.960	0.936	0.161	0.031	0.039	-0.055	0.040	0.194	0.102	-0.054	24.0	25.9	1.9
77.5	26.4	0.961	0.942	0.185	0.075	0.038	-0.058	0.036	0.133	0.097	-0.022	23.2	25.6	2.4
80.0	26.9	0.934	0.871	0.185	0.107	0.040	-0.025	0.012	0.353	0.047	-0.019	24.5	26.4	1.9
82.5	27.4	0.936	0.931	0.088	0.132	0.039	-0.075	0.013	0.162	0.096	-0.029	24.8	26.9	2.1
85.0	27.9	0.974	0.946	0.097	0.077	0.073	-0.077	0.101	0.140	0.150	0.009	23.3	25.9	2.6
87.5	28.4	0.982	0.960	0.118	0.065	0.050	-0.070	0.024	0.127	0.137	-0.002	23.5	26.0	2.5
90.0	28.9	0.963	0.917	0.214	0.026	0.061	-0.046	0.049	0.187	0.180	-0.009	21.8	24.6	2.8
92.5	29.6	0.969	0.954	0.059	0.065	0.065	-0.026	0.043	0.080	0.194	-0.029	23.9	26.4	2.5
95.0	30.4	0.983	0.943	0.184	0.034	0.100	0.020	0.071	0.129	0.152	-0.061	22.5	24.8	2.3
97.5	31.1	0.970	0.916	0.186	0.031	0.069	0.000	0.019	0.217	0.209	-0.027	22.2	24.8	2.5
100.0	31.9	0.975	0.917	0.139	0.042	0.073	0.041	0.061	0.201	0.248	-0.019	22.4	25.0	2.6
102.5	32.6	0.979	0.907	0.177	0.066	0.064	0.074	0.030	0.213	0.253	0.032	21.6	24.7	3.1
105.0	33.3	0.980	0.929	0.150	0.019	0.040	0.019	0.056	0.240	0.177	0.021	22.7	25.5	2.8
107.5	34.1	0.961	0.929	0.151	0.045	0.057	0.058	0.026	0.093	0.242	0.006	22.2	25.3	3.1
110.0	34.8	0.981	0.922	0.205	0.070	0.053	-0.011	0.135	0.187	0.168	-0.008	22.1	24.7	2.7
112.5	35.5	0.945	0.902	0.232	0.035	0.049	-0.031	0.021	0.180	0.199	0.026	21.3	24.5	3.3
115.0	36.3	0.993	0.963	0.142	0.074	0.034	-0.018	0.049	0.066	0.171	0.053	22.5	25.7	3.2
117.5	37.0	0.975	0.946	0.171	0.019	0.030	-0.038	0.026	0.113	0.189	-0.003	22.5	25.4	2.9
120.0	37.8	0.928	0.852	0.218	0.084	0.023	-0.017	0.034	0.349	0.155	-0.027	22.9	25.0	2.2
122.5	38.5	0.969	0.899	0.207	0.047	0.017	0.020	0.039	0.257	0.217	-0.033	22.3	24.8	2.5
125.0	39.2	0.980	0.932	0.187	0.029	0.051	-0.019	0.062	0.219	0.141	-0.024	22.8	25.1	2.3
127.5	40.0	0.963	0.924	0.172	0.019	0.032	0.004	0.073	0.111	0.245	-0.019	22.1	25.2	3.1
130.0	40.7	0.965	0.910	0.137	0.045	0.041	0.014	0.051	0.196	0.272	-0.005	22.3	25.2	2.9
132.5	41.4	0.966	0.907	0.143	0.001	0.040	-0.007	0.052	0.269	0.213	-0.031	22.9	25.4	2.4
135.0	42.2	0.911	0.849	0.141	0.138	0.025	-0.022	0.027	0.330	0.193	-0.053	24.1	25.9	1.8
137.5	42.9	0.933	0.894	0.153	0.031	0.024	0.068	0.022	0.184	0.264	-0.030	22.5	25.4	2.9
140.0	43.7	0.938	0.884	0.225	0.079	0.055	-0.003	0.072	0.215	0.213	0.001	21.5	24.4	2.9
142.5	44.4	0.928	0.909	0.108	0.012	0.072	0.034	0.039	0.184	0.211	-0.071	23.6	25.9	2.3
145.0	45.1	0.809	0.742	0.198	0.111	0.031	-0.031	0.009	0.422	0.158	-0.034	22.8	24.9	2.1
147.5	45.9	0.928	0.902	0.205	0.002	0.039	0.027	0.030	0.162	0.191	-0.079	22.6	25.1	2.5
150.0	46.6	0.905	0.886	0.212	0.044	0.036	-0.075	0.070	0.187	0.161	0.008	21.9	25.0	3.0
152.5	47.3	0.901	0.891	0.152	0.001	0.056	-0.011	0.029	0.151	0.233	-0.051	22.6	25.5	2.8
155.0	48.1	0.940	0.837	0.197	0.063	0.064	-0.009	0.102	0.362	0.226	0.007	21.3	23.9	2.6
157.5	48.8	0.922	0.886	0.226	0.006	0.067	0.047	0.050	-0.006	0.276	-0.021	21.3	24.8	3.6
160.0	49.6	0.972	0.876	0.221	0.005	0.076	0.006	0.074	0.313	0.213	0.037	20.6	23.8	3.1
162.5	50.3	0.973	0.954	0.099	0.007	0.054	-0.045	0.027	-0.026	0.216	0.021	22.6	26.0	3.4
165.0	51.0	0.988	0.929	0.229	0.019	0.030	-0.021	0.082	0.135	0.213	0.034	21.1	24.5	3.4
167.5	51.8	0.970	0.938	0.132	0.001	0.026	-0.043	0.023	0.224	0.135	-0.029	24.1	26.2	2.2
170.0	52.5	0.961	0.884	0.245	0.019	0.026	-0.026	0.049	0.287	0.179	-0.022	21.8	24.4	2.5

depth (cm)	age (kyrs)	COMM.	Factor 1	Factor 2	Factor 3	Factor 4	Factor 5	Factor 6	Factor 7	Factor 8	Factor 9	Est. Tc 0-50m (°C)	Est. Tw 0-50m (°C)	seasonality
172.5	53.2	0.936	0.926	0.146	0.069	0.025	-0.030	0.023	0.145	0.166	-0.042	23.5	26.0	2.4
175.0	54.0	0.720	0.755	0.167	0.036	0.058	0.108	0.060	0.161	0.216	-0.170	23.2	25.8	2.6
177.5	54.7	0.887	0.885	0.150	0.049	0.028	0.023	0.016	0.149	0.218	-0.084	23.4	25.8	2.5
180.0	55.5	0.925	0.904	0.223	0.066	0.030	-0.008	0.046	0.142	0.158	-0.073	22.8	25.1	2.4
182.5	57.6	0.943	0.927	0.158	0.015	0.032	-0.009	0.020	0.183	0.127	-0.092	24.2	26.0	1.8
185.0	59.8	0.984	0.961	0.174	0.063	0.026	-0.074	0.046	0.106	0.074	0.013	23.1	25.7	2.6
187.5	61.9	0.965	0.944	0.183	0.038	0.051	-0.126	0.029	0.084	0.099	0.057	22.0	25.2	3.2
190.0	64.1	0.968	0.918	0.284	0.046	0.039	-0.045	0.050	0.171	0.063	-0.055	22.5	24.6	2.1
192.5	64.8	0.985	0.955	0.219	0.006	0.028	-0.040	0.046	0.110	0.080	-0.041	23.0	25.2	2.2
195.0	65.5	0.922	0.863	0.242	0.045	0.038	-0.096	0.053	0.291	0.124	-0.055	22.7	24.7	2.0
197.5	66.2	0.932	0.924	0.145	0.021	0.018	-0.087	0.057	0.131	0.164	-0.036	23.3	26.0	2.7
200.0	66.9	0.919	0.877	0.227	0.029	0.025	-0.075	0.057	0.274	0.106	-0.046	23.1	25.1	2.1
202.5	67.6	0.935	0.924	0.132	0.060	0.028	-0.083	0.083	0.158	0.140	-0.015	23.5	26.1	2.6
205.0	68.4	0.924	0.889	0.194	0.018	0.031	-0.059	0.035	0.260	0.144	-0.047	23.2	25.4	2.2
207.5	69.1	0.921	0.842	0.145	0.003	0.030	-0.057	0.028	0.400	0.128	-0.097	25.0	26.0	1.0
210.0	69.8	0.923	0.907	0.130	0.017	0.041	-0.062	0.058	0.205	0.166	-0.060	23.8	26.0	2.2
212.5	70.5	0.876	0.873	0.110	0.001	0.031	0.042	0.082	0.234	0.155	-0.119	24.7	26.6	1.9
215.0	71.2	0.903	0.858	0.164	0.019	0.028	-0.004	0.054	0.302	0.182	-0.109	23.8	25.6	1.7
217.5	71.9	0.947	0.923	0.125	-0.001	0.021	0.018	0.022	0.156	0.230	-0.046	23.3	26.0	2.7
220.0	72.6	0.950	0.920	0.109	0.023	0.031	-0.007	0.052	0.174	0.236	-0.031	23.3	26.0	2.7
222.5	73.3	0.978	0.945	0.088	-0.001	0.026	-0.043	0.031	0.195	0.189	-0.004	23.8	26.4	2.6
225.0	74.0	0.949	0.899	0.096	0.011	0.032	0.030	0.058	0.237	0.252	-0.081	23.7	25.9	2.2
227.5	74.7	0.906	0.904	0.107	0.000	0.027	0.027	0.036	0.164	0.191	-0.105	24.4	26.5	2.2
230.0	75.5	0.952	0.907	0.158	0.009	0.012	-0.005	0.036	0.243	0.191	-0.090	23.8	25.7	2.0
232.5	76.2	0.943	0.874	0.132	0.000	0.025	0.053	0.033	0.323	0.211	-0.091	23.8	25.7	1.9
235.0	76.9	0.945	0.831	0.187	0.022	0.021	0.045	0.025	0.434	0.144	-0.083	23.9	25.4	1.5
237.5	77.6	0.950	0.851	0.147	0.001	0.022	0.060	0.023	0.386	0.205	-0.097	23.8	25.5	1.7
240.0	78.3	0.930	0.883	0.161	0.001	0.035	0.013	0.047	0.294	0.173	-0.069	23.5	25.6	2.0
242.5	79.2	0.871	0.807	0.120	0.001	0.032	0.102	0.043	0.327	0.264	-0.125	23.3	25.5	2.2
245.0	80.2	0.907	0.864	0.137	0.001	0.024	0.067	0.033	0.266	0.230	-0.108	23.6	25.8	2.2
247.5	81.1	0.881	0.811	0.146	0.002	0.025	0.037	0.025	0.376	0.221	-0.088	23.4	25.4	2.0
250.0	82.1	0.932	0.888	0.133	0.001	0.029	0.054	0.039	0.285	0.174	-0.098	24.2	26.0	1.8
252.5	83.0	0.910	0.882	0.119	0.001	0.021	0.060	0.037	0.248	0.175	-0.148	24.9	26.5	1.6
255.0	84.0	0.946	0.921	0.104	0.011	0.027	0.081	0.040	0.183	0.211	-0.030	23.5	26.2	2.7
257.5	84.9	0.918	0.902	0.096	0.001	0.022	0.050	0.017	0.224	0.195	-0.054	24.2	26.6	2.4
260.0	85.9	0.909	0.898	0.106	0.010	0.017	0.175	0.009	0.178	0.157	-0.062	24.1	26.7	2.6
262.5	86.8	0.794	0.749	0.071	0.000	0.027	0.323	-0.001	0.240	0.229	-0.113	23.6	26.7	3.2
265.0	87.8	0.890	0.846	0.113	0.010	0.021	0.231	0.020	0.248	0.193	-0.093	23.6	26.3	2.6
267.5	88.7	0.900	0.825	0.121	0.002	0.017	0.328	0.011	0.215	0.195	-0.111	23.2	26.1	2.9
270.0	89.7	0.893	0.793	0.164	0.011	0.030	0.258	0.037	0.332	0.215	-0.109	22.4	25.1	2.7
272.5	90.6	0.784	0.759	0.075	-0.002	0.031	0.304	0.004	0.168	0.264	-0.103	23.4	26.7	3.2
275.0	91.6	0.827	0.753	0.150	0.020	0.027	0.176	0.011	0.442	0.085	-0.054	24.1	26.6	2.6
277.5	92.5	0.916	0.885	0.105	0.002	0.018	0.178	0.009	0.265	0.104	-0.092	24.9	27.0	2.1
280.0	93.5	0.956	0.930	0.107	0.010	0.026	0.192	0.008	0.172	0.107	0.001	23.8	26.6	2.8
282.5	94.4	0.932	0.930	0.067	-0.001	0.025	0.110	0.014	0.151	0.151	-0.060	24.8	27.1	2.3
285.0	95.4	0.969	0.942	0.115	0.012	0.019	0.061	0.030	0.167	0.188	0.001	23.4	26.2	2.8
287.5	96.3	0.946	0.919	0.093	0.002	0.022	0.249	0.019	0.131	0.115	-0.021	23.9	26.6	2.8
290.0	97.3	0.959	0.955	0.090	0.001	0.017	0.068	0.016	0.121	0.134	0.030	24.0	26.8	2.8
292.5	98.2	0.936	0.945	0.084	0.002	0.014	0.110	0.015	0.087	0.122	-0.009	24.4	27.0	2.6
295.0	99.2	0.905	0.896	0.104	0.004	0.025	0.173	0.017	0.218	0.113	-0.033	24.3	26.9	2.6
297.5	100.1	0.904	0.879	0.089	0.003	0.020	0.237	0.029	0.197	0.146	-0.087	24.3	26.8	2.5
300.0	101.1	0.943	0.942	0.142	0.013	0.028	0.081	0.053	0.136	0.068	0.055	23.4	26.3	2.9
302.5	102.0	0.910	0.893	0.201	0.004	0.011	0.143	0.013	0.198	0.032	-0.103	24.4	26.2	1.8
305.0	103.0	0.804	0.768	0.168	0.005	0.037	0.111	0.023	0.391	0.139	0.002	22.8	25.9	3.1
307.5	103.9	0.849	0.859	0.219	0.005	0.009	0.152	0.009	0.175	0.081	-0.058	23.4	26.0	2.6
312.5	105.8	0.845	0.858	0.087	0.000	0.018	0.290	0.003	0.027	0.122	-0.022	24.3	27.0	2.7
315.0	106.8	0.937	0.906	0.119	0.003	0.027	0.231	0.041	0.186	0.105	0.028	23.3	26.5	3.2
317.5	107.7	0.876	0.838	0.230	0.005	0.010	0.226	0.013	0.261	0.025	-0.030	23.3	26.1	2.8
320.0	108.6	0.958	0.931	0.219	0.005	0.006	0.171	0.029	0.110	0.041	-0.016	23.1	25.5	2.4
322.5	109.6	0.952	0.912	0.191	0.004	0.006	0.190	0.015	0.195	0.096	-0.020	23.1	25.9	2.7
325.0	110.5	0.960	0.947	0.126	0.002	0.014	0.156	0.021	0.091	0.120	-0.009	23.7	26.3	2.6
327.5	111.5	0.944	0.929	0.178	0.003	0.010	0.171	0.019	0.087	0.106	0.002	23.1	25.9	2.8
330.0	112.4	0.947	0.891	0.191	0.006	0.009	0.254	0.023	0.181	0.132	0.027	22.3	25.6	3.3
332.5	113.4	0.922	0.875	0.194	0.005	0.010	0.157	0.033	0.261	0.158	-0.026	22.7	25.6	2.9
335.0	114.3	0.972	0.910	0.134	0.002	0.020	0.233	0.032	0.198	0.171	-0.030	22.9	25.9	2.9
337.5	115.3	0.977	0.959	0.140	0.001	0.015	0.064	0.029	0.134	0.121	-0.017	23.7	26.2	2.5
340.0	116.2	0.948	0.880	0.163	0.003	0.010	0.175	0.032	0.260	0.202	-0.078	23.0	25.5	2.6
342.5	117.2	0.958	0.905	0.231	0.004	-0.002	0.074	0.024	0.228	0.152	-0.067	22.9	25.2	2.4
345.0	118.1	0.907	0.864	0.137	0.001	0.024	0.067	0.033	0.266	0.230	-0.108	23.6	25.8	2.2

depth (cm)	age (kyrs)	COMM.	Factor 1	Factor 2	Factor 3	Factor 4	Factor 5	Factor 6	Factor 7	Factor 8	Factor 9	Est. Tc 0-50m (°C)	Est. Tw 0-50m (°C)	seasonality
347.5	119.1	0.905	0.871	0.305	0.007	-0.012	0.064	0.026	0.121	0.169	-0.072	21.8	24.7	2.9
350.0	120.0	0.863	0.797	0.217	0.015	0.011	0.183	0.036	0.320	0.168	-0.123	22.9	25.2	2.3
352.5	121.0	0.766	0.771	0.278	0.007	-0.009	0.097	0.017	0.168	0.192	-0.140	22.4	25.2	2.8
355.0	121.9	0.813	0.787	0.172	0.005	0.011	0.204	0.017	0.261	0.177	-0.154	23.6	26.0	2.4
357.5	122.9	0.732	0.713	0.199	0.006	-0.004	0.262	0.006	0.232	0.090	-0.233	24.4	26.4	2.1
360.0	123.8	0.812	0.799	0.241	0.032	0.000	0.193	0.032	0.221	0.088	-0.142	23.6	25.8	2.2
362.5	124.4	0.835	0.805	0.107	0.004	0.009	0.295	0.012	0.194	0.120	-0.192	24.7	26.9	2.2
365.0	124.9	0.810	0.786	0.151	0.006	0.017	0.159	0.006	0.338	0.092	-0.147	25.0	26.8	1.8
367.5	125.5	0.812	0.777	0.155	0.003	0.015	0.200	0.007	0.302	0.149	-0.173	24.3	26.3	2.1
370.0	126.1	0.945	0.921	0.270	0.007	0.019	-0.021	0.038	0.129	0.068	-0.041	22.6	24.9	2.3
372.5	126.6	0.952	0.910	0.228	0.003	0.021	0.066	0.020	0.238	0.054	-0.090	23.9	25.6	1.7
375.0	127.2	0.983	0.970	0.133	0.000	0.056	-0.001	0.023	0.131	0.037	0.045	23.7	26.1	2.4
377.5	127.8	0.981	0.965	0.147	0.029	0.033	0.144	0.019	0.063	0.024	-0.029	23.7	25.8	2.1
380.0	128.3	0.963	0.951	0.232	0.005	0.016	0.005	0.023	0.033	0.052	-0.025	22.8	25.2	2.3
382.5	128.9	0.977	0.943	0.151	0.002	0.029	-0.020	0.021	0.234	0.086	-0.026	24.2	26.2	2.0
385.0	129.5	0.961	0.960	0.126	0.001	0.010	0.043	0.028	0.043	0.064	-0.120	24.9	26.5	1.6
387.5	130.0	0.934	0.907	0.234	0.003	0.031	-0.006	0.030	0.167	0.162	-0.040	22.2	24.9	2.7
390.0	130.6	0.978	0.955	0.200	0.002	0.035	-0.009	0.034	0.111	0.099	-0.051	23.1	25.3	2.2
392.5	131.2	0.982	0.963	0.122	0.045	0.099	-0.025	0.014	0.113	0.104	-0.058	23.7	25.6	1.9
395.0	131.7	0.957	0.883	0.224	0.014	0.062	0.049	0.031	0.307	0.149	-0.061	22.6	24.7	2.1
400.0	132.8	0.979	0.898	0.287	0.017	0.072	-0.020	0.044	0.257	0.125	0.008	21.1	23.8	2.7
405.0	134.0	0.990	0.939	0.219	0.004	0.082	-0.054	0.095	0.135	0.150	0.000	21.6	24.3	2.8
410.0	135.1	0.950	0.913	0.209	0.014	0.070	-0.027	0.130	0.176	0.121	-0.064	22.7	24.9	2.2
415.0	136.1	0.935	0.838	0.179	0.016	0.062	0.025	0.058	0.391	0.188	-0.072	22.9	24.7	1.8
420.0	137.2	0.977	0.891	0.216	0.013	0.069	-0.022	0.088	0.329	0.117	-0.018	22.4	24.6	2.1
425.0	138.2	0.930	0.916	0.148	0.018	0.109	0.063	0.040	0.153	0.158	-0.058	22.9	25.3	2.4
430.0	139.3	0.964	0.931	0.176	0.012	0.069	-0.043	0.056	0.157	0.176	-0.023	22.4	25.0	2.6
435.0	140.3	0.942	0.921	0.143	0.000	0.099	-0.008	0.071	0.136	0.202	0.016	22.1	25.1	3.1
440.0	141.3	0.973	0.909	0.223	0.028	0.044	-0.055	0.081	0.211	0.198	0.032	21.1	24.3	3.2
450.0	145.3	0.967	0.940	0.161	0.000	0.072	-0.035	0.033	0.193	0.110	-0.024	23.3	25.5	2.2

depth (cm)	age (kyrs)	DSML	STDEV	Mean analog Tc0-50m (°C)	STDEV	Mean analog Tw0-50m (°C)	STDEV	Mean annual analog T75m (°C)	STDEV	Mean annual analog T100m (°C)	STDEV	Mean annual analog T150m (°C)	STDEV	SIM	STEV
0.0	7.4	0.053	0.010	25.9	0.5	27.9	0.5	26.0	0.6	25.1	0.7	22.6	1.2	0.974	0.005
2.5	8.1	0.066	0.009	26.0	0.2	27.9	0.2	25.9	0.5	25.0	0.8	22.4	1.2	0.967	0.005
5.0	8.8	0.102	0.015	25.9	0.4	27.9	0.5	26.0	0.5	25.1	0.7	22.6	1.1	0.949	0.007
7.5	9.4	0.053	0.008	26.0	0.3	27.8	0.2	25.7	0.6	24.7	1.0	21.9	1.6	0.973	0.004
10.0	10.1	0.082	0.019	25.9	0.4	27.9	0.4	25.9	0.5	25.0	0.7	22.4	1.1	0.959	0.010
12.5	10.8	0.060	0.007	25.7	0.6	27.6	0.6	25.6	0.8	24.5	1.1	21.7	1.7	0.970	0.004
15.0	11.4	0.056	0.006	25.9	0.2	27.9	0.2	25.8	0.4	24.8	0.7	22.1	1.2	0.972	0.003
17.5	12.1	0.059	0.013	25.9	0.2	27.9	0.2	25.8	0.4	24.8	0.7	22.2	1.2	0.971	0.006
20.0	12.8	0.130	0.009	25.8	0.4	27.7	0.4	25.8	0.4	24.7	0.6	21.6	2.1	0.935	0.004
22.5	13.5	0.084	0.015	25.6	0.5	27.5	0.7	25.6	0.6	24.5	0.9	21.8	1.4	0.958	0.008
25.0	14.1	0.097	0.013	25.5	0.6	27.5	0.7	25.4	0.6	24.3	0.9	21.6	1.4	0.952	0.007
27.5	14.8	0.084	0.012	25.8	0.4	27.8	0.4	25.8	0.4	25.0	0.5	22.6	0.7	0.958	0.006
30.0	15.5	0.199	0.014	25.8	0.8	27.8	0.5	25.9	0.7	24.8	1.0	21.6	2.7	0.901	0.007
32.5	16.2	0.124	0.015	25.9	0.2	27.8	0.3	25.6	0.7	24.6	0.9	21.9	1.4	0.938	0.007
35.0	16.8	0.129	0.014	25.4	1.1	27.5	1.1	25.4	1.2	24.5	1.1	22.0	1.5	0.936	0.007
37.5	17.5	0.121	0.015	24.9	1.4	27.4	1.1	25.0	1.4	24.1	1.4	21.9	1.2	0.939	0.007
40.0	18.2	0.145	0.012	24.3	1.6	26.8	1.5	23.8	2.9	22.7	3.3	20.1	3.5	0.928	0.006
42.5	18.9	0.136	0.014	23.2	1.6	25.6	1.6	21.9	2.6	20.6	3.2	17.7	3.2	0.932	0.007
45.0	19.5	0.135	0.012	25.4	0.8	27.5	0.8	24.8	2.7	23.8	2.8	21.3	2.7	0.933	0.006
47.5	20.2	0.136	0.017	23.8	1.8	26.0	1.5	20.5	3.9	18.8	4.4	16.5	4.0	0.932	0.009
50.0	20.9	0.183	0.025	25.4	1.1	27.9	0.2	25.6	0.9	24.7	0.8	22.4	0.7	0.909	0.013
52.5	21.4	0.127	0.015	25.0	1.3	27.0	1.3	24.9	1.4	23.9	1.3	21.0	1.9	0.937	0.007
55.0	21.9	0.120	0.010	24.2	1.8	26.5	1.4	21.3	4.2	19.7	4.7	17.3	4.3	0.940	0.005
57.5	22.4	0.177	0.011	23.3	1.5	25.6	1.4	20.6	3.3	18.9	3.8	16.5	3.4	0.912	0.006
60.0	22.9	0.198	0.017	25.1	1.2	27.2	1.2	25.1	1.3	24.2	1.2	21.5	1.6	0.901	0.009
62.5	23.4	0.179	0.008	23.9	2.1	26.2	1.8	21.8	4.2	20.4	4.8	18.0	4.5	0.910	0.004
65.0	23.9	0.155	0.017	23.1	1.6	25.5	1.6	20.9	3.4	19.6	3.9	16.9	3.6	0.923	0.008
67.5	24.4	0.209	0.018	22.7	1.1	25.3	1.2	19.5	3.0	18.1	3.4	15.9	3.0	0.896	0.009
70.0	24.9	0.187	0.009	23.7	1.6	26.1	1.5	22.1	3.3	20.6	4.1	18.2	4.0	0.907	0.005
72.5	25.4	0.150	0.013	23.8	1.5	26.0	1.3	22.0	3.3	20.6	4.0	18.0	3.8	0.925	0.007
75.0	25.9	0.137	0.013	25.4	0.8	27.5	0.7	25.4	0.8	24.5	0.8	22.0	1.0	0.932	0.007
77.5	26.4	0.164	0.009	25.5	1.4	27.2	1.4	24.8	2.5	23.4	2.7	20.3	3.0	0.918	0.005
80.0	26.9	0.183	0.011	25.1	1.6	27.0	1.2	24.4	2.8	23.1	3.2	20.0	3.2	0.909	0.005
82.5	27.4	0.166	0.007	25.8	0.6	27.7	0.6	25.6	0.8	24.7	1.0	22.1	1.5	0.917	0.003
85.0	27.9	0.170	0.010	25.8	0.5	27.8	0.5	25.6	0.7	24.7	0.9	22.1	1.4	0.915	0.005
87.5	28.4	0.138	0.014	25.5	0.6	27.4	0.7	25.3	0.7	24.3	0.8	21.6	1.3	0.931	0.007
90.0	28.9	0.171	0.007	25.4	1.0	27.6	0.9	24.9	2.8	23.9	2.9	21.6	2.8	0.915	0.004
92.5	29.6	0.127	0.015	25.5	0.6	27.4	0.6	25.3	0.6	24.3	0.8	21.6	1.4	0.936	0.007
95.0	30.4	0.147	0.006	24.3	2.1	26.6	1.3	21.5	4.2	20.0	4.4	17.7	3.7	0.926	0.003
97.5	31.1	0.144	0.006	25.1	1.3	27.3	0.9	23.9	3.5	22.6	3.8	20.1	3.5	0.928	0.003
100.0	31.9	0.151	0.012	25.8	0.4	27.8	0.4	25.7	0.5	24.6	0.8	21.9	1.4	0.924	0.006
102.5	32.6	0.177	0.016	24.7	1.6	26.7	1.4	23.3	3.3	21.9	3.9	19.2	3.6	0.912	0.008
105.0	33.3	0.133	0.012	24.9	1.5	26.7	1.2	23.6	3.1	22.1	3.7	19.0	3.4	0.934	0.006
107.5	34.1	0.162	0.010	25.7	0.4	27.5	0.7	24.9	2.2	23.7	2.8	21.0	2.8	0.919	0.005
110.0	34.8	0.194	0.012	24.7	1.9	26.8	1.4	23.0	3.8	21.7	4.3	19.2	3.8	0.903	0.006
112.5	35.5	0.164	0.009	25.3	1.4	27.5	0.9	24.2	3.7	23.1	4.0	20.8	3.7	0.918	0.005
115.0	36.3	0.163	0.006	25.2	1.3	27.3	1.0	24.2	3.3	22.9	4.0	20.5	3.7	0.919	0.003
117.5	37.0	0.125	0.012	25.6	0.8	27.7	0.7	24.8	2.8	23.8	2.9	21.3	2.8	0.938	0.006
120.0	37.8	0.190	0.011	25.2	1.1	27.4	0.9	24.6	2.8	23.7	2.8	21.2	2.7	0.905	0.005
122.5	38.5	0.179	0.021	25.5	0.8	27.6	0.7	24.8	2.7	23.8	2.9	21.3	2.8	0.910	0.011
125.0	39.2	0.151	0.012	25.9	0.2	27.7	0.3	25.5	0.7	24.4	1.1	21.6	1.6	0.925	0.006
127.5	40.0	0.136	0.012	25.9	0.2	27.8	0.2	25.7	0.5	24.6	0.9	21.9	1.5	0.932	0.006
130.0	40.7	0.147	0.013	25.9	0.2	27.9	0.2	25.8	0.4	24.8	0.7	22.2	1.2	0.927	0.006
132.5	41.4	0.124	0.019	25.7	0.4	27.8	0.4	25.6	0.5	24.6	0.8	21.9	1.4	0.938	0.010
135.0	42.2	0.202	0.014	25.9	0.2	27.8	0.2	25.7	0.5	24.6	0.9	21.9	1.5	0.899	0.007
137.5	42.9	0.143	0.013	25.8	0.4	27.7	0.4	25.7	0.5	24.6	0.8	21.9	1.4	0.929	0.007
140.0	43.7	0.197	0.008	25.3	1.4	27.5	0.9	24.2	3.7	23.0	4.0	20.2	3.9	0.902	0.004
142.5	44.4	0.144	0.015	25.9	0.2	27.8	0.2	25.7	0.5	24.6	0.9	21.9	1.5	0.928	0.008
145.0	45.1	0.232	0.018	25.5	0.9	27.5	0.6	25.4	0.8	24.2	0.9	21.2	2.1	0.884	0.009
147.5	45.9	0.144	0.017	25.3	1.4	27.4	0.9	24.1	3.6	22.9	4.0	20.4	3.6	0.928	0.009
150.0	46.6	0.199	0.010	25.0	1.7	27.3	1.0	24.0	3.6	22.7	4.1	20.0	3.8	0.900	0.005
152.5	47.3	0.157	0.012	25.6	0.8	27.6	0.7	24.9	2.8	23.9	2.9	21.4	2.8	0.921	0.006
155.0	48.1	0.189	0.014	25.9	0.2	27.9	0.1	25.9	0.2	24.9	0.5	22.0	2.0	0.905	0.007
157.5	48.8	0.171	0.017	24.4	2.1	26.8	1.4	22.3	4.4	21.2	4.4	19.0	3.8	0.915	0.009
160.0	49.6	0.177	0.010	25.0	1.5	27.2	1.3	24.5	2.8	23.5	3.2	20.9	3.0	0.912	0.005
162.5	50.3	0.119	0.011	25.2	1.4	27.3	1.0	23.9	3.4	22.7	3.8	20.2	3.4	0.941	0.005
165.0	51.0	0.169	0.014	25.5	1.2	27.7	0.7	25.0	2.7	23.8	3.2	21.3	3.0	0.915	0.007

depth (cm)	Est Tc0-50m (°C)	Est Tw0-50m (°C)	Est. annual T75m (°C)	Est. annual T100m (°C)	Est. annual T150m (°C)	#best Analogs
0.0	25.9	27.9	26.0	25.1	22.6	10
2.5	26.0	27.9	25.9	25.0	22.4	10
5.0	25.9	27.9	26.0	25.1	22.6	10
7.5	26.0	27.8	25.7	24.7	21.9	10
10.0	25.9	27.9	25.9	25.0	22.4	10
12.5	25.7	27.6	25.6	24.5	21.7	10
15.0	25.9	27.9	25.8	24.8	22.1	10
17.5	25.9	27.9	25.8	24.8	22.2	10
20.0	25.8	27.7	25.8	24.7	21.6	10
22.5	25.6	27.5	25.6	24.5	21.8	10
25.0	25.5	27.5	25.4	24.3	21.6	10
27.5	25.8	27.8	25.8	25.0	22.6	10
30.0	25.8	27.8	25.9	24.8	21.6	10
32.5	25.9	27.8	25.6	24.6	21.9	10
35.0	25.4	27.5	25.4	24.5	22.0	10
37.5	24.9	27.4	25.0	24.1	21.9	10
40.0	24.3	26.8	23.8	22.7	20.1	10
42.5	23.2	25.6	21.9	20.6	17.7	10
45.0	25.4	27.5	24.8	23.8	21.3	10
47.5	23.8	26.0	20.5	18.8	16.5	10
50.0	25.4	27.9	25.6	24.7	22.4	10
52.5	25.0	27.0	24.9	23.9	21.0	10
55.0	24.2	26.5	21.3	19.7	17.3	10
57.5	23.3	25.6	20.6	18.9	16.4	10
60.0	25.1	27.2	25.1	24.2	21.5	10
62.5	23.9	26.2	21.8	20.4	18.0	10
65.0	23.1	25.5	20.9	19.6	16.9	10
67.5	22.7	25.3	19.5	18.1	15.8	10
70.0	23.7	26.1	22.1	20.6	18.2	10
72.5	23.8	26.0	22.0	20.6	18.0	10
75.0	25.4	27.5	25.4	24.5	22.0	10
77.5	25.5	27.2	24.8	23.4	20.3	10
80.0	25.1	27.0	24.4	23.1	20.0	10
82.5	25.8	27.7	25.6	24.7	22.1	10
85.0	25.8	27.8	25.6	24.7	22.1	10
87.5	25.5	27.4	25.3	24.3	21.6	10
90.0	25.4	27.5	24.9	23.9	21.6	10
92.5	25.5	27.4	25.4	24.3	21.6	10
95.0	24.3	26.6	21.5	20.0	17.7	10
97.5	25.1	27.3	23.9	22.6	20.1	10
100.0	25.8	27.8	25.7	24.6	21.9	10
102.5	24.7	26.7	23.3	21.8	19.1	10
105.0	24.9	26.7	23.6	22.1	19.0	10
107.5	25.7	27.5	24.9	23.7	21.0	10
110.0	24.7	26.8	23.0	21.7	19.2	10
112.5	25.3	27.5	24.2	23.1	20.8	10
115.0	25.2	27.3	24.2	22.9	20.5	10
117.5	25.6	27.7	24.9	23.8	21.3	10
120.0	25.2	27.4	24.6	23.7	21.2	10
122.5	25.5	27.6	24.8	23.8	21.4	10
125.0	25.9	27.7	25.5	24.4	21.6	10
127.5	25.9	27.8	25.7	24.6	21.9	10
130.0	25.9	27.9	25.8	24.8	22.2	10
132.5	25.7	27.8	25.6	24.6	21.9	10
135.0	25.9	27.8	25.7	24.6	21.9	10
137.5	25.8	27.7	25.7	24.6	21.9	10
140.0	25.3	27.5	24.2	23.0	20.2	10
142.5	25.9	27.8	25.7	24.6	21.9	10
145.0	25.5	27.6	25.4	24.2	21.2	10
147.5	25.3	27.4	24.1	22.9	20.4	10
150.0	25.0	27.3	24.0	22.7	20.0	10
152.5	25.6	27.6	24.9	23.9	21.4	10
155.0	25.9	27.9	25.9	24.9	22.0	10
157.5	24.4	26.8	22.3	21.2	19.0	10
160.0	25.0	27.2	24.5	23.5	20.9	10
162.5	25.2	27.3	23.9	22.7	20.2	10
165.0	25.5	27.7	25.0	23.8	21.3	10

depth (cm)	age (kyrs)	DSML	STDEV	Mean analog Tc0-50m (°C)	STDEV	Mean analog Tw0-50m (°C)	STDEV	Mean annual analog T75m (°C)	STDEV	Mean annual analog T100m (°C)	STDEV	Mean annual analog T150m (°C)	STDEV	SIM	STEV
167.5	51.8	0.093	0.014	25.6	0.4	27.6	0.5	25.5	0.5	24.5	0.8	21.8	1.3	0.954	0.007
170.0	52.5	0.143	0.011	25.6	1.2	27.7	0.7	25.0	2.7	23.8	3.2	21.3	3.0	0.929	0.005
172.5	53.2	0.148	0.018	25.7	0.4	27.7	0.4	25.6	0.5	24.6	0.8	21.9	1.4	0.926	0.009
175.0	54.0	0.162	0.016	25.2	1.6	27.3	1.1	23.9	3.6	22.8	3.7	20.2	3.3	0.919	0.008
177.5	54.7	0.137	0.020	25.6	0.8	27.6	0.7	24.9	2.8	23.9	2.9	21.4	2.8	0.932	0.010
180.0	55.5	0.145	0.012	25.6	0.8	27.7	0.7	24.9	2.8	23.9	2.9	21.4	2.8	0.928	0.006
182.5	57.6	0.118	0.011	25.4	0.8	27.5	0.8	24.7	2.7	23.6	2.8	21.0	2.8	0.941	0.006
185.0	59.8	0.138	0.006	24.6	1.6	26.7	1.4	24.1	2.8	23.1	3.2	20.4	3.1	0.931	0.003
187.5	61.9	0.163	0.012	23.1	1.2	26.0	1.2	22.7	2.2	21.7	2.7	19.5	2.6	0.918	0.006
190.0	64.1	0.140	0.012	24.2	1.8	26.6	1.5	22.5	4.0	21.2	4.5	18.8	4.4	0.930	0.006
192.5	64.8	0.110	0.014	23.8	1.8	26.0	1.4	21.3	3.5	19.7	4.0	17.0	3.4	0.945	0.007
195.0	65.5	0.175	0.013	24.6	1.6	27.0	1.3	23.5	3.5	22.5	3.9	20.1	3.6	0.913	0.007
197.5	66.2	0.118	0.016	25.8	0.3	27.9	0.2	25.7	0.4	24.7	0.7	22.2	1.2	0.941	0.008
200.0	66.9	0.172	0.015	25.6	0.8	27.7	0.7	25.0	2.8	24.1	2.9	21.7	2.7	0.914	0.007
202.5	67.6	0.153	0.014	25.8	0.3	27.9	0.2	25.8	0.5	24.8	0.7	22.2	1.2	0.923	0.007
205.0	68.4	0.132	0.015	25.8	0.3	27.9	0.2	25.7	0.4	24.7	0.7	22.2	1.2	0.934	0.008
207.5	69.1	0.118	0.020	25.7	0.4	27.7	0.4	25.6	0.5	24.6	0.8	21.9	1.4	0.941	0.010
210.0	69.8	0.135	0.015	25.8	0.3	27.9	0.2	25.7	0.4	24.7	0.7	22.2	1.2	0.933	0.008
212.5	70.5	0.123	0.016	25.8	0.2	27.9	0.1	25.9	0.1	25.0	0.2	22.6	0.5	0.938	0.008
215.0	71.2	0.121	0.017	25.8	0.3	27.9	0.2	25.7	0.4	24.7	0.7	22.2	1.2	0.940	0.008
217.5	71.9	0.121	0.015	25.7	0.4	27.7	0.4	25.6	0.5	24.6	0.8	21.9	1.4	0.940	0.007
220.0	72.6	0.132	0.015	25.8	0.3	27.9	0.2	25.7	0.4	24.7	0.7	22.2	1.2	0.934	0.008
222.5	73.3	0.120	0.015	25.6	0.4	27.6	0.5	25.6	0.5	24.5	0.8	21.8	1.3	0.940	0.008
225.0	74.0	0.098	0.015	25.9	0.2	27.9	0.2	25.8	0.4	24.8	0.7	22.1	1.2	0.951	0.008
227.5	74.7	0.117	0.025	25.8	0.3	27.8	0.2	25.6	0.5	24.5	0.9	21.8	1.4	0.942	0.013
230.0	75.5	0.101	0.019	25.8	0.3	27.9	0.2	25.7	0.4	24.7	0.7	22.2	1.2	0.949	0.009
232.5	76.2	0.106	0.013	25.7	0.4	27.7	0.4	25.6	0.5	24.6	0.8	21.9	1.4	0.947	0.007
235.0	76.9	0.129	0.013	25.8	0.4	27.7	0.4	25.7	0.5	24.6	0.8	21.8	1.4	0.936	0.006
237.5	77.6	0.096	0.017	25.8	0.4	27.7	0.4	25.7	0.5	24.6	0.8	21.8	1.4	0.952	0.008
240.0	78.3	0.136	0.018	25.9	0.1	27.8	0.2	25.7	0.5	24.6	0.9	21.8	1.5	0.932	0.009
242.5	79.2	0.127	0.017	25.9	0.2	27.9	0.2	25.8	0.4	24.8	0.7	22.1	1.2	0.937	0.008
245.0	80.2	0.096	0.013	25.9	0.2	27.8	0.2	25.8	0.4	24.8	0.7	22.1	1.1	0.952	0.007
247.5	81.1	0.101	0.013	25.5	1.2	27.8	0.3	25.5	1.0	24.6	1.0	22.1	1.2	0.949	0.006
250.0	82.1	0.094	0.005	25.9	0.1	27.9	0.2	25.8	0.4	24.8	0.7	22.2	1.2	0.953	0.003
252.5	83.0	0.087	0.015	25.9	0.2	27.9	0.2	25.8	0.4	24.8	0.7	22.1	1.2	0.956	0.008
255.0	84.0	0.097	0.011	25.8	0.4	27.7	0.4	25.7	0.5	24.6	0.8	21.9	1.4	0.952	0.006
257.5	84.9	0.077	0.015	25.8	0.4	27.7	0.4	25.6	0.5	24.6	0.8	21.8	1.3	0.962	0.008
260.0	85.9	0.082	0.013	25.7	1.0	27.7	0.9	25.3	2.2	24.1	2.8	21.5	3.1	0.959	0.006
262.5	86.8	0.126	0.014	25.8	0.2	27.9	0.2	25.8	0.4	24.8	0.7	22.3	1.1	0.937	0.007
265.0	87.8	0.088	0.012	25.9	0.1	27.9	0.2	25.8	0.4	24.9	0.7	22.3	1.1	0.956	0.006
267.5	88.7	0.096	0.009	25.3	1.1	27.4	1.1	24.6	2.6	23.2	3.4	20.5	3.9	0.952	0.005
270.0	89.7	0.102	0.012	25.8	0.2	27.9	0.2	25.8	0.4	24.8	0.7	22.3	1.1	0.949	0.006
272.5	90.6	0.121	0.017	25.9	0.1	27.9	0.2	25.8	0.4	24.9	0.7	22.3	1.1	0.940	0.008
275.0	91.6	0.146	0.022	25.8	0.4	27.8	0.5	25.8	0.6	24.8	0.9	22.3	1.5	0.927	0.011
277.5	92.5	0.084	0.008	25.6	0.9	27.6	0.8	25.1	2.1	24.0	2.7	21.4	3.0	0.958	0.004
280.0	93.5	0.089	0.006	25.6	1.0	27.6	0.9	25.2	2.2	24.0	2.8	21.3	3.2	0.956	0.003
282.5	94.4	0.075	0.014	25.7	0.6	27.6	0.7	25.6	0.8	24.5	1.1	21.7	1.8	0.962	0.007
285.0	95.4	0.075	0.008	25.9	0.1	27.9	0.2	25.8	0.4	24.8	0.7	22.2	1.2	0.963	0.004
287.5	96.3	0.079	0.010	24.5	1.6	26.3	1.5	22.2	3.9	20.5	4.4	17.7	4.4	0.961	0.005
290.0	97.3	0.077	0.010	25.6	1.0	27.6	0.9	25.2	2.2	24.1	2.9	21.3	3.2	0.962	0.005
292.5	98.2	0.082	0.009	25.1	1.6	27.0	1.4	23.7	3.3	22.0	4.5	19.2	5.1	0.959	0.004
295.0	99.2	0.097	0.010	25.2	1.2	27.0	1.3	23.8	3.5	22.3	4.1	19.6	4.3	0.952	0.005
297.5	100.1	0.094	0.008	25.0	1.3	26.9	1.4	23.2	3.6	21.6	4.3	18.9	4.6	0.953	0.004
300.0	101.1	0.123	0.013	25.3	1.8	27.3	1.2	24.6	3.0	23.5	3.4	20.6	3.5	0.938	0.007
302.5	102.0	0.109	0.010	25.3	1.2	27.4	1.1	24.4	3.4	23.3	3.9	20.9	3.9	0.945	0.005
305.0	103.0	0.165	0.022	25.9	0.3	27.9	0.2	25.9	0.5	25.0	0.8	22.5	1.2	0.918	0.011
307.5	103.9	0.143	0.015	24.8	1.6	26.6	1.6	22.7	4.2	21.3	4.6	18.9	4.4	0.929	0.007
312.5	105.8	0.161	0.013	25.6	1.0	27.6	0.9	25.2	2.2	24.0	2.9	21.4	3.2	0.920	0.007
315.0	106.8	0.130	0.009	25.1	1.5	27.1	1.3	23.5	4.0	22.2	4.5	19.7	4.3	0.935	0.005
317.5	107.7	0.138	0.011	24.5	1.8	26.5	1.3	21.9	4.1	19.9	4.6	17.0	4.4	0.931	0.005
320.0	108.6	0.116	0.006	24.2	2.0	26.1	1.4	20.6	4.1	18.5	4.5	16.0	4.0	0.942	0.003
322.5	109.6	0.115	0.009	23.8	1.8	26.0	1.5	20.6	4.1	18.7	4.7	16.5	4.6	0.943	0.004
325.0	110.5	0.102	0.010	25.2	1.5	27.2	1.3	24.1	3.2	22.5	4.2	19.7	4.6	0.949	0.005
327.5	111.5	0.118	0.010	24.2	1.9	26.1	1.5	20.9	4.0	18.9	4.8	16.7	4.8	0.941	0.005
330.0	112.4	0.133	0.009	23.6	1.6	25.8	1.4	20.1	3.6	18.0	4.1	15.6	4.1	0.934	0.005
332.5	113.4	0.152	0.010	24.9	1.8	27.1	1.5	23.6	4.1	22.4	4.7	20.1	4.5	0.924	0.005
335.0	114.3	0.114	0.008	24.5	1.7	26.5	1.6	22.7	3.6	20.9	4.4	17.8	4.7	0.943	0.004

depth (cm)	Est Tc0-50m (°C)	Est Tw0-50m (°C)	Est. annual T75m (°C)	Est. annual T100m (°C)	Est. annual T150m (°C)	#best Analogs
167.5	25.6	27.6	25.5	24.5	21.8	10
170.0	25.6	27.7	25.0	23.8	21.3	10
172.5	25.7	27.7	25.6	24.6	21.9	10
175.0	25.2	27.3	23.9	22.7	20.2	10
177.5	25.6	27.6	24.9	23.9	21.4	10
180.0	25.6	27.7	24.9	23.9	21.4	10
182.5	25.4	27.5	24.7	23.6	21.0	10
185.0	24.6	26.7	24.1	23.1	20.4	10
187.5	23.1	26.0	22.7	21.7	19.6	10
190.0	24.2	26.6	22.5	21.2	18.8	10
192.5	23.8	26.0	21.3	19.7	17.0	10
195.0	24.6	27.0	23.5	22.5	20.1	10
197.5	25.8	27.9	25.7	24.7	22.2	10
200.0	25.6	27.7	25.0	24.1	21.7	10
202.5	25.8	27.9	25.8	24.8	22.2	10
205.0	25.8	27.9	25.7	24.7	22.2	10
207.5	25.7	27.7	25.6	24.6	21.9	10
210.0	25.8	27.9	25.7	24.7	22.2	10
212.5	25.8	27.9	25.9	25.0	22.6	10
215.0	25.8	27.9	25.7	24.7	22.2	10
217.5	25.7	27.7	25.6	24.6	21.9	10
220.0	25.8	27.9	25.7	24.7	22.2	10
222.5	25.6	27.6	25.6	24.5	21.8	10
225.0	25.9	27.9	25.8	24.8	22.1	10
227.5	25.8	27.8	25.6	24.5	21.8	10
230.0	25.8	27.9	25.7	24.7	22.2	10
232.5	25.7	27.7	25.6	24.6	21.9	10
235.0	25.8	27.7	25.7	24.6	21.8	10
237.5	25.8	27.7	25.7	24.6	21.8	10
240.0	25.9	27.8	25.7	24.6	21.8	10
242.5	25.9	27.9	25.8	24.8	22.1	10
245.0	25.9	27.8	25.8	24.8	22.1	10
247.5	25.5	27.8	25.5	24.6	22.1	10
250.0	25.9	27.9	25.8	24.8	22.2	10
252.5	25.9	27.9	25.8	24.8	22.1	10
255.0	25.8	27.7	25.7	24.6	21.9	10
257.5	25.8	27.7	25.6	24.6	21.8	10
260.0	25.7	27.7	25.3	24.1	21.5	10
262.5	25.8	27.9	25.8	24.8	22.3	10
265.0	25.9	27.9	25.8	24.9	22.3	10
267.5	25.3	27.4	24.6	23.2	20.5	10
270.0	25.8	27.9	25.8	24.8	22.3	10
272.5	25.9	27.9	25.8	24.9	22.3	10
275.0	25.8	27.8	25.8	24.8	22.3	10
277.5	25.6	27.6	25.1	24.0	21.4	10
280.0	25.6	27.6	25.2	24.0	21.3	10
282.5	25.7	27.6	25.6	24.5	21.7	10
285.0	25.9	27.9	25.8	24.8	22.2	10
287.5	24.5	26.3	22.2	20.5	17.7	10
290.0	25.6	27.6	25.2	24.1	21.4	10
292.5	25.1	27.0	23.7	22.0	19.2	10
295.0	25.2	27.0	23.8	22.3	19.6	10
297.5	25.0	26.9	23.2	21.6	18.9	10
300.0	25.3	27.3	24.7	23.5	20.6	10
302.5	25.3	27.4	24.4	23.4	20.9	10
305.0	25.9	27.9	25.9	25.0	22.5	10
307.5	24.8	26.6	22.7	21.3	18.9	10
312.5	25.6	27.6	25.2	24.0	21.4	10
315.0	25.1	27.1	23.5	22.2	19.7	10
317.5	24.5	26.5	21.8	19.9	17.0	10
320.0	24.2	26.1	20.6	18.5	16.0	10
322.5	23.8	26.0	20.6	18.7	16.5	10
325.0	25.2	27.2	24.1	22.5	19.8	10
327.5	24.2	26.1	20.9	19.0	16.7	10
330.0	23.6	25.8	20.1	18.0	15.6	10
332.5	24.9	27.1	23.6	22.4	20.1	10
335.0	24.5	26.5	22.7	20.8	17.8	10

depth (cm)	age (kyrs)	DSML	STDEV	Mean analog Tc0-50m (°C)	STDEV	Mean analog Tw0-50m (°C)	STDEV	Mean annual analog T75m (°C)	STDEV	Mean annual analog T100m (°C)	STDEV	Mean annual analog T150m (°C)	STDEV	SIM	STEV
337.5	115.3	0.092	0.005	25.9	0.6	27.8	0.7	25.7	1.1	24.6	1.7	21.8	2.7	0.954	0.003
340.0	116.2	0.095	0.007	25.0	1.6	26.9	1.6	23.3	4.0	22.1	4.4	19.7	4.2	0.953	0.003
342.5	117.2	0.105	0.008	25.3	1.6	27.3	1.5	24.3	3.5	23.1	3.9	20.5	3.9	0.948	0.004
345.0	118.1	0.096	0.013	25.9	0.2	27.8	0.2	25.8	0.4	24.8	0.7	22.1	1.1	0.952	0.007
347.5	119.1	0.134	0.008	24.4	1.7	26.5	1.5	21.6	4.3	20.2	4.5	17.8	4.1	0.933	0.004
350.0	120.0	0.120	0.010	25.0	1.6	26.9	1.6	23.3	4.0	22.1	4.4	19.7	4.2	0.940	0.005
352.5	121.0	0.148	0.012	25.1	1.6	27.3	1.1	24.0	3.6	23.0	3.7	20.5	3.3	0.926	0.006
355.0	121.9	0.122	0.010	24.9	1.6	27.0	1.5	23.3	4.0	22.0	4.3	19.4	4.1	0.939	0.005
357.5	122.9	0.135	0.015	24.7	1.3	26.6	1.3	21.6	4.4	20.3	4.6	18.0	4.2	0.933	0.008
360.0	123.8	0.129	0.010	23.9	1.9	26.2	1.5	20.7	4.3	19.2	4.5	17.0	4.0	0.935	0.005
362.5	124.4	0.111	0.015	24.5	1.7	26.5	1.5	22.1	3.9	20.4	4.3	17.5	4.3	0.944	0.008
365.0	124.9	0.095	0.010	25.4	1.0	27.3	1.2	24.2	3.2	23.0	3.7	20.5	3.6	0.952	0.005
367.5	125.5	0.104	0.013	25.2	1.2	27.1	1.2	23.4	3.9	22.1	4.2	19.6	4.0	0.948	0.007
370.0	126.1	0.120	0.008	24.4	1.9	26.5	1.8	22.1	4.4	20.9	4.8	18.6	4.6	0.940	0.004
372.5	126.6	0.114	0.009	24.3	1.7	26.5	1.5	21.7	4.2	20.2	4.8	18.0	4.4	0.943	0.005
375.0	127.2	0.089	0.007	23.8	1.5	25.6	1.3	22.1	2.7	20.4	3.2	16.8	3.1	0.956	0.003
377.5	127.8	0.101	0.008	24.0	1.8	26.1	1.0	21.2	3.4	18.9	3.8	15.5	3.3	0.950	0.004
380.0	128.3	0.101	0.007	23.5	1.8	25.9	1.4	19.3	3.8	17.5	4.3	15.8	4.0	0.950	0.004
382.5	128.9	0.089	0.007	25.0	1.7	26.9	1.6	23.9	3.2	22.5	3.7	20.0	3.5	0.955	0.004
385.0	129.5	0.088	0.008	25.3	1.2	27.1	1.1	23.6	3.5	22.1	4.1	19.4	4.0	0.956	0.004
387.5	130.0	0.135	0.014	24.1	1.8	26.3	1.6	21.5	4.1	20.0	4.8	17.8	4.3	0.933	0.007
390.0	130.6	0.096	0.006	24.8	1.6	26.9	1.4	22.9	3.9	21.4	4.4	18.8	4.2	0.952	0.003
392.5	131.2	0.135	0.007	24.9	1.5	26.9	1.2	24.0	2.6	22.6	3.1	19.7	3.1	0.933	0.003
395.0	131.7	0.145	0.007	24.7	1.6	26.7	1.3	22.7	3.8	21.2	4.3	18.5	4.0	0.928	0.004
400.0	132.8	0.143	0.018	22.8	1.1	25.0	0.9	20.3	2.5	18.7	3.0	15.7	2.3	0.928	0.009
405.0	134.0	0.163	0.010	23.4	1.7	25.6	1.4	21.0	3.3	19.5	3.7	16.7	3.3	0.919	0.005
410.0	135.1	0.159	0.012	24.7	2.0	27.0	1.5	23.7	3.8	22.4	4.1	19.4	4.0	0.920	0.006
415.0	136.1	0.143	0.014	25.7	0.4	27.7	0.4	25.6	0.5	24.6	0.8	21.9	1.4	0.928	0.007
420.0	137.2	0.157	0.010	25.1	1.5	27.2	1.5	25.0	1.9	24.0	2.1	21.2	2.9	0.922	0.005
425.0	138.2	0.165	0.006	25.2	0.9	27.5	0.9	24.7	2.2	23.6	2.8	21.3	2.7	0.917	0.003
430.0	139.3	0.137	0.009	25.4	1.2	27.7	0.7	24.9	2.6	23.7	3.1	21.3	2.9	0.932	0.004
435.0	140.3	0.150	0.007	24.6	1.9	26.9	1.4	23.7	3.6	22.5	4.0	20.0	3.8	0.925	0.003
440.0	141.3	0.170	0.012	25.1	1.6	27.4	1.3	24.6	3.0	23.4	3.5	20.8	3.7	0.915	0.006
450.0	145.3	0.130	0.010	24.7	1.3	26.7	1.3	23.9	2.2	22.8	2.7	20.0	2.7	0.935	0.005

depth (cm)	Est Tc0-50m (°C)	Est Tw0-50m (°C)	Est. annual T75m (°C)	Est. annual T100m (°C)	Est. annual T150m (°C)	#best Analogs
337.5	25.9	27.8	25.7	24.6	21.8	10
340.0	25.0	26.9	23.3	22.1	19.7	10
342.5	25.3	27.3	24.3	23.1	20.5	10
345.0	25.9	27.8	25.8	24.8	22.1	10
347.5	24.4	26.5	21.6	20.2	17.8	10
350.0	25.0	26.9	23.3	22.1	19.7	10
352.5	25.2	27.3	24.0	23.0	20.5	10
355.0	24.9	27.0	23.3	22.0	19.4	10
357.5	24.7	26.6	21.6	20.3	18.0	10
360.0	23.9	26.2	20.7	19.2	17.0	10
362.5	24.5	26.5	22.1	20.4	17.5	10
365.0	25.4	27.3	24.2	23.0	20.5	10
367.5	25.2	27.1	23.4	22.1	19.6	10
370.0	24.4	26.5	22.1	20.9	18.6	10
372.5	24.3	26.5	21.7	20.2	18.0	10
375.0	23.8	25.6	22.1	20.4	16.8	10
377.5	24.0	26.1	21.2	18.9	15.5	10
380.0	23.5	25.9	19.3	17.5	15.8	10
382.5	25.0	26.9	23.9	22.5	20.0	10
385.0	25.3	27.1	23.6	22.1	19.4	10
387.5	24.1	26.3	21.5	20.0	17.8	10
390.0	24.8	26.9	22.9	21.4	18.8	10
392.5	24.9	26.9	24.0	22.6	19.7	10
395.0	24.7	26.7	22.7	21.2	18.5	10
400.0	22.8	25.0	20.3	18.7	15.7	10
405.0	23.4	25.6	21.0	19.5	16.7	10
410.0	24.7	27.0	23.7	22.4	19.4	10
415.0	25.7	27.7	25.6	24.6	21.9	10
420.0	25.1	27.2	25.0	24.0	21.2	10
425.0	25.2	27.5	24.7	23.6	21.3	10
430.0	25.4	27.7	24.9	23.7	21.3	10
435.0	24.6	26.9	23.7	22.5	20.0	10
440.0	25.1	27.4	24.6	23.4	20.8	10
450.0	24.7	26.7	23.9	22.8	20.0	10

Core ID	Lat.(N)	Long.(W)	water depth (m)	AEQ	BUL	CAL	CAV	CON	CRA	DEH	DIG	DUT	FAL	GLU	HIR	HUM	INF	MEN	NIT	OBL
M35002-1	12.032	-61.177	1506	5.2	0.4	1.2	0.0	0.5	0.3	0.1	0.0	7.3	0.1	8.8	0.0	0.0	0.1	2.1	0.4	0.5
M35003-6	12.085	-61.245	1299	2.7	0.3	1.0	0.0	0.8	0.0	0.1	0.0	7.5	0.0	7.7	0.0	0.0	0.3	1.5	1.0	0.3
M35004-1	14.410	-61.662	2885	3.6	0.3	1.9	0.0	0.7	0.3	0.0	0.2	3.4	0.0	11.1	0.0	0.0	0.0	0.5	0.7	0.2
M35005-1	15.453	-62.232	2289	3.9	0.3	2.5	0.0	0.7	0.2	0.2	0.2	7.8	0.0	9.5	0.0	0.0	0.0	1.1	1.4	0.7
M35006-6	16.422	-62.453	888	5.4	0.1	0.0	0.0	0.6	0.2	0.0	0.0	5.8	0.0	11.4	0.0	0.0	0.0	1.2	1.0	0.6
M35008-1	18.032	-64.163	2820	5.1	0.3	1.3	0.0	0.9	0.0	0.1	0.8	6.2	0.3	14.0	0.0	0.0	0.0	1.3	1.1	0.6
M35010-2	18.933	-64.090	2696	5.1	0.5	0.1	0.0	2.8	0.1	0.1	0.0	5.3	0.0	7.6	0.0	0.0	0.0	1.0	0.2	0.3
M35012-6	18.305	-63.627	1121	4.0	0.0	1.5	0.0	1.1	0.1	0.3	0.0	7.6	0.0	12.9	0.0	0.0	0.1	1.5	0.4	0.5
M35013-3	18.315	-63.450	899	3.1	0.0	1.0	0.0	0.2	0.0	0.1	0.0	2.6	0.0	8.1	2.0	0.0	0.0	0.6	0.1	0.1
M35014-1	17.842	-63.737	1604	4.1	0.1	2.3	0.0	1.1	0.0	0.0	0.0	7.0	0.2	12.5	0.0	0.0	0.0	1.9	0.6	0.0
M35015-1	17.993	-63.452	1230	4.1	0.5	2.0	0.0	0.5	0.2	0.0	0.2	6.4	0.0	8.7	0.0	0.0	0.0	2.2	0.3	0.1
M35018-1	17.575	-65.370	1728	6.6	0.2	2.6	0.0	0.5	0.0	0.1	0.3	5.5	0.0	10.5	0.0	0.0	0.0	2.2	0.2	0.3
M35019-1	17.672	-65.435	1815	8.0	0.7	0.0	0.0	0.8	0.2	0.2	0.0	6.1	0.0	9.1	0.0	0.0	0.0	2.9	2.1	0.6
M35020-2	17.930	-65.670	2005	4.0	0.0	1.4	0.0	0.7	0.0	0.2	0.0	7.3	0.0	11.2	0.0	0.0	0.0	2.7	1.8	0.3
M35023-3	17.603	-65.682	1192	6.5	0.7	0.0	0.0	0.6	0.0	0.1	0.0	7.0	0.3	7.4	0.0	0.0	0.5	3.3	0.2	0.7
M35024-6	17.043	-66.002	4710	4.3	1.1	1.2	0.0	0.3	0.0	0.6	0.0	4.5	0.0	13.1	0.0	0.0	0.0	2.2	0.3	0.1
M35026-2	17.508	-67.043	3815	6.3	0.4	2.4	0.0	0.6	0.0	0.0	0.0	4.3	0.0	19.2	0.0	0.0	0.0	1.3	1.1	0.2
M35030-1	16.755	-78.610	1298	5.2	0.0	2.2	0.0	0.4	0.5	0.3	0.2	3.3	0.4	8.5	0.0	0.0	0.0	5.6	0.2	0.0
M35033-1	16.913	-79.018	1124	3.0	0.6	0.0	0.0	0.3	0.2	0.1	0.0	3.1	0.0	7.6	0.0	0.0	0.0	7.4	0.0	0.0
M35035-1	16.893	-79.132	1252	3.4	0.5	0.0	0.0	0.4	1.1	0.2	0.0	3.6	0.0	11.4	0.0	0.0	0.0	3.4	1.1	0.3
M35039-1	17.927	-79.145	1142	9.3	0.0	1.0	0.0	0.6	0.1	0.3	0.0	4.5	0.0	6.0	0.0	0.0	0.1	4.2	0.1	0.0

Core ID	PAL	PAR+	QUL	QUR	QUS	RUR	RUW	RUS	TRL	SAC	SCI	TEN	TRL	TRR	TRUS	TUMI	UNIV	UVU	MENT	PDI
M35002-1	0.0	0.4	0.0	0.0	0.0	18.9	34.7	1.3	9.1	3.0	2.2	0.3	0.0	0.4	0.4	0.3	2.0	0.0	2.5	0.4
M35003-6	0.0	1.7	0.0	0.0	1.0	19.3	32.6	0.5	11.0	6.1	1.8	0.0	0.0	0.6	0.6	0.1	1.5	0.0	1.6	1.0
M35004-1	0.0	0.6	0.0	0.0	0.0	20.1	39.0	2.6	7.6	3.5	1.4	0.4	0.0	0.5	0.5	0.1	1.0	0.0	0.6	0.5
M35005-1	0.0	0.4	0.0	0.0	0.0	12.6	33.1	2.2	12.2	5.4	0.8	0.0	0.1	0.3	0.4	1.4	2.8	0.0	2.5	0.4
M35006-6	0.0	0.8	0.0	0.0	0.0	11.0	39.5	3.9	7.7	4.5	0.0	1.7	0.2	0.5	0.7	0.9	2.0	0.0	2.1	0.4
M35008-1	0.0	0.4	0.0	0.0	0.0	11.3	32.4	3.8	10.2	4.1	0.5	0.0	0.1	0.3	0.5	1.7	2.5	0.0	3.0	0.4
M35010-2	0.0	0.4	0.0	0.0	0.0	14.5	36.0	4.1	6.4	6.9	0.0	1.0	0.8	2.5	3.3	1.3	2.4	0.0	2.2	0.2
M35012-6	0.0	0.7	0.0	0.0	0.0	15.0	37.0	1.9	7.3	4.3	0.0	0.5	0.0	0.8	0.8	0.3	2.0	0.0	1.8	0.2
M35013-3	0.0	0.2	0.0	0.0	0.0	13.5	54.6	5.1	2.8	3.2	0.0	0.0	0.0	0.3	0.3	0.2	0.9	0.0	0.8	0.2
M35014-1	0.0	0.2	0.0	0.0	0.0	14.1	28.8	3.9	8.1	5.4	0.8	0.4	0.0	1.1	1.1	1.3	5.4	0.0	3.2	0.0
M35015-1	0.0	0.1	0.0	0.0	0.0	17.7	37.8	3.0	7.3	3.8	0.2	0.7	0.0	0.6	0.6	0.0	2.5	0.0	2.2	0.1
M35018-1	0.0	0.8	0.0	0.0	0.0	10.4	37.5	3.2	5.6	6.3	0.6	0.0	0.0	0.1	0.1	0.8	5.0	0.0	3.0	0.0
M35019-1	0.0	1.6	0.0	0.0	0.0	8.7	36.9	2.1	6.2	5.2	2.1	0.0	0.0	1.2	1.3	0.9	3.4	0.0	3.7	0.2
M35020-2	0.0	1.0	0.0	0.0	0.0	16.6	31.1	5.0	8.4	3.7	0.0	0.0	0.3	0.9	1.2	0.3	3.0	0.0	3.1	0.3
M35023-3	0.0	0.9	0.0	0.0	0.0	12.0	37.9	2.0	5.6	5.2	0.3	0.7	0.2	0.8	1.0	2.2	2.6	0.0	5.6	0.0
M35024-6	0.0	1.7	0.0	0.0	0.0	4.9	43.1	2.6	10.2	3.0	1.1	1.6	0.1	0.1	0.3	1.8	0.9	0.0	4.0	0.6
M35026-2	0.0	0.7	0.0	0.0	0.0	11.7	28.4	5.7	7.9	4.3	0.4	0.4	0.0	0.6	0.6	1.2	2.7	0.0	2.5	0.0
M35030-1	0.7	0.2	0.0	0.0	0.0	8.3	44.2	1.8	9.1	4.1	0.4	0.4	0.0	0.0	0.0	1.7	1.9	0.0	7.3	0.2
M35033-1	0.0	1.3	0.0	0.0	0.0	10.2	47.0	5.0	10.1	1.6	0.1	0.6	0.0	0.8	0.8	0.2	0.9	0.0	6.6	0.0
M35035-1	0.0	0.0	0.0	0.0	0.0	7.4	41.7	3.8	8.2	5.5	0.8	0.8	0.0	0.8	0.8	3.7	1.9	0.0	7.1	0.0
M35039-1	0.0	0.1	0.0	0.0	0.0	10.0	37.0	0.0	9.5	6.5	0.0	1.0	0.1	1.0	1.1	5.1	2.2	0.0	9.3	0.0

Core ID	PAR	Σ
M35002-1	0.0	1097
M35003-6	0.6	706
M35004-1	0.1	922
M35005-1	0.0	1107
M35006-6	0.4	685
M35008-1	0.0	683
M35010-2	0.1	526
M35012-6	0.5	621
M35013-3	0.0	523
M35014-1	0.2	526
M35015-1	0.0	653
M35018-1	0.8	517
M35019-1	1.4	629
M35020-2	0.7	655
M35023-3	0.9	555
M35024-6	1.1	672
M35026-2	0.7	544
M35030-1	0.0	446
M35033-1	1.3	339
M35035-1	0.0	541
M35039-1	0.1	459

GEOMAR REPORTS

1 GEOMAR FORSCHUNGSZENTRUM FÜR MARINE GEOWISSENSCHFTEN DER CHRISTIAN-ALBRECHTS-UNIVERSITÄT ZU KIEL. BERICHT FÜR DIE JAHRE 1987 UND 1988. 1989. 71 + 6 pp. In German

2 GEOMAR FORSCHUNGSZENTRUM FÜR MARINE GEOWISSENSCHAFTEN DER CHRISTIAN-ALBRECHTS-UNIVERSITÄT ZU KIEL. JAHRESBERICHT/ANNUAL REPORT 1989. 1990. 96 pp. In German and English

3 GEOMAR FORSCHUNGSZENTRUM FÜR MARINE GEOWISSENSCHAFTEN DER CHRISTIAN-ALBRECHTS-UNIVERSITÄT ZU KIEL. JAHRESBERICHT/ANNUAL REPORT 1990. 1991. 212 pp. In German and English

4 ROBERT F. SPIELHAGEN
DIE EISDRIFT IN DER FRAMSTRASSE WÄHREND DER LETZTEN 200.000 JAHRE. 1991. 133 pp.
In German with English summary

5 THOMAS C. W. WOLF
PALÄO-OZEANOGRAPHISCH-KLIMATISCHE ENTWICKLUNG DES NÖRDLICHEN NORDATLANTIKS SEIT DEM SPÄTEN NEOGEN (ODP LEGS 105 UND 104, DSDP LEG 81). 1991. 92 pp. In German with English summary

6 SEISMIC STUDIES OF LATERALLY HETEROGENOUS STRUCTURES – INTERPRETATION AND MODELLING OF SEISMIC DATA. Ed. by ERNST R. FLUEH
Commission on Controlled Source Seismology (CCSS), Proceedings of the 8th Workshop Meeting, held at Kiel – Fellhorst (Germany), August 27-31, 1990. 1991. 359 pp. In English

7 JENS MATTHIESSEN
DINOFLAGELLATEN-ZYSTEN IM SPÄQUARTÄR DES EUROPÄISCHEN NORDMEERES: PALÖKOLOGIE UND PALÄO-OZEANOGRAPHIE. 1991. 104 pp. In German with English summary. Out of print

8 DIRK NÜRNGERG
HAUPT- UND SPURENELEMENTE IN FORAMINIFERENGEHÄUSEN – HINWEISE AUF KLIMATISCHE UND OZEANOGRAPHISCHE ÄNDERUNGEN IM NÖRDLICHEN NORDATLANTIK WÄHREND DES SPÄTQUARTÄRS.
1991. 117 pp. In German with English summary. Out of print

9 KLAS S. LACKSCHEWITZ
SEDIMENTATIONSPROZESSE AM AKTIVEN MITTELOZEANISCHEN KOLBEINSEY RÜCKEN (NÖRDLICH VON ISLAND). 1991. 133 pp. In German with English summary. Out of print

10 UWE PAGELS
SEDIMENTOLOGISCHE UNTERSUCHUNGEN UND BESTIMMUNG DER KARBONATLÖSUNG IN SPÄTQUARTÄREN SEDIMENTEN DES ÖSTLICHEN ARKTISCHEN OZEANS. 1991. 106 pp.
In German with English summary

11 FS POSEIDON. EXPEDITION 175 (9.10.-1.11.1990)
175/1:OSTGRÖNLÄNDISCHER KONTINENTALRAND (65°N)
175/2: SEDIMENTATION AM KOLBEINSEYRÜCKEN (NÖRDLICH VON ISLAND).
Hrsg. von J. MIENERT und H.-J. WALLRABE-ADAMS. 1992. 56 pp. + app. In German with some English chapters

12 GEOMAR FORSCHUNGSZENTRUM FÜR MARINE GEOWISSENSCHAFTEN DER CHRISTIAN-ALBRECHTS-UNIVERSITÄT ZU KIEL. JAHRESBERICHT/ANNUAL REPORT 1991. 1992. 152 pp. In German and English.
Out of print

13 SABINE E. I. KÖHLER
SPÄTQUARTÄRE PALÄO-OZEANOGRAPHISCHE ENTWICKLUNG DES NORDPOLARMEERES UND EUROPÄISCHEN NORDMEERES ANHAND VON SAUERSTOFF- UND KOHLENSTOFF-ISOTOPENVERHÄLTNISSEN DER PLANKTISCHEN FORAMINIFERE *Neogloboquadrina pachyderma* (sin.).
1992. 104 pp. In German with English summary

14 FS SONNE. FAHRTBERICHT SO78 PERUVENT: BALBOA, PANAMA - BALBOA, PANAMA, 28.2.1992-16.4.1992
Hrsg. von ERWIN SUESS. 1992. 120 pp. In German with some English chapters. Out of print

15 FOURTH INTERNATIONAL CONFERENCE ON PALEOCEANOGRAPHY (ICP IV): SHORT- AND LONG-TERM GLOBAL CHANGE: RECORDS AND MODELLING. 21-25 SEPTEMBER 1992, KIEL/GERMANY.
PROGRAM & ABSTRACTS. 1992. 351 pp. In English

16 MICHAELA KUBISCH
DIE EISDRIFT IM ARKTISCHEN OZEAN WÄHREND DER LETZTEN 250.000 JAHRE. 1992. 100 pp.
In German with English summary

17 PERSISCHER GOLF: UMWELTGEFÄHRDUNG, SCHADENSERKENNUNG, SCHADENSBEWERTUNG AM BEISPIEL DES MEERRESBODENS; ERKENNEN EINER ÖKOSYSTEMVERÄNDERUNG NACH ÖLEINTRÄGEN. Schlußbericht zu den beiden BMFT-Forschungsvorhaben 03F0055 A + B. 1993. 108 pp. In German with English summary

18 TEKTONISCHE ENTWÄSSERUNG AN KONVERGENTEN PLATTENRÄNDERN / DEWATERING AT CONTINENTAL MARGINS. Hrsg. von/ed. by ERWIN SUESS. 1993. 196 + 32 + 68 + 16 + 22 + 38 + 4 + 19 pp.
Some chapters in English, some in German

19 THOMAS DICKMANN
DAS KONZEPT DER POLARISATIONSMETHODE UND SEINE ANWENDUNGEN AUF DAS SEIMISCHE VEKTORWELLENFELD IM WEITWINKELBEREICH. 1993. 121 pp. In German with English summary

20 GEOMAR FORSCHUNGSZENTRUM FÜR MARINE GEOWISSENSCHAFTEN DER CHRISTIAN-ALBRECHTS-UNIVERSITÄT ZU KIEL. JAHRESBERICHT/ANNUAL REPORT 1992. 1993. 139 pp. In German and English

21 KAI UWE SCHMIDT
PALYNOMORPHE IM NEOGENEN NORDATLANTIK - HINWEISE ZUR PALÄO-OZEANOGRAPHIE UND PALÄOKLIMATOLOGIE. 1993. 104 + 7 + 41 pp. In German with English summary

22 UWE JÜRGEN GRÜTZMACHER
DIE VERÄNDERUNGEN DER PALÄOGEOGRAPHISCHEN VERBREITUNG VON *Bolboforma* - EIN BEITRAG ZUR REKONSTRUKTION UND DEFINITION VON WASSERMASSEN IM TERTÄR. 1993. 104 pp.
In German with English summary

23 RV PROFESSOR LOGACHEV. Research Cruise 09 (August 30 - September 17, 1993): SEDIMENT DISTRIBUTION ON THE REYKJANES RIDGE NEAR 59°N. Ed. by H.-J. WALLRABE-ADAMS & K.S. LACKSCHEWITZ. 1993. 66 + 30 pp.
In English

24 ANDREAS DETTMER
DIATOMEEN-TAPHOZÖNOSEN ALS ANZEIGER PALÄO-OZEANOGRAPHISCHER ENTWICKLUNGEN IM PLIOZÄNEN UND QUARTÄREN NORDATLANTIK. 1993. 113 + 10 + 25 pp. In German with English summary

25 GEOMAR FORSCHUNGSZENTRUM FÜR MARINE GEOWISSENSCHAFTEN DER CHRISTIAN-ALBRECHTS-UNIVERSITÄT ZU KIEL. JAHRESBERICHT/ANNUAL REPORT 1993. 1994. 69 pp. In German and English

26 JÖRG BIALAS
SEISMISCHE MESSUNGEN UND WEITERE GEOPHYSIKALISCHE UNTERSUCHUNGEN AM SÜD-SHETLAND TRENCH UND IN DER BRANSFIELD STRASSE - ANTARKTISCHE HALBINSEL. 1994. 113 pp.
In German with English summary

27 JANET MARGARET SUMNER
THE TRANSPORT AND DEPOSITIONAL MECHANISM OF HIGH GRADE MIXED-MAGMA IGNIMBRITE TL, GRAN CANARIA: THE MORPHOLOGY OF A LAVA-LIKE FLOW. 1994. 224 pp. In English with German summary. Out of print

28 GEOMAR LITHOTHEK. Ed. by JÜRGEN MIENERT. 1994. 12 pp + app. In English. Out of print

29 FS SONNE. FAHRTBERICHT SO 97 KODIAK-VENT: KODIAK - DUTCH HARBOR - TOKYO - SINGAPUR, 27.7.-19.9.1994. Hrsg. von ERWIN SUESS. 1994. Some chapters in English, some in German. Out of print

30 CRUISE REPORTS:
RV LIVONIA CRUISE 92, KIEL-KIEL, 21.8.-17.9.1992: GLORIA STUDIES OF THE EAST GREENLAND CONTINENTAL MARGIN BETWEEN 70°AND 80°N
RV POSEIDON PO200/10, LISBON-BREST-BREMERHAVEN, 7.-23.8.1993: EUROPEAN NORTH ATLANTIC MARGIN: SEDIMENT PATHWAYS, PROCESSES AND FLUXES
RV AKADEMIK ALEKSANDR KARPINSKIY, KIEL-TROMSÖ, 5.-25.7.1994: GAS HYDRATES ON THE NORTHERN EUROPEAN CONTINENTAL MARGIN
Edited by JÜRGEN MIENERT. 1994. 186 pp.
In English; report of RV AKADEMIK ALEKSANDR KARPINSKIY cruise in English and Russian

31 MARTIN WEINELT
BECKENENTWICKLUNG DES NÖRDLICHEN WIKING-GRABENS IM KÄNOZOIKUM - VERSENKUNGSGESCHICHTE, SEQUENZSTRATIGRAPHIE, SEDIMENTZUSAMMENSETZUNG. 1994. 85 pp.
In German with English summary

32 GEORG A. HEISS
CORAL REEFS IN THE RED SEA: GROWTH, PRODUCTION AND STABLE ISOTOPES. 1994. 141 pp.
In English with German summary

33 JENS A. HÖLEMANN
AKKUMULATION VON AUTOCHTHONEM UND ALLOCHTHONEM ORGANISCHEM MATERIAL IN DEN KÄNOZOISCHEN SEDIMENTEN DER NORWEGISCHEN SEE (ODP LEG 104). 1994. 78 pp.
In German with English summary

34 CHRISTIAN HASS
SEDIMENTOLOGISCHE UND MIKROPALÄONTOLOGISCHE UNTERSUCHUNGEN ZUR ENTWICKLUNG DES SKAGERRAKS (NE NORDSEE) IM SPÄTHOLOZÄN. 1994. 115 pp. In German with English summary

35 BRITTA JÜNGER
TIEFENWASSERERNEUERUNG IN DER GRÖNLANDSEE WÄHREND DER LETZTEN 340.000 JAHRE / DEEP WATER RENEWAL IN THE GREENLAND SEA DURING THE PAST 340,000 YEARS. 1994. 6 + 109 pp.
In German with English summary

36 JÖRG KUNERT
UNTERSUCHUJNGEN ZU MASSEN- UND FLUIDTRANSPORT ANHAND DER BEARBEITUNG REFLEXIONSSEISMISCHER DATEN AUS DER KODIAK-SUBDUKTIONSZONE, ALASKA. 1995. 129 pp.
In German with English summary

37 CHARLOTTE M. KRAWCZYK
DETACHMENT TECTONICS DURING CONTINENTAL RIFTING OFF THE WEST IBERIA MARGIN: SEISMIC REFLECTION AND DRILLING CONSTRAINTS.1995. 133 pp. In English with German summary

38 CHRISTINE CAROLINE NÜRNBERG
BARIUMFLUSS UND SEDIMENTATION IM SÜDLICHEN SÜDATLANTIK - HINWEISE AUF PRODUKTIVITÄTSÄNDERUNGEN IM QUARTÄR. 1995. 6 + 108 pp. In German with English summary

39 JÜRGEN FRÜHN
TEKTONIK UND ENTWÄSSERUNG DES AKTIVEN KONTINENTALRANDES SÜDÖSTLICH DER KENAI-HALBINSEL, ALASKA. 1995. 93 pp. In German with English summary

40 GEOMAR FORSCHUNGSZENTRUM FÜR MARINE GEOWISSENSCHAFTEN DER CHRISTIAN-ALBRECHTS-UNIVERSITÄT ZU KIEL. JAHRESBERICHT/ANNUAL REPORT 1994. 1995. 125 pp. In German and English.
Out of print

41 FS SONNE. FAHRTBERICHT / CRUISE REPORT SO 103 CONDOR 1 B: VALPARAISO-VALPARAISO, 2-21.7.1995. Hrsg. von ERNST R. FLUEH. 1995. 140 pp. Some chapters in German, some in English

42 RV PROFESSOR BOGOROV CRUISE 37: CRUISE REPORT "POSETIV": VLADIVOSTOK-VLADIVOSTOK, September 23 - October 22, 1994. Edited by CHRISTOPH GAEDICKE, BORIS BARANOV, and EVGENY LELIKOV. 1995. 49 + 33 pp. In English

43 CHRISTOPH GAEDICKE
DEFORMATION VON SEDIMENTEN IM NANKAI-AKKRETIONSKEIL, JAPAN. BILANZIERUNG TEKTONISCHER VORGÄNGE ANHAND VON SEISMISCHEN PROFILEN UND ERGEBNISSEN DER ODP-BOHRUNG 808. II + 89 pp. In German with English summary

44 MARTIN ANTONOW
SEDIMENTATIONSMUSTER UM DEN VESTERIS SEAMOUNT (ZENTRALE GRÖNLANDSEE) IN DEN LETZTEN 250.000 JAHREN. 1995. 121 pp. In German with English summary

45 INTERNATIONAL CONGRESS: CORING FOR GLOBAL CHANGE - ICGC '95. KIEL, 28 - 30 June, 1995.
Edited by JÜRGEN MIENERT and GEROLD WEFER. 1996. 83 pp. In English

46 JENS GRÜTZNER
ZUR PHYSIKALISCHEN ENTWICKLUNG VON DIAGENETISCHEN HORIZONTEN IN DEN SEDIMENTBECKEN DES ATLANTIKS. 1995. 96 pp. In German with English summary

47 INGO A. PECHER
SEISMIC STUDIES OF BOTTOM SIMULATING REFLECTORS AT THE CONVERGENT MARGINS OFFSHORE PERU AND COSTA RICA. 1996. 159 pp. In English with German summary

48 XIN SU
DEVELOPMENT OF LATE TERTIARY AND QUATERNARY COCCOLITH ASSEMBLAGES IN THE NORTHEAST ATLANTIC. 1996. 120 pp. +7 pl. In English with German summary

49 FS SONNE - FAHRTBERICHT/CRUISE REPORT SO108 ORWELL: SAN FRANCISCO - ASTORIA, 14.4. - 23.5.1996
Edited by ERNST R. FLUEH and MICHAEL A. FISHER. 1996. 252 pp. + app. In English with German summary

50 GEOMAR FORSCHUNGSZENTRUM FÜR MARINE GEOWISSENSCHAFTEN DER CHRISTIAN-ALBRECHTS-UNIVERSITÄT ZU KIEL. JAHRESBERICHT/ANNUAL REPORT 1995. 1996. 93 pp. In German and English

51 THOMAS FUNCK
STRUCTURE OF THE VOLCANIC APRON NORTH OF GRAN CANARIA DEDUCED FOM REFLECTION SEISMIC, BATHYMETRIC AND BOREHOLE DATA. 1996.VI, 144 pp. In English with German summary

52 PETER BRUNS
GEOCHEMISCHE UND SEDIMENTOLOGISCHE UNTERSUCHUNGEN ÜBER DAS SEDIMENTATIONSVERHALTEN IM BEREICH BIOSTRATIGRAPHISCHER DISKONTINUITÄTEN IM NEOGEN DES NORDATLANTIK, ODP LEG 104, SITES 642B UND 643A. 1996. V, 73 pp. In German with Englliish summary

53 CHRISTIANE C. WAGNER
COLD SEEPS AN KONVERGENTEN PLATTENRÄNDERN VOR OREGON UND PERU: BIOGEOCHEMISCHE BESTANDSAUFNAHME. 1996. 108, XXXVI pp. In German with English summary

54 FRAUKE KLINGELHÖFER
MODEL CALCULATIONS ON THE SPREADING OF SUBMARINE LAVA FLOWS. 1996. 98 pp.
In English with German summary

55 HANS-JÜRGEN HOFFMANN
OBJEKTORIENTIERTE ANALYSE UND MIGRATION DIFFRAKTIERTER WELLENFELDER UNTER VERWENDUNG DER STRAHLENMETHODE UND DER EDGE-WAVE-THEORIE. 1996. XXI, 153 pp. In German with English summary

56 DIRK KLÄSCHEN
STRAHLENSEISMISCHE MODELLIERUNG UNTER BERÜCKSICHTGUNG VON MEHRFACHDIFFRAKTIONEN MIT HILFE DER EDGE-WAVES: THEORIE UND ANWENDUNGSBEISPIELE 1996. X, 159 pp.
In German with English summary

57 NICOLE BIEBOW
DINOFLAGELLATENZYSTEN ALS INIKATOREN DER SPÄT- UND POSTGLAZIALEN ENTWICKLUNG DES AUFTRIEBSGESCHEHENS VOR PERU. 1996. IV, 100, 17, 14 (7 pl.) pp. In German with English summary

58 RV SONNE. CRUISE REPORT SO109: HYDROTRACE ASTORIA-VICTORIA-ASTORIA-VICTORIA. MAY 23 - JULY 8, 1996. Ed. by PETER HERZIG, ERWIN SUESS, and PETER LINKE. 1997. 249 pp. In English

59 RV SONNE. CRUISE REPORT SO110: SO - RO (SONNE - ROPOS). VICTORIA-KODIAK-VICTORIA. JULY 9 - AUGUST 19, 1996. Ed. by ERWIN SUESS and GERHARD BOHRMANN. 1997. 181 pp. In English

60 RV AKADEMIK M. A. LAVRENTYEV CRUISE 27. CRUISE REPORT: GREGORY. VLADIVOSTOK-PUSAN-OKHOTSK SEA-PUSAN-VLADIVOSTOK. SEPTEMBER 7 - OCTOBER 12, 1996.
Ed. by DIRK NÜRNBERG, BORIS BARANOV, and BORIS KARP.1997. 143 pp. In English

61 GEOMAR FORSCHUNGSZENTRUM FÜR MARINE GEOWISSENSCHAFTEN DER CHRISTIAN-ALBRECHTS-UNIVERSITÄT ZU KIEL. JAHRESBERICHT / ANNUAL REPORT 1996. 1997. 169 pp.
In German and English

62 FS SONNE. FAHRTBERICHT/CRUISE REPORT SO123: MAMUT (MAKRAN MURRAY TRAVERSE - GEOPHYSIK PLATTENTEKTONISCHER EXTREMFÄLLE). Maskat - Maskat, 07.09 - 03.10.1997. Ed. by ERNST R. FLUEH, NINA KUKOWSKI, and CHRISTIAN REICHERT. 1997. 292 pp. In English with German summary

63 RAINER ZAHN
NORTH ATLANTIC THERMOHALINE CIRCULATION DURING THE LAST GLACIAL PERIOD: EVIDENCE FOR COUPLING BETWEEN MELTWATER EVENTS AND CONVECTIVE INSTABILITY. 1997. 133 pp. In English

64 FS SONNE. FAHRTBERICHT/CRUISE REPORT SO112 HIRESBAT (HIGH RESOLUTION BATHYMETRY). Victoria, B.C., Canada - Apra Harbor, Guam. 17.09 - 08.10.1996. Hrsg. von WILHELM WEINREBE. 1997. 90 pp.
Some chapters in German, some in English

65 NIELS NØRGAARD-PEDERSEN
LATE QUATERNARY ARCTIC OCEAN SEDIMENT RECORDS: SURFACE OCEAN CONDITIONS AND PROVENANCE OF ICE-RAFTED DEBRIS. 1997. 115 pp. In English with German summary

66 THOMAS NÄHR
AUTHIGENER KLINOPTILOLITH IN MARINEN SEDIMENTEN - MINERALCHEMIE, GENESE UND MÖGLICHE ANWENDUNG ALS GEOTHERMOMETER. 1997. 119, 43 pp. In German with English summary

67 MATTIAS KREUTZ
STOFFTRANSPORT DURCH DIE BODENGRENZSCHICHT: REGIONALISIERUNG UND BILANZIERUNG FÜR DEN NORDATLANTIK UND DAS EUROPÄISCHE NORDMEER. 1998. IV, 166 pp. In German with English summary

68 AMIT GULATI
BENTHIC PRIMARY PRODUCTION IN TWO DIFFERENT SEDIMENT TYPES OF THE KIEL FJORD (WESTERN BALTIC SEA). 1998. 139 pp. In English with German summary

69 RÜDIGER SCHACHT
DIE SPÄT- UND POSTGLAZIALE ENTWICKLUNG DER WOOD- UND LIEFDEFJORDREGION NORDSPITZBERGENS. 1999. 123 pp. + app. In German with English summary

70 GEOMAR FORSCHUNGSZENTRUM FÜR MARINE GEOWISSENSCHAFTEN DER CHRISTIAN-ALBRECHTS-UNIVERSITÄT ZU KIEL. JAHRESBERICHT/ANNUAL REPORT 1997. 1998. 155 pp. In German and English

71 FS SONNE. FAHRTBERICHT/CRUISE REPORT SO118 BIGSET (BIOGEOCHEMICAL TRANSPORT OF MATTER AND ENERGY IN THE DEEP SEA). MUSCAT (OMAN) - MUSCAT (OMAN). 31.03.-11.05.1997. Ed. by OLAF PFANNKUCHE and CHRISTINE UTECHT. 1998. 188 pp. In English

72 FS SONNE. FAHRTBERICHT/CRUISE REPORT SO131 SINUS (SEISMIC INVESTIGATIONS AT THE NINETY EAST RIDGE OBSERVATORY USING SONNE AND JOIDES RESOLUTION DURING ODP LEG 179). KARACHI - SINGAPORE. 04.05-16.06.1998. Ed. by ERNST R. FLUEH and CHRISTIAN REICHERT. 1998. 337 pp. In English

73 THOMAS RICHTER
SEDIMENTARY FLUXES AT THE MID-ATLANTIC RIDGE: SEDIMENT SOURCES, ACCUMULATION RATES, AND GEOCHEMICAL CHARACTERISATION. 1998. IV, 173 + 29 pp. In English with German summary

74 BARBARA MARIA SPRINGER
MODIFIKATION DES BODENNAHEN STRÖMUNGSREGIMES UND DIE DEPOSITION VON SUSPENDIERTEM MATERIAL DURCH MAKROFAUNA. 1999. 112 pp. In German

75 SABINE JÄHMLICH
UNTERSUCHUNGEN ZUR PARTIKELDYNAMIK IN DER BODENGRENZSCHICHT DER MECKLENBURGER BUCHT. 1999. 139 pp. In German

76 WOLFRAM W. BRENNER
GRUNDLAGEN UND ANWENDUNGSMÖGLICHKEITEN DER MIKRO-ABSORPTIONSPHOTOMETRIE FÜR ORGANISCH-WANDIGE MIKROFOSSILIEN. 1999. 141 pp. In German with English summary

77 SUSAN KINSEY
TERTIARY BENTHIC FORAMINIFERAL BIOSTRATIGRAPHY AND PALAEOECOLOGY OF THE HALTEN TERRACE, NORWAY. 1999. VI, 145 pp. In English with German summary

78 HEIDI DOOSE
REKONSTRUKTION HYDROGRAPHISCHER VERHÄLTNISSE IM CALIFORNIENSTROM UND IM EUROPÄISCHEN MITTELMEER ZUR BILDUNGSZEIT ORGANISCH KOHLENSTOFFREICHER SEDIMENTE. 1999. IV, 111 pp. + app. In German with English summary

79 CLAUDIA WILLAMOWSKI
VERTEILUNGSMUSTER VON SPURENMETALLEN IM GLAZIALEN NORDATLANTIK: REKONSTRUKTION DER NÄHRSTOFFBILANZ ANHAND VON CADMIUMKONZENTRATIONEN IN KALKSCHALIGEN FORAMINIFEREN. 1999. 86, XXI pp. In German with English summary

80 FS SONNE. FAHRTBERICHT/CRUISE REPORT SO129. BIGSET (BIOGEOCHEMICAL TRANSPORT OF MATTER AND ENERGY IN THE DEEP SEA). PORT SULTAN QUABOOS - DUBAI. JANUARY 30 - MARCH 9, 1998. Ed. by OLAF PFANNKUCHE and CHRISTINE UTECHT. 1999. 107 pp. In English

81 FS SONNE. FAHRTBERICHT/CRUISE REPORT SO138. GINCO-2 (GEOSCIENTIFIC INVESTIGATIONS ON THE ACTIVE CONVERGENCE ZONE BETWEEN THE EAST EURASIAN AND AUSTRALIAN PLATES ALONG INDONESIA). JAKARTA - JAKARTA. 29.12.1998 - 28.01.1999. Ed. by ERNST R. FLUEH, BERND SCHRECKENBERGER, and JÖRG BIALAS. 1999. 333 pp. In English

82 CRUISE REPORTS: KOMEX I and II (KURILE OKHOTSK SEA MARINE EXPERIMENT)
RV PROFESSOR GAGARINSKY CRUISE 22
RV AKADEMIK M. A. LAVRENTYEV CRUISE 28
VLADIVOSTOK - PUSAN - OKHOTSK SEA - PUSAN - VLADIVOSTOK. 7 JULY - 12 SEPTEMBER 1998. Ed. by NICOLE BIEBOW and EDNA HÜTTEN. 1999. 188, 89 pp. In English

83 GREGOR REHDER
QUELLEN UND SENKEN MARINEN METHANS ZWISCHEN SCHELF UND OFFENEM OZEAN. REGIONALE VARIABILITÄT UND STEUERNDE PARAMETER DER METHANVERTEILUNG UND DER AUSTAUSCH MIT DER ATMOSPHÄRE. 1999. 161, 20 pp. In German with English summary

84 SVEN-OLIVER FRANZ
PLIOZÄNE ZEITREIHEN ZUR REKONSTRUKTION DER TIEFENWASSERZIRKULATION UND DER SILIZIKLASTISCHEN AMAZONASFRACHT IM ÄQUATORIALEN WESTATLANTIK (CEARA SCHWELLE, ODP LEG 154). 1999. 183 pp. In German with English summary

85 SYLKE HLAWATSCH
Mn-Fe-AKKUMULATE ALS INDIKATOR FÜR SCHAD- UND NÄHRSTOFFFLÜSSE IN DER WESTLICHEN OSTSEE. 1999. 132 pp. In German with English summary

86 BETTINA GEHRKE
ZUSAMMENSETZUNG UND VERTEILUNG DER LITHOGENEN FEINFRAKTION IN SPÄTQUARTÄREN SEDIMENTEN DES MITTELATLANTISCHEN REYKJANES RÜCKENS (59°N) - TONMINERALE ALS INDIKATOREN FÜR LIEFERGEBIETE, TRANSPORTMECHANISMEN UND ABLAGERUNGSPROZESSE. 1999. 102 pp.
In German with English summary

87 JENS GREINERT
REZENTE SUBMARINE MINERALBILDUNGEN: ABBILD GEOCHEMISCHER PROZESSE AN AKTIVEN FLUIDAUSTRITTSSTELLEN IM ALEUTEN- UND CASCADIA-AKKRETIONSKOMPLEX. 1999. 196, XX pp.
In German with English summary

89 FS SONNE. FAHRTBERICHT/CRUISE REPORT SO136. TASQWA (QUATERNARY VARIABILITY OF WATER MASSES IN THE SOUTHERN TASMAN SEA AND THE SOUTHERN OCEAN, SW PACIFIC SECTOR). WELLINGTON - HOBART. OCTOBER 16 - NOVEMBER 12, 1998. Ed. by JÖRN THIEDE, STEFAN NEES et al. 1999. 78, 106 pp. In English

90 FS SONNE. FAHRTBERICHT/CRUISE REPORT SO142. HULA (INTERDISCIPLINARY INVESTIGATIONS ON THE TIMING OF THE HAWAII-EMPEROR BEND AND THE ORIGIN OF LITHOSPHERIC ANOMALIES ALONG THE MUSICIAN SEAMOUNT CHAIN. MIDWAY - HONOLULU. MAY 30 - JUNE 28, 1999. Ed. by ERNST R. FLUEH, JOHN O'CONNOR, JASON PHIPPS MORGAN, AND JOCHEN WAGNER. 1999. 224 pp. In English

91 J. HAUSCHILD, T. GINDLER, D. RISTOW, A. BERHORST, C. BÖNNEMANN, K. HINZ
DFG-FORSCHUNGSPROJEKT *„KRUSTENSPLITTER"*. 3D-MAKRO-GESCHWINDIGKEITSBESTIMMUNGEN UND 3D-TIEFENMIGRATION DES SEISMISCHEN 3D-COSTA-RICA-DATENSATZES. 1999. 85 pp.
In German with English summary

92 FS AKADEMIK MSTISLAV KELDYSH. Fahrtbericht Reise Nr. 40: Norwegisch-Grönländische See, 27.6.-29.7.1998. Hrsg. von J. MIENERT, A. OMLIN, T. GÖLZ, D. LUKAS, J. POSEWANG. 1999. 65, 7 pp. In German

93 FS SONNE. FAHRTBERICHT/CRUISE REPORT SO143 TECFLUX. Ed. by GERHARD BOHRMANN, PETER LINKE, ERWIN SUESS, AND OLAF PFANNKUCHE. In English

94 FS SONNE. FAHRTBERICHT/CRUISE REPORT SO144-1&2. PAGANINI (PANAMA BASIN AND GALAPAGOS "PLUME" - NEW INVESTIGATIONS OF INTRAPLATE MAGMATISM). SAN DIEGO - CALDERA. SEPTEMBER 7 - NOVEMBER 7, 1999. Ed. by JÖRG BIALAS, ERNST R. FLUEH, AND GERHARD BOHRMANN. 437 pp. + app. In English

95 CHRISTIAN MATTHIAS HÜLS
MILLENNIAL-SCALE SST VARIABILITY AS INFERRED FROM PLANKTONIC FORAMINIFERAL CENSUS COUNTS IN THE WESTERN SUBTROPICAL ATLANTIC. 2000. 81 pp. + app. In English with German summary